EUROPEAN COMMISSION

nuclear science and technology

A Critical Evaluation of the Dissolution Mechanisms of High-level Waste Glasses in Conditions of Relevance for Geological Disposal (GLAMOR)

P. Van Iseghem[1], M. Aertsens[1], S. Gin[2], D. Deneele[2],
B. Grambow[3], P. McGrail[4], D. Strachan[4], G. Wicks[5]

[1] SCK•CEN, Mol (Belgium)
[2] CEA, Bagnols-sur-Cèze (France)
[3] Subatech, Nantes (France)
[4] PNNL, Richland (USA)
[5] SRNL, Aiken (USA)

Contract N° FIKW-CT-2001-00140

Final report

Work performed as part of the European Atomic Energy Community's research and training programme in the field of nuclear energy 1998-2002 (Fifth Framework Programme)
Key action: Nuclear fission
Area: Safety of the fuel cycle

Directorate-General for Research
2007 Euratom EUR 23097

Contents

Executive summary

Different theories have been proposed worldwide in the past for interpreting the results from experimental programmes on the dissolution of nuclear waste glasses. The common and important trend is that the dissolution rate of nuclear waste glass decreases with increasing time of exposure to the contacting solution under static conditions. The interpretations are diverging in that the decrease may be attributed to saturation effects in the solution, to protecting effects of the reaction layer formed on the glass surface, or to ion exchange processes between solution and glass. Currently these different interpretations relate to either a thermodynamically (affinity) or with kinetically controlled dissolution behaviour.

The first objective of the GLAMOR[1] project was to achieve a common understanding amongst the participants on the interpretation of the decrease in dissolution rate of nuclear waste glasses as observed in most experimental programmes and referring to geological disposal conditions. The project started from a selection of existing experimental data and existing analytical models as the basis of its work. A group of acknowledged international experts identified the experimental data to be used in the project and applied the models to the data. The experimental data were produced by various laboratories and under various experimental conditions (i.e. different glass compositions, pure solutions, solutions loaded with solids referring to disposal concepts). The second objective of the project was to better define and quantify the uncertainties associated with the calculations performed in modelling, for instance the uncertainty of the parameters used in the models. This modelling was done so that laboratory data would be properly interpreted and correctly extrapolated beyond the laboratory time scale of several years.

As a result of this project we achieved a common view of the different glass dissolution processes, and the different individual views on certain processes were integrated into an overall picture characterised by the following observations:

- Glass dissolution is strongly linked to the concentration of dissolved silica and as much as 10 000 times lower long-term dissolution rates relative to the initial dissolution rate can be achieved when Si concentrations are high.
- The principal source of high Si concentration is the glass itself. As long as the silica from the glass is not consumed by reaction with near-field materials, high silica concentrations in solution are expected to be achieved in a few months, and correspondingly low glass dissolution rates.

Even though there is a general agreement on these observations and on their mathematical treatment in conceptual models, there is still large uncertainty on how to interpret in detail the mechanism by which high silica concentrations slow down the dissolution rates. Two key interpretations were evaluated in detail in the project: (1) affinity-limited dissolution and (2) rate decrease by transport limitation through the reaction layer. We conclude that both affect the rate decrease. By applying the analytical models we realised a better understanding of the role of the different parameters considered in the models and of the impact of the uncertainties of these parameters. We were however unable to quantify the uncertainties associated with the calculations performed in modelling because of the large uncertainties on some of the modelling parameters still existing.

The following report provides a summary involving detailed discussions of the two main models and their potential use to explain the long-term behaviour of nuclear waste glasses under conditions relevant for geological disposal conditions.

[1] GLAMOR = A Critical Evaluation of the Dissolution Mechanisms of High-level Nuclear Waste Glasses in Conditions of Relevance for Geological Disposal.

Introduction and objectives

Different theories have been proposed worldwide in the past for interpreting the results from experimental programmes on the dissolution of nuclear waste glasses. The common and important trend is that the dissolution rate of nuclear waste glass decreases with increasing time of exposure to the contacting solution under static or low-flow conditions. The interpretations are diverging in that the decrease may be attributed to saturation effects in the solution, to protecting effects of the reaction layer formed on the glass surface, or to ion exchange processes between solution and glass. Currently these different interpretations relate to either a thermodynamically (affinity) or with kinetically controlled dissolution behaviour.

The first objective of the GLAMOR project was to achieve a common understanding amongst the participants on the interpretation of the decrease in dissolution rate of nuclear waste glasses as observed in most experimental programmes and referring to geological disposal conditions. The project started from a selection of existing experimental data and existing analytical models as the basis of its work. A group of acknowledged international experts identified the experimental data to be used in the project and applied the models to the data. The experimental data were produced by various laboratories and under various experimental conditions (i.e. different glass compositions, pure solutions, solutions loaded with solids referring to disposal concepts). The second objective of the project was to better define and quantify the uncertainties associated with the calculations performed in modelling – for instance the uncertainty of the parameters used in the models. This modelling was done so that laboratory data would be properly interpreted and correctly extrapolated beyond the laboratory timescale of several years.

We expected that by organising discussions amongst a group of experts on a selected set of experimental data and models we would create the most *efficient* condition for achieving a common understanding. We also believed that through such a Concerted Action type project we would achieve the most *economical* way of getting to that scientific common understanding.

The work plan of GLAMOR was organised as follows:

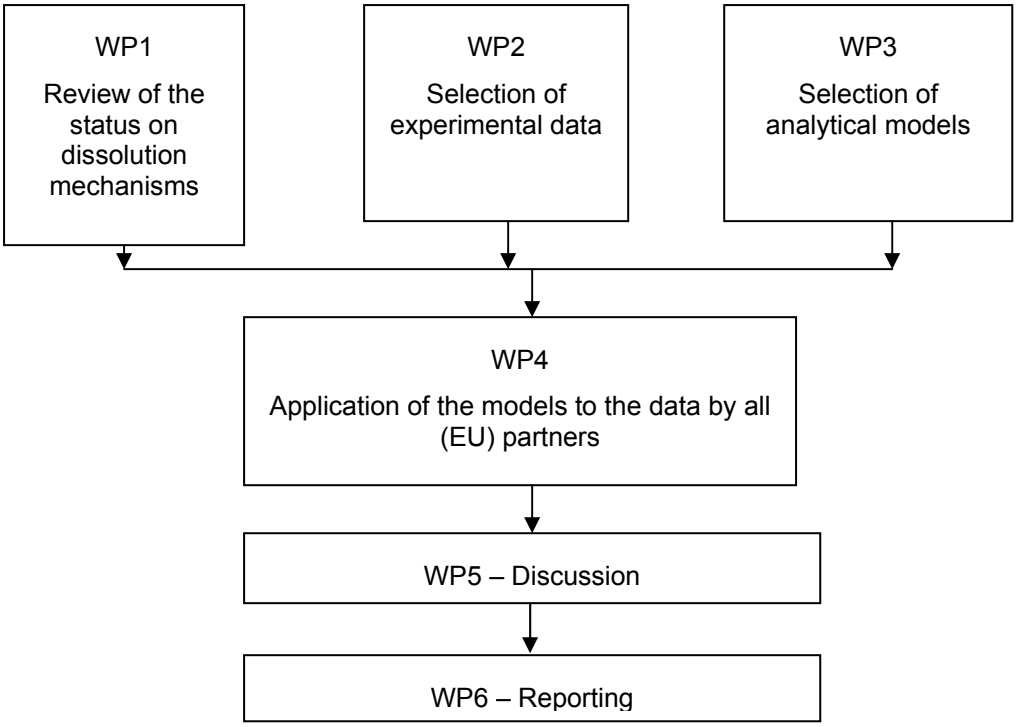

Figure 1: Scheme of the different work packages of GLAMOR and the relations among them

1 Work package 1: Overview of the status of the dissolution mechanisms of HLW glasses

1.1 General overview

A global view of the dissolution of high-level waste (HLW) glass in confined conditions is shown in Figure 2.

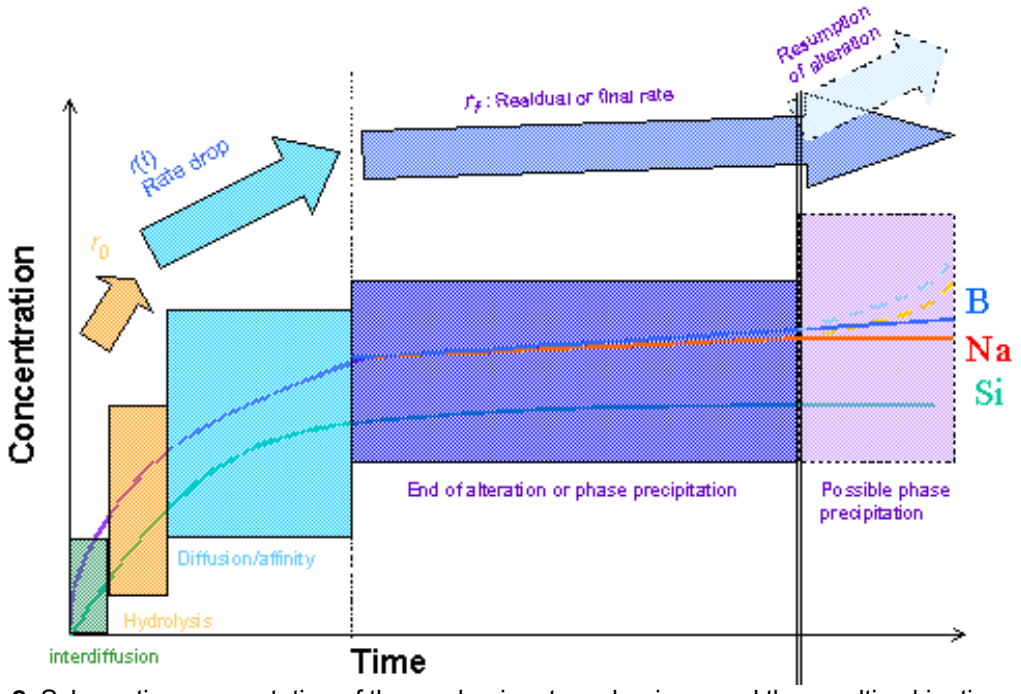

Figure 2. Schematic representation of the predominant mechanisms and the resulting kinetics as they affect the concentration versus time of the glass alteration elements Si, B and Na. This diagram is applicable to any type of glass, but the relative importance – or even the existence – of each phase depends on the glass composition and the alteration conditions (for example, a resumption of alteration is not applicable to all glass compositions, or only in extreme situations)

The initial stages of glass dissolution refer to the first two stages in Figure 2: interdiffusion and hydrolysis of the silicate network bonds.

Interdiffusion (ion exchange) occurs between the alkali metals of the glass network and H^+ or H_3O^+ ions in aqueous solution:

$$Si\text{-}O\text{-}Na + H^+ \leftrightarrow Si\text{-}OH + Na^+$$

This dissolution is selective, because only network-modifying cations weakly bonded to oxygen atoms can be exchanged. It is accompanied by an increase of the pH.

Hydrolysis of the silicate network occurs when the nucleophilic attack by an OH^- ion on a Si-O-Si bond results in depolymerisation followed by dissolution of the glass network. This will occur at alkaline pH values.

$$Si\text{-}O\text{-}Si + OH^- \leftrightarrow Si\text{-}OH + Si\text{-}O^-$$

$$Si\text{-}O^- + H_20 \leftrightarrow Si\text{-}OH + OH^-$$

The interdiffusion and hydrolysis mechanisms are competitive and have been well characterised in the international literature.

The following stages are much more subjected to controversy. After some time, especially in closed systems (representative for most geological disposal situations) the dissolution rate will drop, because of either silica saturation in solution, or because of the protection from the reaction layers formed on top of the glass. The first hypothesis considers thermodynamic equilibria controlling the process of rate decrease, based on the general law proposed by Aagaard and Helgeson [11]:

$$r = k^{+} \exp(-E_a/RT) \prod_i a_i^{ni} [1-(Q/K)^{\sigma}],$$

where r is the dissolution rate, k^{+} the forward rate constant ($g.m^{-2}\ s^{-1}$), E_a the activation energy ($J.mol^{-1}$), a_i the activity of i_{th} aqueous species and n_i the corresponding stochiometric coefficient, Q is the ion-activity product of the rate controlling reaction, K the equilibrium constant of this reaction and σ the net reaction order. A simplified expression of this law is

$$r = r_0 [1- (Q/K)^{\sigma}],$$

where r_0 is the initial dissolution rate (depending mainly on the glass composition, on the temperature and on the pH) and $1-(Q/K)^{\sigma}$ is an affinity term characterizing the decreasing solution aggressiveness with respect to the glass as it becomes increasingly concentrated in dissolved elements and as the ion activity product Q of the reactive species approaches the material solubility product K.

This kinetic law was adapted by Grambow [6], who postulated that hydrolysis of the silica in the glass is the rate limiting step

$$r = r_0 (1- C_{Si\ (solution)}/C^*_{Si\ (saturation)})$$

This expression is Grambow's "first-order law", in which only the silica from the glass is assumed to limit the dissolution reaction. This type of law assumes that an intrinsic saturation constant C^* exists for the SiO_2 that is supposed to represent the glass, and that it depends only on the glass composition, temperature and pH.

The second hypothesis considers kinetic processes as dominant. Alteration "protective gel" layers are formed during the glass dissolution that act as a diffusion barrier for the glass constituents, in particular silicon.

As a consequence of this rate drop, a "final" rate of dissolution may be reached in the next stage. These two stages (rate drop, final rate) constitute the main discussion of this project. The current disagreement on which process causes the rate drop is reviewed in Section 1.2.

Well-documented reviews on nuclear waste glass dissolution can be found in [1-5].

1.2 Consensus and disagreement on the glass corrosion mechanism: uncertainties in the conceptual models

Model uncertainty with respect to the affinity law

The affinity concept is one of the principal theories invoked to explain the decrease of glass corrosion rates with time as well as the effect of S/V and ground water flow rates on these rates [6-10]. It states that there is a thermodynamic driving force (affinity) for glass corrosion and the decrease of reaction rates is due to a reduction of this affinity. "Affinity" is a term used in the context of irreversible thermodynamics and of transition state theory [11] to quantify the deviation of a homogeneous or heterogeneous chemical reaction system from equilibrium. Close to equilibrium the reaction rate decreases proportional to the decreasing affinity. The problem is to identify the affinity controlling reaction step within the overall series of processes governing glass corrosion.

Some authors [12, 13] considered leaching to cease when silica is saturated in solution, but from a theoretical point of view this seems to be unlikely. Today there is general consensus that the glass phase can never come to equilibrium with aqueous solution because glasses

are thermodynamically unstable with respect to an assemblage of crystalline phases with a similar bulk composition to the glass [6, 14]. However, the pristine glass phase comes never in direct contact with an aqueous solution because diffusion processes prior to potential equilibration processes modify the original glass surface compositions: alkali depletion, surface hydration, hydrogen ion uptake…The affinity concept may thus be applied to the glass surface composition instead of bulk glass composition. Bourcier [10] proposed a model that did not postulate any "equilibrium" between the glass and solution. The glass alteration rate is assumed to follow a gel dissolution chemical affinity function calculated from the gel composition.

In the simplest case the silica rich glass surface composition may be simulated by amorphous silica resulting in the so-called first order dissolution rate law. In this form the affinity term is only controlled by the dissolved silica concentration in the aqueous solution contacting the glass. In a more sophisticated affinity model, the glass surface composition would be considered as a solid solution of silicate and oxide end members. The first order dissolution rate law and derived concepts are used for nuclear waste glass performance predictions since 1984. In the first order dissolution concept, the dissolution of silica from the surface is considered rate limiting for the release of soluble elements from the glass. Today there are not yet sufficient data to quantify the effect of other constituents of the alkali depleted glass surface (Al …) on the affinity term.

There are indications that there might be problems with the applicability of the first order rate law [15]. Fresh glass or prealtered glass samples were put in solutions over-saturated with silica. A decrease in reaction rates by as much as a factor of 10 was observed, but the rates remained much higher than predicted from a first order rate law. It was argued that "none of the kinetic models based on the notions of "chemical affinity" and "deviation from equilibrium" is adapted to describe the kinetics of glass corrosion. In contrast, the formation of a surface gel and condensation of silanol groups is considered responsible for the decrease in reaction rates.

The critique of the concept of affinity driven glass dissolution and of corresponding transition state theory applications is motivated in summary by the following experimental and theoretical observations:

- The glass/water equilibrium ("intrinsic glass solubility") cannot be a reference state for affinity controlled (limited) glass dissolution because glass is metastable. A true thermodynamic equilibrium will never exist
- Transition state theory is valid only for elementary reactions. The glass water reaction is dynamic system where a single rate limiting elementary reaction cannot be defined. Instead there is a series of coupled reactions. The first order dissolution rate law, which is based on this concept, therefore is also not valid.
- Experimental results show that saturation concentrations are not intrinsic glass properties but vary with the environmental conditions and with the exposure history of glass to water.
- Glass dissolution continues even if silica concentrations are higher than the apparent saturation concentration. The initial dissolution rate of a fresh glass exposed to a silica-saturated solution is only slightly lower than the initial rate in deionised water. In the long term the reaction rates are about 10 000 times lower than the initial rates. Thus, this cannot be a result of saturation but protective layer formation is considered as alternative explanation for the decrease of corrosion rates with time (see below).
- Glass dissolution continues at relatively high rate also in concentrated clay slurries with high silica concentration in solution [46].

The proponents of the affinity concept agree that these experimental and theoretical observations are valid but they refuse to draw a conclusion against the affinity concept and propose ways how to integrate these observations within an overall theory:

- The argument that transition state theory is valid only for elementary reactions would apply to all types of heterogeneous reactions, where potentially rate limiting elementary reactions are hardly known. Yet saturation phenomena are common in solid/water interactions of various minerals.

- There are other explanations for deviations from the affinity law, not only the hypothesis of a “protective gel”, but also other hypotheses put forward in the literature: “water diffusion/ion exchange” [38] “ion exchange” [47], phase separation of glasses [48].
- Tests performed at temperatures well above 100 ^{o}C show that glass corrosion continues with a low rate despite silica saturation [6, 16-17]. Precipitation of Si containing secondary phases such as quartz or water diffusion/ion exchange were invoked as mechanism for keeping final dissolution affinities higher than zero.
- There is consensus that an affinity-based rate law cannot alone be used to describe all the contributions to the observed decrease in reaction rate, especially for glasses with very complex compositions. The affinity theory can only be validated or invalidated if it is not considered in isolation, but as part of an overall mechanism that includes ion exchange, water diffusion, inter-diffusion, hydrolysis, dissolution, secondary phase formation, affinity reduction, protective layer formation, long-term corrosion.
- The existence of a protective gel layer - one in which the transport of a rate limiting species is hindered - is not only consistent with an affinity-based reaction mechanism, affinity differences as a function of distance from the dissolving glass surface provide even the thermodynamic driving force governing mass transfer across the protective transport barrier.
- Monte Carlo calculations [18] have shown that some type of surface restructuration (alkali depletion, silanol recondensation) is necessary before saturation effects become fully effective in controlling long-term release of soluble glass constituents. This explains why the saturation concentration is a function of time (in the first hours of experiment)

Affinity-unrelated protective layer theory

The formation of dense surface layers is considered responsible by certain authors for explaining the saturation effect [19-20]. Recent experimental results revealed the renewed dissolution of a pristine glass specimen in an apparently saturated solution. Such behaviour, which cannot be explained in terms of only a saturation effect, seems to depend on the protective effect of the gel formed during alteration.

A possible hypothesis for the formation of a protective gel is that the solubility of the precipitating phase is reached at the reaction interface under conditions where the dissolving phase (glass) is far from a potentially never achievable equilibrium. The situation would be comparable to the dissolution of metals which are thermodynamically instable in aqueous media (Zr, Ti, Al, Cr …) but which become stabilised by the formation of a passivation layer attributed to the onset of saturation with respect to an oxide or a hydroxide at the reaction surface [21].

It is proposed that only a dynamic process of hydrolysis and condensation of silicon at the glass/gel interface can account for the formation of the gel layer. The glass alteration rate under silica saturation conditions would thus be highly dependent on the silicon recondensation rate. The hypothesis of glass alteration rate being controlled by the rate at which the hydrolyzed species recondense, allows to explain an S/V effect, since the recondensation rate in turn depends on the number of available recondensation sites and thus on the S/V . Silicon release would be controlled by the initial glass dissolution kinetics, while recondensation may be assumed to depend on the dissolved silicon concentration in the homogeneous solution. Silicon diffusion in the water is assumed to occur quickly, and recondensation may occur at any point on the glass surface. Steady-state conditions will occur in solution when the concentration of silicon remains constant. According to the affinity unrelated protective layer theory, this steady state reflects only the equal flows of hydrolysis and recondensation and does not correspond to equilibrium between the dissolving initial (glass) phase and solution. In the mathematical formulation of this concept a limiting silicon concentration C* at the gel/glass interface is used at which glass corrosion ceases. Glass corrosion rates decrease on the approach of this concentration, but the limiting value is interpreted not as a thermodynamic value but as a property of the dynamic glass/gel/solution system.

The critique of the concept of affinity unrelated protective layer formation, as limit for glass dissolution in saturated environments, is motivated by the following experimental and theoretical observations:

- While there are circumstances under which the gel layer can be protective, layers are non protective under other conditions
- Until now, no relation between layer thickness and corrosion rate at any given layer thickness has been demonstrated
- The mathematical model for the effect of a protective layer is based on silica transport limitation, but this concept does not make sense if the affinity concept is invalid
- The affinity concept provides the principal theoretical framework to explain the protective layer effect: the layer may be formed by solubility effects and/or the layer plays the role of a silica diffusion barrier limiting glass dissolution rates according to the first order rate law at the interface between the pristine glass and the surface layer.
- Concerning the balance of the rates of hydrolysis and recondensation reactions of silica bonds, two cases must be distinguished: an equilibrium state with the surface (not the bulk) of the dissolving glass or a steady state, where the glass dissolves at its initial rate and recondensation of silanol groups leads to the formation of a gel as a secondary phase. In both cases solution concentrations of Si become almost constant, but in the steady state case, the glass would become transformed into a gel with its initial rate. Experimental observations show that this is not the case. Hence, it is the dissolving phase which is stabilized by recondensation of silanol groups, not a secondary phase. This validates the affinity concept.
- There are conflicting arguments: the argument of a steady state between initial glass corrosion rates and recondensation rates implies as consequence a constant rate of glass/gel transformation; whereas the concept of C* implies as consequence that the glass/gel transformation rate decreases with the approach to this value.
- Silicon recondensation rates in the gel can explain diverse steady state concentrations at the glass/gel interface, depending on glass matrix alteration rate and different silicon removal rates, but they cannot explain, why and in which way this steady state concentration would slow down glass/gel transformation with increasing concentration of Si at the gel/glass interface. Higher concentrations should increase the recondensation rate of Si in the gel without being able to reduce the initial glass corrosion rate. What then is the reason for the slow down of glass /gel transformation (glass matrix alteration rate) once steady state concentrations approach C*? The only plausible explanation is that silica recondensation not only occurs in the gel but as well at the surface of the dissolving phase (glass). This recondensation would then stabilize the glass surface. This explanation of a balance of dissolution and recondensation rates at the glass surface is thus equal to the kinetic interpretation of glass surface equilibrium by equal forward and backward rates; hence we come back to the affinity term.

The proponents of the affinity unrelated protective layer concept agree to certain statements and disagree to others:

- Agreement is on the fact that certain gel layers are protective, others not. Protective gel layers are formed in silica rich solutions, because the degree of silanol group condensation will produce very dense gel layers.
- Mass transfer of Si across the gel layer is an important rate-limiting step, but this is not related to a dissolution affinity. The saturation concentration at the glass/gel interface is not a thermodynamic value but merely a steady state value, which could be different from experiment to experiment.

The “residual” or “final” rate

This process probably will govern the long-term behaviour of glass in a geologic repository. This process and its fundamental driving forces (possibly a combination of secondary phase formation and ion exchange) have been invoked as rate controlling since about 1984 without serious progress since then in the development of our predictive capacities in the assessment of secondary phase effects driving glass corrosion. There are no major inconsistencies in the approaches of the various partners of the GLAMOR project on this issue, but model uncertainties will occur, once the different models are applied to the same experimental data.

Interdiffusion – water diffusion – ion exchange

Experimental results show that glass network hydration and ion exchange are important in short term laboratory tests and in certain cases (closed system) also in the long term. For example, "inter-diffusion" may relate to a chemical process with a rate that is important at the very beginning of the glass-water interaction and much later as all the rates of the other processes decrease. Recent literature suggests that the interdiffusion (ion exchange, water diffusion) coupled to the affinity concept might become rate limiting in the long-term as all the other processes slow down [36, 47]. This literature suggests that the "interdiffusion" part of the glass-water interaction might not always have a square root of time dependence. A certain time dependence might be masked by the uncertainties in the results that can be estimated from propagating all the errors in the measurements leading to the results (temperature measurement errors that lead to errors in the computed activation energy, etc). Low dissolution affinity is a necessary condition for the long-term validity of the ion exchange/water diffusion concept, but reaction rates do not slow down immediately to zero, in case were the glass dissolution affinity approaches zero.

The critique of the concept of ion exchange/water diffusion/interdiffusion in saturated environments is motivated by the following experimental and theoretical observations:

- Ion exchange and water diffusion are short term processes, if applicable in the long term, its contribution to long-term performance would be negligible
- The glass alteration rate at silica saturation should not depend on the available glass reactive surface area if water diffusion is dominant.

The proponents of the affinity coupled water diffusion concept agree to these statements but they would like to clarify the following:

- Agreement is to the fact that the long-term contribution of ion exchange is probably negligible. This effect however is not negligible in the experiments, which are used to sustain a model for long-term predictions. Ion-exchange/water diffusion must therefore be considered in the analysis of the experimental results before conclusions on a long-term model can be derived from these experimental data.
- It is correct that the water diffusion driven rate should be independent on the S/V, but this is not the case for the time period necessary to approach a condition where the dissolution affinity becomes close to zero. There are many experimental data, particularly in salt media, showing that the long-term glass dissolution rate is indeed independent on the S/V effect.

1.3 Data and understanding of the long-term dissolution of HLW glass in closed systems

a) Approach followed

The GLAMOR project aims to achieve a common understanding of the mechanisms by which the dissolution rate decreases with time, when saturation effects (mainly of silica) in the solution are occurring. One may consider this in two ways:

- in the stage where the glass dissolution is decreasing from the initial rate to smaller values,
- in the subsequent stage, when the glass dissolution has slowed down very strongly, and may tend to a stable value.

We opt for reviewing the situation for the second case, because this stage will be representative for the long-term dissolution behaviour. A "final rate of dissolution" is sometimes defined in that stage.

We have reviewed the literature for experiments that cover the dissolution of HLW glasses in closed (therefore static) systems, and that preferably run for long durations and/or high reaction progress[2]. In reviewing the literature, our interest was:

- first to look for the dissolution **mechanisms** (ion exchange, diffusion of species inside the glass, congruent dissolution, precipitation, etc.) that were reported to explain the long-term dissolution behaviour,
- second to look for the underlying hypotheses or explanations for these mechanisms.

Further points of interest were:

- composition of the glass and of the medium
- temperature, surface to volume ratio, duration
- analyses done after the test (solution, surface, others).

b) Overview of experimental data

a. Data from FZ Karlsruhe (Germany)

Large experimental programmes have been conducted at FZK and prior to them at HMI (Hahn-Meitner Institute, Berlin) on the dissolution of different reference HLW glasses since the early 80's. The media chosen were usually either pure water (deionised water) or different brines (salt being until recently the candidate host rock in Germany). Experimental data that provide a long-term perspective are reported in [22-23]. The experimental parameters are summarized in Table I.

Table I: Experimental conditions considered in the FZK studies

Parameter	Value
Glass	SON68 (inactive, radioactive)[3]
Solution	Halite saturated $MgCl_2$ or NaCl rich brines
S/V (in m^{-1})	10; 210; 2,100; 21,000 (geometrical S/V)
Geometric form of glass	Powder; average size 240 µm (inactive), 86 µm (radioactive)
Duration	t_{max} = 3 years
Temperature (°C)	110, 150, 190
Analyses	Solution analysis (ICP-OES for inactive elements)

Reaction progress values of as high as 10^5 $g.m^{-3}$ were achieved this way at 190°C. At the lower temperature reaction progress values of ~ 2 x 10^4 $g.m^{-3}$ were reached. The normalized elemental concentrations were plotted as a function of (S/V)*t or (S/V)*√t, to check whether the dominating dissolution process is congruent dissolution or selective leaching (diffusion). A few typical plots are shown in Figures 3-5. They were obtained in two different $Mg(Cl_2)$ rich brines, with initial pH between 4.0 and 5.0 (full details see [24-25].

The long-term glass dissolution under silica saturated conditions appears to be controlled by a diffusion process, as concluded from the linear fit in the (S/V)*√t plots. Water diffusion is proposed as being the rate controlling diffusion process, rather than ion-ion exchange (H_30^+-M^+). Water diffusion is causing soluble glass constituents (alkali's and B) to leach with the same rate.

---

[2] Reaction progress : the normalized concentration of the trace element (B, Li) in solution, per-unit solution volume ($g.m^{-3}$)

[3] The glass was specially prepared by CEA. Reprocessing HLW was used, with a somewhat different radioactivity level than the radioactive R7T7 glass.

The data referred too so far were obtained at basic pH condition – pH is further decreasing with further reaction progress. In the NaCl rich brine pH is evolving from ~6.5 initially to higher pH values. The pH and glass dissolution data do not show nice linear relationships as in the $Mg(Cl_2)$ rich brines, but diffusion within the glass matrix is proposed as the rate controlling process as well [23].

The time dependence of the dissolution of the radioactive glass is the same as for the inactive glass.

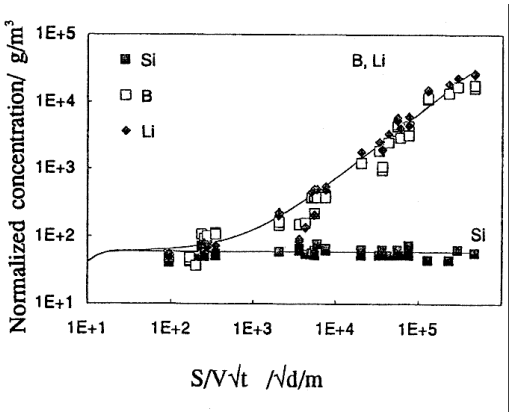

Figure 3: Normalised solution concentration of B, Li and Si as a function of S/V*√t for glass SON68 in $MgCl_2$ rich brine at 110 °C

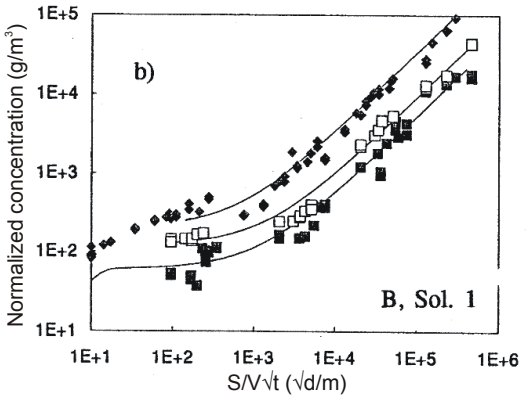

Figure 4: Normalised solution concentrations of B as a function of S/V*√t at various temperatures in a $MgCl_2$ rich brine (inactive R7T7 glass)
■ 190°C □ 150°C ♦ 110°C

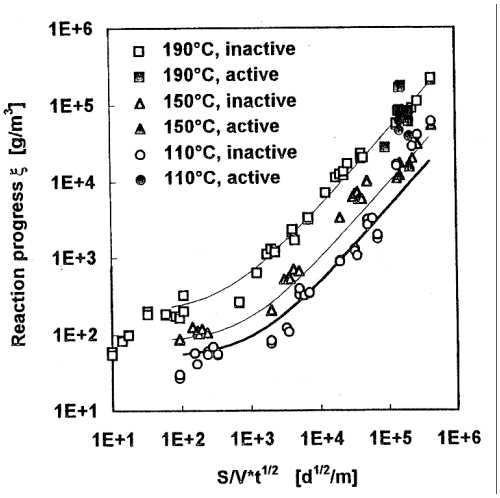

Figure 5: Time and temperature dependence of CEA-R7T7 glass corrosion in a Mg(Ca)Cl_2-rich brine

b. Data from CEA Valrhô (France)

CEA has been conducting experimental programmes on HLW glass dissolution since the early 80's as well. These programmes were more general than others essentially because no candidate geological formation so far was defined in France. The selection of the reference SON68 glass for the R7T7 vitrification plant in La Hague resulted in the onset of a very large database on this glass, in France and in many other countries.

In this review we concentrate on CEA studies that covered or focussed on "long-term" dissolution data. Significant progress has been achieved in this area in the past years, resulting in amongst others in the hypothesis of the "protective gel".

We summarize the experimental approach in Table II. A few typical plots taken from the papers are shown in Figures 6-12. A basic detail is that solution aliquots taken from the container at different intervals – only one test container was used to monitor the time dependence of dissolution.

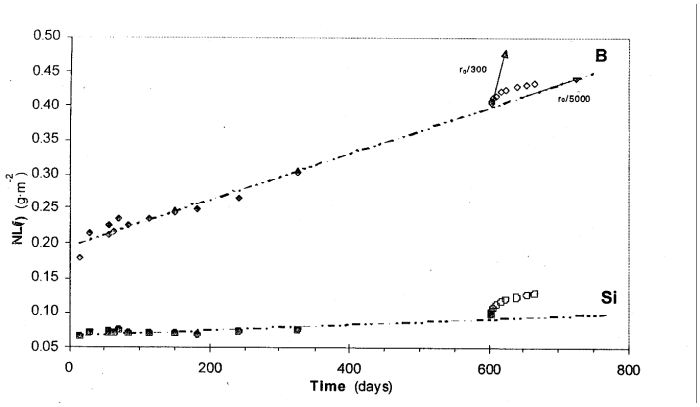

Figure 6 : Normalised glass mass losses calculated from the B and Si concentrations in the 600 days static experiment (solid symbols) and after renewed leaching in pure water after 600 days of leaching (open symbols) for glass SON68

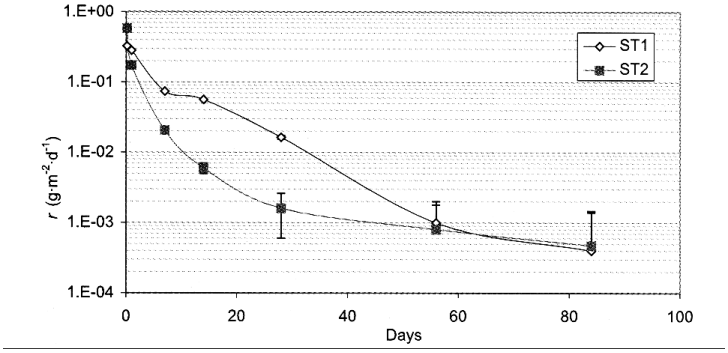

Figure 7: Glass alteration rates in static tests ST1 (glass specimen previously altered under flowing conditions) and ST2 (pristine glass coupon) versus time at 90°C and S/V = 500 m^{-1} for glass SON68. The estimated uncertainty on alteration rates is 10^{-3} $g.m^{-2}.d^{-1}$

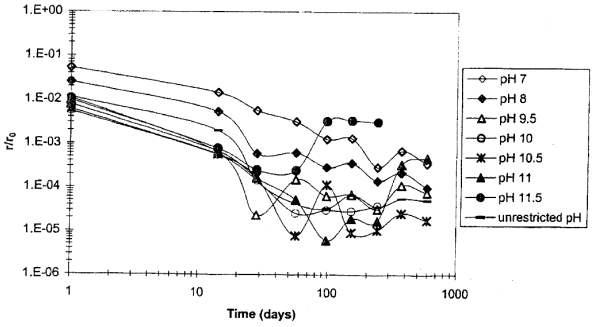

Figure 8: Evolution of the ratio between the alteration rate (r) and the initial rate (r0) for glass SON68 at various pH values. The precision on the r/r0 ratio below 10^{-4} is poor and the fluctuations are not significant

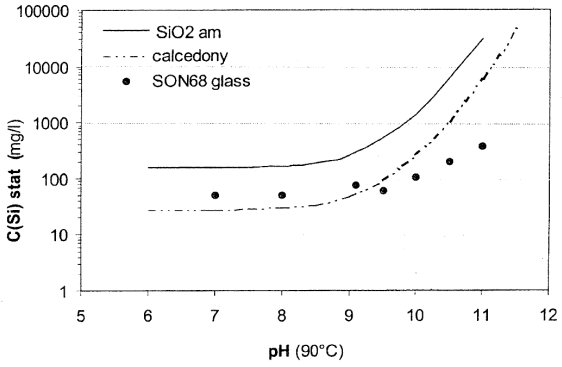

Figure 9: Apparent solubility of SON68 glass at S/V = 5 000 m^{-1} and imposed pH; comparison between silica and chalcedony

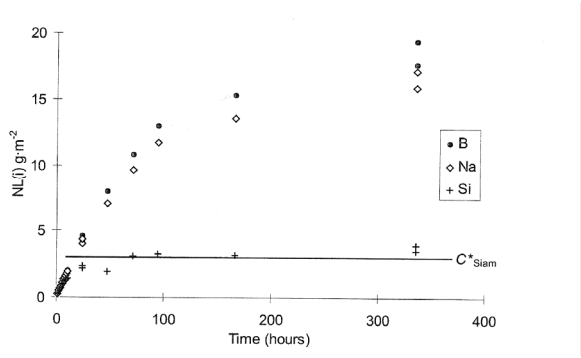

Figure 10: Normalised Si, B and Na mass losses versus time during the first 14 days of glass alteration under static conditions at 90°C, pH 9 and S/V 400 m^{-1}. After about 50h the alteration rate (determined from the B and Si release) gradually diminished to approximately $r_0/10$ after 14 days

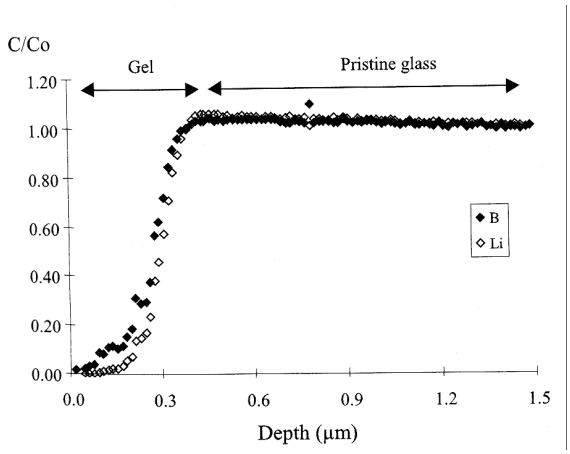

Figure 11: SIMS profiles for B and Li at the surface of a pristine glass specimen immersed in a saturated leachate (S/V = 10 m^{-1}) for glass SON68

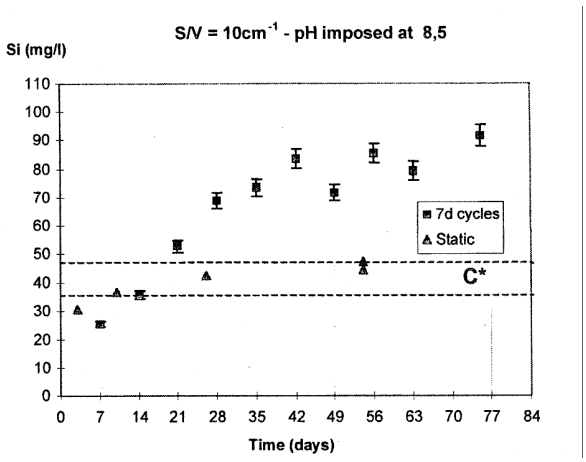

Figure 12: Static leaching behaviour of SON68 glass at 90°C with and without glass powder renewal

In view of the objectives of this work package within the GLAMOR project, the CEA experiments have provided data on the long-term dissolution rate, and some hypotheses on the possible underlying mechanism.

Reaction progress went up to similar values as in the data reported by Grambow (see a.). The CEA studies [26, 28, 30] conclude on a "final" dissolution rate r_f of 2 or 3 x 10^{-4} $g.m^{-2}.d^{-1}$, which is about 5,000 times smaller than r_0 (the initial rate of dissolution). The amount of data to support this final rate is still relatively limited, however. No discussion was made so far to associate this final rate to mechanisms. Interdiffusion and precipitation of a secondary phase were proposed as potential mechanisms [26]. The rate therefore is not necessarily constant with time.

The solution pH values associated with the "final" dissolution rate data are within the 9.0 – 9.5 range. Corrosion resumption was observed only at pH of 10.9 and above. This potentially important phenomenon was attributed to the precipitation of an alkali-alumino-silicate phase [30]. The data are characterized by the initial achievement of very low reaction rates (similar as in the experiments at lower pH) but after a delay which at pH 10.9 (at 90°C) reaches one year a strong increase in reaction rates is observed. The cut-off pH at which definitely no rate resumption is observed is not very clearly known, but since this phenomenon was never observed at pH 10.5 one may conclude that the critical pH is probably higher than pH 10.5 but lower than pH 11.

These studies provided several indirect proofs that a protective "gel" reaction layer on top of the glass caused the very strong drop in the dissolution rate in silica saturated solution. The concept of "silica solubility" was also reconsidered. Indeed it was shown that the measured silica solubility depends on the type of experiment done – this was well demonstrated in the cyclic test reported in [29] – see also Table II. The apparent solubility does not fit with that from a pure silica mineral, and other elements such as Al, Ca, Zr and rare earth elements are present as well.

Table II: Experimental conditions considered in the CEA studies

Common parameters	Reference	Test concept	Specific parameters
SON68 90 °C	[26]	2 step test: powdered glass is dissolved in DW for 600d, then leachate is renewed	S/V = 5,000m^{-1} Reaction progress < 10^3 $g.m^{-3}$
Use of powdered glass; surface determined by BET Deionised water (DW)	[27]	2 step test: powdered glass is dissolved in DW for 90d to achieve saturated solution ($r_f = r_0/5,000$) then pristine glass is added to the saturated solution	S/V = 5,000m^{-1} in step 1; 1,000m^{-1} in step 2
	[28]	2 step test: powdered glass is dissolved in flowing DW to generate a low-density gel then the powdered glass is transferred to fresh DW	Step 1: flow rate 1.3 ml/min , duration 7d S/V = 500 m^{-1} in step 2 Powder fraction 160-250µm
	[29]	Powdered glass dissolved for 800d	S/V = 200,000 m^{-1}
	[29]	2 parallel tests: - powdered glass is dissolved (t_{max} 84d) - same, but altered glass replaced by pristine glass every 7d	S/V = 1,500 m^{-1}
	[30]	Tests were done at different fixed pH values (7 values between 7 and 11.5); tmax = 600d	Powder fraction 63-100 µm
Ternary glass Si/Na/B, simulating SON68*	[31]	Static test to follow the elements leaching until silica saturation is reached ; t_{max} = 14d (90°C, DW)	Reaction progress < 10^4 $g.m^{-3}$ Powder fraction 40-100 µm; S/V = 400m^{-1}

* (ternary glass in mol%: 67.73 SiO_2, 14.23 Na_2O, 18.04 B_2O_3).

c. Data from SCK•CEN Mol (Belgium)

SCK•CEN has conducted nuclear waste glass dissolution studies since the early 80's. It considered two kinds of HLW glasses: the "SON68-type HLW glasses" (designed for reprocessed commercial reactor fuel), and high-Al_2O_3 glasses (designed for reprocessed research reactor fuel). The latter glasses have an Al_2O_3 content of ~20 wt%, SiO_2 ~40 wt%, B_2O_3 ~20 wt% (see [5], p. 88). The studies included parametric studies in pure water (DW) and in clay solutions (clay water or clay slurries). We review the studies that provided long-term data in these media. We refer to [32-33].

Table III summarises the experimental conditions applied.

Table III: Experimental conditions in the SCK•CEN studies

Parameter	Value
Glass	SON68, SM527 (high Al_2O_3) Simple glasses with various Si/Al ratios [4]
Solution	Distilled water Synthetic boom clay water Boom clay slurry (500g/l)
S/V (in m^{-1})	100; 500; 2,500; 10,000 (geometrical surface area 0.012 m^2/g)
Geometrical form of the glass	Powder fraction 125-250 µm
Duration (d)	T_{max} = 980d
Temperature (°C)	90, 150 (150°C data not discussed in this report)
Analyses	Solution (ICP-AES)

Reaction progress values of as high as 2 x 10^4 $g.m^{-3}$ were achieved this way at 90°C. The normalized elemental concentrations were plotted in function of (S/V)*t or (S/V)*√t, to find out whether the dominating dissolution process is congruent dissolution or selective leaching (diffusion). A few typical plots are shown in Figures 13-15. Solution pH remains below 10 in the pure solutions and below ~ 9.2 when clay is present.

At 90°C, the long-term glass dissolution under silica saturated conditions appears to be controlled by a diffusion process, as concluded from the linear fit in the (S/V)*√t plots. This is observed for the different glass compositions studied, and in the two different solutions. Effective diffusion coefficients for boron were in the order of 10^{-19}-10^{-20} $m^2.s^{-1}$, suggesting ion exchange reactions between H_30^+ or H^+ and Na^+/Li^+.

The "saturation" silica concentrations in solution are not necessarily constant with time. Increasing silica concentrations (up to 300 $mg.L^{-1}$) were measured for the low Al_2O_3/high SiO_2 model glass, whereas the saturation Si concentrations were stable for the other glasses at 50-60 $mg.l^{-1}$. This difference does not affect the long-term leaching of the soluble elements however.

When solids (clay) are present in the solution, the methodology in applying powdered glass and different S/V is not useful, because other processes occur in addition, such as sorption of leached species onto the clay [32]. So we did not succeed in obtaining long-term dissolution rate data and mechanisms this way.

[4] The composition of these glasses is (in mol%):
M3 : 28.5 SiO_2, 18.2 $AlO_{1.5}$
M5 : 34 SiO_2, 12.7 $AlO_{1.5}$
M7 : 40 SiO_2, 6.7 $AlO_{1.5}$
(balance: 14.92 $NaO_{0.5}$, 14.5 $LiO_{0.5}$, 21.17 $BO_{1.5}$, 2.71 CaO).

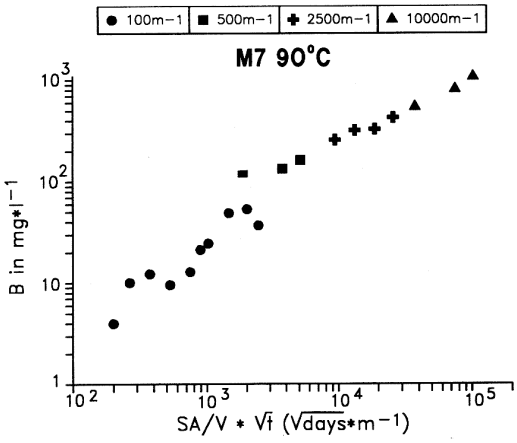

Figure 13: B solution data for glass M7 at 90°C, for various S/V conditions

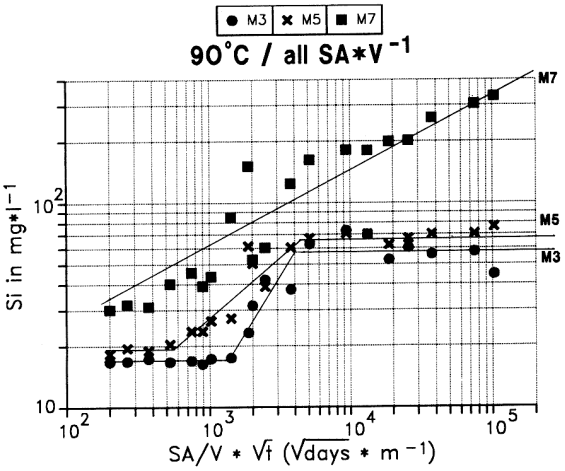

Figure 14: Si solution data for glasses M3, M5 and M7 at 90°C, for various S/V conditions. The lines are a guide for the eye

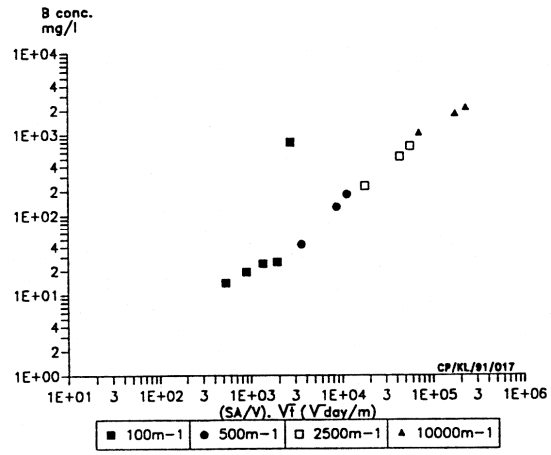

Figure 15: B solution data as function of S/V*√t for glass SM527 at 90°C in synthetic interstitial clay water

d. Data from PSI (Switzerland)

A series of long-term leaching tests were started in 1990 at PSI on two reference HLW glasses (SON68 and MW), used to solidify reprocessed radioactive HLW from the Swiss nuclear power plants. The main objective was to obtain reliable and precise long-term corrosion rates of the glasses. The test conditions were similar to those in the tests reported in the previous sections (powdered glass, deionised water, 90 °C). The interesting point is that the tests were running for very long time (13 years). Details are listed in Table IV. Some experimental results are shown in Figures 16-17. More information can be found in [49, 50].

Table IV: Experimental conditions in the PSI studies

Parameter	Value
Glass	SON68, MW (*)
Solution	Distilled water
S/V (in m^{-1})	1 200 (specific surface measured by stereological analysis is 0.03 m^2/g – [51])
Geometric form of glass	Powder
Duration (years)	13 (maximum duration)
Temperature (°C)	90
Analyses	ICP-AES, SEM/TEM/STEM of reacted glass surface

* The MW glass is selected by BNFL (U.K.). Compared to SON68 the SiO_2 content is similar, CaO is 0% (4% for SON68), MgO is 5.9% (0% for SON68), ZnO is 0% (2.5% for SON68) and the content of fission products and actinides is 8.6% (10.4% for SON68).

It was concluded that beyond ~ 500 days of test, the dissolution rate was constant till some 3650 days. This is based on a linear regression model of the data, although the data for B and Li leaching did not evolve in a perfect linear way over the whole time period. Values for this long-term dissolution rate are

1.3 (± 0.2) x 10^{-4} g m^{-2} d^{-1} for SON68 (based on B or Li)
9.6 (± 5.3) x 10^{-4} g m^{-2} d^{-1} for MW (based on B) or 6.8 x 10^{-4} g m^{-2} d^{-1} (based on Li)

The Si concentrations in solution were quite constant, after about 1 000 days. The "saturation" concentration is ~90 mg/l. The alteration layers of the SON68 and MW glasses were studied after 5.5 and 12.2 years of corrosion, and revealed that a number of clay minerals had formed in a outer precipitation layer.

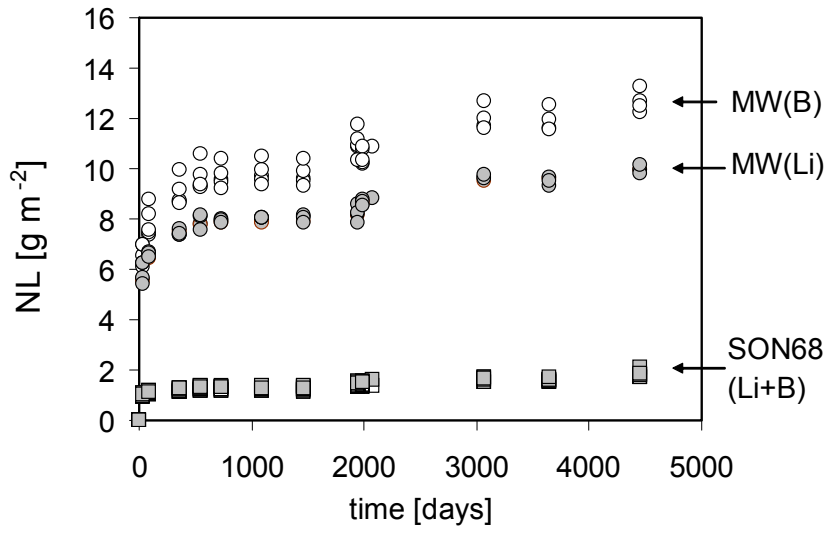

Figure 16: Normalised B and Li mass losses for glasses MW and SON68 (DW; 90 °C; 1 200 m^{-1})

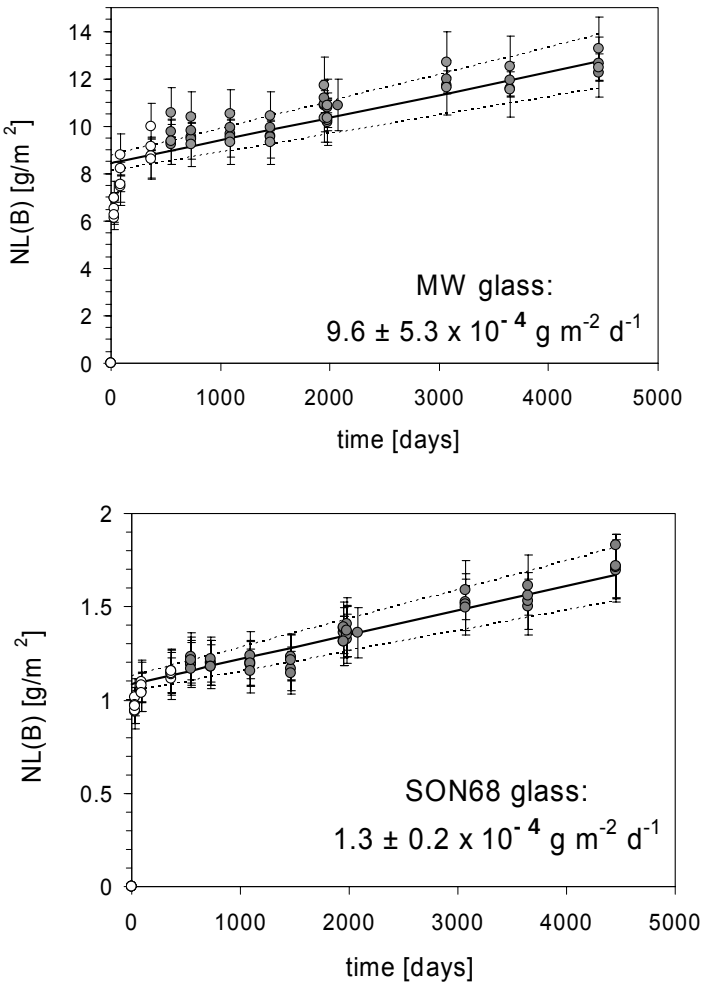

Figure 17: Normalised B mass losses and their deviations, used to calculate the dissolution rate. Only data > 500 days were considered

e. Data from other sources

Studies reported by Wicks *et al* in the early '80s discuss the mechanisms when different HLW glasses were submitted to the standard MCC1 test (S/V = 10m^{-1}, 90°C, t_{max} = 6 months) [12]. The longer term data in these tests could be interpreted as being controlled by diffusion of silicate through a precipitation layer at the outside of the gel layer. A mathematical model was developed accordingly [12].

The contribution of these tests to identifying the long-term dissolution behaviour as intended within GLAMOR is not that straightforward however. The maximum reaction progress achieved was ~10^3 g.m^{-3} and the results did not reveal the glass dissolution stage beyond silica saturation in solution.

Mitsui *et al* performed more recently glass dissolution experiments in the presence of bentonite, iron and magnetite. Amorphous silica was added sometimes, to assess its effect on the alteration in these integrated conditions [34]. It was found that the glass alteration in these silica saturated conditions is dominated by hydration, and the release of soluble elements follows a square root of time dependence.

c) Conclusions

The various data covering the "long-term" stage (the stage beyond saturation of the solution) do not unanimously show that a final dissolution rate is obtained that further decreases (proportional with √t,

data by FZK and SCK), or remains more or less stable (CEA). The respective databases are not that large either, but they cover both basic and acidic pH ranges. The considerations on the final dissolution behaviour were made for reaction progress values in the order of 10^3-10^4 g.m^{-3} (at 90 °C), and at high S/V conditions by using powdered glass. The conditions for achieving the final dissolution behaviour can't be achieved by using monolithic glass samples without presence of powdered glass, if a sufficiently high solution volume is used to allow reliable solution analyses.

Overall, we can conclude for pH values < 10.5 that for very large reaction progress values very small dissolution rates are obtained (e.g. 5 000 times smaller than the initial rate of dissolution as concluded by CEA), that tend to further decrease with time. It would be of interest to use a similar graphical representation for the data of the different laboratories.

Various hypotheses have been proposed to account for the long-term dissolution:
- water diffusion into the glass
- ion-ion exchange reactions between alkali's (glass) and H^+ (solution)
- network hydrolysis
- precipitation of secondary phases.

Presently, it is uncertain if a single process dominates in all experimental conditions. The real mechanism controlling the long-term dissolution might be a combination of different processes. For instance, the diffusion processes might be different depending on the temperature. Diffusion processes appear to be a common hypothesis for all laboratories, however. Matrix dissolution might occur as well when (typically water) diffusion would be rate limiting. The aqueous solutions generated by long-term glass corrosion are typically supersaturated in quartz and possibly in other minerals capable for consuming large quantities of dissolved silica. Assuming that any of these minerals would form sufficiently slowly for not being detectable in the experiments, one would conclude that a diffusion mechanism would dominate long-term glass corrosion. However, since the diffusion rate might steadily decrease with time, there might come a moment at which the secondary phase formation rate is higher than the diffusion rate, hence secondary phase formation might become rate limiting. This is why a square root of time-rate law shall not be extrapolated to the long-term for experimental times longer than experimentally measured.

It is important to note as well that diffusion coefficients for water are today only estimated from accumulation of dissolved glass constituents in solution (= leaching tests), and in some cases from solid state concentration profiles at the glass surface. However, these estimations all use the hypothesis that the diffusion coefficient is constant with reaction depth. However, this may not be the case. If the diffusion coefficients decrease with water penetration depth, no square root of time dependency of glass corrosion might be expected and constant rate terms might occur.

Remark: one should be careful in interpreting simply a $\sqrt{t}$ dependence in a log-log plot of normalized mass loss as a function of time as corresponding to a diffusion process (see for instance the data of FZ Karlsruhe and SCK•CEN; see also the methodology to correlate data at different S/V values in e.g. [76]). A $\sqrt{t}$ dependence may as well be due to a matrix dissolution process coupled with precipitation of secondary phases and diffusion processes.

d) Further actions

- This literature search for long-term HLW glass dissolution should be completed with data from other sources and with data when solids (clays or other materials) are present in solution.
- The cut-off pH at which no resumption of glass dissolution occurs should be documented, though it is not a process that is expected to occur in any condition (e.g. for pH below 10).
- This literature survey did reveal some uncertainties for further consideration:
    - What are the uncertainties in measuring very low corrosion rates of ~10^{-4} g.m^{-2}.d^{-1} and less? What's the lowest dissolution rate that is measurable?
    - How can the data for powdered glass be correlated with the data on monoliths? Are diffusion coefficients (M^+, etc) similar between powdered glass and monoliths for the same reaction progress?
    - Which kind of diffusion process is controlling the long-term dissolution rate? Is the process the same at different temperatures?
    - Is there competition between water diffusion and secondary phase formation?

2 Work package 2: Selection of experimental data

2.1 Major parameters to consider

Two types of parameter must be taken into account. The first depends only on the glass considered: the glass chemical composition, the radioactivity and the reactive surface area. The second depends on the environment: the pH, the solution chemical composition and redox potential, the glass-surface-area-to-solution-volume ratio, the solution flow rate, the nature and reactivity of the materials near the glass (metal canister corrosion products, clay engineered barrier), the pressure, the temperature.

a) Effect of the glass composition

This is a very important parameter. All basic mechanisms depend on the glass composition. The selection of glass accounts for the following considerations:

- Silica is the main element responsible for the diminishing rate.
- The relative concentrations of boron and the alkalis significantly affect the pH. This is one of the main environmental parameters that must be taken into account.
- Elements liable to form secondary phases such as magnesium or phosphorus favour high residual rates or subsequent resumption of alteration.
- Cross-linking elements such as zirconium or the rare earth elements have a favourable effect on the glass alteration kinetics.
- The role of aluminium depends on its concentration in the glass. In small quantities, it accentuates the rate drop. In excessive amounts, however, it results in renewed alteration due to zeolite precipitation.
- Calcium appears to enhance the protectiveness of the gel.

Glass SON68 (the R7T7 reference glass) can be considered as the reference glass in this project. It has been studied most extensively until today. The compositions of the glasses studied within GLAMOR are listed in Annex III.

b) Effect of radioactivity

Radioactivity can affect the glass alteration kinetics, but the effect is always small. Recently it was shown that highly radioactive R7T7 glass (10^9 to 10^{10} $Bq.g^{-1}$ of βγ emitters) display similar forward and residual alteration rates as the inactive reference glass [71]. But it was found that radiolysis can delay the slowdown in the alteration rate by modifying the protective properties of the gel or more probably by diminishing the pH of the leachate. As a result, a larger quantity of glass (by a factor of 3 to 5 at low S/V ratios for R7T7 glass) is altered during this time, because the glass will dissolve longer at the forward dissolution rate. This effect is appreciable only for $\beta\gamma$ radiation, and would thus be a potential problem only if the glass is exposed to water during the period of $\beta\gamma$ emission, i.e. during the first 300 years of the package lifetime.

Considering that the conditions under which this effect was observed are largely unrelated to repository conditions, we feel this parameter can be disregarded, at least initially.

c) Effect of surface area

This parameter concerns the surface area of the glass package. This is an important parameter for performance calculations in the repository, because then the normalized release rates are multiplied by the available surface area. Is irrelevant for this study however insofar as we are testing the applicability of models using laboratory data. In any event, the glass sample surface area is taken into account below, notably through the S/V parameter.

d) Effect of pH

The pH is an essential factor because H^+ and OH^- species directly affect the equilibrium and steady state concentrations of various solution species (e.g. silica) in solution, and these are

related with the mechanisms of hydrolysis and recondensation of elements from the glass. The initial rate, the rate drop, the residual rate and any resumption of alteration all depend on the pH.

In order to discuss the ability of the models to account for the effect this parameter we selected several tests over a pH range extending from 2.5 to 11.5.

e) Effect of the solution chemical composition

Many chemical species in the repository solutions are liable to alter the glass package, by affecting for instance the mechanisms of hydrolysis and recondensation of the glass constituting elements. Enhancing or inhibiting effects are possible.

Given the objective of this contract and the nature of the models tested, we suggest concentrating initially on the behaviour of silica. Silica is the main - and in most cases the only - kinetically limiting element taken into account in the models. The mechanisms of silica feedback on the glass dissolution kinetics are currently at the heart of the debate.

We also added experiments in which phosphate ions were present, as they significantly modify the gel properties.

f) Effect of the redox potential

The solution redox potential has no significant influence on the glass matrix alteration kinetics [72]. Insofar as the models considered do not describe the specific behaviour of radionuclides, this parameter can be disregarded in the study.

g) Effect of S/V

S/V is an important parameter during the diminishing rate phase of glass alteration. Generally, the higher S/V, the faster the glass element concentrations rise in solution and the sooner the glass alteration rate diminishes. The increasing concentrations of glass elements in solution are considered to diminish the reaction affinity and/or to favour the development of a protective gel layer.

The experiments considered here cover a very wide range of S/V values (between 100 and 200 000 m^{-1}).

h) Effect of the flow rate

Experimentally, a flowing solution is known to delay the formation of a protective gel and/or to diminish the chemical affinity. The higher the flow rate, the slower the rate drop. As this parameter significantly affects the alteration rate, we selected several dynamic experiments.

Currently there is a preference to use flow tests to determine parameters such as the forward dissolution rate used in the glass dissolution models. We refer to the single-pass flow-through experiment (SPFT) [73, 74]. By providing a continuous flow of fresh influent solution, the build-up of reaction products is prevented, and the bulk solution composition is maintained throughout the experiment, thus providing a direct measure of the dissolution rate.

i) Effect of environmental materials

The presence of environmental materials in contact with the glass can significantly modify the glass alteration kinetics. Many processes particular to these systems may be involved. Strong coupling is generally observed between chemical reactions and the transport of reactive species. The effects therefore depend on the chemical nature of the materials and their transport properties. For example, the nature of the mineral phases in clays or metallic corrosion products causes them to bind glass constituent elements such as silicon. Boom clay and FoCa 7 clay are both known to consume silica from the glass. Siliceous additives can avoid these undesirable effects, saturate the medium and form a protective gel.

We selected several experiments in which environmental materials were present.

j) Effect of pressure

The pressure does not directly modify the glass alteration kinetics, although it can indirectly affect the transport properties of the reactive species.

We decided not to take this parameter into account.

k) Effect of temperature

The reaction kinetics depends on the temperature. The activation energies involved depend on the type of reaction considered (diffusion, surface reaction). In the case of R7T7 glass, although the kinetics (initial rate, rate drop and residual rate) depend on the temperature, it is acknowledged that the predominant mechanisms are the same between 50 and 150°C. Moreover, considering the high-level waste glass disposal concepts proposed around the world, the range between 50 and 90 °C appears to correspond to realistic alteration temperatures.

For the initial selection, we considered tests conducted at temperatures between 50 and 150°C.

l) Summary

Table V summarises the parameters liable to affect nuclear glass alteration mechanisms as well as those for which the effect can be discussed on the basis of the experiments selected for this work.

Table V. Summary of main parameter effects on the principal phases of nuclear glass alteration. The "+" sign means that the parameter has an effect on this kinetic step, and the degree of the effect is indicated by the number of "+" signs. An empty space means the effect is nonexistent or negligible, and a question mark indicates that the possible effect is unknown. The last column in the table indicates whether the experiments considered in this work take this parameter into account

Parameter	Initial rate	Rate drop	Residual rate	Resumption of alteration	Considered in this study
Glass composition	+++	+++	+++	+++	Yes
Radioactivity		+	?	?	No
Package surface area					No
pH	+++	+++	+++	+++	Yes
Solution composition	+	+	++	++	Partially
Eh					No
S/V ratio		+++	+	+	Yes
Flow rate		+++			Yes
Environmental materials		+++	?	?	Yes
Pressure					No
Temperature	+++	++	++	+	Yes

2.2 List of experiments

For the initial selection we have considered 50 experiments conducted by the CEA, SCK and Subatech. Table VI shows the main characteristics of the experiments considered.

Table VI: List of the experiments selected for consideration in GLAMOR

Experiment	Glass	pH	Solution composition	S/V (m^{-1})	Flow rate (ml/day)	Environment material	T (°C)	Duration (days)
A1	SON68	free	HPW[(1)]	200,000	0	-	90	1,219
A2	SON68	free	HPW	5,000	0	-	90	594
A3	SON68	7	KOH	5,000	0	-	90	594
A4	SON68	8	KOH	5,000	0	-	90	594
A5	SON68	9.5	KOH	5,000	0	-	90	594
A6	SON68	10	KOH	5,000	0	-	90	594
A7	SON68	10.5	KOH	5,000	0	-	90	594
A8	SON68	11	KOH	5,000	0	-	90	594
A9	SON68	11.5	KOH	5,000	0	-	90	240
A10	SON68	8	KOH	150	144	-	90	23
A11	SON68	8	60 ppm Si	150	144	-	90	23
A12	SON68	8	120 ppm Si	150	144	-	90	23
A13	SON68	9	KOH	1,500	0	-	90	192
A14	SON68	9	100 ppm P	1,500	0	-	90	192
A15	SON68	free	HPW	5,000	0	-	90	604
A16	SON68[(2)]	9	KOH	5,000	0	-	90	61
A17	SON68	free	HPW	50	0	-	90	364
A18	SON68	free	HPW	50	0	-	150	364
A19	SON68	free	Volvic	78	0.3	Granite	90	6,328
A20	SON68	free	Clay water	607	0.4	Boom clay	90	4,404
A21	AVM6	free	HPW	5,500	0	-	50	1,092
A22	AVM10	free	HPW	5,500	0	-	50	1,092
B1	CJ1	free	HPW	8,000	0	-	90	1,533
B2	CJ3	free	HPW	8,000	0	-	90	1,824
B3	CJ6	free	HPW	8,000	0	-	90	1,864
B4	CJ9	free	HPW	8,000	0	-	90	1,374
FZK1	GPWAK1	2.6	buffer	1,000	0	-	50	79
FZK2	GPWAK1	3	buffer	1,000	0	-	50	79
FZK3	GPWAK1	3.5	buffer	1,000	0	-	50	79
FZK4	GPWAK1	4	buffer	1,000	0	-	50	79
FZK5	GPWAK1	4.5	buffer	1,000	0	-	50	79
FZK6	GPWAK1	5.1	buffer	1,000	0	-	50	84
FZK7	GPWAK1	6.1	buffer	1,000	0	-	50	84
FZK8	GPWAK1	7.1	buffer	1,000	0	-	50	84
FZK9	GPWAK1	8.1	buffer	1,000	0	-	50	84
FZK10	GPWAK1	9.1	buffer	1,000	0	-	50	84
FZK11	GPWAK1	10.1	buffer	1,000	0	-	50	86
E1	SON68	pH 5	Sat. leach. [(3)]	4,000	14.4	-	50	50
E2	SON68	pH 5	Sat. leach.	12,000	14.4	-	50	50
E3	SON68	pH 5	Sat. leach.	50	14.4	-	50	50
E4	SON68	pH 7	Sat. leach.	4,000	14.4	-	50	32
E5	SON68	pH 7	Sat. leach.	12,000	14.4	-	50	32
E6	SON68	pH 7	Sat. leach.	50	14.4	-	50	32
E7	SON68	pH 9.8	Sat. leach.	4,000	14.4	-	50	55
SCKgl31/42	SON68	free	Clay water	100	0	-	90	710
SCKgl46/57	SON68	free	Clay water	2,500	0	-	90	710
SCKgl151/162	SON68	free	Clay water	100	0	Boom clay	90	704
SCKgl166/177	SON68	free	Clay water	2,500	0	Boom clay	90	704
SCKgl264/275	SON68	free	Clay water	0	0	Boom clay	90	714
SCKbox7/63	SM527	free	Clay water	100	0	-	90	971

(1) High-purity water
(2) Pre-altered glass specimen in experiment A15
(3) Saturated leachate: 60 ppm Si, 380 ppm B, > 1 000 ppm Na

2.3 Data presentation and management

The experimental data are grouped in Excel files. A separate file is created for each experimental category. Each file includes a general worksheet called "Experiments" listing all the input data (reference, type of glass, experimental conditions, etc.) as well as a series of worksheets containing the analysis results (at least the dissolved element concentrations and normalized elemental mass losses).

The files are managed by the CEA, which is responsible for updating them and sending them to the other contractors (and for sending the final version to the American partners). All exchanges will be by e-mail.

Each file is named as follows: GLAMOR-WP2-**AAA**a-v**l** where AAA represents the first three letters of the organization supplying the data (e.g. SCK, SUB, CEA), **a** the data series considered and **l** the file version number.

2.4 Input data

The following data sheets show the input data for the selected experiments. They contain comprehensive data concerning the glass compositions. The sheets are attached as Annex II.

3 Work package 3: Description of the models used in GLAMOR

The models intended for use in GLAMOR are conceptual models, by which we mean a simple, robust and reasonably conservative model that focuses on the essential mechanisms controlling the long-term behaviour of the glass package under the alteration conditions specified by the user. Two models were selected to represent the major lines of thought on long-term glass dissolution: the models r(t) [35] and GM2001/2003 [36].

The r(t) model and GM2001/2003 address the following processes: build-up of a gel layer which is potentially protective, description of protective gel properties by transport limitations of dissolved silica, accumulation of dissolved silica in bulk solution, retention of silica in the gel and incongruent release of soluble glass constituents and the use of a limiting solution concentration of dissolved silica at the glass surface at which glass corrosion ceases. The GM model does not account for geochemical constraints such as the pH dependency of affinity-controlled reactions or of solubility-controlled secondary phase formation and it also does not account for the effects of pH evolution during the proceeding reaction. Diffusion coefficients, rate constants, surface layer porosities and solubility constants are considered to be constant. The model treats glass dissolution as a one-dimensional phenomenon. A constant final rate term can be added to both models if necessary, but this was not done in their original form (which is discussed in this Section). The model GM2001/2003 addresses the following additional process: water diffusion/ion exchange. The formal similarity of the two models shall not mask the quite different interpretation of each input parameter. However, the GM2001/2003 model can operate as well in a mode of the hypotheses of the r(t) model, thus allowing direct model verification (verification = assessment whether there are no major coding errors, the question to be answered is: does the code behave in a way it is intended to behave).

However, no model (and no theory) is ever complete and it is always a simplification of the real world. There does not yet exist an overall modelling tool combining the different processes in an overall view. Instead both codes are overlapping and cover different degrees of integrations of the various processes. There are more detailed molecular level codes (based on Monte Carlo approaches etc.). These models increase our understanding of the principal glass corrosion mechanism but these models are not yet sufficiently developed to describe long-term glass corrosion in an operational manner.

In both models, different reaction rates and empirical rate laws (time exponents) are interpreted as resulting from of the various reaction steps in the overall reaction scheme, as shown below for the two models graphically in terms of resistors representing rates and a capacitor representing solubility. In parallel reactions the fastest rate (lowest resistance) determines the overall rate whereas in sequential reactions the slowest rate (highest resistance) is rate determining.

Description of the r(t) model

The r(t) model is shown schematically in Figure 18. The principal parameters to describe glass corrosion in the frame of the r(t) model are the initial rate r_o, the diffusion coefficient Dg for dissolved silica transport across the gel layer, the fraction of dissolved silica retained in the gel and a reference silica concentration at the gel/glass interface at which glass/gel transformation(and glass corrosion) ceases. All these parameters are functions of the environmental conditions (pH …) and on the S/V ratio. The new idea of the r(t) model is that the concentration C_g (or C*) at the glass gel interface is a dynamic function of the glass/gel system which may represent a thermodynamic equilibrium, but which is not possible to determine it a priori because it evolves continuously.

The reaction scheme is as follows: Initial surface reaction and Si diffusion in the gel are sequential reactions, indicating that the slowest process is dominating the overall reaction behavior. Initially there is no gel. Hence, diffusion is fast (only governed by an immobile water boundary layer at the surface) and the initial rate is dominant. Nevertheless, saturation of the bulk solution is an intrinsic property of the mathematical structure of the r(t) model. If the bulk solution is at the critical concentration C*, there is no transport gradient anymore and the concentration at the glass/gel interface also becomes C*. Diffusion in the gel and saturation in

bulk solution are also sequential processes. If transport across the gel is very slow, saturation in the bulk solution may never be reached. Si transport in the gel and approach of the critical silica concentration C* are parallel reactions. If C* is very high, even a slow diffusion of dissolved silica might not limit the release of soluble elements such as B from the glass. Retention of silica in the gel is also a parallel process to these reactions, implying that stronger retention of silica will retard the approach of C* at the gel/glass interface.

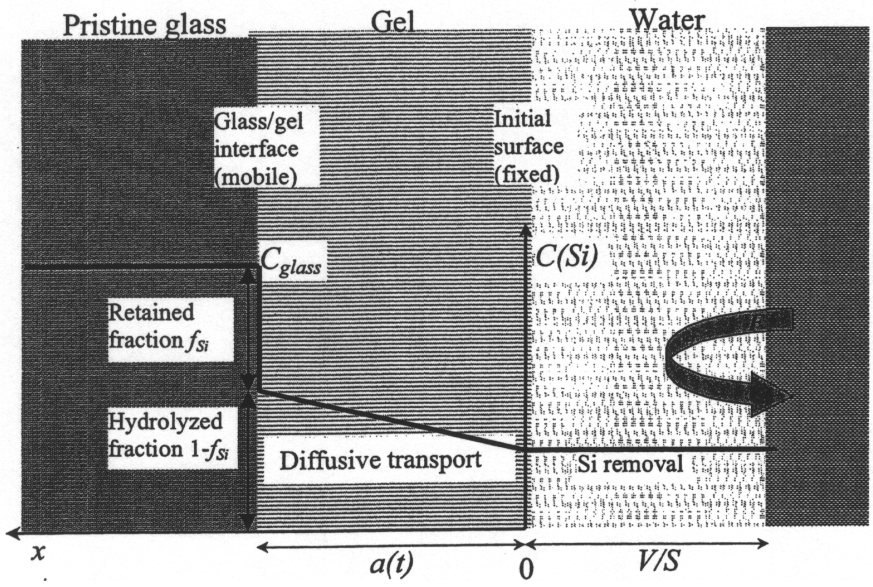

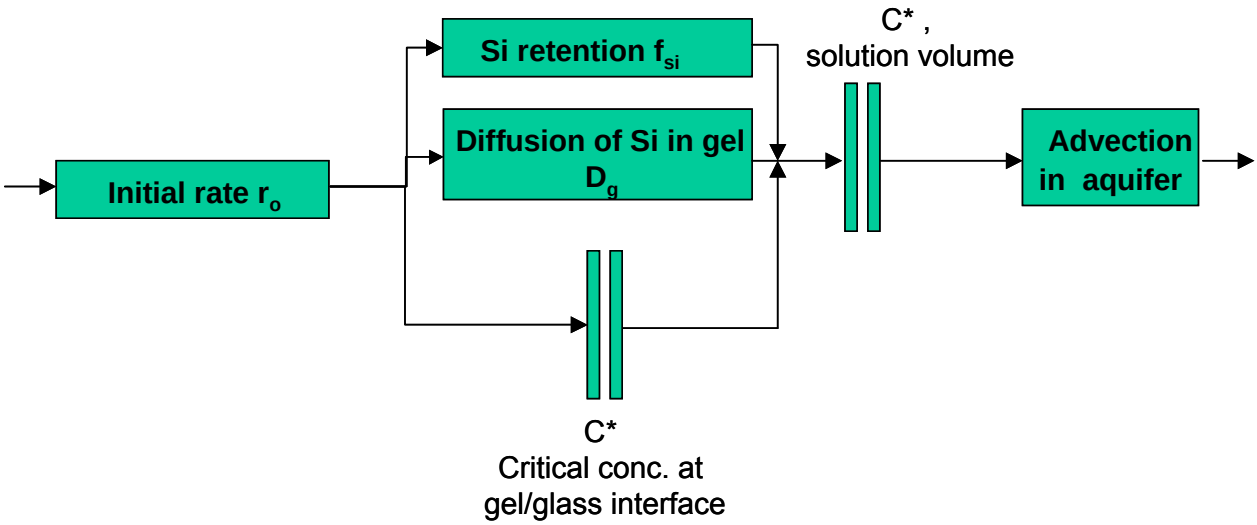

Figure 18: r(t) model: Scheme of interrelationship of rate controls in the dissolution process of glass, expressed in terms of resistors (for rates) and capacitors (for saturation)

Description of the GM2001/GM2003 model

The principal parameters of r(t) are used (sometimes with different symbols) also in GM2001/2003. However, none of the parameters is considered to be a function of S/V. The new idea in the GM2001 model is the consideration of a diffusion layer, whose formation is governed by water diffusion and ion exchange. This diffusion layer is considered to be a part of the glass phase; it is not a secondary reaction product. A graphical representation of the model is given in Figure 19.

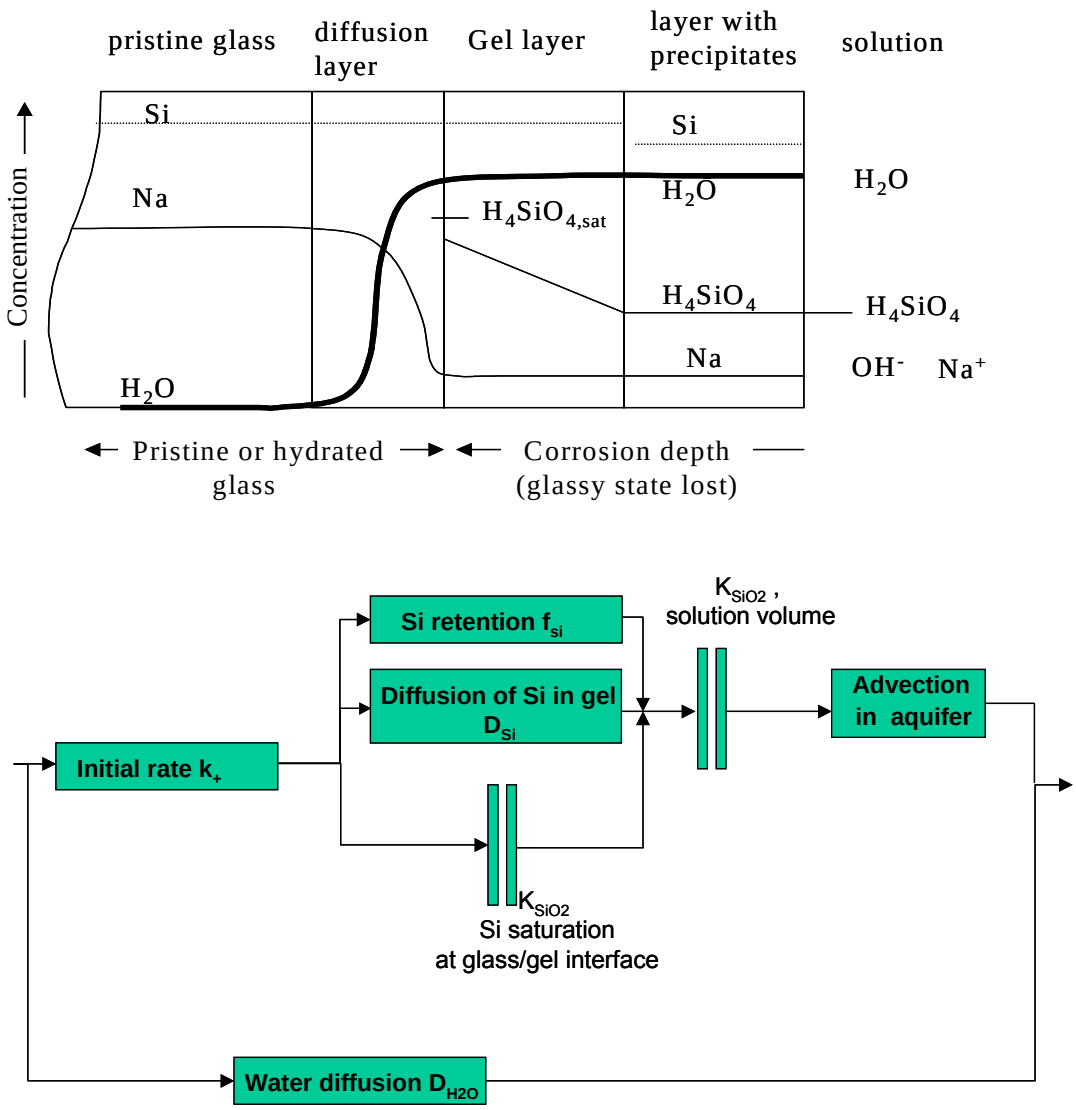

Figure 19: GM2001 model: Scheme of interrelationship of rate controls in the dissolution process of glass, expressed in terms of resistors (for rates) and capacitors (for saturation)

The GM2001 model has principally the same reaction scheme as the r(t) model. Additionally water diffusion is considered. Glass hydration and Alkali/H^+ ion exchange on the one hand and initial glass network dissolution on the other are parallel reactions [37-40]. The model is consistent with the observation that the initial surface modification in the glass/water reaction is diffusion controlled glass hydration accompanied by alkali/H^+ ion exchange. Matrix dissolution is considered in the model to occur as a parallel reaction implying that the rate of water diffusion/ion exchange is initially faster and decreases with the square root of time until it becomes equal to the rate of matrix dissolution. Under these steady state conditions the rate becomes constant with time and a stationary water/alkali diffusion profile of constant depth is established at the corroding glass surface.

A similar steady state with constant rates and diffusion profiles would also result from surface transformation in the absence of surface dissolution. If sufficient network bonds are hydrolyzed, a transformed layer [41] (gel) is formed, often with a clear phase boundary to the glassy phase. The transformed surface layers are porous [42], containing molecular water [43-44] and allowing for high ionic mobility [45] as well as high water mobility. Thus, water transport in this gel layer cannot be rate limiting. The rate limiting diffusion step is in a thin diffusion layer at the interface between the pristine glass and the gel layer. Mathematically, in the context of the GM2001 model, the in-situ transformation of the surface layer is equivalent to a matrix dissolution process,

if a large quantity of the silica content of the dissolved glass is retained in the surface gel. The matrix dissolution front then is the interface between the water/alkali diffusion profile and the transformed layer.

Table VII summarises the fitting parameters considered in both models. A more detailed discussion of the r(t) and GM models (*) is given in Annex I.

Table VII. Different parameters used in both models used in the GLAMOR project

Parameter considered	*r(t) model*	*GM2001 model* [1]
Environmental parameters	Renewal rate of solution S/V (surface to volume) T (temperature) Partial pressure of CO_2 solution pH	Renewal rate of solution S/V (surface to volume) T (temperature)
Fitting parameters	α (Si retention factor in the gel: the fraction of silica retained in the gel is 1 - $e^{(-\alpha C)}$ with C the silica concentration in solution)	α (Si retention factor in the gel: the fraction of silica retained in the gel is 1 - $\exp^{(-\alpha C)}$ with C the silica concentration in solution) – sometimes the additional notation 1 – exp (-f_x *C/C**) is used instead of 1 - exp(-αC)) [2] or f_{ret}(Si retention factor in the gel: a constant fraction f_{ret} of silica is retained in the gel)
	D_g (effective Si diffusion coefficient for the gel)	D_{Si} (T) (pore Si diffusion coefficient for the gel)
	C* (Si concentration at the glass-gel interface)	C* (T, pH) (Si saturation concentration in solution with respect to an alkali depleted surface region, T, pH) D_{H2O} (water diffusion coefficient in the glass and/or diffusion layer) K_d(B), K_d(Li) (apparent sorption constants for boron and lithium, respectively, to account for the slightly higher mobility of water molecules as compared to B and Li in the diffusion layer)
	r_{fin} (residual dissolution rate) [3]	r_{fin}(residual dissolution rate) [3]

[1] The term GM2001 is used to describe the model used as published in [36]. In the project, small changes were made to allow using the model by other partners. The modified code was named GM2003. This includes as well to use similar notations to the r(t) model as far as possible, provided that the underlying physical chemical concept was similar. This was in particular the case for describing silica retention in the surface layer.

[2] The meaning of f_x and f_{ret} is further explained in Annex I.

[3] The residual dissolution rate is not considered in the original version of both models, but will be taken into account in the next chapter.

4 Work package 4: Application of the models

In this chapter, we attempt to reproduce the experimental data by using both models. First, some interpretation of the datasets is given. Next, the application of both models is discussed. This includes: how the optimal parameters for both models are obtained, some specific problems of each model and a numerical comparison between both models. Third, the optimal parameter values for some experiments are presented. *Note:* For most examples presented here we only show and discuss data and calculations for Si (determining the glass dissolution behaviour) and B (one of the main mobile glass constituents).

4.1 Interpretation of the data-sets

This section summarises how the laboratories having generated the respective datasets did interpret the experimental data, before interpreting them by modelling.

Datasets A1and A17 (tests at 90 °C, DW, with different S/V) were amongst the main data-sets discussed within GLAMOR – see 4.3.1. Long-term static glass dissolution tests are currently interpreted essentially in terms of a dissolution rate (based on Boron release) that decreases after the initial dissolution, to transit into a residual dissolution rate [26, 29, 49]. This was argued for tests A1 and A17 as well.

The interpretation of the long-term dissolution (i.e. after the rate decrease stage) as measured in the PSI test in terms of a constant residual rate has been argued on a mathematical basis in [49]. Linear regression was applied to the data from Figures 16-17 (see 2.3.) between 500 (end of initial dissolution and subsequent rate decreasing stages) and 3,650 days, and a long-term dissolution rate was calculated. The leaching data show that changes in slope do occur after 1,500 days of interaction: the mean rate is almost zero between 500 and 1,500 days, increases up to ~3,000 days, and becomes negligible afterwards. However, the apparent changes in slope after 500 days are not significant, since all NL_i values and their uncertainties fall within the regression's uncertainty. Interesting to note is that B and Li do leach nearly congruently, in agreement with current assumptions.

The altered glass surfaces of tests A1, A2, A17 were analysed by TEM [53]. TEM analysis of the altered glass grains after the A1 test revealed an alteration layer consisting of an inner, amorphous layer, on top of which clay-type precipitates were seen. A combination of SEM, TEM, XRD and EDS was used to characterize the dissolved glass surfaces from the PSI test [50]. This enabled to identify an amorphous, porous zone and an external clay zone (constituted of precipitates mainly).

4.2 The application of the r(t) and GM2003 models to experimental data – general

4.2.1 How are the optimal model parameters obtained?

In general optimal parameter values are found by minimising a χ^2 function representing the distance between calculated and experimental data. Nowadays, this optimisation is generally automated: apart from the optimal parameter values, also estimates of the error on each parameter and the correlations between the parameters are provided by a fit program. None of both models (*r(t)* and GM) has a fit routine associated with it. GM provides calculated values (concentrations, normalised mass loss, pH, gel layer thickness) for a large suite of time steps but it does not attempt to provide calculated results for a pre-selected time step to compare directly with an experimental data point (at an additional effort, this value can be obtained by interpolation). As a consequence the calculation of some χ^2 function (which could be minimised by hand) is even more cumbersome. Besides, defining an appropriate χ^2 function is not straightforward since several curves (e.g. boron and silica concentration in solution as a function of time), having different absolute magnitudes, need to be optimised simultaneously. Using the same χ^2 function for fitting concentrations in solution as a function of time would also lead to other optimal parameter values than fitting the corresponding release rates as a function of time.

Due to the lack of an automated fit routine, the optimal parameter values are determined by eyeballing, without the use of any χ^2 function. Evidently, this makes the search for optimal parameter values not only very cumbersome, but also the results not very reliable since both models have many fit parameters of which some are strongly correlated (see 4.5). So, in order to be able to compare the parameter values of several experiments, a similar fit strategy must be used for fitting several experiments: which parameters should be kept constant and which should be varied? Evidently, the parameter values obtained in this way need to have the expected order of magnitude, which is by preference measured in an independent way. Such estimates are given in Annex I.

4.2.2 Strategy followed in r(t)

The calculated data were stepwise fitted manually on the experimental data for both the boron and silicon concentrations. The three main parameters (α, D_g and C^*) were determined as follows. The concentration levels were fitted by modifying C^*, then the shape of the rate decrease with D_g, and finally the difference between B and Si with α.

Note: This approach can sometimes lead to numerical instability and a drift in the calculated boron concentrations because of a sudden pH increase. This occurs in case of "dissolution excursions" (see also 5.3.1, under test A1), when dissolution is resuming at a rate much larger than the residual dissolution rate. Another set of C^*, D_g and α parameters must then be used to reproduce the experimental data. In extreme cases, fitting is impossible with the pH calculation module, and the pH must be assigned the experimental value. The origin of the drift and instability is unknown.

When the $r(t)$ model parameters were fitted over a very extensive experimental dataset [35], D_g and C^* could not be assigned a single value describing all experimental data. Different α, D_g and C^* values were even required within the same experiment, see Figures 20 and 21. The parameter values chosen in Figure 20 are suited to reproduce the longer term data, not those during the dissolution rate decrease during the first 50 days. Figure 21 clearly shows that the values of the parameters may be different for the short and the longer term data. The main difference is the use of a residual rate to fit the longer-term data.

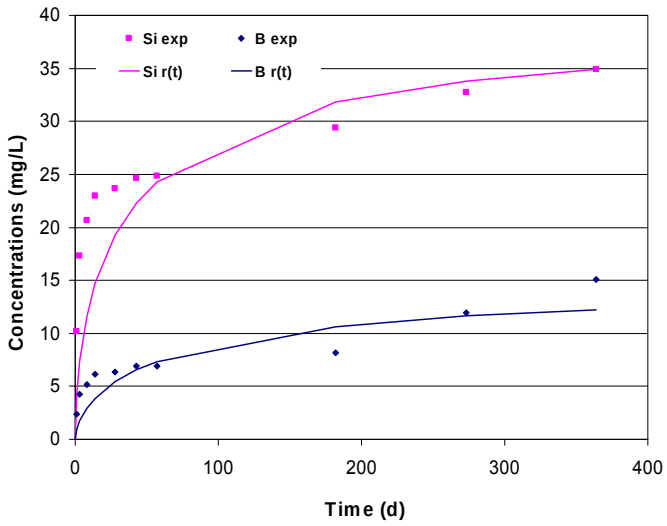

Figure 20: Fit obtained with $r(t)$ model parameters α, *Dg* and *C* (experiment A17:90°C, 50 m^{-1})*

The strategy of r(t) is to describe the rate decrease using the α, *Dg* and C^* parameters. A constant residual rate is added to allow adjustment to concentration increases once silica saturation solution has been reached. The use of a constant residual rate acknowledges that the r_{fin} parameter, together with the preceding three parameters, provides a better description of the experimental data. At the present the underlying mechanism is not yet completely established. In *r(t)* a constant residual rate parameter affects not only the boron concentrations but also the silicon concentrations. This is illustrated in Figure 21, where a satisfactory fit is obtained using the four parameters α, D_g, C^* and r_{fin}. Adding the fourth parameter reduces the variation range of the

α, D_g and C^* parameters and more closely accounts for the experimental data, as shown in Figure 21-B.

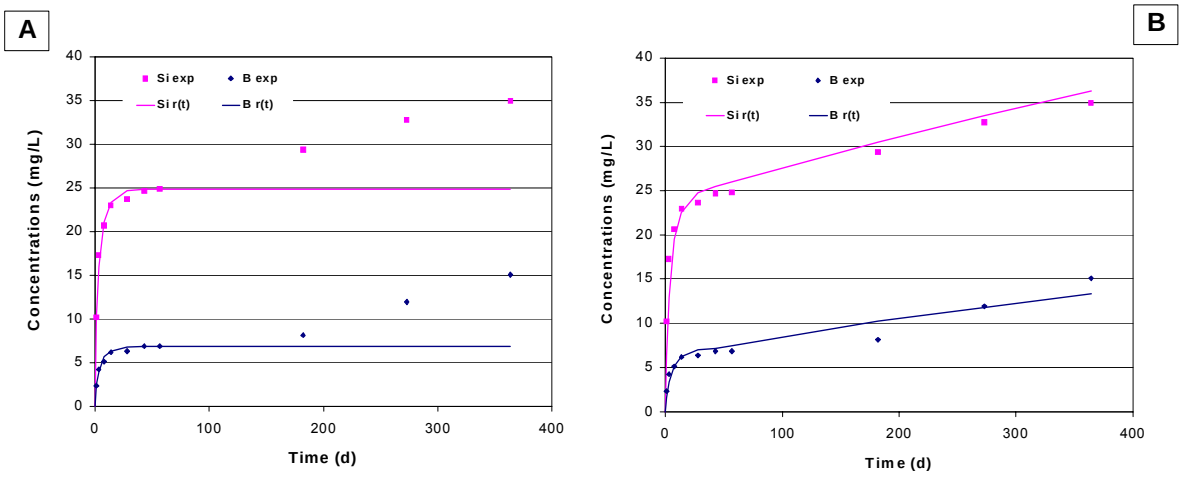

Figure 21: Application of the $r(t)$ model to experiment A17 (90°C, 50 m^{-1}) using only the α, D_g and C^* parameters to describe the rate decrease (A), then with a constant residual rate parameter (B)

In Annex I, 4.1.2 it is already mentioned that *r(t)* has a geochemical part and that the *r(t)* code can be executed in two ways: at fixed pH, or at calculated pH. In the second case, pH (and the ionic strength of the solution) is calculated by considering the concentration in solution of the major glass elements, the temperature and the partial pressure of CO_2. These last two parameters have a constant value, chosen by the user of the model. In the present chapter, a partial CO_2 pressure of 10^{-20} atm. is considered for each experiment. This value corresponds to an atmosphere free of CO_2.

The initial dissolution rate of R7T7 glass is calculated as a function of the pH and temperature according to the relation determined from the experimental data [54]) (see Annex I, 4.1.2). For GPWAK, AVM and CJ glasses, the initial dissolution rate is assigned an experimentally determined value: respectively 0.27 $g \cdot m^{-2} \cdot d^{-1}$ [36], 0.2 $g \cdot m^{-2} \cdot d^{-1}$ [55] and 5 $g \cdot m^{-2} \cdot d^{-1}$ [15]. Table VIII summarizes the parameters required by the $r(t)$ model. The parameter values are assigned via a single interface (Lixiver 1.9), except for the C^* parameter, which is set in the geochemical database (filename: corps.in).

Table VIII: Summary of r(t) parameters

	r(t) parameters
Experimental parameters	Temperature (°C)
	Surface to volume ratio (S/V, cm^{-1})
	Flow Rate of the solution
	Fixed pH or calculated pH
	Initial elementary concentrations in solution (in mg/L)
	Partial pressure of CO_2 (colog (PCO_2) atm.)
Fixed parameters	Initial rate r_o, fixed or pH-dependent (in g m^{-2} day^{-1})
Fitting parameters	D_g, effective Si-diffusion coefficient in the gel layer
	C^*, concentration at which the glass to gel transformation ceases (in mol H_4SiO_4)
	α, a coefficient of the silica retention function (ppm^{-1})
	r_{fin}, constant residual rate (in g m^{-2} day^{-1})

4.2.3 Strategy followed in the GM2003 model

4.2.3.1 Versions, reproducibility, step and system sizes

Contrary to the *r(t)* model, several versions of GM exist. The version discussed in the GLAMOR project is called GM2003. GM is written in mathcad and the source code is available to every user. This is very interesting from a scientific point of view, but it is a dangerous from the view of reproducibility of results: a line in the code is easily changed (intentionally or not), resulting in a new 'version' without the user being aware of it. GM solves numerically the (linearised) silica diffusion equation and the water diffusion equation. Silica diffusion is solved completely automatically (see Annex I, 4.2.2.2). For water diffusion, the user needs to define a time step Δx , a time step Δt and the length L of system (the water diffusion profile needs to be thinner than the system size) in a way that the final result becomes independent on these three 'iteration parameters'. Apart from this, choosing an appropriate step (so that the stability criteria are fulfilled and the calculation time remains reasonably low) is not always simple. In most results mentioned later in this chapter, tmax (= the number of time steps) is fixed at 2,000; Jmax (= the number of position steps) at 100 and Δx, Δt and the system size have variable values. It is recommended that the code for GM is adapted in such a way, that the iteration variables Δx, Δt and the system size L are given values by the program (as already happens for the silica diffusion part) instead of by the user.

4.2.3.2 Fit strategy of GM2003

This model uses a larger number of parameters than the $r(t)$ model. The values of some of these parameters were fixed for the purposes of this exercise. For the experiments with R7T7 glass at 50° and 90°C, the initial dissolution rates were set at 0.04 $g \cdot m^{-2} \cdot d^{-1}$ and 0.7 $g \cdot m^{-2} \cdot d^{-1}$ respectively. These values were measured experimentally at pH 8. For GPWAK, AVM and CJ glass, the initial dissolution rate was assigned the same way as with the *r(t)* model (see 4.2.2.) The initial dissolution rate has little effect on the model calculation. In every simulation the gel porosity was set at 0.2, which approximates the concentration of mobile glass constituents. The silicon diffusion coefficient in the gel is often given a value of about 5.0×10^{-14} $m^2 \cdot s^{-1}$, as determined using the GLASSOL geochemical calculation code to fit experimental data under dynamic conditions at a low S/V ratio (0.1 cm^{-1}) at 90°C: 1.0×10^{-14} $m^2 \cdot s^{-1} < D_{si} < 1.0 \times 10^{-13}$ $m^2 \cdot s^{-1}$ [56].

The other parameters are adjusted for each new experiment to obtain the best possible fit. The K_{SiO2} parameter is assigned first to set the silicon saturation concentration level. The B and alkali concentrations are fitted using three parameters: α, the water diffusion coefficient D_{H2O}, and K_{di} . One K_{di} value is defined for each species (B, Li, Na, Mo) and for each experiment. $K_{d,i}$ values have no inherently optimum value; instead, the best combination of $K_{d,ii}$ and D_{H20} is determined for each experiment. Note, $K_{d,i}$ and D_{H20} are clearly correlated to each other (see 4.5) The α parameter is used mainly to describe boron and alkali behaviour during the decreasing rate phase, but even in case of rapid slow down of dissolution rates (experiments at high S/V) it has a strong effect on the initial difference between the normalised boron and alkali release on the one hand and silica release on the other hand.

For the residual rate phase two fitting strategies are possible. First, a residual rate of similar value as that used in the *r(t)* model can be used. The transition between initial and a fixed final rate is then governed by a combination of affinity effects and water diffusion, using the parameters D_{H20} and K_{di}. The residual alteration rate (affecting only the boron and alkali concentrations, not silicon) was set at a value of $7\ 10^{-5}$ $g.m^{-2}.d^{-1}$. This strategy has been used by Subatech. Residual rates can alternatively be described by using only a combination of D_{H2O} and K_{di} with an infinitely small final rate. This strategy was used by CEA when adopting the GM2003 model. SCK•CEN considered the residual rate as one of the fitting parameters, and followed a strategy depending on the dataset.

Table IX summarises the parameters required by the GM2003 model.

Table IX: Summary of GM2003 parameters

	GM2003 parameters
Experimental parameters	Temperature (in K)
	Surface to volume ratio S/V (m^{-1})
	Volumetric Flow rate (kg day^{-1})
	m_{CCB}([1]), molality of Si in advective fluid (mole kg^{-1})
Fixed parameters	The forward rate constant k^+ (in kg m^2 day^{-1}), fixed at a given temperature
	Porosity of the gel, ϕ = 0.2
	D_{si}, (pore) Si-diffusion coefficient in the gel (m^2 s^{-1})
Iteration parameter	tfin= the last experimental step (in days)
	Tmax (number of time increments), typical value: 2 000
	Δx, space increment (in meter)
	Jmax, number of equal space steps, typical value: 100
	System size, L
Fit parameters	K_{SiO2} *or* C^*_{tot}, total silica saturation constant at the gel/hydrated glass interface (in ppm) ([2])
	α *or fx* or f_{ret} parameter, retention factor of silica in the gel
	D_{H20} diffusion coefficient of water in the glass (m^2 s^{-1})
	Kd,i (I = B, Li, Na, …) sorption constant for boron, lithium, …in the hydrated glass (in kg m^{-3}), a fixed value is used if only one element out of B, Li and Na is to be fitted.
	r_{fin} constant residual rate (kg m^2 d^{-1})

([1]) The term CCB refers to “constant concentration boundary” hence it is the Si concentration in the water not affected by the glass. So it is an input parameter which may be lower or higher than C*.
([2]) C^*_{tot} is the total of the concentration of $Si(OH)_4$ and a number of anionic silica species ($SiO(OH)_3^-$, $SiO_2(OH)_2^{2-}$, $Si_4O_6(OH)_6^{2-}$) that become more predominant when pH increases above 9.

4.2.3.3 Numerical comparison of r(t) and GM2003 models

For an arbitrarily chosen data set (A17: R7T7 glass, 90 °C, S/V = 50 m^{-1}, free pH) it is verified that with similar parameter values, both models produce the same calculated concentrations as a function of time or not. Due to the similar mathematics of both models this is possible. Roughly spoken, GM is *r(t)* with water diffusion and without a geochemical part. So, to verify numerical agreement between both models one needs to keep pH constant (or take an experiment where pH varies only a little), and have very few boron and alkali diffusion through the diffusion layer. This can be obtained by a very high value of the water diffusion coefficient in the diffusion layer, and/or a low value of the corresponding K_d.

Practically, the experimental data have been first 'fitted' with *r(t),* in a mode of variable pH. Next, nearly the same parameter values have been used with GM. The experimental data as well as the predictions by *r(t)* and GM are shown in Figure 22. The fit parameter values used in both models are given in Table X.

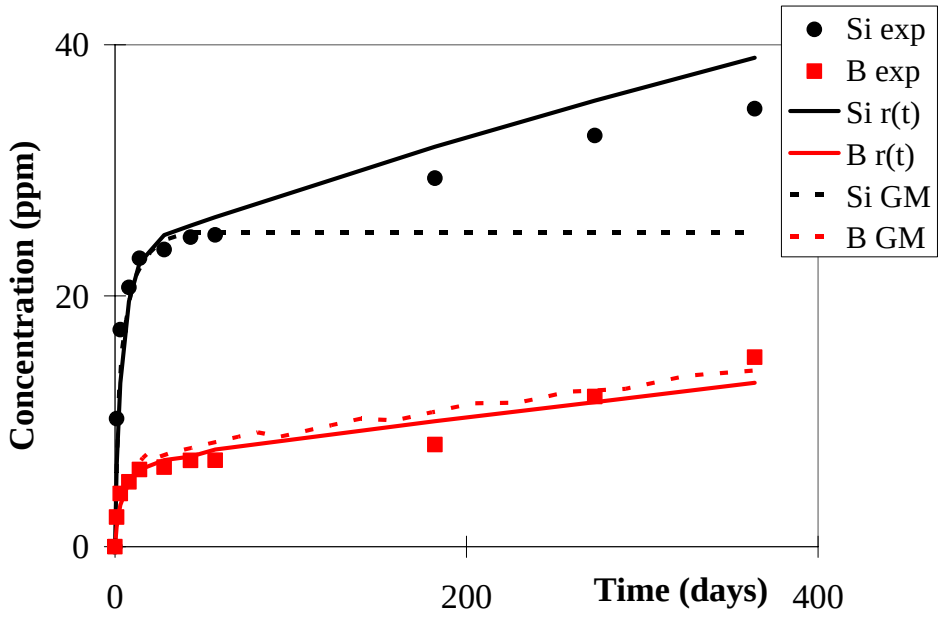

Figure 22. Predicted and experimental data for the A17 experiment (90 °C, 50 m^{-1})

Table X: Summary of r(t) and GM2003 parameters used for the A17 experiment

	FIG 20 r(t) (CEA)	FIG 21a r(t) (CEA)	FIG 21b r(t) (CEA)	FIG 22 (r(t) SCK•CEN	FIG 22 GM 2003 SCK•CEN
Forward rate ($g\ m^{-2}\ day^{-1}$)	r_o= *f*(pH) ~1.5	r_o= *f*(pH) ~0.95	r_o= *f*(pH) ~2.5	r_o= *f*(pH) ~1.33	0.7
Silica saturation ($mg.L^{-1}$)	C^*=35 , C^*_{tot}~66	C^*=16 , C^*_{tot}~25	C^*= 16 , C^*_{tot}~30	C^*= 16 , C^*_{tot}~25	K_{SiO2} =25.05
Si-diffusion coefficient ($m^2\ s^{-1}$)	D_g=7.0 10^{-16}	D_g=5.0 10^{-14}	D_g=5.0 10^{-14}	D_g=5.0 10^{-14}	D_{si}=2.6 10^{-13}
Si-retention α (ppm^{-1})	0.031	0.023	0.023	0.022	0.022
Final rate, r_{fin} ($g\ m^{-2}\ day^{-1}$)	1.0 10^{-8}	1.0 10^{-8}	6.5 10^{-3}	8 10^{-3}	8.0 10^{-3}
Water diffusion coefficient D_{H2O} ($m^2\ s^{-1}$)	Not considered	Not considered	Not considered	Not considered	5.0 10^{-21}
Kd_B ($kg\ m^{-3}$)	Not considered	Not considered	Not considered	Not considered	100

Before commenting Figure 22, all parameter values from Table X are discussed:

- initial rate: since the experiment is performed at 90°C, the model *r(t)* automatically takes equation (30) (see Annex I, 4.1.2) for the forward rate. The calculated pH by r(t) is approximately constant during the duration of the experiment (8.38 after one day up to 8.9 after one year). Substituting such a value in equation (30) leads to a forward rate of 1.33 g m^{-2} day^{-1}. This value is higher than the value used in GM2003 (0.7 g m^{-2} day^{-1}). However, this parameter has very little influence on the calculated data, and a value of 0.7 or 1.33 $g{\cdot}m^{-2}{\cdot}d^{-1}$ does not modify the overall fit.
- the 'saturation concentration': since C* refers to the concentration in solution of only $Si(OH)_4$, it needs to be converted to the total silica concentration in solution (for which the notation C^*_{tot} is used), to allow comparison with K_{SiO2} (see Annex I, 4.3.1). Without final rate, the final silica concentration in both models is the same ($C^*_{tot} \approx K_{SiO2} \approx 25$ ppm). Since *r(t)* allows a final silica rate, silica concentrations in *r(t)* can rise above 'saturation'. This is probably due to pH and/or ionic strength evolution in the experiments.
- the silica diffusion coefficient: it is discussed in Annex I, chapter 4 that (i) D_g is an effective diffusion coefficient and D_{Si} a pore diffusion coefficient, and (ii) that their values are related to each other by expression (59) (from Annex I, 4.3.1). A fixed gel porosity of 0.2 in all calculations leads to D_{Si} = 5 D_g. Since this relation is fulfilled in Table X, both models use the same silica diffusion coefficient there.

- both models use the same expression and the same value for silica retention.
- The water diffusion coefficient in the diffusion layer as well as the K_d for boron are not relevant for *r(t).* For GM, values have been chosen so that the contribution of boron leached from the gel to the boron concentration in solution is negligible.

Figure 22 shows a good numerical agreement between the predictions by both models for the concentration of boron in solution, and for the concentration of silica in solution up to saturation. When silica 'saturation' occurs, the predictions for the silica concentration diverge since *r(t)* considers a non-zero final silica dissolution rate, while in GM there is a zero silica dissolution rate.

4.3 Predicted data versus experimental data

Because of the strong correlations between the parameters of *r(t)* and GM2003, the obtained optimal parameter values with both models can only be compared by taking the 'fit' strategy into account. The general fit strategies of both models have already been explained in 4.2. Here, a discussion is presented of the quality of the fits and it is tried to relate the obtained parameter values to the (fixed) experimental parameters (S/V, pH, temperature, composition of the alteration solution, and renewal rate of the solution) for the glasses R7T7 and AVM. Only a few experiments are considered here. The complete set of the fits and the parameter values is presented in Annex IV

4.3.1 S/V variation

We consider an experiment at a low S/V (see 4.2.2), followed by an experiment at a high S/V. More specific, this concerns experiments A17 and A1 with R7T7 glass powder under static conditions at 90°C with an unconstrained pH, at S/V values of 50 and 200,000 m^{-1}, respectively. The calculated data are compared with the experimental data in Figure 22 for the experiment at low S/V (A17), and in Figure 23 for the experiment at high S/V (A1).

The fitted data of experiment A17 have already been shown in Figures 20-22 (see 4.2.2). Fig. 22 shows the fitted data with nearly identical parameter values for both models (see 4.2.3). As expected, similar data by the models need to similar predicted results (at least if water diffusion is sufficiently low). The residual rate r_{fin} of 8 10^{-3} $g \cdot m^{-2} \cdot d^{-1}$ is relatively high. This rate is quite high compared with the value currently used in this report – 10^{-4} $g.m^{-2}.d^{-1}$ or lower; this is because in the A17 experiment reaction progress achieved is not that high, consequently the conditions for achieving the final rate are not really suitable.

Figures 23 (a-f) and Table XI show the result of applying both models to the experiment at the highest S/V (experiment A1). In this test running for nearly five years, very high reaction progress is achieved. B and Na concentrations increase up to 3,000; resp. 4 000 $mg.L^{-1}$. We used the current way of interpreting the experimental data: saturation of the solution in silica is assumed to occur at the end of the rate drop, followed by a period of residual dissolution – exactly the way it was done in experiment A17. During this residual dissolution a resumption of the dissolution (see B and Si data) is observed after some 300 days duration, however. This is explained as being due to (Li, Na) phyllo-silicate secondary phase formation [58]. For this experiment, *r(t)* is used in a no-variation pH mode (pH is fixed at 9.36). The fits by CEA with both *r(t)* and GM2003 are presented in Fig 23a and Fig 23b, which is a detail of the first year of the experiment. Fig 23c and Fig 23d show the results obtained with GM2003 by Subatech and SCK•CEN, respectively. All parameter values are summarized in Table XI. Most interesting in this Table is the large variety in the parameter values obtained by the three institutes for fitting the data with the GM model. This set of parameter values is discussed in the remainder of this section.

For r(t) the situation is simple: only CEA managed to obtain a more or less decent fit for experiment A1. This fit is obtained at the cost of using a fixed pH in a free pH experiment, which appeared to be the only way to avoid the problem mentioned in the note of 4.2.2). Neglecting water diffusion, the models *r(t)* and GM are largely identical and consequently the same parameter values give the same predictions with both models (see Fig 22). Combining this knowledge with the fact that the predicted silica concentration with GM does not depend on water diffusion, it might seem evident that CEA uses for both models similar values for the silica saturation concentration as well as for the silica diffusion coefficient in the gel. Table XI shows that this is indeed the case for the silica saturation concentration, but the values of the silica diffusion coefficient in the gel differ by about five orders of magnitude (D_{Si} = 5 10^{-14} m^2/s for GM

and D_{Si} = 5 D_g = 5 10^{-19} m^2/s for *r(t)*). This difference can be considered as an indication of the very large uncertainty on the value of the silica diffusion coefficient in the gel.

We discuss the modelling parameters in more detail:

- Silica diffusion coefficient.

By choosing a relatively high value for the silica diffusion coefficient in the gel, as Subatech does in the GM2003 model, the solution becomes saturated with silica very fast and the predicted silica concentration is often substantially higher than the measured silica concentration (see Fig. 23 c). Choosing a smaller value for the silica diffusion coefficient in the gel means that the silica concentration in the solution raises more slowly. By choosing a small value for the silica diffusion coefficient in the gel, SCK•CEN clearly manages to obtain a much better agreement between the prediction with GM and the experimental data than both other institutes (see Fig 23 a-c-d). It is however questionable if such low diffusion coefficients physically make sense (see also Annex I). Similarly problematic is whether with such low diffusion coefficients the assumption of a constant linear concentration gradient in the gel, which both *r(t)* and GM make (see also Annex I), is still valid and that the results produced by the models are correct.

- Silica saturation concentration.

For determining the value of the silica saturation concentration, different strategies were used by CEA on one hand and by Subatech and SCK•CEN on the other hand. CEA chooses the silica saturation concentration at the concentration where the initial fast rise in silica concentration stops. Since the experimentally measured pH remains more or less constant with time in experiment A1, this strategy leads to the problem of how to explain the increase of silica in solution after 'saturation'. Although theoretically impossible, this problem is handled in *r(t)* by introducing a non-zero constant final silica dissolution rate r_{fin}. In GM, a non-zero constant final silica dissolution rate does not exist, and so the predicted behavior by CEA is from the moment of reaching 'silica saturation' on, always much smaller than the observed behaviour. By choosing the value of the silica saturation concentration larger than or close to the last measured silica concentration, Subatech and SCK•CEN do not face this problem.

- Water diffusion coefficient and apparent sorption constant for Boron.

For the boron data, it is less obvious to decide by eyeballing which institute provides the best fit with GM. Since the water diffusion coefficient and the $K_{d,B}$ value are nearly totally correlated (see 4.5 and Annex I) not their individual values, but only their ratio matters. All three institutes obtain similar values (at least the same order of magnitude) for the ratio D_{H2O}/K_{dB} characterizing the boron leaching due to leaching out of the diffusion layer.

- Final dissolution rate.

A constant dissolution rate is clearly observed in Fig. 23d of SCK•CEN and not (yet) in the GM predictions of Subatech or CEA. This is due to the higher r_{fin} and/or the higher D_{H20} used by SCK•CEN. Since for CEA and Subatech at all measurement times, release associated to water diffusion dominates the constant final release of Boron, the exact value of the final rate is not very important (explaining the difference in magnitude between CEA and Subatech). Since in *r(t)*, diffusion in the diffusion layer does not exist, boron leaching can only be described by the final dissolution rate. Since silica saturation is reached fast, according to the (*r(t)* like) interpretation by CEA most (more than ninety percent) of the dissolution of this experiments occurs under 'residual rate conditions' (see Fig. 23a). Note also from Fig. 23a, that although the final (=residual) rate fits the boron release at large times relatively well, this is not so for the corresponding silica release (in *r(t),* only one value exists for the final rate, and this value should describe the release of silica as well as of boron).

- Silica retention factor.

Both Subatech and CEA use a constant silica retention factor f_x, while CEA uses an exponential silica retention function

In Figures 23e-23f we show a calculation with r(t) obtained by optimized curve fitting. The main parameter values resulting from this best fit are listed in Table XI. The best fit heavily relies on D_g to calculate the evolution of the Si and B concentrations with time, although we discuss elsewhere that D_g is subject to very strong uncertainties. The final dissolution rate is not taken into account, although it is one of the most important parameters in the r(t) model.

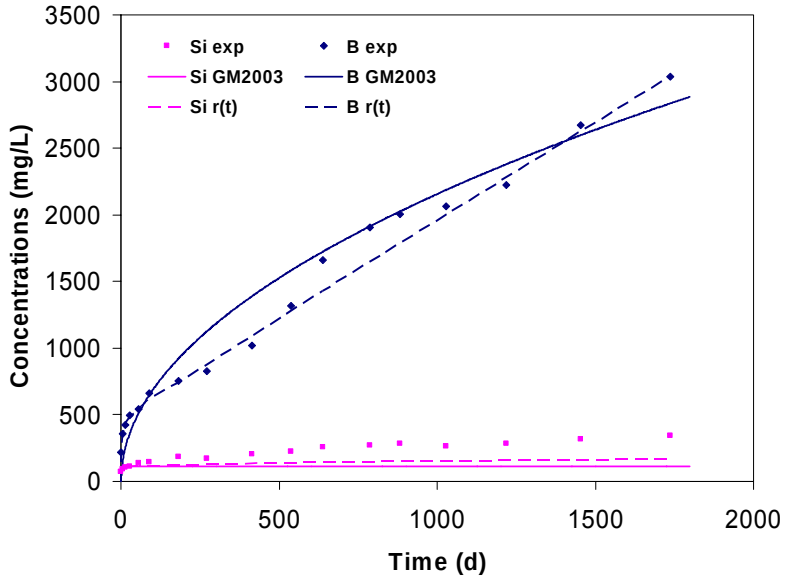

Figure 23a: Experiment A1 modelled with r(t) and GM2003 by CEA

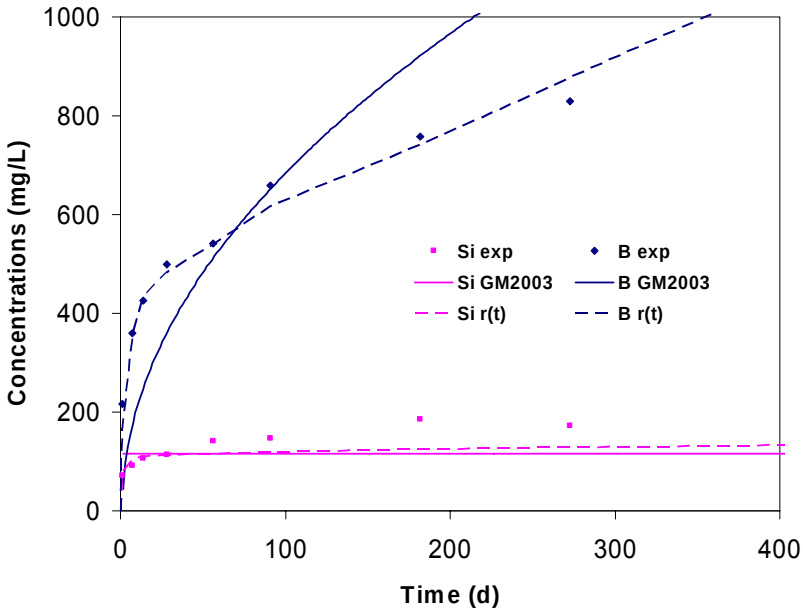

Figure 23b: Same figure as Figure 23a, but focusing on the first year of alteration

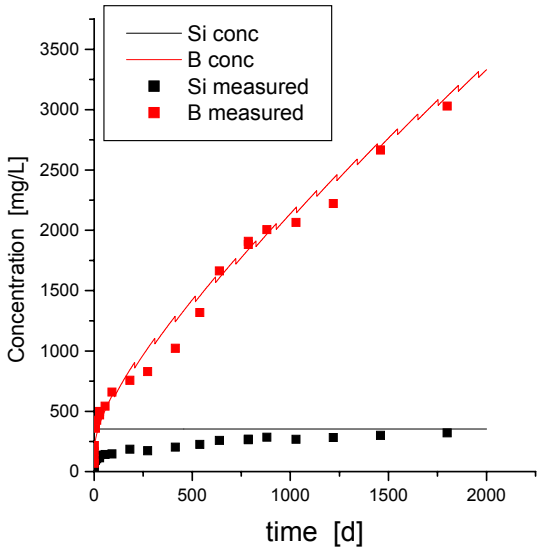

Figure 23c: Experiment A1 modelled with GM2003 by Subatech

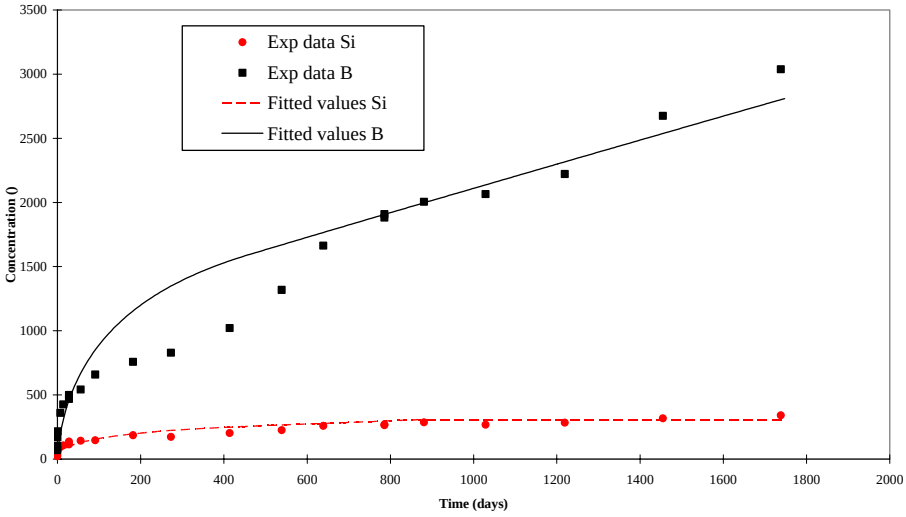

Figure 23d: Experiment A1 modelled with GM2003 by SCK•CEN

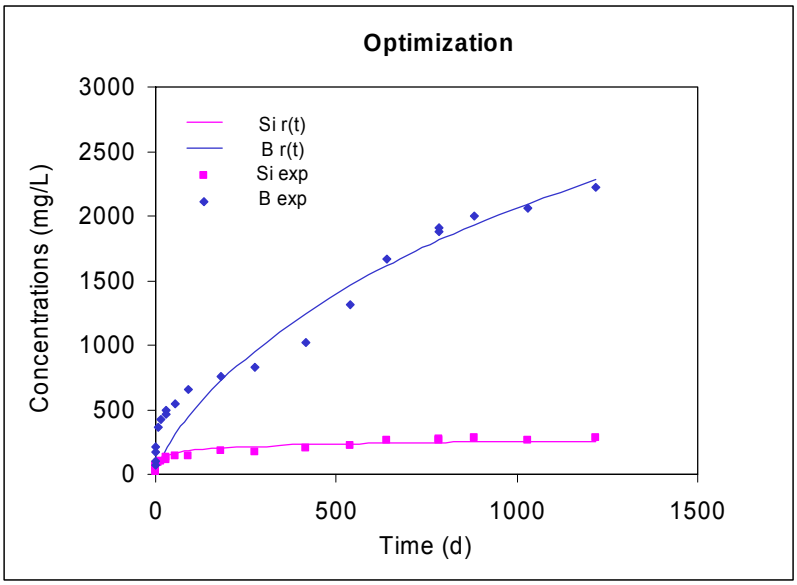

Figure 23e: Optimised curve fitting with the r(t) model for experiment A1 by CEA

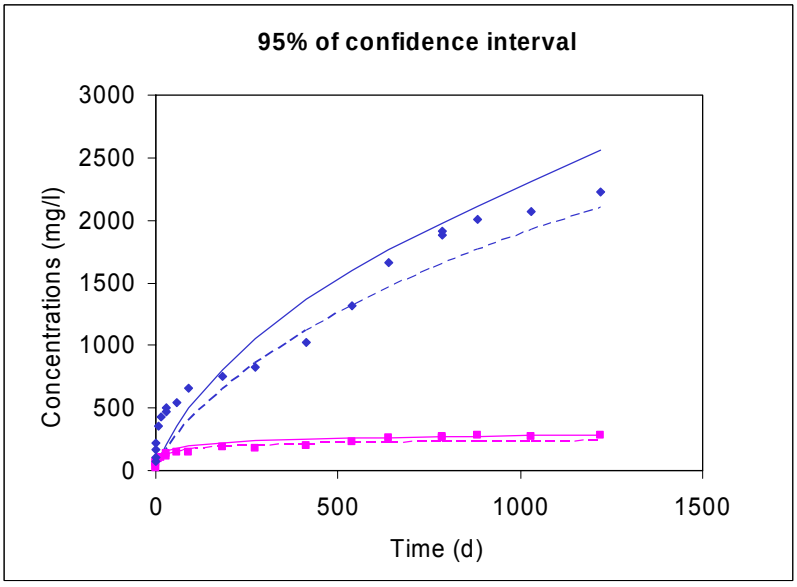

Figure 23f: 95 % confidence interval upon optimized curve fitting with the r(t) model for experiment A1 by CEA

Table XI: Summary of parameters used with r(t) and GM2003 for experiment A1. C^*_{tot} is the total silica concentration in solution at saturation

	r(t) (CEA)	r(t) (CEA) (curve fitting)	GM2003 (CEA)	GM 2003 (Subatech)	GM 2003 (SCK•CEN)
Forward rate ($g.m^{-2}.d^{-1}$)	r_o=f(pH) ~3.2	1.5	0.7	0.7	0.69
Silica saturation concentration ($mg.L^{-1}$)	C^*=32 C^*_{tot}=115	C*=284	K_{SiO2} =115	K_{SiO2}=350	K_{SiO2}= 307
Si-diffusion coefficient ($m^2\ s^{-1}$)	D_g =1.0 10^{-19}	Dg=2.5 10^{-21}	D_{Si}= 5.2 10^{-14}	D_{Si}= 5.2 10^{-14}	D_{Si}= 5.2 10^{-20}
Si-retention α (ppm^{-1})	0.038	0.020	0.004	0.025	fx=0.97
Final rate, r_{fin} ($g\ m^{-2}\ day^{-1}$)	1.5 10^{-4}	0	7.0 10^{-11}	8 10^{-5}	1.0 10^{-4}
Water diffusion coefficient D_{H2O} ($m^2\ s^{-1}$)	Not considered	Not considered	5.0 10^{-23}	2.5 10^{-23}	7 10^{-20}
K_{dB} ($kg\ m^{-3}$)	Not considered	Not considered	70	100	10^{+5}
Ratio D_{H2O}/ K_{dB}	Not considered	Not considered	7 10^{-25}	2 10^{-25}	7 10^{-25}

Discussion

In this section, we covered very diverging S/V conditions – including an extremely large value (200 000 m^{-1} in test A1) that exhibited a complicated dissolution behaviour for elements such as boron. This was done to explore the limits of the applicability of the models. We observe that both models produce a reasonable fit for the rate decreasing stage in both tests (S/V of 50 m^{-1} – test A17 – and 200 000 m^{-1} – test A1). The consideration of a residual dissolution rate beyond the silica saturation stage appears to be necessary to fit the long-term boron release data. It is also advisable that the analysis and interpretation of the experimental data beyond silica saturation in test A1 should be done in more detail, to define the processes dominating the different stages. Geochemical modelling of the element speciation and of secondary phases formed might be one way of doing.

Discussing the influence of S/V on the values of the fit parameters, we limit ourselves to the silica saturation concentration. Due to the large differences in values proposed by the different labs, it does not make sense to try to find out with the current data how the other parameters depend on S/V. In particular, the uncertainly on the silica diffusion coefficient in the gel is very high (several orders of magnitude). Additionally, there is also the (not described by the models) protective effect due to silica condensation (see Annex I, 3.3.), which is observed to be more important at high S/V than at low S/V.

The difficulty to define C* in the very high S/V test (200,000 m^{-1}, test A1) as introduced above is another problem. C* is currently defined from the mechanistic interpretation of the experimental data. As mentioned above the higher value (>300 $mg.L^{-1}$) provides a better fit of the model calculation with the data. This interpretation is in conflict with the current interpretation: at silica saturation boron leaching would slow down after the initial dissolution stage - rather suggesting the lower C* value as most acceptable (~115 $mg.L^{-1}$). This latter value is also closer to the theoretical solubility of silica of ~ 100 $mg.L^{-1}$ at pH ~9.4 [57]. This classical interpretation of solubility must be questioned, however. Recent work showed that in this high S/V test the Si_{tot} increase is due to $NaHSiO_3$ complexes [58] (in addition to H_4SiO_4 that controls Si solubility at the early stages of glass dissolution). This evolving C* would in this test be associated with the dissolution resumption (see B data in test A1). The true solubility of poorly soluble minerals even may be reached in various consecutive steps, leaving the question open what the real silica solubility in such high S/V tests would really be [59].

The choice of a value for the silica diffusion coefficient D_{Si} is only very poorly supported by independent experimental data. Dedicated tests to measure D_{Si} in the glass alteration layer [64,50] only provide evidence for D_{Si} in the range 10^{-13} to 5 10^{-14} m^2/s, but in the model predictions discussed here D_{Si} as low as 10^{-21} m^2/s were used.

4.3.2 The pH variation

This section discusses the data predicted with both models for the same experiment performed at different pH – the A3 and A8 experiment (R7T7 glass, 90 °C, fixed pH to 7 and 11, S/V 5 000 m^{-1}). In these experiments, S/V is moderate, resulting in much lower reaction progress values than experiment A1, but higher than in experiment A17. Since an illustration of the differences between the fit results obtained by the three institutes with the same models have already been illustrated in the previous section, only the predictions of one institute with both models is presented here.

The experimental results as well as the predictions with *r(t)* and GM for experiment A3 are presented in Figure 24. The experimental curves show a decrease in dissolution rate within the first 240 days, transiting in a residual dissolution of B. As for the previously discussed experiments, *r(t)* and GM predictions present a fit of moderate quality, in particular for Si.

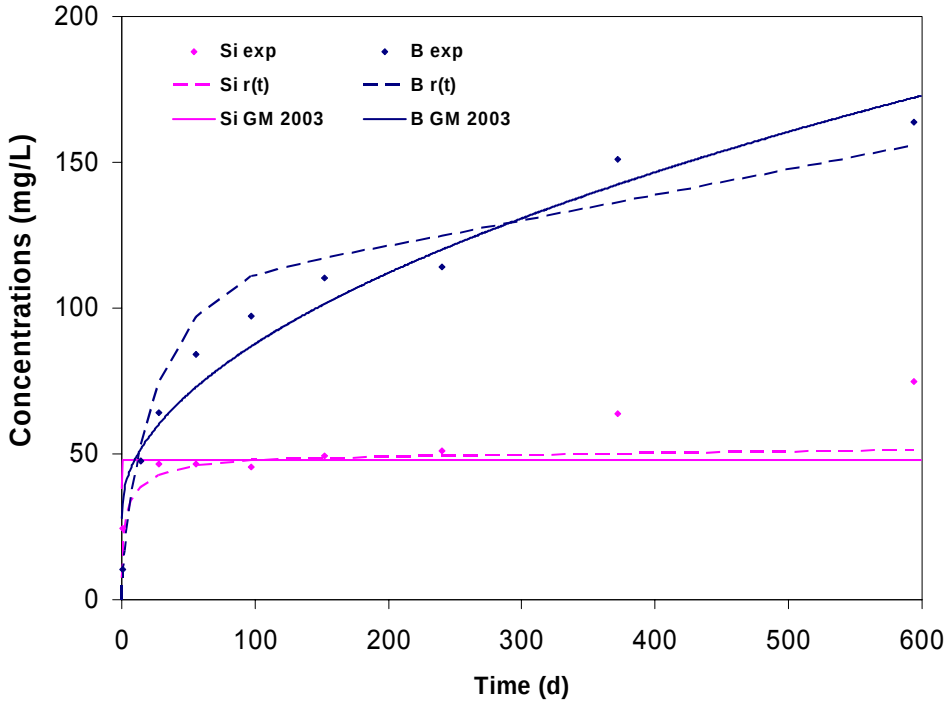

Figure 24: Predicted data with r(t) and GM2003 for experiment A3 (S/V = 5 000 m^{-1}, pH = 7)

For both models, the total Si concentration at saturation is set at 48 $mg.L^{-1}$. With a silicon diffusion coefficient equal to the value used with GM2003 (5×10^{-14} $m^2 \cdot s^{-1}$), silicon saturation is reached in one day. Conversely, with the *r*(*t*) model using a silicon diffusion coefficient of 1.0×10^{-17} $m^2 \cdot s^{-1}$, silica saturation is reached after ~100 days . The delayed saturation in this case assigns greater weight to the gel barrier function (in fact a higher D_{Si} would yield a better fit for the Si data before saturation). However none of the fittings correctly describes the boron behaviour up to saturation. The *r*(*t*) model on the other hand is unable to account for the behaviour of silicon, which appears to reach saturation after only a few weeks. The fit obtained with GM2003 describes the experimental data more satisfactorily than r(t), by monitoring the boron behaviour via water diffusion coupled with the boron distribution coefficient in the hydrated glass, Kd_B (note: with GM diffusion controls the B release up to the last data point. This is also because the r_{fin} chosen is much too small (10^{-11} $g.m^{-2}.d^{-1}$), whereas Subatech currently assumes an r_{fin} of 8 10^{-5} $g.m^{-2}.d^{-1}$but the modelling calculation is not that sensitive to the r_{fin} value). Similar to experiment A17 (see Fig. 22), there seems to be a final silica dissolution rate in experiment A3 (see Fig. 24). Note also that contrary to experiment A17, experiment A3 is executed at fixed pH. The parameter values used for this experiment are listed in Table XII.

Table XII: Summary of r(t) and GM2003 parameters used for experiment A3

	r(t)	**GM2003**
Forward rate ($g.m^{-2}.d^{-1}$)	r_o = f(pH) ~0.4	0.7
Silica saturation ($mg.L^{-1}$)	C^* = 48, C^*_{tot}=48.6	K_{SiO2} =48
Si-diffusion coefficient ($m^2\ s^{-1}$)	D_g=1.0 10^{-17}	D_{Si}=5.2 10^{-14}
Si-retention α (ppm^{-1})	0.078	0.02
Final rate, r_{fin} ($g\ m^{-2}\ day^{-1}$)	3.0 10^{-4}	1.0 10^{-11} (*)
Water diffusion coefficient D_{H2O} ($m^2\ s^{-1}$)	Not considered.	3.0 10^{-22}
K_{dB} ($kg\ m^{-3}$)	Not considered	30
Ratio D_{H20}/K_{dB}	Not considered	10^{-23}

(*) A value of 10^{-11} g m^{-2} $day^{-1}$was used, although GM currently uses a value for r_{fin} of 8 10^{-5} g m^{-2} day^{-1}. In this test the modelling however is insensitive to the value of r_{fin}.

Two alteration regimes can be identified in experiment A8 (see Figure 25): the boron and silica concentrations stabilize after 200 days at about 120 and 350 mg·L^{-1}, then increase significantly afterwards. This has been explained elsewhere as due to zeolite secondary phase formation [60]. However, because of the small amount of data, as well as to the fluctuations of these data, it is hard to draw conclusions in this region. We therefore decided not to take the data of 400 days duration and longer into consideration.

The parameter values are presented in Table XIII. The *r(t)* prediction fits rather well the rate decreasing stage, suggesting that a silicon diffusion coefficient of 1.0 × 10^{-17} m^2·s^{-1} better reproduces the experimental data than the corresponding value used with GM.

Table XIII: Summary of r(t) and GM2003 parameters used for experiment A8

	r(t)	**GM2003**
Forward rate ($g.m^{-2}.d^{-1}$)	r_o = f(pH) ~14	0.7
Silica saturation ($mg.L^{-1}$)	C^* = 3.1, C^*_{tot}=350	K_{SiO2} =340
Si-diffusion coefficient ($m^2\ s^{-1}$	D_g=1.7 10^{-17}	D_{Si}=5.2 10^{-14}
Si-retention α (ppm^{-1})	0.003	0.002
Final rate, r_{fin} ($g\ m^{-2}\ day^{-1}$)	1.0 10^{-8}	1.0 10^{-11} (*)
Water diffusion coefficient D_{H2O} ($m^2\ s^{-1}$)	Not considered.	2.0 10^{-23}
K_{dB} ($kg\ m^{-3}$)	Not considered	70
Ratio D_{H20}/K_{dB}	Not considered	2.8 10^{-25}

(*) A value of 10^{-11} g m^{-2} $day^{-1}$was used, although GM currently uses a value for r_{fin} of 8 10^{-5} g m^{-2} day^{-1}. In this test the modelling however is insensitive to the value of r_{fin}.

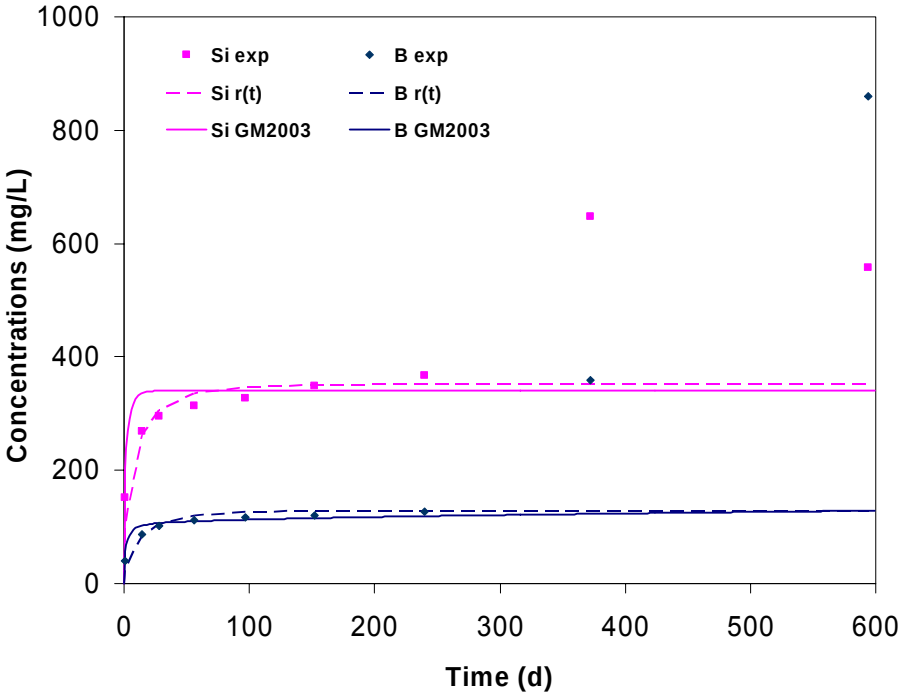

Figure 25: Predicted data with r(t) and GM2003 for experiment A8 (S/V = 5 000 m^{-1}, pH =11)

Discussion

In agreement with the increase in solubility of silica with pH above 7, C^*_{tot} increased from 50 (test at pH 7) to 350 $mg.L^{-1}$ (test at pH 11).

The value of the silica diffusion coefficient was kept more or less constant in both tests, but differed about three orders of magnitude (since for *r(t)* is $D_{Si} = 5\ D_g \approx 8\ 10^{-14}\ m^2.s^{-1}$) between both models. This difference is due to the fit strategy used for each model.

For the *r(t)* model, the value of the α parameter decreased from 0.078 at pH 7 to 0.003 ppm^{-1} at pH 11. The same trend is observed with GM.

Given the large uncertainty on the data above 'saturation' (according to *r(t)* terminology) as well as the influence of 'fit strategy', it is not useful to compare final rate values (which were given such a small value that they were not relevant) or diffusion layer parameter values (for GM only) between both tests.

4.3.3 The saturation of the solution

This section presents the data predicted using the GM2003 model for experiments with silicon-saturated solution. The *r*(*t*) model cannot simulate these experiments because it does not consider the water diffusion process after silica has reached saturation and glass dissolution is considered to proceed from the first day on at its final rate value.

The experiments were performed at 90°C under flowing conditions (14.4 $mL{\cdot}d^{-1}$) with R7T7 glass at pH 8.9 and 7.5, with solutions containing Si (120 $mg{\cdot}L^{-1}$), B (380 $mg{\cdot}L^{-1}$) and Na (> 1 000 $mg{\cdot}L^{-1}$) with an S/V ratio of 26 or 12 000 m^{-1}. The specific objective of these experiments was to estimate the water diffusion coefficients [61]. They involved monitoring the Li concentrations in solution; the data predicted by GM2003 therefore assume a lithium distribution coefficient, Kd_{Li}. The predictions obtained using GM2003 are compared with the experimental data in Figures 26 and 27. The parameter values used are listed in Table XIV.

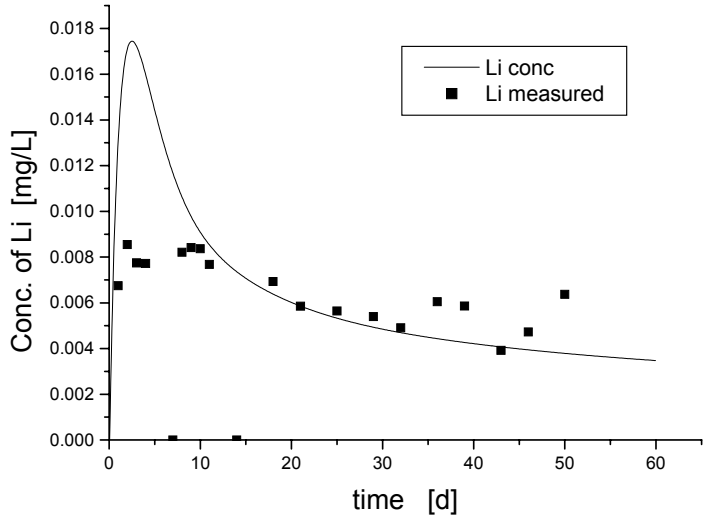

Figure 26: Data predicted with GM2003 data for experiment E16 (pH 8.9, S/V 26 m^{-1}, flow rate 14.4 ml/d, 90 °C)

The leaching curve of Li shows a continuous decrease with time after an initial peak. Predicted data were in agreement with experimental data, by using a water diffusion coefficient as only fit parameter and a Kd_{Li} of 10 kg m^{-3}. The reason for this choice of Kd_{Li} was to provide consistency with values used for the fit of Li data from static tests. In fact, except for the experiment A1, the Kd for Li was fixed at a value of 10 for all other static or dynamic experiments.

Table XIV: Summary of GM2003 parameters used for experiment E16 and E9 performed in silica saturated solutions at 90 °C and a water flow rate of 14 ml/day and a solution volume of 35 mL

	E16	**E9**
pH	8.9	7.1
S/V m^{-1}	26	12,000
Forward rate ($g.m^{-2}.d^{-1}$)*	*0.7*	0.7
Silica saturation ($mg.L^{-1}$)	70	70
Si-diffusion coefficient (m^2 s^{-1})*	$D_g = 5.2\ 10^{-14}$	$D_{Si} = 5.2\ 10^{-14}$
Si-retention α (ppm^{-1})*	insensitive	insensitive
Final rate, r_{fin} ($g\ m^{-2}\ day^{-1}$)*	$1.0\ 10^{-5}$	$1.0\ 10^{-5}$
Water diffusion coefficient D_{H2O} (m^2 s^{-1})	$2.0\ 10^{-21}$	$8.0\ 10^{-22}$
K_{dLi} ($kg\ m^{-3}$)	10	10
Ratio D_{H20}/K_{dLi}	$2\ 10^{-22}$	$8\ 10^{-23}$

* Fit not sensitive to choices of parameter values.

For all experiments (also those not shown, e.g. documented in [61]) the model predicts a fast initial rise of Li concentration and a subsequent slower decrease with time. This is indeed observed experimentally. The fit is relatively good for the experiment E9 but worse for E16. The worse fit at lower S/V and higher pH may be associated to larger analytical uncertainties at the very low Li concentrations measured (< 0.01 mg/L). It is interesting to note that the parameters used for the experiment E9 are rather similar to those used for a static test at similar high S/V at a similar pH (experiment A3).

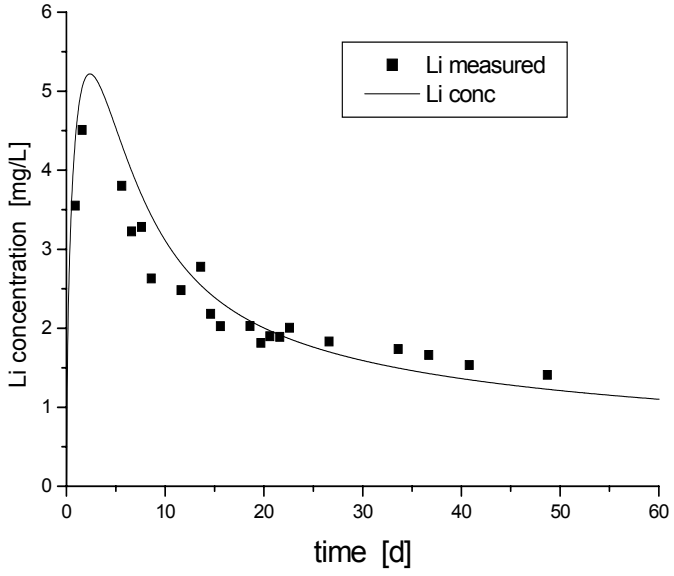

Figure 27: Data predicted with GM2003 for experiment E9 (pH 7.5; S/V 12,000 m^{-1}, flow rate 14.4 ml/d, 90°C)

4.3.4 Effect of the glass composition

This concluding section discusses experiment A21 on AVM6 glass, which has higher Al, Na and Mg concentrations than R7T7 glass, but lower B and Si concentrations. The experiment was carried out at 50°C, with an S/V ratio of 5,500 m^{-1}. The calculated and experimental data are compared in Figure 28.

In this test, running for nearly three years, very high reaction progress is achieved and B and Na concentration increase till 1,700; resp. 2,200 mg/L. The experimental curve shows a continuous increase of B concentration in solution which slows down after 700 days. Si concentration decreases with time, after 100 days.

Figure 28 shows that modelling of the experimental data is not really satisfactory. The best fit is obtained by Subatech, by using an appropriate combination of r_{fin} and D_{H2O} values – see Table XV. The Boron (and Lithium) data are relatively well reproduced. The main difference compared between the data on glass AVM6 and glass SON68 (see 4.2.3.3 and 4.3.1) is that in Figure 28 the Si saturation is achieved must faster. The subsequent lowering of the Si concentration in solution was not observed for glass SON68 either. The reason is probably the precipitation of secondary phases, containing Na, Li, Si and Al. There is no detailed documentation of this phenomenon in this test, but we may refer to [70], where similar secondary (analcime) phases were measured and predicted for high Al_2O_3 glass in similar conditions. They were associated to a resumption of the glass dissolution in silica saturated solution. However, none of the models is able to take into account this secondary phase formation, if it is affecting the dissolution in a non-linear way (we acknowledged before the occurrence of secondary phase formation as part of the final dissolution rate). Such secondary phase formation was also observed on SON68 glass enriched in Mg, yielding a Mg-rich secondary phase.

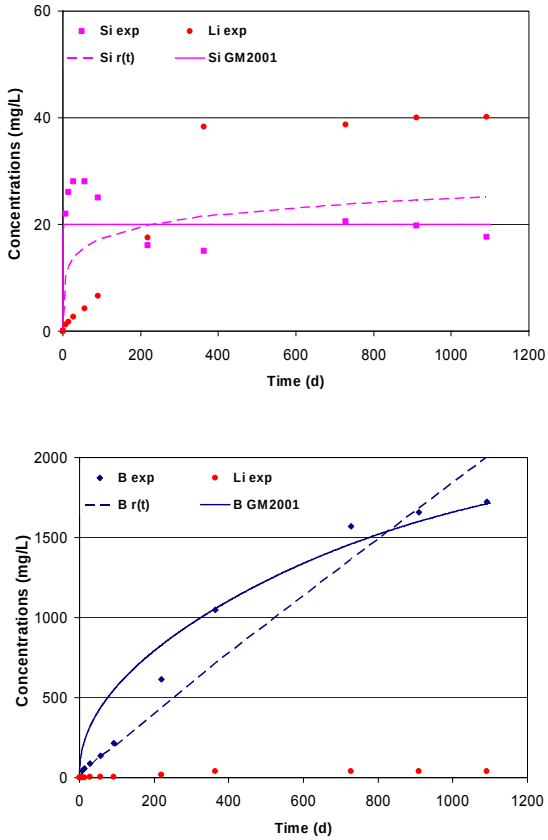

Figure 28a: Predicted data with r(t) and GM2003 for A21 experiment (AVM6 glass) – CEA. The upper figure shows the Si data, the lower figure the B data

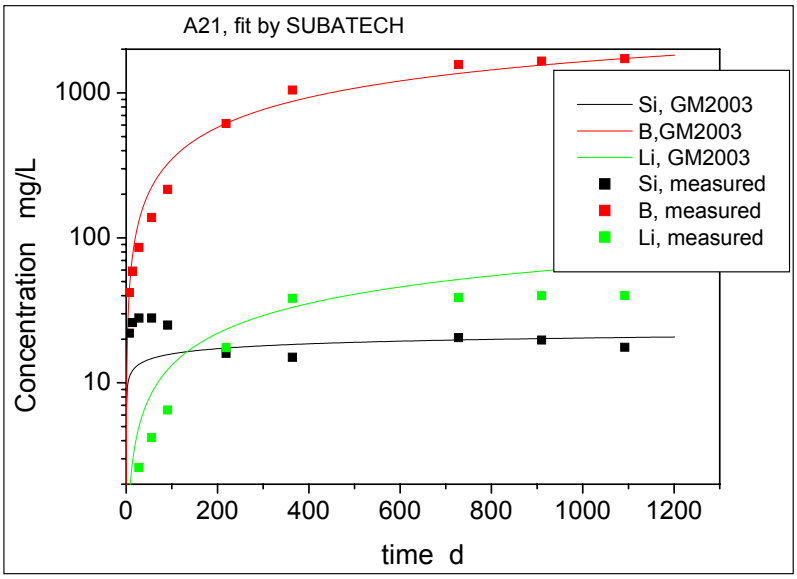

Figure 28b: Predicted data with GM2003 for A21 experiment (AVM6 glass) – Subatech

Table XV: Parameter values used for modelling test A21 (50 °C, S/V = 5 500 m^{-1}, free pH)

	r(t) – CEA	GM2003 – CEA	GM2003 – Subatech
r_o **(g.m^{-2}.day^{-1})**	0.02	0.04	0.04
C*/ K_{SiO2} (ppm)	10	20	20
Dg/D_{Si} (m².s^{-1})	5.0 10^{-14}	2.8 10^{-13}	2.8 10^{-13}
α(ppm^{-1})	0.003	0.15	0.419
r_{fin}**(g.m^{-2}.day^{-1})**	5.0 10^{-3}	1.0 10^{-11}	7.0 10^{-8}
D_{H20} (m².s^{-1})	n.c.	3.0 10^{-20}	3.0 10^{-24}
Kd_B (kg.m$^{-3)}$	n.c.	100	100

4.4 Conclusion from this comparison between model and experiment

In the previous sections we showed that both models can produce a reasonable fit in the rate decreasing stage for various types of tests. The modelling was done by using a number of known or proposed parameter values, and according to the fit strategy of the two models. However, beyond the saturation stage (which is currently assumed to occur following the rate decreasing stage) the agreement between the modelling predictions and experimental data is worse. Main deviations are (i) with the GM2003 model Si concentration after saturation does not increase any longer, contrary to observations, and (ii) in case of (different kinds of) resumptions of dissolution beyond the saturation stage. As discussed in 4.3.1, the first deviation may be overcome by properly choosing C* (this might be applicable to 4.3.2 as well). This also leaves the question open if additional changes in C* will occur at still higher reaction progress than we achieved so far in the experiments. The second deviation (resumption of dissolution) could be handled by the models if this resumption would not prevent that a single final dissolution rate can be proposed beyond silica saturation. This is hardly possible in the very high S/V test A1 (see Figure 23 in 4.3.1).

We must mention that even if predictions with both models might be satisfactory for a specific experimental dataset, the agreement between both models for longer-term data might become worse. This is because of the different mathematics. With r(t) a constant residual rate is used, whereas in GM the long-term prediction will depend on the relative weight of water diffusion and the residual rate. But at the end the residual rate will control the long-term when using the GM model, as well.

Improvement of the modelling predictions will depend on improved or enhanced knowledge or understanding of the modelling parameters:

- During the past years, considerable progress has been achieved on identifying and quantifying r_{fin} and D_{H20}. However, the mechanism controlling r_{fin} needs yet to be identified.
- C* is determined from the experimental plots. However, assuming that silicon will achieve a steady state saturation concentration during glass dissolution can never be completely true in reality, because the whole system glass-water can only be in steady state equilibrium if all constituents are transformed into crystalline form. Practically we observed this problem at high reaction progress (see e.g. test A1 in 4.3.1.), leading to different potential C* values. Additional calculations of the silica speciation may be a way to better argue the choice of C* – see the discussion in 4.3.1.
- D_{Si} is subject to large uncertainties. The value of the Si diffusion coefficient through the reaction layer is very uncertain. The barrier effect of the reaction layer might be due to silica condensation in the reaction layer as well – or a combination of silica condensation and diffusion. We can consider D_{Si} as a parameter that enables to reproduce the rate decrease before silica saturation.
- r_{fin} is considered in both models as a fitting parameter, that should affect the concentrations in solution of B, Si, and other glass constituents. However the affinity term in both *r(t)* and GM2003 models is incompatible with an increase of silica concentration beyond saturation.

Optimised curve fitting as shown in 4.3.1 produces the best fit of the model with the experimental data, but it does not take into account the agreed dissolution processes (in particular the final dissolution rate). This way of curve fitting is not the recommended way to model experiments in a scientific way – which is the way looked for in GLAMOR. Neglecting the residual rate (as resulting from optimal curve fitting) is not an option, for instance.

We haven't made a systematic evaluation of the role of the glass composition within GLAMOR. We focussed on glass SON68, for which a very large database exists. Although different glass compositions might display some differences in dissolution behaviour (see e.g. in 4.3.4, secondary phases result in a decrease of silica in the silica saturated solution), the general scheme of glass dissolution as proposed by CEA (see Chapter 2) is generally valid. The according conclusions from GLAMOR therefore appear to be applicable to other compositions.

In conclusion, there are no clear-cut arguments to reject or to favour one of the two models (r(t) or GM2003. Both models succeed to reproduce the dissolution rate decrease and the residual dissolution in the "silica saturation" stage, by optimizing values of D_{Si}, C*, r_{fin}, D_{H20}, etc. As argued above, the quality of the modelling fits (predictions, simulations) will rather be determined by the qualification of the (key) modelling parameters. This is more important than one could conclude from the modelling examples discussed in the previous sections. Indeed, for instance diffusion controlled kinetics for the final dissolution rate (which yet are not demonstrated) would lead to much longer HLW glass lifetimes than a constant final dissolution rate

4.5 Relationships between the model parameters, after performing the model application

Due to the poor quality of some of the fits, as well as to the lack of automatically calculated correlation coefficients between the model parameters (no automatic fit routines), it is clear that obtaining information about correlations from the fits alone is not evident. Most information is derived from the mathematical discussion of the models (Annex I, Chapter 4): this discussion shows where correlations should lie and the fit results are used to see if the expected correlations occur indeed. Other correlations, based on physical grounds are discussed afterwards.

First, the correlations based on the mathematics of the models are discussed. It is reminded that both models use a different definition of silica diffusion coefficient (a pore diffusion coefficient in GM and an effective diffusion coefficient in *r(t)*) and of 'silica saturation concentration' (referring only to $Si(OH)_4$ in *r(t)* and including also the dissociated silica species in GM), but the conversion formulas are known (see Annex I, 4.3). In both models, the initial (= maximal) silica dissolution rate is measured and thus not considered a fit parameter. The three common fit parameters of both models are the 'silica saturation concentration', the silica retention α (see expression (28) in Annex I, Chapter 4), and the 'silica diffusion coefficient in the gel'. It has been shown theoretically (see expression (54) in Annex I, chapter 4), that the silica diffusion coefficient in the gel is strongly correlated to the 'silica saturation concentration' and silica retention. In particular, it was demonstrated (see Annex I, 4.2.2.1) that high values of the 'silica saturation concentration' correspond to low values of the silica diffusion coefficient in the gel. This behaviour was clearly confirmed while fitting the experiments.

For GM, it is expected (see Annex I, 4.2.1) that the water diffusion coefficient and the $K_{d,i}$ values are strongly correlated. An illustration of this expected behaviour is shown for boron in Figure 29. Since in the GM model, the boron concentration in solution comes partly from the gel layer, and partly from the diffusion layer, an additional correlation is expected between both parts, characterized by the silica retention coefficient α (for the gel part) and the $K_{d,B}$ of boron/ water diffusion coefficient (both for the diffusion layer part). Due to the already mentioned correlation between $K_{d,B}$ and the water diffusion coefficient, this second correlation was not searched for when fitting the experiments. Anyway, for fitting the selected set of dissolution data, GM is clearly over-parameterised and accurate values for the fit parameters can only be obtained by fitting, if some parameters (like in the fit strategy of GM was done with the silica diffusion coefficient in the gel or the forward rate constant) are assigned a constant value. The situation would have been different if a larger set of experimental data would have been used to calibrate/fit the model. If a model is insensitive to a given parameter for a given set of conditions, one may argue that the model is over-parameterised; however, when changing the conditions, this parameter may become significant. In the GM approach for example, the choice of a couple D(H2O) and Kd(Li, B …) is clearly an over-parameterisation if apart of silica concentration only

one other element (e.g. B) needs to be fitted. However, if the release of more elements needs to be fitted and if the NL values of soluble elements like Li, B, Na… were different, the introduction of a second parameter is necessary to account for this different behaviour of mobile elements.

Apart from the just discussed correlations due to the mathematics of the models, there are also physically related correlations. The protective effect (see Annex I, 3.3), caused by the densification of the gel due to silica condensation, is most pronounced at high surface to volume ratios, which corresponds to high pH values [62]. A more dense (condensed) pore structure does not only lead to lower values of the initial silica dissolution rate (as observed experimentally), but also hampers diffusion. This explains the low fitted values of the silica diffusion coefficient in the gel (see [27]) and low values of the water diffusion coefficient (see [36]) measured at high surface to volume ratio and high pH values.

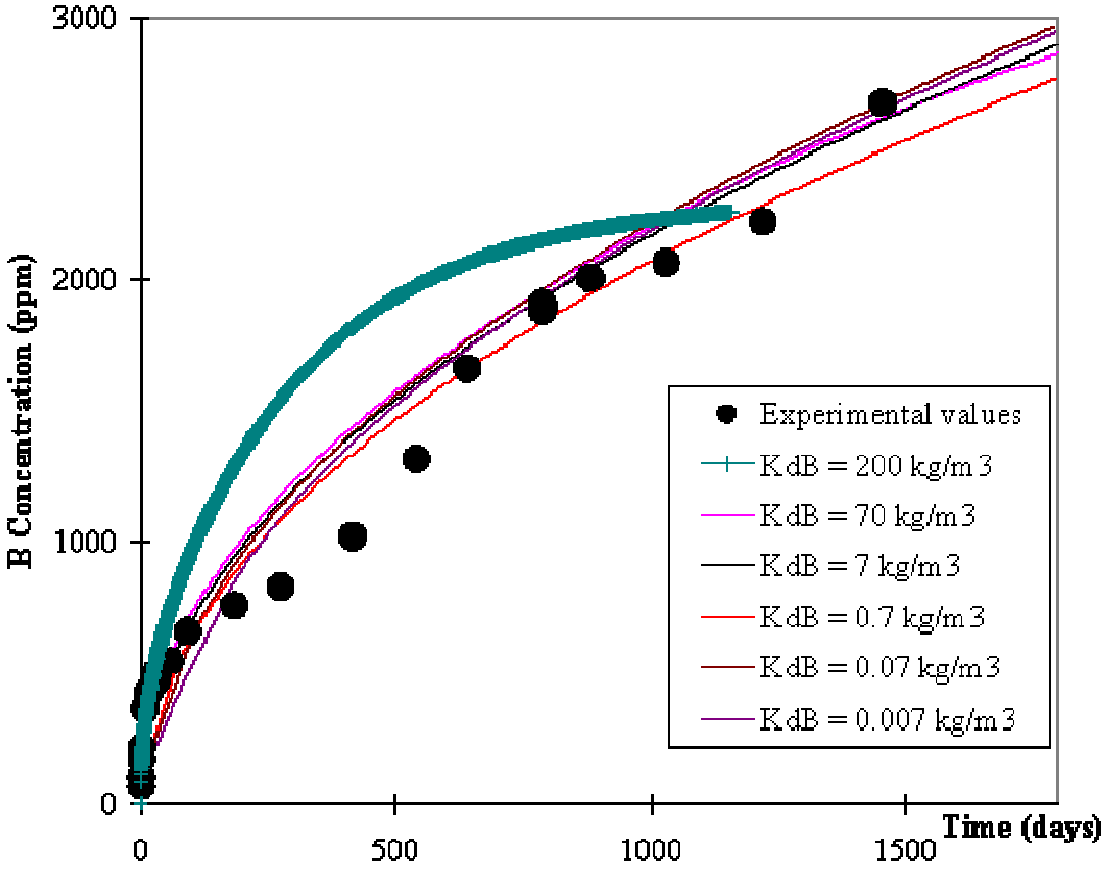

Figure 29: The predicted boron release of experiment A1 according to the GM model for several values of the $K_{d,B}$ of boron, while adapting simultaneously the water diffusion coefficient to get close to the experimental data. Obviously, both model parameters are correlated. For the fits shown, the corresponding value of the water diffusion coefficient decreases from 3 10^{-22} m^2/sec (for K_{dB} = 200 kg/m^3) to 2.8 10^{-24} m^2/s at K_{dB} = 0.007 kg/m^3

5 Work package 5: Discussion

5.1 Main parameters

5.1.1 Overview of parameter field

The previous chapter gave various examples (see 4.3) showing that various parameters are correlated and not entirely independent (see 4.5). Uncertainties may to a certain degree be reduced if the evaluation of the quality of the fit includes a criterion on the consistency of selected parameters when comparing different experiments with each other. As an example, the following Table XVI summarises the parameter values used in the parameterisation of GM model by Subatech, applied to all data of the GLAMOR project obtained at 90 °C. The plots are given in Annex IV. Distinction is made between interdependent parameters and parameters, which are insensitive for the fit of a given experiment. One should mention that the C* values listed are in a few cases (static test, high S/V) different from the rationale used in Chapter 4; see for instance C* = 350 ppm for test A1 (see 4.3.1). The C* values in Table XVI are closer to the C^*_{H4SiO4} values than to the C^*_{tot} as argued in Chapter 4. Various observations can be made:

Table XVI: Summary of parameter values used by Subatech when applying the GM model to the tests at 90°C (pH values listed are those measured at t_{max})

Exp.	tmax d	pH	S/V m-1	F mL/d	mccb ppm	Dsi m2/s	DH2O m2/s	C* ppm	KdB	KdLi	fx	k+ g/m2d	rfin
A1	1200	9.5	200000	0	0	5.20E-14	2.50E-23	85	100	100	1.2	0.7	7.00E-08
A2	600	9	5000	0	0	5.20E-14	4.00E-23	95	100	10	1.2	0.7	7.00E-08
A3	600	7.4	5000	0	0	5.20E-14	1.00E-21	75.6	100	100	1.5	0.7	7.00E-08
A4	600	8	5000	0	0	5.20E-14	1.50E-22	75.6	100	50	1.5	0.7	7.00E-08
A5	600	9.5	5000	0	0	5.20E-14	1.00E-23	60	100	10	1	0.7	7.00E-08
A6	600	10	5000	0	0	5.20E-14	1.00E-23	75.6	100	10	1	0.7	7.00E-08
A7	600	10.5	5000	0	0	5.20E-14	2.00E-23	213.3	100	10	1	0.7	7.00E-08
A8	600	11	5000	0	0	5.20E-14	2.00E-23	338	100	10	1	0.7	7.00E-08
A9	240	11.2	5000	0	0	5.20E-14	2.00E-23	674	100	10	1	0.7	7.00E-08
PSI	3600	9.7	1200	0	0	5.20E-14	2.50E-23	84.9	100	10	2.1	0.7	7.00E-08
E9	48	7.5	12000	14.4	120	5.20E-14	8.00E-22	75.6	100	10		0.7	7.00E-08
E10-a	30	5.2	26	14.4	120	5.20E-14	8.00E-19	75.6	100	10		0.7	7.00E-08
E10-a	50	5.2	26	14.4	120	5.20E-14	3.00E-19	75.6	100	10		0.7	7.00E-08
E11	37	8.1	4330	14.4	120	5.20E-14	5.00E-22	75.6	100	10		0.7	7.00E-08
E12	37	8.1	12000	14.4	120	5.20E-14	2.00E-22	75.6	100	10		0.7	7.00E-08
E13	37	8.1	26	14.4	120	5.20E-14	4.00E-21	75.6	100	10		0.7	7.00E-08
E15-a	10	8.9	12000	14.4	120	5.20E-14	1.70E-22	75.6	100	10		0.7	7.00E-08
E15-b	50	8.9	12000	14.4	120	5.20E-14	5.00E-23	75.6	100	10		0.7	7.00E-08
E16	50	8.9	26	14.4	120	5.20E-14	2.00E-21	75.6	100	10		0.7	7.00E-08
A10	23	8.1	150	144	0	5.20E-14	2.00E-20	84	100	10	1.2	0.7	7.00E-08
A11	23	8.1	150	144	60	5.20E-14	2.00E-20	84	100	10	1.2	0.7	7.00E-08
A12	23	8.1	150	144	120	5.20E-14	2.00E-20	84	100	10		0.7	7.00E-08
A17	370	8.6	50	0	0	3.50E-15	5.00E-21	48	100	10	1	0.7	7.00E-08
B1	1600	9.3	8000	0	0	5.20E-14	5.00E-23	400	10	10	4.8	1.5	9.00E-06
B4	1200	9.2	8000	0	0	5.20E-14	1.00E-25	300	10	10	3.1	1.5	7.00E-08
GL31-42	700	8.6	100	0	2	5.00E-15	1.00E-22	51	100	10	0.6	0.7	7.00E-08

= fit insensible to selected value = value strongly correlated to D(H2O)

a. None of the parameter values was sensitive to the forward reaction rate constant K+. This is because the selected set of experiments did not include experiments at very low S/V (<10 m^{-1}) which would be necessary to calibrate this value. On the other hand, the forward reaction rate constant is fairly well known as a function of temperature and pH. The value of 0.7 used in the present fit does not reflect this knowledge. It is an arbitrary value, without a strong influence on the fit results. Since the set of experiments used in the GLAMOR project reflects better real disposal conditions than tests at very low S/V ratio, one may conclude that uncertainties in the forward rate constant do not influence long-term predictions.

b. Almost no data were sensitive to the residual rate value (r_{fin}). The r_{fin} value in Table XVI is an arbitrary value chosen sufficiently low for not being rate limiting. This however may not reflect reality but is the outcome of a fit-strategy, which tried to optimise the agreement between experimental results and model predictions, using the water diffusion process as key parameter in high S/V experiments. Some experimental data may indeed allow a better fit if a lower water diffusion coefficient and a higher residual rate is used. NOTE: This shows that the D_{H20} and r_{fin} parameters may compete to reproduce the rate decrease in silica saturation conditions. r_{fin} is definitely required in the r(t) model (see e.g. Fig 21 in 4.2.2), as that does not consider water diffusion.

c. There are only few experiments, which were sensitive to the diffusion coefficient of silica D_{Si} in the gel, see Table XVI. This reflects the selected fitting strategy by Subatech for GM, focussing on describing the long-term rate decrease at high S/V or in Si rich solution by water diffusion**.** It was shown however (SCK•CEN modelling, see Fig 23d in 4.3.1 and Table XI) that the fit with the experimental data could be much improved by varying D_{Si}, although there's no experimental evidence for those values of D_{Si} (10^{-20} m^2/s). In the r(t), model, this parameter is of course very sensitive.

d. The selected parameterisation strategy allowed providing a relative consistent set of parameters for the entire field of experimental observations, including large variations of S/V, water flow rate and initial dissolved silica concentration. The Figures 30 to 32 show the parameters C*, D_{H2O} and the silica retention parameter f_x as a function of pH.

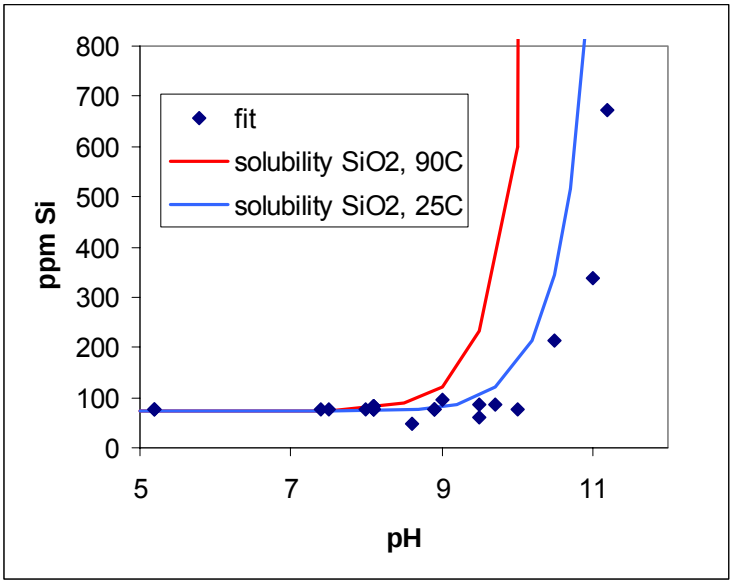

Figure 30: pH dependency of the parameter C* at 90°C in Subatech's parameterisation of the GM2003 model. Only tests with glass SON68 are considered. The experimental data for C* taken from Annex IV (Subatech's calculations) are compared with the solubility curve for a SiO_2 polymorph at 25 and 90 °C (stability constants were adapted so that the solubility curves fit the data at pH < 8

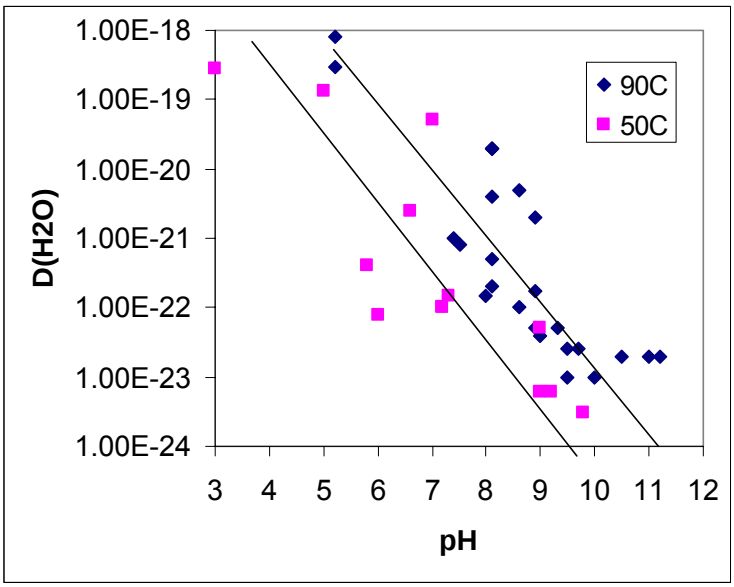

Figure 31: Diffusion coefficient of water in the glass as a function of pH, obtained by Subatech's parameterisation of the GM2003 model both for 50 and for 90°C. Only tests with glass SON68 are considered

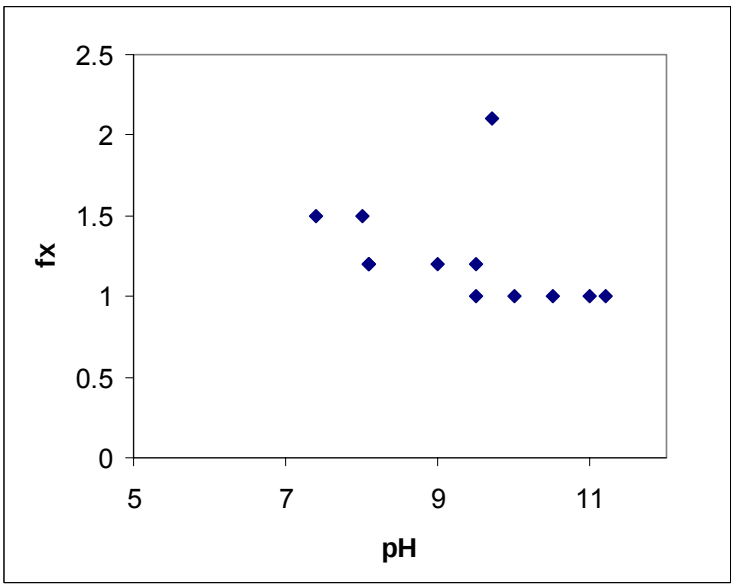

Figure 32: Factor describing the retention of silica in the gel obtained by Subatech's parameterisation of the GM2003 model. Only tests with glass SON68 are considered

5.1.2 Silica saturation concentration in solution (C*, K_{SiO2})

There is overwhelming experimental evidence showing that the accumulation of dissolved silica at a critical concentration C* or K_{SiO2} either in bulk solution or in the pore-water of the surface gel layer is associated to a decrease of release rates of soluble elements from the glass. This "saturation effect" can be described by an affinity [6] or a transport driven rate law, implying that a local equilibrium is reached between dissolved silica and the alkali-depleted glass surface. The Gibbs free energy of formation of the glass phase does not control this affinity term; rather, only the Gibbs free energy of the outer surface [6]. A true thermodynamic equilibrium between the pristine glass phase and the solution is not to be expected, since soon after being in contact with the solution it is not the bulk glass, but the compositionally different, depleted glass surface region that is in contact with an aqueous solution. Local equilibrium between this hydrated silica-rich and alkali-depleted glass is likely to occur, with equilibrium silica concentrations in solutions resembling those of various silica polymorphs.

There is some confusion in the use of the terms “saturation” and “affinity” when they are applied to the bulk glass phase. It was observed [15] that a fresh glass (without the presence of a steady-state, alkali-depleted surface) at neutral pH showed only limited reduction of reaction rates in silica-rich solutions, contrary to what would have been expected from an affinity-type rate law applied to the bulk glass. This initial fast corrosion in silica rich solutions is confirmed by the experiments E1-E16 included in the present project. This observation lead some researchers to conclude that an affinity driven dissolution rate law was invalid, and it was postulated that the reduction of reaction rate with time is due to the formation of protective layers [15]. This approach [27] considered the mass transfer of dissolved silica across the leached layer as rate-limiting, replacing the connotation of a thermodynamic, affinity related saturation concentration C(sat.) by an empirical solubility limit, C*. This “apparent solubility” is observed when the amount of silica dissolved from the glass and the gel corresponds exactly to the one amount recondensed into the gel. This stationary state is strongly dependent on the way by which this state is reached. The drawback of this approach is that its mathematical formulation is in no way different from the affinity-driven rate law, if the affinity law is considered valid at the glass/gel layer interface. As a consequence, the term C* has a similar mathematical significance both in the r(t) and the GM2003 model. Hence, this theory cannot explain why relatively high initial dissolution rates are observed in solutions with dissolved silica concentrations larger than C* (experiments E1 to E16). Even if C* cannot be calculated today from thermodynamic equations, the consistent trend as a function of pH of the fitted C* data in Figure 30 indicates that it is not merely an empirical concept but has some thermodynamic meaning. It was postulated [6] that the affinity term controlling glass dissolution may just be formulated with respect to the SiO_2 component of the glass (since the surface is silica rich and alkali depleted). Frugier *et al* [58] have shown with silica saturation concentrations for the experiment A1 as example, that the evolution of the silica concentration with reaction progress is entirely due to hydrolysis and formation of sodium complexes of dissolved silicic acid, while the concentration of H_4SiO_4 stays constant (see also 4.3.1.). This indicates achievement of solubility equilibrium. However the interpretation of the trend in Figure 30 in a way of pH dependency of SiO_2 solubility is not straightforward. The calculated (PHREEQC) solubility curve for a silica polymorph increases for 90°C much earlier with pH than the measured values. Various explanations might be invoked to explain this behaviour:

a) this is not a solubility equilibrium but a kinetic steady state which might follow other pH dependencies than the solubility of SiO_2

b) there is a change with pH in the composition of the hydrated, alkali-depleted glass

c) there is an effect of temperature. The pH was typically measured at temperature (90°C) but the solution composition at room temperature. It cannot be excluded that the experimentally measured solution concentrations of Si do not reflect solubility at 90 but at 25°C. The solubility curve calculated for 25°C matches the fitted C* parameter much better

d) there is a problem of conservation of solution concentrations prior to analyses. Typically solutions are acidified prior to ICP analyses. This may cause precipitation of Si if this is done for Si solutions > pH10.

Even though a consistent pH dependency of the C* parameter has been obtained by the fit with GM2003, it must be stated that in general the fit is not optimal: the approach of Si saturation concentrations is correctly described but after reaching saturation, the dissolved silicon concentration is considered constant, whereas the experimental Si concentrations continue to rise even after saturation. The continued rise of dissolved Si concentrations after saturation is a thermodynamic consequence of the continued leaching of alkali elements (controlled by water diffusion or residual rate) after Si saturation. The change in pH, the increase in Na concentrations and the increase in ionic strength increase the hydrolysis and Na silicate complex concentrations, hence the total Si concentration rises even if the H_4SiO_4 concentration remains constant (see calculations in [58]. These reactions are not included in GM2003. GM2003 can neither calculate the evolution of pH nor of ionic strength with reaction progress. This drawback in the fit of Si concentrations is without effect on the fit of the release data of soluble elements such as B, Na *etc.* Nevertheless, a new version (GM2004) has been created in the course of the project, which accounts for the evolution of pH and ionic strength, by including the respective chemical equilibrium in aqueous solution. Indeed, a much better fit of dissolved Si concentrations was obtained. However, this version was not used in the GLAMOR project since it was not available at the beginning of the project.

5.1.3 What is the diffusing species?

Strong experimental evidence, mostly based on measuring element profiles of the glass constituents elements [e.g. 63, 64, 65, 66], shows the diffusion of boron and the alkalis from the glass towards solution and of 'water' (under which form like H_2O, H^+, OH^- or OH_3^+ is less important) from solution into the glass. These processes, described by a diffusion equation, are not contested. It is an advantage of GM that, contrary to *r(t),* it explicitly describes these processes.

As discussed in Annex I, 5.4, the major problem is silica diffusion. More in particular:

(a) It is clear that dissolved Si diffusion does occur. However it is less clear under which conditions this process may become rate limiting: in the r(t) model this process is considered rate-limiting at high S/V and describes the whole rate-drop towards the residual rate whereas in the GM2003 model the rate drop is due to both Si and water diffusion. Because of the lack of detailed information and the very high uncertainty on the D_{Si} values, we can't elucidate the relative importance of both parameters. There is a consensus amongst the GLAMOR partners that Si diffusion is rate-limiting at low S/V and in certain dynamic tests. At high S/V condition (e.g. test A1, see 4.3.1.), the GLAMOR partners had different positions towards the D_{Si} parameter applied

(b) Is it according to the silica diffusion/dissolution mechanism as stated in both *r(t)* and GM, (e.g. does silica dissolve form the glass/gel boundary (instead of e.g. from the gel/solution interface)? does this occur according to equations like expression (27) or (39) from Annex I, Chapter 4)

Answering question (a), every species diffuses (although possibly with a very low diffusion coefficient and the diffusion process can be disturbed by other simultaneously occurring phenomena). The only independent (= not obtained by fitting some dissolution behaviour as a function of time with models like GM or *r(t)*) measurements of an (apparent) silica diffusion coefficient in the gel were performed by Valle [64] (see also Annex I, 5.4.2). By measuring the diffusion profile of tracer silica from a solution in an already existing gel, she obtains estimates of the silica diffusion coefficient in a gel. D_{Si} values measured this way were between 10^{-13} and 10^{-14} m^2/s. Smaller D_{Si} could not be measured. Depending on how the gel was formed, the value of this diffusion coefficient can change over some orders of magnitude (see Annex I, 5.4).

It is shown in Annex I, 4.2.2.1, that if the value of the silica diffusion coefficient in the gel is sufficiently large, silica diffusion in the gel is not rate determining. Besides, models (see e.g. the STORM model, [67]), not taking silica diffusion into account, claim to be able to describe glass dissolution. Since these models were not part of the GLAMOR program, it is uncertain that they would better describe experiments than *r(t)* of GM.

On the other hand, if the diffusion coefficient of Si in a very dense gel is very low, Si diffusion may also not be rate limiting. This is because under these conditions, Si concentration gradients will break down if the dissolution rate of Si from the outer gel surface is faster than the mass transfer of dissolved silica across the dense gel layer.

Gel dissolution is also very important for dissolution of glass next to a porous medium like clay. Experiments of glass dissolution next to clay clearly show a retreat of the glass/clay interface, definitely not in agreement with the fixed glass (gel) solution interface assumed in both *r(t)* and GM. However, even if gel dissolution at the clay/gel interface occurs, it is not clear whether this process is rate limiting.

For dissolution in water and apart from measuring diffusion profiles with isotopic tracers, as already mentioned in Annex I, 5.4, the major 'proof' of the silica diffusion/dissolution mechanism of *r(t)* and GM, is the fact that better fits are obtained with this mechanism (where the silica diffusion coefficient is an additional fit parameter) than without it. Adding Si diffusion in the gel layer to the linear rate law, makes it possible to describe decreasing solution concentrations measured in dynamic tests at low dissolved Si-concentrations (example: experiment A10). A model like STORM will probably predict achievement of constant steady state concentrations. Also there is no way to describe this decrease in solution concentration in the experiment A10 by water diffusion. Water diffusion cannot be rate limiting in this experiment since the bulk aqueous solution is under-saturated with respect to C. However, computer simulations [18] suggest that silica does not only dissolve from the gel/diffusion layer (but from the entire gel and even more from the gel/solution interface) and that due to silica condensation (which is experimentally observed but not taken into account explicitly in GM or *r(t)*) the movement of silica through the gel is more complicated than described by a simple diffusion behaviour. Indirectly Si dissolution and recondensation in the gel is considered in the Si retention factor, which has the character of

some kind of a distribution coefficient. Future model development may ask for a more rigorous coupling of diffusion and retention/dissolution in the gel.

5.2 Processes controlling the rate decrease

The following is based on the literature survey made at the start of GLAMOR, and on the further discussions within GLAMOR. We conclude that both affinity- and kinetics- controlled processes will intervene during the rate decreasing stage.

- It is accepted, and extensively documented, that glass dissolution becomes much slower when dissolved silica in solution reaches a “saturation” value. However,
    - The dissolution does not fully stop when the silica concentration in solution is equal to the silica saturation concentration. This minimum rate, that can be time-dependent and even zero, corresponds to the residual rate.
    - The silica saturation concentration value is not necessarily constant with time (for a specific glass composition, temperature and pH), but may change as a function of the reaction progress [58, 59].
    - One might extend the notion of saturation of the solution with respect to silica to all glass constituents, defining a total glass solubility limit [e.g. 7, 11, 68].
- It is as well accepted that kinetic effects associated to the alteration layer affect the glass dissolution:
    - The protective effect of the alteration layer has been argued by various authors [e.g.12, 19]. A dedicated test to demonstrate the protective effect – see Figure 5 – shows that for an already leached glass for which the leaching solution was replaced by pure water, the initial dissolution rate after build-up of the alteration layer was 1/300 of the initial dissolution rate if no alteration layer is present. However, the total Boron release is still ~ 20 % of the amount if no alteration layer is present. This effect is accounted for a by diffusion coefficient for Si. The effect is accepted, although its extent is open to interpretation
    - The diffusion of water as a rate-limiting process [61] has been accepted. It is coupled to the subsequent release of mobile glass constituents (Li, B, Na for instance). Water diffusion can contribute in the rate deceasing stage and in the residual dissolution stage. The way in which water diffusion is coupled to the release of mobile glass constituents still needs to be investigated. There are glasses (e.g. obsidians) where water diffusion and alkali release are largely decoupled (water diffusion depth much faster than Na depletion depth) whereas for nuclear waste glasses, close relation between water diffusion and mobile element release does exist. Recently it has been shown that under silica saturated conditions the ratio between water uptake and mobile element release is constant, independent on temperature and pH and appears to be governed by the stoichiometric of the glass [61,69]

5.3 Uncertainties in modelling

The prediction of the long-term performance of nuclear waste glasses in a repository environment relies essentially on models, since time periods of millions of year are experimentally inaccessible and the performance proof by comparison to million year old natural analogue glasses is not straightforward and relies essentially as well on models. This puts directly the question to the uncertainties in the modelling approach. Different uncertainties must be distinguished in this regard: (1) model uncertainties, which concern the choice of the model and the question whether all potentially rate-limiting processes are accounted for in the model, (2) parameter uncertainty, which covers uncertainties in the underlying experimental data, and (3) uncertainties in the boundary conditions and evolution scenarios. This latter uncertainty will not be treated in the present context.

Parameter uncertainty is typically taken into account in performance modelling by probability distribution functions, model uncertainty by changing model hypothesis and looking for the effects

on the outcome of performance calculations. The outcome of the present project shows that with respect to model and parameter uncertainties we need a change in paradigm. This is because parameter and model uncertainty are strongly coupled. We observe for example in the present project as much as seven orders of magnitude of uncertainties in the diffusion coefficient of dissolved silica (example: experiment A1) as to whether the r(t) or the GM2003 model is used or which parameterisation strategy is used. Even though the significance of this parameter is the same in both models, different parameterisation strategies lead to this uncertainty. In the GM2003 by Subatech, the rate drop in the experiment A1 is thought to being caused by water diffusion, hence a Si-diffusion coefficient from other experiments was used which is insensitive to the data of the experiment A1. In the GM2003 application by SCK•CEN it was found that a low D_{Si} value was leading to the best fit with the experimental data. On the other hand, in the model r(t) Si diffusion is a key parameter to describe the rate drop, hence a very low diffusion coefficient was selected. Indeed one would need additional physical-chemical evidence to reduce overall modelling uncertainty. Such evidence may for example for the experiment A1 be provided by the recent work of Frugier *et al.* [58] showing that H_4SiO_4 concentrations are essentially constant in solution, suggesting absence of rate control by Si diffusion. On the other hand, for experiments, where the parameterisation strategy was similar, uncertainties in the diffusion coefficients of dissolved silica in the gel are very low. This was the case for example for the experiment A10 where both in the r(t) and in the GM2003 approach water diffusion was not considered rate limiting.

Another source of uncertainties is the strong coupling in various parameters. This is the case in the GM2003 model for coupling between the water diffusion constant and the K_d for B, Li *etc*.. An attempt has been made to limit this uncertainty by fixing the K_d value of B at a constant value (see Table XVI above). This is also the case for the correlation between the diffusion coefficient of dissolved silica and C* in the r(t) model.

In order to reduce uncertainties, certain parameters can be measured in dedicated experiments and may be kept fixed in others where strong couplings occur, or where the data are insensitive to a given parameter. This is the case for the forward rate constant which needs to be determined in experiments at low S/V for time periods after steady state between ion exchange and network corrosion has been achieved but before saturation effects become effective and gel layers are still of low density, to avoid Si diffusion control. Currently there is a preference to use flow tests such as the single-pass flow-through experiment (SPFT) to determine the forward dissolution rate – see also 2.1.h. By providing a continuous flow of fresh influent solution, the build-up of reaction products is prevented, and the bulk solution composition is maintained throughout the experiment, thus providing a direct measure of the dissolution rate. Diffusion coefficients of silica in the gel can be obtained with only little correlation to the choice of C* only in dynamic experiments in aqueous solutions that do not contain initial Si concentrations or by the measurement of diffusion profiles in the gel. However, the dynamic range of these methods is limited to diffusion coefficients in the range between 10^{-12} and 10^{-14} m^2/s.. Lower diffusion coefficients of Si related to more dense surface layers can only be obtained from static experiments at high S/V in a way which is strongly coupled to the choice of C* and there is debate as to whether Si-diffusion is at all rate limiting under such conditions (key question in the comparison between r(t) and GM2003 approaches). C* can be obtained reliably in experiments at very high S/V if solution speciation of dissolved silica is accounted for (see work of Frugier *et al*. [58]). However, since C* is no intrinsic glass property but that of an alkali-depleted Si rich surface, within a certain range, C* is not necessarily constant with S/V and with reaction progress. So C* values determined at high S/V may not be valid at low S/V.

A very important question is to which degree the above mentioned uncertainties relate to uncertainties in conceptual models and in the results of long-term predictions. It shall be noted that an operational model does not provide an exact description of the glass dissolution process but provides an upper limit assuring that real glass dissolution shall occur at lower rates than those predicted by the operational model. There is agreement on the main stages of such an operational model: (1) fast initial rate, (2) rate drop if silica concentrations are becoming high (3) no rate drop if Si concentrations are kept low by sorption on near-field materials (4) constant final rate. Even though the question of constant or decreasing long-term rate strongly affects long-term predictions, the use of a constant long-term rate as upper limit creates a situation where all these uncertainties relate to the question on how much better the real glass performance is when comparing it to the upper limit. However, since Si concentrations provide the principal coupling between glass performance and near-field constraints (sorption, diffusion), uncertainties related to the understanding of C* are of critical importance for any operational model which wants to account for the rate drop.

5.4 Points of consensus and disagreement

There is a consensus that both affinity- and transport-kinetics-controlled processes are occurring during the dissolution of HLW glass in pure solutions in closed conditions. Both kinds of processes are accounted for in the models considered in GLAMOR. There is disagreement on the relative importance of the two kinds of processes when interpreting experimental data: arguments are given that the silica saturation in solution will induce only a limited decrease of the dissolution rate, but similarly arguments are forwarded that the protective effect (which is hard to quantify) of the alteration layer induces only a limited effect on the dissolution rate. The main disagreement exists with respect to the value attributed to the Si diffusion coefficient (D_{Si}) in the alteration layer at very high S/V values.

There is a consensus that the mechanism of silica diffusion is demonstrated and parameterised to a small extent only. Agreement has been achieved that silica diffusion is contributing to the rate decrease at low S/V and for tests under dynamic conditions far away from saturation (note: This may seem conflicting, but the dissolution rate may decrease with time to a minor extent under dynamic conditions as well), although no single numerical value can be proposed. Its use in the models is essentially to obtain good fits with the experimental data.

There is a consensus that a residual ("final" but not necessarily constant with time) dissolution rate exists beyond the rate-decreasing stage, at least in the conditions considered in GLAMOR (pure solutions, closed system). There is also a consensus that this residual rate will significantly control the long-term performance of the glass. It may become an input parameter in the performance-assessment studies. There is agreement that high silica concentrations are a necessary but not a sufficient condition for low residual rates. Disagreement exists as to whether additional conditions refer to the build-up of dense surface gel layers or to the build-up of a silica-rich alkali (and boron) depleted glass surface.

6 Recommendations

At the end of the GLAMOR project, we present the following recommendations:

- In future R&D on the long-term durability of HLW glass in geological disposal, focus should be on the residual ("final") dissolution rate rather than on the preceding stages. This is true as well if one considers the presence of near- or far field solid materials (clays, corrosion products, etc.) in the interacting system. Once these become saturated with glass matrix constituents (mainly Si), the conditions for achieving a final dissolution rate (whatever its kinetics: constant with time or square root of time dependent) will be met as well.
- Detailed surface analyses should be made on the dissolved glasses, in addition to solution analyses. Electron microscopy (SEM, TEM) is frequently used already, and other techniques are able to provide sometimes very specific information (FTIRRS, NMR, XRD, etc.). Depth-profiling techniques by e.g. SIMS however are recommended for a more in-depth characterisation of the alteration layers (occurrence of sub-layers, composition as a function of the depth, speciation of water). Care should be taken here to carefully monitor the accuracy of such analysis (density corrections, normalisation of the element analyses). Detailed surface analyses will help to identify the dissolution processes occurring in the residual dissolution regime.
- The chemistry and the geochemistry in the system must be considered. The solution characteristics (pH, Eh, pCO_2, cation and anion concentration) together with the generation of secondary phases should be carefully monitored during the test, whenever relevant. Geochemical models are useful to predict the formation of secondary phases.
- New computation techniques such as ab initio, Monte Carlo and molecular dynamics should be further developed to obtain a better support for the basic assumptions of the conceptual models for glass dissolution.
- The uncertainty on the output parameters of the tests should be carefully identified. We mention: the residual dissolution rate, the diffusion coefficient of H_2O, and the saturation concentration for Si. Both models *r(t)* and GM should be coupled with a fit routine, although optimised model predictions have to be interpreted with caution (as argued in Section 4.4).
- Models should be exchanged between different laboratories and should be elaborated jointly. Activities of benchmarking and validation (as done in GLAMOR) are recommended as well, because they will increase confidence in the models and in their predictions.
- The mathematical analysis of the models by the partners leads to the following proposed improvements in the models:
    - In many cases, the water-diffusion part of the GM model can to a very good approximation be solved analytically, instead of the present time-consuming and hard-to-use numerical code.
    - The silica diffusion coefficient in *r(t)* should be considered as an effective diffusion coefficient, not as an apparent one.
    - In GM, the retention coefficient $K_{d,i}$ and the water diffusion coefficeint D_{H2O} are very strongly correlated, making the individuall values of these parameters very inaccurate. To avoid this correlation, it should be tried to replace both parameters by one single parameter, e.g. a boron/alkali diffusion coefficient.
    - Both models should use the same silica dissolution rate law. At first sight, both models seem to use the same rate law, but due to their different handling of silica dissolution this is not the case.
    - Mathematically, both models assume that the silica concentration profile in the gel is stationary and linear. Due to the small thickness of the gel, this approximation is probably valid for Si diffusion coefficients of the order of e.g. 10^{-13} m^2/s, but it is not likely that this is the case when the order is 10^{-20} m^2/s.
- Efforts should be done to make scientific models applicable to the interaction between HLW glass and near-field surroundings (including solids).

- Ancient glasses – both natural and historical – can be very useful to argue about the long-term dissolution performance of HLW glasses. Some of them at least were found to have quite similar dissolution behaviour as HLW glass (activation energy for the forward rate, further dissolution processes including a final rate) [75]. Ancient glasses may therefore contribute to a better understanding of the dissolution of HLW glass.

7 Conclusions

We conclude that the first objective of GLAMOR – achieving a common understanding of the rate decrease of HLW glass – was met. By applying the selected models to the test data, we could conclude that both mechanisms proposed (affinity-limited dissolution, rate decrease by transport limitation through the reaction layer) are affecting the rate decrease. We did not fulfil the second objective – quantify the uncertainty of the model calculations. This was found to be unrealistic, as the uncertainties of the different model parameters are poorly known only.

Some conclusions of GLAMOR were not expected in the beginning of the project:

- Emphasis should be more on the residual dissolution rate (and the mechanisms controlling it) than on the preceding rate-decreasing stage
- The process of Si diffusion through the alteration layer is only poorly demonstrated and parameterised. Its use in analytical models can only be based on pragmatic arguments.
- The silicon saturation concentration must be determined with better precision. The use of speciation calculations can be very helpful to do this.
- Mechanistic interpretation of the experiments should be done in more detail, in support of the modelling.

Part of the objectives defined at the beginning of GLAMOR was not fully achieved. The determination of the uncertainties of the model parameters was found not to be a realistic objective. We did not manage to apply the GLAMOR methodology to data in solutions including solids (e.g. clay), because of time limitations.

The approach of GLAMOR to evaluate with scientists from different laboratories a selected set of data with selected models proved to be very useful. It enabled the participants to acquire a detailed understanding of the different approaches developed by them – for instance the strategy followed in the models and the application of the models. It proved to be at the same time an excellent review of the corresponding literature! The participants agreed about the dissolution rate decrease, the occurrence of water diffusion and of a long-term “residual” dissolution rate. The role of the model parameters (Si diffusion coefficient, Si saturation concentration, Si retention in the reaction layer, water diffusion coefficient, boron/lithium retention factors, and residual rate) in the predictions was evaluated. GLAMOR in a way contributed to validate both models. Finally we made progress in getting an understanding of the uncertainties in the model predictions.

8 References

[1] W. Lutze. Silicate glasses, in Radioactive waste forms for the future. Ed. W. Lutze and R. Ewing., 1988

[2] High-level waste borosilicate glass. A Compendium of corrosion characteristics. US-DOE-EM-0177 (3 volumes), 1994. Ed. J.C. Cunnane. See also: W. L. Ebert and J.J. Mazer, Mat. Res. Soc. Symp. Proc. Vol 333, 1994, 27-40.

[3] Glass as a waste form and vitrification technology: summary of an international workshop (Washington, 1996). Ed National Academic Press

[4] GLASS. Scientific research for high-performance containment. CEA/VALRHO summer session proceedings, 1998

[5] Glass in its Disposal Environment. Proceedings of a topical workshop. Journal of Nuclear Materials, Vol 298, 2001

[6] Grambow B. , "A general rate equation for nuclear waste glass corrosion", , Mat. Res. Soc. Symp. Proc. vol. 44, 1985, pp. 15-27.

[7] Advocat T., Chouchan J.L., Crovisier J.L., Guy C., Daux V., Jégou C., Gin S. and Vernaz E.Y. Borosilicate nuclear waste glass alteration kinetics: chemical inhibition and affinity control , Mat. Res. Soc. Symp. Proc., vol. 506, 1998, pp. 63-70.

[8] McGrail B.P., Ebert W.L., Bakel A.J. and Peeler D.K. (1997), J. Nucl. Mat., vol. 249, pp. 175-189.

[9] Abraitis P.K., McGrail B.P. and Trivedi D.P. , "The effects of silicic acid, aluminate ion activity and hydrosilicate gel development on the dissolution rate of a simulated British Magnox waste glass", in Scientific Basis for Nuclear Waste Management XXII, Mat. Res. Soc. Symp. Proc. Vol 556, 1999, 401-408

[10] Bourcier W.L., Pfeiffer D.W., Knauss K.G., McKeegan K.D. and Smith D.K. (1990), "A kinetic model for borosilicate glass dissolution based on the dissolution affinity of a surface alteration layer", Mat. Res. Soc. Symp. Proc. Vol. 176, 1990, pp. 209-216

[11] Aagaard P. and Helgeson H.C. (1982), "Thermodynamic and kinetic constraints on reaction rates among minerals and aqueous solutions. I. Theoretical considerations", Am. J. Sci., vol. 282, pp. 237-285.

[12] R. Wallace and G. Wicks, "Leaching chemistry of defense borosilicate glass". Mat. Res. Soc. Symp. Proc. Vol 15 (1983), 23-28

[13] S.J. Zavoshy, P.L. Chambre, and T.H. Pigford, "Mass transfer in a Geologic Environment", Mat. Res. Soc. Symp. Proc. Vol 44, 1985, pp 311-322

[14] W.E. Dibble Jr. and W.A. Tiller, Non-equilibrium water/rock interactions I. Model for interface-controlled reactions, Geochimica et Cosmochimica Acta, 45 pp. 79, 1981

[15] Jégou, Mise en évidence expérimentale des mécanismes limitant l'altération du verre R7T7 en milieu aqueux. Critique et proposition d'évolution du formalisme cinétique, Ph.D thesis, Université de Montpellier, France, 207 pages. (1998)

[16] H.T. Fullam, *Solubility* Effects in Waste-Glass / Demineralized-Water Systems, Pacific Northwest Laboratory Raport (1981)

[17] Freude E., B. Grambow, W. Lutze, H. Rabe, and R.C. Ewing. "Long-Term Release from High-Level Waste Glass - Part IV: The Effect of Leaching Mechanism." Mat. Res. Soc. Symp. Proc. **44**, 99-106 (1985)

[18] M. Aertsens, Testing the Grambow glass dissolution model by comparing it with Monte Carlo simulation results, Mat. Res. Soc. Symp. Proc. 556 (1999) 409-419

[19] S. Gin, « Protective Effect of the Alteration Gel : A key Mechanism in the Long-term Behavior of Nuclear Waste Glass", Mat. Res. Soc. Symp. Proc. 663 (2000)

[20] C. Jégou, S. Gin, F.Larché, “Alteration kinetics of a simplified nuclear waste glass in an aqueous medium: effects of solution chemistry and of protective gel properties on diminishing the alteration rate”, J. Nuc. Mater. 280 (2000) 216-229

[21] Philibert J., Vignes A., Bréchet Y. and Combrade P. (1998) Métallurgie, du minerai au matériau, Masson, Paris.

[22] B. Grambow, W. Lutze, R. Müller, "Empirical dissolution rate law for the glass R7T7 contacting halite- and silica-saturated brines", Mat. Res. Soc. Symp. Proc. Vol 257, 1992, 143-150

[23] B. Grambow, A. Loïda, L. Kahl, W. Lutze, "Behaviour of Np, Pu, Am, Tc upon glass corrosion in a concentrated $Mg(Ca)Cl_2$ solution". Mat. Res. Soc. Symp. Proc. Vol 353, 1995, 39-46

[24] W. Lutze, R. Müller, W. Montserrat, "Chemical corrosion of Cogema glass R7T7 in high saline brines – part II", Mat. Res. Soc. Symp. Proc. Vol 127, 1989, 81-88

[25] B. Grambow, L. Kahl, H. Geckeis, E. Bohnert, A. Loida, W. Lutze, P. Dressler, R. Pejsa, "Retention of Pu, Am, Np and Tc in the corrosion of Cogema glass R7T7 in salt solutions". EUR 17114, 1997

[26] S. Gin, "Protective effect of the alteration gel: A key mechanism in the long-term behaviour of nuclear waste glass". Mat. Res. Soc. Symp. Proc. Vol 663, 2001, 207-215

[27] E. Vernaz, S. Gin, C. Jégou, I. Ribet, "Present understanding of R7T7 glass alteration kinetics and their impact on long-term behavior modeling". Journal of Nuclear Materials 298 (2001), 27-36

[28] S. Gin, I. Ribet, M. Couillard, "Role and properties of the gel formed during nuclear glass alteration: importance of gel formation conditions". Journal of Nuclear Materials 298 (2001), 1-10

[29] E. Vernaz and S. Gin, "Apparent solubility limit of nuclear glass", Mat. Res. Soc. Symp. Proc. Vol 663, 2001, 217-225

[30] S. Gin and J.P. Mestre, "SON68 nuclear glass alteration kinetics between pH 7 and 11.5". Journal of Nuclear Materials 295 (2001), 83-96

[31] C. Jégou, S. Gin, F. Larché, "Alteration kinetics of a simplified nuclear glass in an aqueous medium: effects of solution chemistry and of protective gel properties on diminishing the alteration rate". Journal of Nuclear Materials 280 (2000), 216-229

[32] K. Lemmens and P. Van Iseghem, "The long-term dissolution behaviour of the PAMELA borosilicate glass SM527 – application of SA/V as accelerating parameter". Mat. Res. Soc. Symp. Proc. Vol 257, 1992, 49-56

[33] P. Van Iseghem, T. Amaya, Y. Suzuki, H. Yamamoto, "The role of Al_2O_3 in the long-term corrosion stability of nuclear waste glasses". Journal of Nuclear Materials 190 (1992), 269-276

[34] S. Mitsui and R. Aoki, Effect of a siliceous additive on aqueous alteration of waste glass with engineered barrier materials, J. of Nuclear Materials, 298 (2001), 184-191.

[35] I. Ribet, S. Gin, Y. Minet, E. Vernaz, P. Chaix, and Do Quang, “Long-term behavior of nuclear waste glass: the r(t) operational model”, GLOBAL international conference on “Back end of the fuel cycle : From research to solutions” Paris 2001

[36] B. Grambow R. Müller, « First order dissolution rate law and the role of surface layers in glass performance assessment », J. of Nuclear Materials, 298 (2001) 112-124

[37] Schröder, H. Glastechn. Ber. 26 (1953) 91-97

[38] Zagar, K., Schillmöller, A. Glastechn. Ber. 33 (1960) 109-116

[39] Douglas, R.W., T.M. ElShamy, J. Amer. Cer. Soc. 50 (1967) 1

[40] Doremus, R.H., Interdiffusion of hydrogen and alkali ions in a glass surface, J. Non-Cryst. Solids 19 (1975) 137-144

[41] H. Schnatter, H. Doremus, W.A. Lanford, J. Non-Cryst. Solids **102**, (1988) 11-18

[42] Bunker, B.C., T.J. Headly and D.C. Douglas, Mat. Res. Soc. Symp. Proc. 32 (1984)

[43] R.D. Aines, H.C. Weed, J.K. Bates, "Hydrogen speciation in hydrated layers on nuclear waste glass", Mat. Res. Soc. Symp. Proc. Vol 84, (1987), 547-558

[44] Ernsberger, F.M., Glastechn. Ber. 56K (1983) 963-968

[45] Doremus, R.H., Y. Mehrotra, W.A. Lanford, C. Burman, J. Mater. Science 18 (1983) 612-622

[46] T. Advocat, P. Jollivet, Y. Minet, B. Luckscheiter, B. Grambow, R. Gens, K. Lemmens, P. Van Iseghem, M. Aertsens, V. Pirlet, E. Curti, "Experimental and modelling studies to formulate a nuclear waste glass source term in representative geological disposal conditions". EUR 19120 (1999).

[47] P. McGrail, J.P. Icenhower, D.K. Shuh, P. Liu, J.G. Darab, D.R. Baer, S. Thevuthasen, M.H. Engelhard, C.H. Booth, P. Nachimuthu, "The structure of Na_2O-Al_2O_3-SiO_2 glass: impact on sodium ion exchange in H_2O and D_2O", J. non-cryst. Solids 296 (2001), 10-26.

[48] P. McGrail, J.P. Icenhower, E.A. Rodriguez, "Origins of discrepancies between kinetic rate law theory and experiments in the Na_2O-B_2O_3-SiO_2 system". Mat. Res. Soc. Symp. Proc. Vol 713 (2002), 537-546.

[49] E. Curti, "Glass dissolution parameters: update for "Entsorgungsnachweis". PSI Bericht Nr 03-18, 2003

[50] I. Ribet, S. Gin, N. Godon, P. Jollivet, Y. Minet, B. Grambow, A. Abdelouas, K. Ferrand, K. Lemmens, M. Aertsens, V. Pirlet, D. Jacques, J.L. Crovisier, G. Aouad, A. Arth, A. Clément, B. Fritz, G. Morvan, I. Munier, M. Del Nero, A. Ozgümüs, E. Curti, B. Luckscheiter, B. Schwyn, "GLASTAB. Long-term behaviour of glass: Improving the glass source term and substantiating the basic hypotheses". Final report of the GLASTAB project.

[51] E. Curti, personal communication

[52] S Gin and P. Frugier, "SON68 glass dissolution kinetics at high reaction progress: experimental evidence of the residual rate", Mat. Res. Soc. Symp. Proc. Vol 757 (2003), 175-182

[53] S Gin, personal communication

[54] T. Advocat, Hydrolysis of R7T7 nuclear waste glass in dilute media : mechanisms and rate as a function of pH, Mat. Res. Soc. Symp. Proc., Vol. 212, p. 57-64, 1991

[55] P. Frugier and JP. Mestre: Comportement à long terme des verres du domaine de composition AVM – Comparaison avec les verres du domaine R7T7. CEA internal report, 2001.23, 79 p.

[56] B. Grambow, H.P. Hermansson, I.K. Björner, H. Christensen, L. Werme . Reaction of nuclear glass with slowly flowing solutions, Advances in ceramics, *Nuclear Waste Management* II, vol 20 (1986) , pp 465-473.

[57] W. Stumm and J.J. Morgan, Aquatic Chemistry, an introduction emphasizing chemical equilibria in natural waters. Socond edition. Publ. Wiley-Interscience. John Wiley & Sons.

[58] P. Frugier, S. Gin, J.E. Lartigue, E. Deloule, "SON68 glass dissolution kinetics at high reaction progress: mechanisms accounting for the residual alteration rate". Mat. Res. Soc. Symp. Proc. Vol 932, 2006, 305-312

[59] R. Tang and G. Nancollas, New mechanism for the dissolution of sparingly soluble minerals, Pure Appl. Chem. Vol 74, No 10, pp 1851-1857, 2002

[60] S. Ribet, S. Gin (2004). Role of neoformed phases on the mechanisms controlling the resumption of SON68 glass alteration in alkaline media**,** *Journal of Nuclear Materials*, Volume 324, vol 2-3, pp 152-164.

[61] K. Ferrand . *Effet de la diffusion d'eau et de la radiolyse alpha et gamma sur la corrosion des verres type SON 68 en solutions aqueuses riches en silicium*, PhD thesis, University of Nantes (France), 2004, 201 pages.

[62] X. Feng, I. Pegg, A glass dissolution model for the effects of S/V on leachate pH, J. Non Cryst. Solids, 175, p. 281-293, 1994

[63] M. Aertsens, K. Lemmens, P. Van Iseghem, Fitting element profiles for predicting glass dissolution rates in synthetic interstitial clay water, Mat. Res. Soc. Symp. Proc., Vol. 757, p. 167-174, 2003

[64] N. Valle, Tracage isotopique (^{29}Si et ^{18}O) des mécanismes de l'altération du verre de confinement des déchets nucléaires: SON68, Ph. D. Thesis, Centre de Recherches pétrographiques et géochimiques, Nancy (France), 2000

[65] T. Richter, G. Frischat, G. Borchardt, Short time leaching of a soda-lime glass in H_2O and D_2O, Phys. Chem. Glasses, Vol. 26 (6), p. 208-212 1985

[66] J. Hamilton, C. Pantano, Effects of glass structure on the corrosion behavior of sodium-aluminiosilicate glasses, J. Non-Cryst. Solids, Vol. 222, p. 167-174, 1997

[67] D.H. Bacon, M.D. White, B.P. McGrail, Subsurface transport over reactive multiphases (STORM): a general, coupled nonisothermal multiphase flow, reactive and porous medium alteration simulator, Version 2, User's Guide, PNNL-13108, Pacific Northwest National Laboratory, Richland, WA

[68] Lasaga A., Rate laws of chemical reactions, in Kinetics of geochemical processes, eds. A. Lasaga, R. Kirkpatrick, Review in mineralogy, v8, p. 1-110, 1981

[69] K. Ferrand, A. Abdelouas and B. Grambow, "Water diffusion in the simulated French nuclear waste glass SON 68 contacting silica rich solutions: Experimental and modeling" Journal of Nuclear Materials, Volume 355, 54-67 (2006)

[70] P. Van Iseghem and B. Grambow, "The long-term corrosion and modelling of two simulated Belgian reference high-level waste glasses". Mat. Res. Soc. Symp. Proc. Vol 112, Publ. Mat. Res. Soc., 631-639 (1988).

[71] T. Advocat, P. Jollivet, J.L. Crovisier, M. del Nero, "Long-term alteration mechanisms in water for SON68 radioactive borosilicate glass". J. Nucl. Mat. 298 (2001), 55-62

[72] Y. Inagaki, A. Ogata, H. Furuya, K. Idemitsu, "Effects of redox condiiton on waste glass corrosion in the presence of magnetite", Mat. Res. Soc. Symp. Proc. Vol 412 (1996), 257-264

[73] Standard practice for measurement of the glass dissolution rate using the single-pass flow-through test method. Test submitted to ASTM committee C26-13

[74] Mc Grail, J.P. Icenhower, P.F. Martin, D.R. Rector, H.T. Schaef, E.A. Rodriguez, J.L. Steele, Low-Activity Waste Glass Studies: FY2000 Summary Report. PNNL-13381.

[75] J. L. Crovisier, T. Advocat, J.L. Dussossoy, "Nature and role of natural alteration gels formed on the surface of ancient volcanic glasses". Journal of Nuclear Materials 321 (1), 91-109 (2003)

[76] A.J. Machiels and C. Pescatore, "The functional dependence of leaching on the surface area-to-solution volume ratio". Mat. Res. Soc. Symp. Proc. Vol 15 (1983), 209-216

ANNEX I

Discussion of the models used in GLAMOR

1 Introduction

The models used in GLAMOR are operational models. This means simple, robust and reasonably conservative models focusing on the essential mechanisms controlling the long-term behaviour of the glass package under the alteration conditions specified by the user. Two models are selected: *r(t)* [1] and GM2003 [2]. Other classes of models (e.g. based on Monte Carlo approaches) increasing the understanding of the glass corrosion were not selected in these report since they are not yet sufficiently developed to describe long-term corrosion in an operational matter.

The mathematical concepts of both selected models *r(t)* and GM are similar and they often use the same mathematical expressions, although their interpretation of the parameters can be different. Therefore, each model is presented using its own notations. Simultaneously, it is tried to present each model so that comparison with the other model gets as easy as possible. Afterwards, a summary and comparison of both models, discussing their differences and similarities, follows.

Since its publication in [1], development of the *r(t)* has stopped. So only one version of *r(t)* exists and it is used in GLAMOR. Contrary to *r(t),* developments of the GM model were still continuing during the GLAMOR project, resulting in several versions. The GM version used in GLAMOR, called GM2003, differs from the version GM2001 published in [2]. More recent versions than GM2003 are not discussed in the present report.

This annex is structured as follows. It starts by introducing theoretical concepts needed for better understanding the basics of the models. Next, the effect of pH, which the *r(t)* model partly tries to take into account, is mentioned. Then both the *r(t)* and the GM model are explained in detail, followed by a comparison of both. Afterwards, the parameters of both models are considered: what are they, how can they can be measured (preferentially in an independent way), and which order of magnitude can be expected for their values. The annex ends with a short summary of both models.

2 Some theoretical concepts

2.1 Silica dissolution and the linear rate law

Glass dissolution is assumed to be controlled by dissolution of its major component: silica. The silica dissolution reaction

$$SiO_2 + 2H_2O \rightarrow Si(OH)_4 \qquad (1)$$

can be considered as the sum of four elementary reactions, where in each elementary reaction a Si-O-Si (siloxane) bond is broken by a neighbouring water particle:

$$\equiv Si - O - Si \equiv + H_2O \rightarrow \equiv Si - OH + OH - Si \equiv \qquad (2)$$

The simplest way to derive the silica dissolution rate is by considering two silica states: dissolved silica (having no siloxane bonds) and silica in the glass (having one up to four siloxane bonds). Silica dissolves with a (forward) rate constant k_f from the glass surface with size *SA*. Dissolved silica is trapped again by the glass. This backward rate is proportional to the concentration *C(t)* of dissolved silica in solution. The proportionality factor is the backward rate constant k_b. At equilibrium, the silica concentration in solution is the silica solubility C_{sat} and the forward and backward rates must be equal. This leads to

$$C_{sat} = \frac{SA\, k_f}{k_b} \tag{3}$$

Note from expression (3) that the forward rate constant k_f is a surface rate, while the backward rate constant k_b is not.

The net silica dissolution rate J_{diss} is the difference of the forward and the backward rate. Due to this net rate, the silica concentration $C(t)$ in a solution volume V rises as a function of time, by

$$\frac{\partial C}{\partial t} = \frac{SA}{V} J_{diss} = \frac{SA}{V} k_f \left(1 - \frac{C}{C_{sat}}\right) \tag{4}$$

Since according to this rate law the net silica dissolution rate J_{diss} is linear as a function of the silica concentration in solution C, the resulting rate law is called 'linear rate law'. Other terms used for it are 'first order rate law' or 'Grambow rate law'.

The linear rate law is the simplest expression describing the influence of silica on the glass dissolution rate. Although generally not in agreement with experimental results (e.g. [3, 4, 5, 6, 7 Fig. 10]), it was confirmed in some cases [7 Fig. 11, 8], suggesting that the linear rate law is an approximation, whose validity depends on the set up of the experiment as well as on experimental conditions.

More complex (and more realistic?) alternatives to the linear rate law are available. The rate law proposed by Aagaard and Helgeson [9, 10, see also section 2.1 of the main part of this report] takes into account other glass components than just silica. Another possibility is to take into account all silica coordination states. It is evident that a silica particle with three siloxane bonds dissolves slower than a silica particle with only one siloxane bond. Deriving the linear rate law, it is assumed that breaking the final siloxane bond takes much more time than breaking siloxane bonds of silica particles having other siloxane bonds. It looks more realistic to assume that the time (energy) needed to break a siloxane bond is independent of the number of siloxane bonds of a silica particle, or due to steric hindrance by other siloxane bonds, to assume that breaking a siloxane bond is most difficult when that particle has the maximum of four siloxane bonds. This last hypothesis is confirmed by ab initio calculations [11]. With such assumptions, silica dissolution can be studied with Monte Carlo simulations (e.g. [12]). No simple analytical expressions for a rate law are available then.

2.2 Theory of kinetically coupled diffusion

Diffusion in a porous medium is described by

$$\eta \frac{\partial C}{\partial t} = \eta D_p \frac{\partial^2 \mathrm{C}}{\partial \mathrm{x}^2} - \frac{\partial S'}{\partial t} \tag{5}$$

with η the diffusion accessible porosity, D_p the pore diffusion coefficient, C the concentration in the pore water accessible for diffusion, S' the sorbed concentration, t time and x position.

The change of the sorbed concentration as a function of time is given by

$$\frac{\partial S'}{\partial t} = \eta\lambda C - \mu' S' \qquad (6)$$

with λ and μ' the rate constants of the sorption/precipitation, resp. desorption/dissolution process.

The porosities η are eliminated from (5-6) by using the notations

$$S' = \eta S \qquad \mu' = \eta\mu \qquad (7)$$

simplifying (5-6) to

$$\frac{\partial C}{\partial t} = D_p \frac{\partial^2 \mathrm{C}}{\partial \mathrm{x}^2} - \frac{\partial S}{\partial t} \qquad (8)$$

$$\frac{\partial S}{\partial t} = \lambda C - \mu S \qquad (9)$$

These equations describe three processes (sorption/precipitation, desorption/dissolution and diffusion), whose relative rates determine the behaviour of the system. The distance $L_* = (D_P/\lambda)^{0.5}$ can be considered as a characteristic distance over which a particle diffuses before it sorbes/precipitates. In the absence of a desorption/dissolution reaction ($\mu = 0$), particles cannot move much farther in the system than this distance. Similarly, $1/\lambda$ (resp. $1/\mu$) are typical times for the sorption/ precipitation (resp. desorption/dissolution) reactions.

If both these processes are fast compared to diffusion, local equilibrium is reached soon. This means that at every position

$$S = \frac{\lambda}{\mu} C \qquad (10)$$

Substituting (10) in (8) leads to

$$\frac{\partial C}{\partial t} = D_p \frac{\partial^2 \mathrm{C}}{\partial \mathrm{x}^2} - \frac{\lambda}{\mu}\frac{\partial C}{\partial t} \qquad (11)$$

which can be transformed in

$$\frac{\partial C}{\partial t} = D_{app} \frac{\partial^2 \mathrm{C}}{\partial \mathrm{x}^2} \qquad (12)$$

where the apparent diffusion coefficient D_{app} is given by

$$D_{app} = \frac{D_p}{R} \qquad (13)$$

and the retardation factor R by

$$R = 1 + \frac{\lambda}{\mu} \qquad (14)$$

Expressions (12-13) show that at local equilibrium the only effect of the sorption process is that it reduces the diffusion coefficient from D_p to D_{app}.

The assumption of local equilibrium is often made, but instead of (10), one writes traditionally

$$S' = \rho K_d C \qquad (15)$$

with ρ the dry density of the bulk and K_d a constant. In this case, the expression (14) looks as

$$R = 1 + \frac{\rho K_d}{\eta} \qquad (16)$$

Comparing (14) and (16) leads to an interpretation of K_d in terms of the rates of the sorption/desorption (or precipitation/dissolution) reaction.

Another limit case of the equation (8-9) is when the rate constants λ and μ are very low compared to the pore diffusion coefficient D_p. In that case, sorption can be neglected and diffusion occurs with the diffusion coefficient D_p.

Apart from the just mentioned limiting cases, both equations (8-9), completed with boundary and initial conditions, need to be solved completely. From the expressions for $C(x,t)$ and $S(x,t)$, the bulk concentration $C_b(x,t)$ is given by

$$C_b(x,t) = \eta\left(C(x,t) + S(x,t)\right) \qquad (17)$$

In the case of local equilibrium, this simplifies to

$$C_b(x,t) = \eta R C(x,t) \qquad (18)$$

Apart from a pore and an apparent diffusion coefficient, an effective (or simple) effective diffusion coefficient D_e exists. It is defined by the product of the porosity η and the pore diffusion coefficient D_p

$$D_e = \eta D_p \qquad (19)$$

2.3 Glass alteration layers

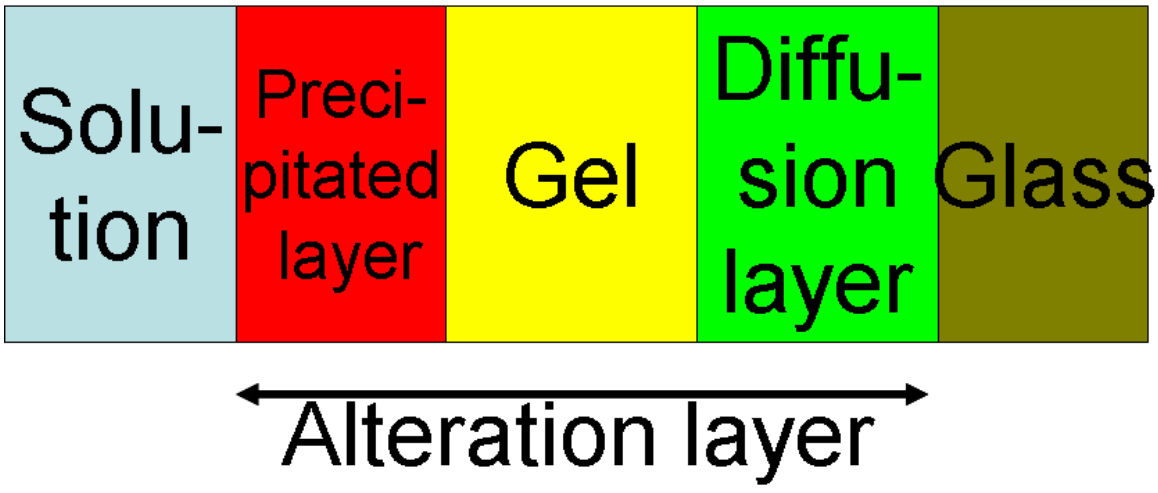

Figure 1: Schematic view of the glass alteration layers

In the present work, the **alteration layer** is defined as all glass altered by a dissolution reaction. In the present report, three types of sub-layers are distinguished (see Figure 1, other distinctions are possible as well). The **diffusion layer** is the layer closest to the pristine glass. In this (thin) layer, high diffusion gradients of alkalis, hydrogen and boron exist. Otherwise the composition of this layer is similar to the pristine glass [13]. If the solution flows sufficiently slow, the layer closest to the solution contains phases which have precipitated from solution. This layer is called the **precipitated layer**. The newly formed phases are called **secondary phases**. The layer between the diffusion layer and the precipitated layer is called the **gel** (layer). Here, the abundance and ordering of secondary phases increases with distance from the glass [13]. Most of the secondary phases have nucleated within the layers [13, 14] suggesting a local equilibrium caused by the reaction of the remaining glass components with the pore solution.

The occurrence of three distinct sub-alteration layers has also clearly been demonstrated by SIMS (Secondary Ion Mass spectroscopy) analyses, see e.g. [44, 45].

3 The effect of pH on silica dissolution

3.1 Effect on solubility

At sufficiently high pH values, next silica dissociation reactions become important

$$Si(OH)_4 \rightarrow H_3SiO_4^- + H^+ \tag{20}$$

$$H_3SiO_4^- \rightarrow H_2SiO_4^{--} + H^+ \tag{21}$$

At 90°C, the equilibrium constants of these reactions are $K_1 = 10^{-8,97}$ and $K_2 = 10^{-10,7}$ [5]. So, the total silica concentration C_{Si}^{tot} in solution can be written as

$$C_{Si}^{tot} = C_{Si(OH)4}\ f(pH) \tag{22}$$

with

$$f(pH) = 1 + \frac{K_1}{[H^+]} + \frac{K_2}{[H^+]^2} = 1 + 10^{pH-8,97} + 10^{2\,pH-10.7} \tag{23}$$

The solubility of $Si(OH)_4$ does not depend on pH, but according to expressions (22-23), at sufficiently high pH, the total silica concentration in solution at silica saturation rises sharply as a function of pH.

3.2 Effect on dissolution rate

Experiments (e.g. [15, 16, 7]) show a higher initial dissolution rate at higher pH values. Ab initio calculations [17, 18] confirm that the activation energy for breaking a siloxane bond by water

(reaction $\equiv Si - O - Si \equiv \quad + \quad H_2O \quad \rightarrow \quad \equiv Si - OH \quad + \quad \equiv Si - OH$)

is higher than the activation energy of breaking this bond by OH^-

(reaction $\equiv Si-O-Si\equiv \;+\; OH^- \;\rightarrow\; \equiv Si-OH \;+\; \equiv Si-O^-$).

3.3 Silica condensation and the protective effect

Silica condensation is the reverse reaction of the silica dissolution reaction (2). So, due to silica condensation, the number of siloxane bonds of a silica particle tends to increase. Silica condensation is demonstrated experimentally [19, 20, 21, 22] and it becomes more important when pH increases [23]. A simple explanation [12] for increased silica condensation with increasing pH is the decreased activation energy E_a (see previous section) of the silica dissolution/condensation reaction (2). Since the reaction rate is determined by the ratio E_a/RT (with R the gas constant and T absolute temperature), a lower activation energy is similar to a higher temperature. Glass is a metastable state, and escaping metastable states (like 2Si-OH instead of the lowest energy configuration Si-O-Si) gets possible by limited temperature increases. This technique is known in optimization theory (where it is called simulated annealing), but also in glass production itself. Cooling a glass smelt fast, the glass gets frozen in metastable states resulting in a low glass density. Cooling the glass at a lower rate allows escaping from metastable states, and results in a higher glass density [24]. Similarly, Bach [21, 22] concludes that a prolonged thermal treatment (annealing) at elevated temperatures (in his case between 230 and 340 °C) results in an increase of the mean bond energy of the atoms, an emanation of water and an increase of the atomic density of silica. So silica rich layers are formed by condensation. These layers contain almost no hydrogen if the thermal treatment takes place immediately after leaching. They act as a diffusion barrier for boron and (Bach considers silica-barium-boron glasses) barium. The mean bond energies measured by Bach also increase with decreasing hydrogen concentration. Since siloxane (Si-O-Si) is a lower energy state than silanol (Si-OH), this looks logical. Similarly logical is that ion exchange (interdiffusion of hydrogen and alkalis) is faster by weak, longer Si-OH bonds than by strong, shorter Si-O-Si bonds. More recent experiments by Rebiscoul [25, 26] confirm that at long leaching times, densification of gel occurs, making diffusion in these layers more difficult.

Due to silica condensation, the mean silica bond energy increases and more Si-O-Si bonds need to be broken to dissolve a silica particle. Hence, silica dissolution (and the measured dissolution rate k_f, see expression (4)) will become slower. The leaching of B and other mobile elements like the alkalis will proceed more slowly because their diffusion through the condensed surface becomes retarded. This is consistent with experimental observations. At low surface-to-volume ratio (and thus a limited pH and limited silica condensation), Chick and Pederson [27] observe that the forward rate k_f does not depend on the leaching history of the glass (redissolving an already leached glass in a new solution without dissolved silica leads to the same value of k_f). For the same glass, at high surface to volume ratios (and thus high pH values and important silica condensation), redissolution of an already leached glass leads to a much lower value of k_f [28]. More recent experiments by CEA [5] confirm this protective effect in experiments with high surface to volume ratios.

Due to silica condensation, the pore structure of the glass changes. This makes not only the forward rate k_f time dependent, but also the silica solubility C_{sat} and diffusion coefficients through the gel (see [5] for experiments and [12] for computer simulations of glass dissolution).

4 The models *r(t)* and GM2003

4.1 The *r(t)* model

4.1.1 Presentation of the model

The *r(t)* model [1] assumes a zero thickness of the diffusion layer and the precipitated layer. Hence, it considers only the gel layer.

The model also assumes that glass constituents dissolve (i) in a congruent way, and (ii) only at the pristine glass/gel interface. From there, the dissolved glass constituents diffuse through the gel towards solution. During transport, some glass components are retained in the gel. Other elements, like e.g. boron, are completely released in solution (no retention in the gel). For this

reason, the glass dissolution rate (= the glass alteration rate) ***r(t)*** (unit: m/s) is considered (defined) to be given by the boron dissolution (= boron leach) rate.

During dissolution, the position of the gel/solution interface remains fixed as a function of time. In other words, glass dissolution is considered as an iso-volume process. The dynamics of glass alteration are therefore described by the progression of the alteration front where the glass is transformed into a gel. An origin *x = 0* is chosen at the gel/solution interface. The gel thickness at time *t* is designated ***a(t)*** (unit: m) and all positions are identified by their distance *x* to the fixed gel/solution interface (where *x* = 0).

Hydrolyzed silica entering the gel at the glass/gel interface *a(t)* is transported by diffusion through the gel. This diffusive transport is described by

$$\frac{\partial C}{\partial t} = D_g \frac{\partial^2 C}{\partial x^2} \qquad (24)$$

with $C(x,t)$ the $Si(OH)_4$ concentration in the pore water of the gel (unit: g/litre),

D_g the apparent silica diffusion coefficient of in the gel pore interstitial water (unit: m^2/s).

Next, for the diffusion equation (24), a boundary condition at the gel/pristine glass and a boundary condition at the gel/solution interface are specified.

Of both boundary conditions, the easiest to derive is the boundary condition at the fixed solution/gel interface *x* = 0. Here, silica conservation for an experiment carried out with a glass surface area *S* (unit: m^2) and a (well stirred) solution volume *V* (unit: m^3) renewed at a rate F_r (unit: 1/s) is:

$$\frac{\partial C}{\partial t} = D_g \frac{S}{V}\left(\frac{\partial C}{\partial x}\right)_{x=0} - F_r C(t) \qquad (25)$$

where the notation *C(t) = C(x=0, t)* is used for the concentration at *x* = 0.

Next, the boundary condition at the gel/pristine glass interface *a(t)* is handled. Here, the matrix dissolution rate *r(t)* (unit: m/s) is given by a linear rate law

$$r(t) = \frac{\partial a}{\partial t} = r_0\left(1 - \frac{C\left(x = a(t), t\right)}{C^*}\right) \qquad (26)$$

with r_0 the maximal glass alteration rate (unit: m/s), and

C^* a glass-gel-solution interaction parameter that can be interpreted as the concentration value $C(x = a(t),t)$ at the alteration front at which the glass-to-gel transformation ceases (unit: g/litre).

It is important to note that, like the silica diffusion coefficient in the gel D_g, the parameter C^* is not an intrinsic property of the glass, but rather of the glass-gel system.

Mass conservation at the gel/pristine glass interface leads to the boundary condition at *x* = 0:

$$-D_g\left(\frac{\partial C}{\partial x}\right)_{x=a(t)} = -\left(1-f_{Si}\left(C\left(x=a(t),t\right)\right)\right)C_{g,Si}\,r(t) \qquad (27)$$

with $f_{Si}(C(x=a(t),\,t))$ the fraction of the hydrolyzed silica retained to form the gel

$1-f_{Si}(C(x=a(t),\,t))$ the fraction of hydrolyzed silica entering the pore solution of the gel, and

$C_{g,Si}$ the silicon concentration of the glass (unit: g/litre)

The silica retention function $f_{Si}(C(x = a(t),\, t))$ reflects the balance between the hydrolysis kinetics and the recondensation kinetics. It is an increasing function of the silica concentration $C(x = a(t),\, t))$ in solution. Recondensation increases as the silica concentration in pore solution of the gel rises. Next empirically derived expression (see Figure 2) is used for the silica retention function:

$$f_{Si}(C) = 1-\exp(-\alpha C) \qquad (28)$$

where α is a fit parameter (unit: $(g/litre)^{-1}$). Note that expression (28) assures that no silica is retained in the gel when the silica concentration in solution is zero. At high silica concentration in solution, almost all silica is retained in the gel.

The initial condition for the diffusion equation (24) depends on the experimental conditions.

In the *r(t)* model, the diffusion equation (24) is solved with the additional assumption that the concentration gradient of dissolved silica in the gel is constant over the gel (stationary state assumption):

$$\left(\frac{\partial C}{\partial x}\right)_{0\le x\le a} = \frac{C(x=a(t),t)-C(t)}{a(t)} \qquad (29)$$

Since the solution of the resulting 'diffusion' equation is the same as in GM, we refer to the GM chapter for it.

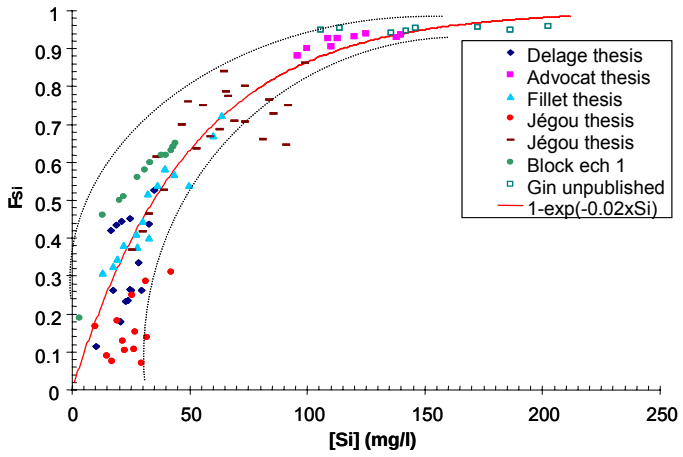

Figure 2: Evolution of the retention factor F_{Si} of silica in the gel (f_{Si}) as a function of the silica concentration in solution. The retention factor F_{Si} (= $f_{Si}(C)$ in expression (28)) is defined by $F_{Si} = 1 - \frac{C_N(t)}{C_{B,N}(t)}$ with $C_N(t)$ the normalized silica concentration in solution and $C_{B,N}(t)$ the normalized boron concentration in solution. It can be shown that this expression for F_{Si} is mathematically consistent with expression (29)

4.1.2 Additional remarks to the *r(t)* model

1. The computer code for the *r(t)* model uses a geochemical part, which also determines the final result. This geochemical part is not described in the present text. Due to this coupling, the results calculated by *r(t)* do not only depend on the already mentioned parameters and constants, but also on all values listed in the used geochemical database.

2. The code for the *r(t)* model can execute in two ways. In the first way, the pH is fixed. In the second way, the pH varies as a function of time and is calculated by the geochemical part of the *r(t)* model. In this case, next expression is used to describe the dependence on pH of the glass alteration rate r_0:

$$r_0 = \frac{k^+}{\rho_{glass}} \left[H^+\right]^{-n} \qquad (30)$$

with at 50°C k^+=1.98 10^{-7} g/(m² day) and n=0.56

at 90 °C, k^+=7.22 10^{-4} g/(m² day) and n=0.39

at 150 °C, k^+=8.08 10^{-3} g/(m² day) and n=0.40

ρ_{glass} = 2779 10^3 g/m^3 the glass density,

[H^+] the hydrogen concentration in solution.

These data result from experimental measurements. At temperatures not mentioned in expression (30), due to lack of experiments, the glass alteration rate r_0 is not adapted by the code to pH variations and r_0 is constant.

3. In the *r(t)* model, the normalized boron concentration in solution is given by

$$C_{N,B}(t) = a(t)\,\frac{S}{V}\,\rho_{glass} \qquad (31)$$

with ρ_{glass} the glass density (unit: kg/m^3)

4.1.3 Summary

The *r(t)* model considers water silica diffusion (through the gel). Dissolution is supposed to be congruent and to occur according to a linear rate law at the gel/diffusion layer interface.

Assuming that the maximal glass alteration r_0 can be measured independently of the other parameters, the *r(t)* model has three remaining fit parameters:

- D_g the pore diffusion coefficient in the gel D_g (unit: m^2/s),
- C^* the concentration at which the glass/gel transformation ceases (unit: g/litre),
- α a coefficient in the silica retention function (unit: litre/g)

All three parameters are not intrinsic properties of the glass, but properties of the glass-gel system. The *r(t)* model is also coupled to a geochemical database.

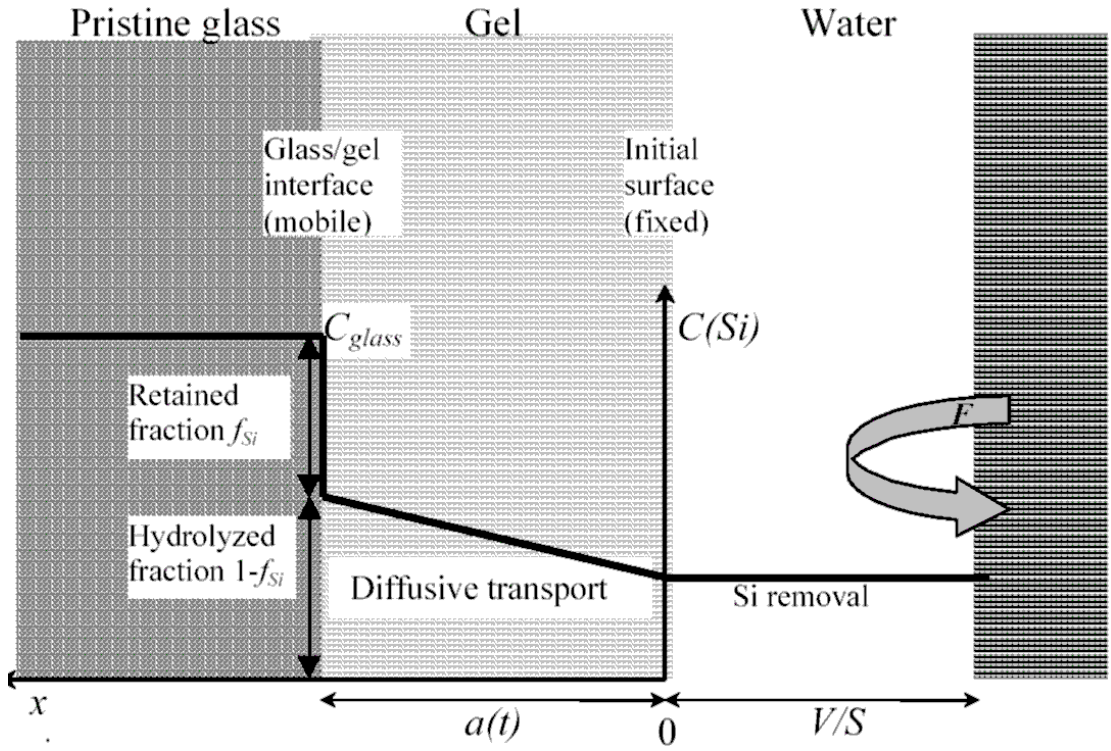

Figure 3: Schematic presentation of the *r(t)* model

4.2 The GM2003 model

4.2.1 Presentation of the model

The GM2003 model considers only the gel layer and the diffusion layer. Glass dissolution is assumed to be the result of two parallel reactions: (i) water diffusion and (ii) congruent dissolution of (part of) the glass components followed by their diffusion through the gel towards solution.

Congruent dissolution of all glass components is assumed to occur at the gel/diffusion layer interface only. From there, the dissolved glass constituents diffuse through the gel towards solution. During transport, some glass components are retained in the gel. Other elements, like e.g. boron, are completely released in solution (no retention in the gel).

During dissolution, the position of the gel/solution interface remains fixed as a function of time. In other words, glass dissolution is considered as an iso-volume process. An origin *x = 0* is chosen at the gel/solution interface. The gel thickness at time *t* is designated ***L(t)*** (unit: m) and all positions are identified by their distance *x* to the fixed gel/solution interface (where *x* = 0). The glass alteration rate ***U(t)*** (unit: m/s) is defined as the growth velocity of the gel thickness *L(t)* (*U(t) = dL/dt)*.

Water diffusion is assumed to be much slower than alkali or boron diffusion. This implies that boron and the alkalis should leach more or less congruently from the glass. This behaviour is in general observed experimentally.

Next the mathematical description of the GM2003 model is presented. The process of congruent dissolution and diffusion through the gel is treated first, followed by water diffusion.

Silica dissolution and silica diffusion in the gel

Matrix dissolution is assumed to occur at the gel/diffusion layer interface. Part of the hydrolyzed silica enters the pore solution of the gel. The remainder is retained to form the gel.

The hydrolyzed silica entering the gel is transported by diffusion through the gel. This diffusive transport is described by

$$\frac{\partial m_{Si}}{\partial t} = D_{Si} \frac{\partial^2 m_{Si}}{\partial x^2} \qquad (32)$$

with m_{Si} the molality of dissolved silica (unit: mole/kg solution), and

D_{Si} the pore diffusion coefficient of silica in the gel (unit: m^2/s).

Next, for the diffusion equation (32), a boundary condition at the gel/diffusion layer and a boundary condition at the gel/solution interface are specified.

At the gel/diffusion layer interface *L(t),* the matrix dissolution rate *U(t)* (unit: m/s) is given by a linear rate law

$$U(t) = \frac{\partial L}{\partial t} = \frac{k^+}{\rho_{glass}} \left(1 - \frac{a_{Si}}{K_{Sio2}} \right) \qquad (33)$$

with

ρ_{glass} the glass density (unit: kg/m^3),

k^+ a forward rate density (unit: kg glass/(m^2 s)),

a_{Si} the total activity of dissolved silica, and

In the context of this formula in the paper and in the code, the notion of activity and concentration are mathematically identical as long as only the ratio aSi/K is used (or Csi/C*) and as long as neither the ionic strength, not the pH changes. Hence, from a mathematical point of view (and only this counts here) there is no discrepancy for what I use in the code and in the paper. Distinction between activity and concentration needed also to be mate for the couplings between advective transport and the first order rate law. The mathematical representations of these couplings are identical in the code and in the paper.

This however is different in the new version of GM (GM2004?), in which case the pH and the ionic strength changes and an explicit distinction between concentration and activity is necessary.

K_{SiO2} the saturation constant at the dissolving glass surface

Mass conservation at the gel/diffusion layer interface leads to

$$-\phi D_{Si} \left(\frac{\partial m_{Si,\mathrm{int}}}{\partial x} \right)_{x=L(t)} \rho_{s\ln} = FS\, \beta\, \rho_{glass}\, U(t) \qquad (34)$$

with ϕ porosity of the gel layer (unit: ())

D_{Si} pore diffusion coefficient of silicic acid in the gel layer (unit: m^2/s)

$m_{Si,int}$ molality of dissolved silica at the gel/diffusion layer interface (unit: mole/kg)

ρ_{sln} solution density (to convert molality units into volumetric concentration units) (unit: kg/litre)

and where *FS* (unit: mole/kg) is a conversion factor from kg glass/(m^2 s) to mole Si/(m^2 s):

$$FS = \frac{f_{SiO2}\left(1 - f_{ret}\right)}{MG_{SiO_2}} \qquad (35)$$

with f_{SiO2} weight fraction of SiO_2 in pristine glass

f_{ret} retention factor describing the weight fraction of initially dissolved silica when it becomes incorporated into secondary alteration products or sorbed on the glass surface

MG_{SiO2} molecular weight of silica (approximately 60 10^{-3} kg/mole)

In order to facilitate comparison with the *r(t)* model, the GM2003 model has been extended so that instead of a constant silica retention factor f_{ret} a silica retention function, similar to equation (28) can be used. In that case, expression (35) is replaced by

$$FS = \frac{f_{SiO2}\left(1 - f_{Si}\left(a_{Si}\right)\right)}{MG_{SiO_2}} \qquad (35a)$$

with

$$f_{Si}\left(a_{Si}\right) = 1 - \exp\left(-f_x \frac{a_{Si}}{K_{SiO2}}\right) \qquad (35b)$$

with f_x a dimensionless fit parameter. Comparing expression (35b) to expression (28) shows directly shows the relation between f_x and α.

The dimensionless factor □ in expression (34) is

$$\beta = \frac{s_r}{s} \qquad (36)$$

with s_r total microscopic interfacial area (unit: m^2)

s macroscopic interfacial area (perpendicular to the mass transport directions) (unit: m^2)

Besides, next relations/notations are introduced as well:

$$\gamma_i = \frac{a_{Si}}{m_{Si}} \qquad (37)$$

with γ_{Si} the activity coefficient of dissolved silica (unit: ()) and m_{Si} the molality of dissolved silica, and for the concentration C_{glass} of silica in the glass (unit: kg/m^3 or kg/litre):

$$C_{glass} = f_{SiO2} \frac{MG_{Si}}{MG_{SiO2}} \rho_{glass} \qquad (38)$$

with MG_{Si} molecular weight of Si (approximately 28 10^{-3} kg/mole).

Substituting (38) and (35) in (34) leads to

$$-\phi D_{Si}\left(\frac{\partial m_{Si,\mathrm{int}}}{\partial x}\right)_{x=L(t)} \rho_{s\ln} MG_{SiO_2} = (1-f_{ret})\beta C_{glass} U(t) \tag{39}$$

The unit of the product $m_{Si,int}\ \rho_{sln}\ MG_{Si}$ is kg/litre.

During the GLAMOR project, the GM2003 was extended so that instead of the constant silica retention factor f_{ret}, also the silica retention expression of the *r(t)* model can be used in GM.

It is assumed that the solution is well stirred. This leads to next boundary condition at the gel/solution interface:

$$\frac{\partial m_{Si,CCB}}{\partial t} = -\phi D_{Si}\frac{\beta s}{V}\left(\frac{\partial m_{Si,CCBi}}{\partial x}\right)_{x=0} - \frac{F}{V} m_{Si,CCB}(t) \tag{40}$$

with $m_{Si,CCB}$ the molality of dissolved silica in the solution (at x = 0) (unit: mole/kg)

V the (macroscopic) solution volume (unit: litre or m^3)

F the flow rate (unit: m^3/s or m^3/year)

Substituting (34) in (40) leads to

$$\frac{\partial m_{Si,CCB}}{\partial t} = \frac{\beta S}{V}\frac{FS\,\rho_{glass}}{\rho_{s\ln}} U(t) - \frac{F}{V} m_{Si,CCB}(t) \tag{41}$$

The initial condition for the diffusion equation (32) depends on the experimental conditions.

In the GM2003 model, the diffusion equation (32) is solved with the additional assumption that the concentration gradient of dissolved silica in the gel is constant over the gel:

$$\left(\frac{\partial m_{Si,\mathrm{int}}}{\partial x}\right)_{0\le x\le L(t)} = \frac{m_{Si,CCB} - m_{Si,\mathrm{int}}}{L} \tag{42}$$

Details on the numerical solution of the solution are provided in 4.2.2.

Water diffusion

The penetration of water in glass is described by the diffusion advection equation

$$\frac{\partial C_{H2O,gl}}{\partial t} = D_{H2O,eff}\frac{\partial^2 C_{H2O,gl}}{\partial x^2} - U(t)\frac{\partial C_{H2O,gl}}{\partial x} \tag{43}$$

with

$C_{H2O,gl}(x,t)$ the concentration of free mobile water in the glass,

x the distance to the gel/solution interface,

$D_{H2O,eff}$ the effective diffusion coefficient of water molecules in the dry glass (unit: m^2/s), and

$U(t)$ the time-dependent matrix dissolution rate (unit: m/s).

To avoid possible confusion, the diffusion coefficient $D_{H2O,eff}$ is an effective diffusion coefficient in the homogeneous solid phase (porosity = zero) not affected by retention (reaction of water with the glass network to form silanol groups), and the definition of the effective diffusion coefficient in porous media according to (19) is not applicable here.

The boundary conditions are:

(i) $C_{H2O,gl}(x=0,\ t>0)$ = 1kg/litre which is the density of water, and
(ii) $C_{H2O,gl}(x\rightarrow\infty,\ t>0) = 0$.

The initial condition is $C_{H2O,gl}\ (x>0,\ t=0) = 0$ where zero time is the moment that glass dissolution starts.

For details on the numerical solution of equation (43), we refer to 4.2.3.

Water diffusion in the diffusion layer from the gel towards the pristine glass is accompanied by diffusion of boron and the alkalis from to pristine glass towards the gel. It is assumed that at every position x in the gel, boron and alkali in the diffusion layer have a mobile fraction $f_{m,i}(x,t)$ (the index i refers to boron or an alkali) supposed to have diffused out of the diffusion layer, and an immobile fraction $f_{im,i}(x,t)$ still present in the diffusion layer. The ratio of both fractions is supposed to be proportional to the free mobile water concentration $C_{H2O}(x,t)$ in the diffusion layer:

$$\frac{f_{m,i}(x,t)}{f_{im,i}(x,t)} = \frac{\phi\, C_{H2O}(x,t)}{K_{d,i}} \qquad (44)$$

with Φ a formal porosity of the glass and $K_{d,i}$ a proportionality constant (unit: kg/litre or kg/m^3). Expression (44) implies that the ratio between the mobile and immobile fractions of an element i in the glass is directly proportional to the water concentration in the hydrated glass with $1/K_{d,i}$ being a proportionality constant. The higher the $K_{d,i}$, the larger is the immobile (retained) fraction in the hydrated glass. In this sense we can speak of a retention coefficient but this distribution parameter in the homogeneous hydrated glass phase in units of kg/m^3 shall not be misunderstood in terms of a distribution coefficient K_d in units of m^3/kg for a heterogeneous porous media (distribution between 2 phases at a phase boundary) as introduced in the expressions (15) and (16). However, similarly to the K_d concept in porous media, where the sorbed concentration is proportional to the concentration in solution, we can say for the homogeneous phase that the mobile fraction of an element i is proportional to the concentration of water.

The quantity Φ is a formal "porosity" of the glass; it must not be confounded with the porosity of the gel layer. It shall however be clarified that in reality, the hydrated glass is a homogeneous phase and is not phase separated into a water filled pore space and a residual water free glass skeleton. The product $C_{H2O,gl}$ Φ corresponds to the mass of water dissolved in a unit volume of glass.

According to GM2003, boron and alkali are depleted from the diffusion layer according to a typical length L_i given by

$$L_i(t) = \int_0^\infty \frac{f_{m,i}(x,t)}{f_{m,i}(x,t) + f_{im,i}(x,t)}\, dx \qquad (44a)$$

In fact the integral in (44a) should go over the diffusion layer only, but since in the pristine glass $f_{m,i}(x,t)$ becomes zero, it can be included in the integral as well. Substituting (44) in (44a) leads to

$$L_i(t) = \int_0^{\infty} \frac{\phi\, C_{H2O}(x,t)}{K_{d,i} + \phi\, C_{H2O}(x,t)}\, dx \qquad (44b)$$

Depending on the value of the $K_{d,i}$ coefficient, the diffusion depth of an element *i* may be larger or smaller than the average penetration depth of water. Depletion depths larger than the penetration depth of water are meaningful for certain cases, as it cannot be excluded that even a partial hydration of the glass phase leads to 100 % mobilisation of a given ion. Depletion depths much smaller than the water penetration depth are likely to occur for many immobile elements.

It is interesting to note the conditions under which the penetration depth of water exactly equals the depletion depth of an element *i:* We may define as depletion depth the depth at which the mobile fraction of a given element is half the total concentration ($f_{m,i}/f_{im,I}$ = 1) and a water penetration depth we may define as the depth where $C_{H2O,gl}$ is half of its maximum value of 1000 kg/m^3. Using a Φ value of 0.2 (as in the present work) we can calculate from Eq (44) that a $K_{d,i}$ of 100 kg/m^3 leads to equal values for depletion depth and penetration depth (see also figure 4). Figure 4 shows the calculated concentration profiles for the experiment A2 at a given time step (a) for a $K_{d,i}$ of 100 kg/m^3 and (b) a $K_{d,i}$ of 10 kg/m^3.

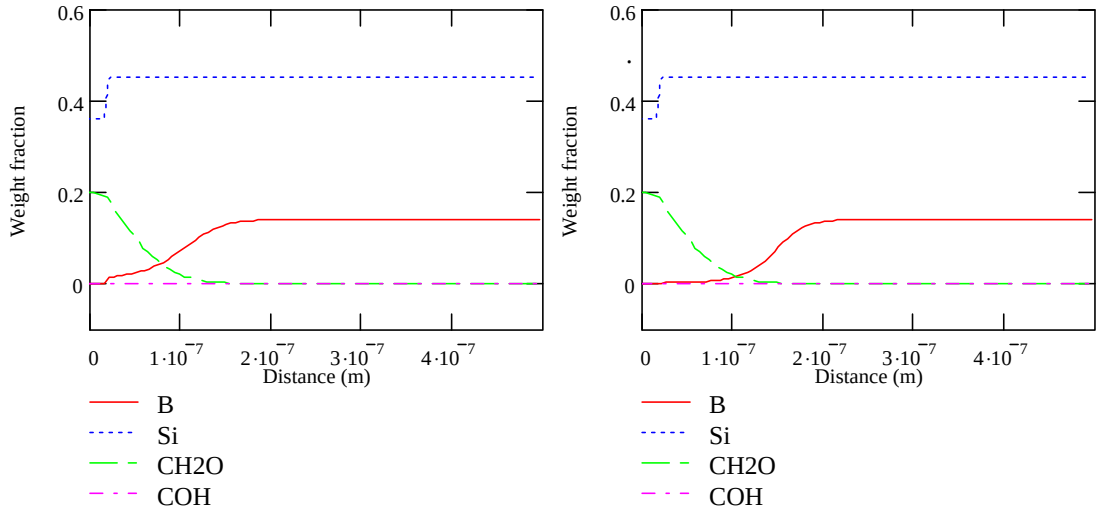

Figure 4: Calculated concentration profiles for B, Si, H2O for the experiment A2 after 596 days. The concentration of SiOH="COH" is included as well but is set at a value of zero. (a) for a $K_{d,B}$ of 100 kg/m^3 and (b) for a $K_{d,B}$ of 10 kg/m^3

It can be seen that for a $K_{d,B}$ of 100 kg/m^3 the depletion depth of B is about equal to the penetration depth of water, while a $K_{d,B}$ of 10 kg/m3 corresponds to a depletion depth of B higher than that of water (which is not impossible but not very realistic).

For large values of $K_{d,i}$ and a sufficiently small time *t*, so that $K_{d,i} >> \Phi\, C_{H2O,gl}(x,t)$, expression 44b becomes

$$L_i(t) \approx \frac{\phi}{K_{d,i}} \int_0^{\infty} C_{H2O,gl}(x,t)\, dx \qquad (45)$$

Expression (45) clearly shows that $L_i(t)$ is proportional to $\int_0^{\infty} C_{H2O,gl}(x,t)\, dx$, which is apart from a constant, the average intrusion length of water in the glass.

The corresponding concentrations in solution *i* are obtained by solving an equation similar to expression (41):

$$\frac{\partial m_i}{\partial t} = \frac{\beta s}{V} \frac{C_{i,glass}}{\rho_{s\ln} MG_i} \frac{\partial L_i}{\partial t} - \frac{F}{V} m_i(t) \qquad (46)$$

with

$C_{i,glass}$	the concentration of element *i* in the glass
MG_i	the molecular weigth of element i

The concentration $C_{i,glass}$ is calculated similar to expression (38) for the silica concentration in the glass. As example, for boron this is

$$C_{glass} = f_{B2O3} \frac{2MG_B}{MG_{B2O3}} \rho_{glass} \qquad (47)$$

with

f_{B2O3}	weight fraction of B_2O_3 in pristine glass
MG_{B2O3}	molecular weight of B_2O_3 (approximately 69.64 10^{-3} kg/mole)
MG_B	molecular weight of Si (approximately 10.82 10^{-3} kg/mole).

Finally, assuming that in the diffusion equation (43) the rate *U(t)* becomes zero very soon, the solution of this equation is in very good approximation given by

$$C_{H2O,gl}(x,t) = C_{H2O,gl}(x=0, t>0)\, erf\left(\frac{x}{2\sqrt{D_{H2O,eff}\, t}}\right) \qquad (48)$$

Substituting expression (48) in expression (45) leads to

$$L_i(t) \approx \frac{\phi}{K_{d,i}} \frac{2\, C_{H2O,gl}}{\sqrt{\pi}} \sqrt{D_{H2O,eff}\, t} \qquad (49)$$

According to expression (49), it is not possible to determine from the leach data of element *i* the values of the two parameters $K_{d,i}$ and $D_{H2O,eff}$ since these parameters are totally correlated.

Hence, as long as solid state diffusion profiles are not measured and as long as diffusion coefficients have to be deduced from solution data, it is important to fix the $K_{d,i}$ value of a reference element such as boron at a value which always allows equal water penetration depth and elemental depletion depth.

4.2.2 Solution of the silica diffusion equation

4.2.2.1 Analytical part of the solution

An analytical solution of equation (34) is possible by assuming that

(i) the concentration gradient $(\delta m_{Si,int}/\delta x)$ is constant over the gel,
(ii) the length L remains constant,
(iii) the molality $m_{Si,CCB}$ (unit: mole/kg) of dissolved silica in the solution (at $x = 0$) remains constant

It is evident that assumptions (ii) and (iii) are not valid during the entire dissolution experiment. However, it remains interesting to consider this case (A) for a better understanding, (B) at infinitesimal time steps the assumptions can be considered as valid, and (C) since equation (3) can also be used for describing glass dissolution next to a porous medium (where assumptions (ii) and (iii) can be realistic).

Assuming (i), (ii) and (iii), leads to

$$\left(\frac{\partial m_{Si,\mathrm{int}}}{\partial x}\right)_{0\le x\le L(t)} = \frac{m_{Si,CCB} - m_{Si,\mathrm{int}}}{L} \qquad (50)$$

which is expression (42), similar to expression (29) in the *r(t)* model. After substituting (50) in (34), the resulting expression can be solved for $m_{Si,int}$. Substituting this expression for m_{Si} in (33) leads to

$$U(t) = \frac{k^+}{\rho_{glass}}\left(1-\gamma_{Si}\frac{k^+ FS\,\beta\,L + \phi\,D_{Si}\,m_{Si,CCB}\,\rho_{s\ln}}{K_{SiO2}\,\phi\,D_{Si}\,\rho_{s\ln} + k^+\,FS\,\gamma_{Si}\,\beta\,L}\right) \qquad (51)$$

This term is used in GM2003 in the numerical model. Introducing the notation

$$L^* = \frac{\phi\,D_{Si}\,\rho_{s\ln}\,K_{SiO_2}}{FS\,\beta\,\gamma_{Si}\,k^+} \qquad (52)$$

the expression (51) can also be written as

$$U(t) = \frac{k^+}{\rho_{glass}}\frac{1}{1+\dfrac{L}{L^*}}\left(1-\frac{\gamma_{Si}m_{Si,CCB}}{K_{SiO_2}}\right) \qquad (53)$$

showing that the dissolution rate *U(t)* depends on **only three 'overall parameters': k^+/ρ_{glass}, L/L^* and $\gamma_{Si}\,m_{Si,CCB}/K_{SiO2}$**. The silica diffusion coefficient D_{Si} only appears in the solution (53) via the combination L/L^*. Substituting expression (35) in expression (52) leads to

$$L^* = \frac{\phi\,D_{Si}\,\rho_{s\ln}\,K_{SiO_2}\,MG_{SiO_2}}{\gamma_{Si}\,k^+\,L\,\beta\,f_{Si}\,(1-f_{ret})} \qquad (54)$$

So when fitting the silica diffusion coefficient D_{Si}, its value is correlated with the values of all other parameters in expression (54), in particular with the saturation constant K_{SiO2} and the silica retention factor f_{ret} (which, apart from D_{Si}, are the only parameters which are fitted, the other parameters are assumed to have a known value in GM). From error propagation theory follows that the relative error on the value of the silica diffusion coefficient is larger than the relative errors on K_{SiO2} and f_{ret}:. Of the three parameters D_{Si}, K_{SiO2} and f_{ret}, the value of D_{Si} is the most

imprecise. Concerning correlations, from expressions (52-53-54) one expects that during fitting, larger values of K_{SiO2} lead to lower values of D_{Si}. Indeed, increasing the value of K_{SiO2} during a fit leads to a larger value of $\left(1-\frac{\gamma_{Si} m_{Si,CCB}}{K_{SiO_2}}\right)$. Since the measured value *U(t)* is constant, this decrease needs to be compensated (see expression 53) by a smaller value of *L**, which means a smaller value of D_{Si} (if all the other parameter values are kept constant).

As a result of the assumptions (i), (ii), (iii), the dissolution rate *U(t)* in expression (53) is independent of time. Evidently, in reality, the width of the gel *L* and the concentration (molality) of dissolved silica in solution $m_{Si,CCB}$ are not constant (assumptions (i) and (ii)) but increase as a function of time. Both the increasing width of the gel and the higher silica concentration in solution lead to a decreasing dissolution rate *U(t).* The dissolution rate *U(t)* becomes zero only at silica saturation ($m_{Si,CCB} = K_{SiO2}/\gamma_{Si}$).

Two limit cases can be distinguished in (53). If ***L* >> L* (strong diffusion)** then according to (50), the dissolution rate *U(t)* is approximated well by

$$U(t) = \frac{k^+}{\rho_{glass}}\left(1-\frac{\gamma_{Si}\, m_{S,CCBi}}{K_{SiO_2}}\right) \qquad (55)$$

Since the overall dissolution rate *U(t)* does not depend anymore on the diffusion coefficient D_{Si}, overall dissolution is controlled by the dissolution at the pristine glass/gel interface.

Alternatively, if ***L* <<L* (weak diffusion)**, the dissolution rate *U(t)* is approximated well by (see 53)

$$U(t) = \frac{1}{\rho_{glass}} \frac{\phi\, D_{Si}\, \rho_{s\ln}\, K_{SiO_2}\, MG_{SiO_2}}{\gamma_{Si}\, L\ \beta\ f_{Si}\left(1-f_{ret}\right)}\left(1-\frac{\gamma_{Si} m_{Si,CCB}}{K_{SiO_2}}\right) \qquad (56)$$

The overall dissolution rate *U(t)* does not depend anymore on the forward rate k^+ and is again controlled by the slowest process: in this case, diffusion through the gel.

The just discussed two limit cases are related to the evolution with time of the system. Indeed, since a pristine glass has no gel, the initial width *L* of the gel is zero. So, at zero time, expression (53) is always reduced to expression (55). From then on, the width *L* of the gel increases, leading to a monotonous decrease of the factor $\frac{1}{1+\frac{L}{L*}}$. After some time, the condition of weak diffusion $L^* << L(t)$ can be reached and expression (53) becomes very well approximated by expression (56). Depending on the parameter values, the condition of weak diffusion $L^* << L(t)$ can be reached far below saturation. In that case, one observes an initial drop of the dissolution rate *U(t)* due to diffusion through the gel, instead of silica saturation. On the other hand, it is possible that during the entire dissolution process $L^* >> L$, so silica diffusion is never relevant. This occurs for instance at high values of the silica diffusion coefficient (see expression (54)). So, at sufficiently high values of the silica diffusion coefficient, its precise value does not influence the dissolution rate at any time.

4.2.2.2 Numerical part of the solution

The overall reaction time t is divided into a sequence of time steps Δt_i and for each time step i, the reaction rate U_i is calculated by (51). The time step Δt_i is sufficiently small for not influencing the results.

The thickness of the gel L is given initially a very small value (e.g. 10^{-10} m). Then with the rate U_i, it is increased by $\Delta L_i = U_i \Delta t_i$.

Similarly, the molality of silica in solution m_{Si} is increased by $\Delta m_{Si,CCB} = U_i FS \Delta t_i s \beta / V + F \Delta t_i m_{i-1,CCB} / V \rho_{sln}$.

4.2.3 Numerical solution of the water diffusion equation

Equation (43) is solved by a finite difference representation, using a forward time-space centred algorithm

$$C_{t+1,j} = C_{t,j} + D_{H2O,eff} \frac{C_{t,j+1} - 2C_{t,j} + C_{t,j+1}}{\Delta x^2} \Delta t - U_t \frac{C_{t,j+1} - C_{t,j-1}}{2\Delta x} \Delta t \qquad (57)$$

4.2.4 Summary

The GM2003 model considers water diffusion (through the gel and through the diffusion layer) as well as silica diffusion (through the gel). Dissolution is supposed to be congruent and to occur according to a linear rate law at the gel/diffusion layer interface.

The model has six fit parameters:

K_{SiO2}	a silica saturation constant at the gel/diffusion layer interface,
f_{ret}	retention factor describing the weight fraction of initially dissolved silica when it becomes incorporated into secondary alteration products or sorbed on the glass surface
D_{Si}	the diffusion coefficient of silica in the gel (unit: m^2/s)
$D_{H2O,eff}$	the effective diffusion coefficient of water molecules in the dry glass (unit: m^2/s)
$K_{d,B}$, $K_{d,Li}$	"sorption constants" for boron and lithium in the diffusion layer (unit: kg/litre)

Other parameters like

k^+	a forward-rate density (unit: kg glass/(m^2 s)),
ϕ	porosity of the gel layer

are not varied and supposed to be known.

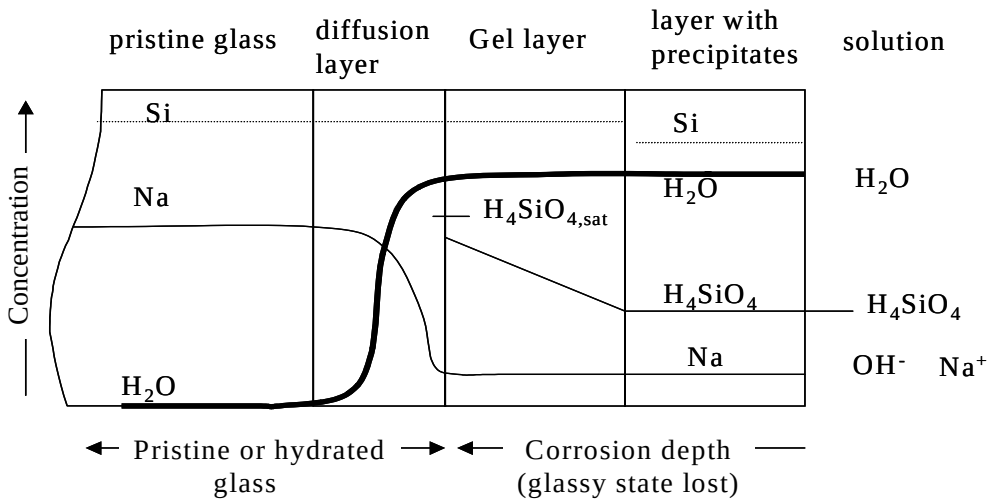

Figure 5: Schematic presentation of the GM2003 model

4.3 Similarities and differences between the *r(t)* model and GM2003

The *r(t)* model and the GM2003 model are to a large extent similar. Both consider silica diffusion in a largely similar way. The major differences between both models are (i) the GM2003 model considers also water diffusion and boron and lithium retention in the diffusion layer, and (ii) the *r(t)* has a geochemical part. The GM model also allows calculating element profiles in the diffusion layer.

4.3.1 The silica dissolution/diffusion parameters

For allowing an immediate comparison between the basic equations and the notations used in both models, the sections describing each model have been structured as much as possible in the same way. Both models describe silica dissolution/diffusion in nearly the same way. They use the same quantities, but not the same notations for these quantities or the same interpretation of these quantities.

In order to be able to compare the numerical values of the same parameters of both models, we must know the relation between them. This is what we list here. The comparison of the interpretation of these parameters is presented in section 5.

The forward rate k_f

Notation used in *r(t):* r_0 (unit: m/s)

Notation used in GM: k^+ (unit: kg glass/(m^2 s))

Relation between both (see expression (33)):

$$r_0 = \frac{k^+}{\rho_{glass}} \qquad (58)$$

with ρ_{glass} the glass density (unit: kg glass/m^3)

Remember (see section 4.1.2) that at some temperatures, the *r(t)* model does not use a constant forward rate r_0, but a forward rate varying with pH (see expression (30)).

The 'saturation concentration' C_{sat}

Notation used in *r(t):* C* (unit: g/litre)

Notation used in GM: K_{SiO2} (unit: mole/kg)

Relation between both:

The constant K_{SiO2} gets a similar unit as C^* by multiplying K_{SiO2} with the product ρ_{sln} MG_{Si} (notations used in GM: ρ_{sln} is the solution density (unit: kg/litre), MG_{Si} is the molecular weight of silica (28 10^{-3} kg/mole)).

Although now both constants have similar units (unit K_{SiO2} ρ_{sln} MG_{SiO2}: kg/litre), the constant C^* refers only to $Si(OH)_4$ while K_{SiO2} considers all silica in solution. This means that C^* needs to be multiplied with a function *f(pH)* of pH (see expressions (22-23)) to get the corresponding K_{SiO2} value. If *r(t)* is used in the mode of variable pH, the most logical pH value to take is the final pH value calculated in the *r(t)* model. The model *r(t)* also allows a non-zero final silica dissolution rate, so that silica concentrations higher than C* can be reached.

The silica diffusion coefficient in the gel

Notation used in *r(t):* D_g (unit: m^2/s)

Notation used in GM: D_{Si} (unit: m^2/s)

Relation between both:

$$D_g = \phi D_{Si} \qquad (59)$$

with ϕ the porosity of the gel layer (unit: ())

This relation looks clear from comparing expressions (25) and (27) in the *r(t)* section with expressions (39) of and (40) in the GM section. Comparing the silica diffusion equations of both models (expressions (24) and (32)), one could incorrectly conclude that $D_g = D_{Si}$. Since in reality both models use a simplified 'diffusion equation' (see section 4.2.2.1) instead of the real diffusion equations (24) and (32), comparison must be based on the simplified equation. Expression (25) also clearly shows that D_g is an effective diffusion coefficient (instead of an apparent diffusion coefficient as pretended in section 4.1.1) (see expression (19)).

The silica retention function

Originally, the GM model only allowed a constant silica retention function f_{ret}. During the GLAMOR program, GM was modified so that also the silica retention function $f_{Si}(C)$ of the *r(t)* model (expression (28)) could be used in it (with exactly the same notations in both models). The value of the constant silica retention function f_{ret} (GM) can also be compared with the values of the silica retention function $f_{Si}(C)$ (see expression (28) of *r(t)*) .

The final dissolution rate

The status of this parameter is not entirely clear. In the published texts of both models [1, 2], this parameter is not mentioned at all. Still, it is included in both models, and it was used during the GLAMOR project (in particular by the *r(t)* model). Although the theoretical origin of this parameter is not entirely clear, it is related to the fact that even at 'silica saturation' the transformation of pristine glass into gel can go on (since glass is a metastable instead of a stable state). Besides, a (constant) final rate is sometimes observed experimentally.

Due to the obscurity of the final rate, it is not surprising that both models apply it in a different way. In GM, the final rate only relates to boron and alkali dissolution. In *r(t),* it also concerns silica dissolution, allowing to increase calculated silica concentrations above the 'silica saturation concentration' C_{sat} and rising questions about the meaning of this parameter.

4.3.2 The silica dissolution/diffusion concept

4.3.2.1 Differences between both models

1. The model *r(t)* is coupled with a geochemical part, calculating e.g. pH.

2. Although both models use at first sight the same rate law, this is not so in the mode of variable pH in the *r(t)* model. The reason is that both models adapt the linear rate law to silica dissociation in a different way.

Using the notations *U(t)* for the matrix dissolution rate and r_0 for the maximal rate, then (apart from an activity coefficient γ in GM, which is supposed to be equal to one) the linear rate law in both models is (see also expression (26) in 4.1 and expression (33) in 4.2)

GM $$U(t) = r_0 \left(1 - \frac{C_{Si}^{tot}}{K'_{SiO2}} \right) \qquad (60)$$

r(t) $$U(t) = r_0 \left(1 - \frac{C_{Si(OH)_4}}{C^*} \right) \qquad (61)$$

with K'_{SiO2} the saturation constant K_{SiO2} expressed in g/litre

C^* the 'saturation' constant of the *r(t)* model

C_{Si}^{tot} the concentration of dissolved silica in the pore water of the gel,

$C_{Si(OH)4}$ the $Si(OH)_4$ concentration in the pore water of the gel,

The relation between the total silica concentration C_{Si}^{tot} and the concentration $C_{Si(OH)4}$ of $Si_{(OH)4}$ is given by the expressions (22-23). According to expression (23) is $C_{Si}^{tot} = C_{Si(OH)4}\ f(pH)$ with pH the actual pH. Expression (23) also converts C^* to K'_{SiO2}, but since both C^* and K'_{SiO2} are constants, the question is which pH should be used in expression (23)? The most obvious choice looks the final pH (for which the notation pH_{fin} is used), leading to

$$K'_{SiO2} = C^*\ f(pH_{fin}) \qquad (62)$$

Substituting the expressions (23) and (62) in expressions (60) gives

GM $$U(t) = r_0 \left(1 - \frac{C_{Si}^{tot}}{K'_{SiO2}} \right) = r_0 \left(1 - \frac{C_{Si(OH)4}}{C^*} \frac{f(pH)}{f(pH_{fin})} \right) \qquad (63)$$

This clearly shows that unless $pH = pH_{fin}$, (which is only true at all times for a fixed pH) the matrix dissolution rate *U(t)* calculated by both models is different.

3. Both models allow the use of a final constant dissolution rate. In *r(t),* this final rate refers to silica, boron and the alkalis. In GM, it only refers to boron and the alkalis, not to silica.

4.3.2.2 Discussion of the similarities in both models

The concept of silica diffusion as it is used in both models is doubtful. Other glass dissolution models (like e.g. STORM [29]) are always based on silica dissolution (although some with an adapted rate law), but most do not consider silica diffusion. This subject is discussed more in detail in 5.4.

Both models allow the use of a final dissolution rate. No physical explanation of this dissolution rate is given. It is not clear how this final dissolution rate affects the gel thickness (or in GM possibly the thickness of the diffusion layer).

Both models do not solve the silica diffusion equation but a linearised simplification of it. Given the small thickness of the gel, for sufficiently high values of the silica diffusion coefficient this simplification is probably OK. For small silica diffusion coefficients, this might not be so.

4.3.3 Water diffusion in the gel

In closed systems, the solution will eventually always become silica 'saturated'. At silica saturation, according to both models, the thickness of the gel will not change anymore as a function of time. At silica saturation, however water diffusion still goes on. So, the width of the diffusion layer will still increase as a function of time. Besides, leaching of boron and the alkalis continues as well.

5 Discussion of the model parameters

Although both models describe silica diffusion by nearly the same mathematics, their interpretation of the model parameters is sometimes different. It is obvious that this difference is only a matter of **semantics**. Therefore, all parameters, as well as their possible different definitions in both models, are discussed. It is also explained how every parameter can be measured (by preference in an independent way), and, if possible, an estimate of the order of magnitude of its value is made. Due to pH variations, and a possible change of the glass pore structure during the dissolution experiment (see the protective effect), the value of some parameters can change during the dissolution experiment. As a result, the values determined experimentally are not always very accurate and are sometimes only representative for a certain period in the dissolution experiment. If the variation of the value remains limited, this does not need to be a problem.

5.1 The forward rate k_f

Since this is the glass dissolution rate for zero silica concentration in solution (see the linear rate law expression (4)), this rate can be determined with standard test procedures [46,47]. Therefore, in both models *r(t)* and GM, this parameter is not considered a fit parameter but given a measured value.

The value of the forward rate depends on pH, which the *r(t)* model takes into account by using expression (30). In the GM version used in GLAMOR, the pH dependency of the forward rate is ignored.

Due to the protective effect, the value of the forward rate can also change during a dissolution experiment, in particular at high pH.

5.2 The saturation concentration C_{sat}

Theoretically, this concentration can easily be measured, since according to the linear rate law (see expression (4)) it is the concentration at which net silica dissolution should stop. This agrees with the definition used in GM: the saturation constant at the dissolving glass surface. The definition used in the *r(t)* model is:

*C** a glass-gel-solution interaction parameter that can be interpreted as the concentration value *C(x=a(t),t*) at the alteration front at which the glass-to-gel transformation ceases

The *r(t)* definition of *C** emphasizes that *C** is the final (large time) silica concentration at the gel/glass interface, which could suggest that the final silica concentration in solution differs from that at the gel/glass interface *C**. According to the mathematics of the model, dissolution stops only when the concentrations in solution and at the gel/glass interface are equal. So *C** also needs to be the final silica concentration in solution.

In the *r(t)* model, it is stressed that ***C** is not an intrinsic property of the glass, but of the glass/gel system**: dissolution experiments performed at different circumstances lead to different gels and thus also different *C** values. This looks acceptable: (at large times,) the solution is only in contact with altered glass, not with pristine glass. Since the gel has a lower energy state than the metastable glass, it looks evident that *C** is some kind of gel 'solubility', having a lower value than 'pristine glass solubility'. Experiments in which pristine glass samples are put in a 'silica saturated' solution of another glass, confirm this [5]. So, according to *r(t)* semantics, 'glass solubility' can change during dissolution experiments and *C** is the some kind of final 'gel solubility'. This situation can be compared to the dissolution of metals, which are thermodynamically unstable in aqueous media, but become stabilized by the formation of a passivation layer.

A remaining major problem for the definition of *C** in the *r(t)* model is that the *r(t)* model allows a non zero constant final silica dissolution rate, allowing silica concentrations to rise to values much higher than *C**. Evidently, silica concentrations above silica saturation (solubility) are impossible. It is not clear how to solve this problem in the interpretation of *C**. In GM, no non-zero constant final silica dissolution rate is allowed, making it possible to use the word 'solubility'. Experiments have to show if a non zero constant final silica dissolution rate exists or not.

Another problem in the interpretation of the 'saturation concentration' is: 'Does it concerns only the $Si(OH)_4$ concentration in solution (like C* in *r(t)*), or the total silica concentration in GM (like K_{SiO2} in GM)? Evidently, this problem is related to how to adapt the linear rate law to silica dissociation. The conversion between the values of the 'saturation concentrations' of both models can be done by using expressions (22-23)

5.3 The silica retention function

The expression for the silica retention function in the *r(t)* model (expression (28), one fit parameter: α) is purely empirical. Its justification comes from fitting the ratio of normalized silica concentration to normalized boron concentration in solution to expression (28) of the *r(t)* model (see also Figure 2).

In the GM model, the same expression can be used for the silica retention factor (this was introduced in order to facilitate comparison with the *r(t)* model) as well as a constant silica retention factor f_{ret}. Similar to *r(t),* this constant factor f_{ret} is determined by fitting solution data.

5.4 The silica diffusion coefficient in the gel

Of all parameters used in both models, this parameter is the most problematic: the reported values for it vary over many orders of magnitude, independent measurements of its value hardly exist and there are doubts about the relevance of silica diffusion for describing glass dissolution (other models like e.g. STORM [29] describe glass dissolution without taking silica diffusion into account).

Why do both models consider silica diffusion? Experiments show the influence of the dissolved silica concentration on the glass dissolution rate, which is in a simple way described by the linear rate law expression (4). This expression provides a simple differential equation for the silica concentration in solution *C(t),* of which the solution is:

$$C(t) = C_{sat}\left(1 - \exp\left(-\frac{k_f\, SAt}{V\, C_{sat}}\right)\right) \qquad (64)$$

This expression contains only two parameters (k_f and C_{sat}), which can both be measured. The problem is that, except at short times (where k_f is measured) and at long times (where C_{sat} is determined), the experimental data are always below the prediction (64). How to explain this? Element profiles of the (altered) glass show that alkalis and boron dissolve not from the glass/solution surface but from the diffusion layer. In general, the alkalis and boron leach congruently, and in the initial stage of dissolution (in a solution without silica), silica mostly leaches congruently as well. So, the assumption is made that silica also dissolves from the diffusion layer (whose thickness is assumed to be zero in the *r(t)* model). Then silica diffuses through the gel layer, causing, compared to the prediction (64), a delay in the rise of silica in solution. This delay is characterized by the silica diffusion coefficient in the gel, which provides an additional fit parameter to expression (64). Varying this parameter allows a better agreement between predicted and experimental data. In particular in dynamic tests, where the silica concentration in solution initially rises up to a maximum after which it decreases again, a silica diffusion coefficient is needed according to Grambow [30, 31] in order to have a silica peak calculated by the model

The assumption of silica dissolution at the glass side of the gel, made in both *r(t)* and GM, has never been proven: only arguments exist. Glass is a metastable state in which a wide distribution of siloxane distances (and thus also bond strengths) exists. It sounds OK to assume that only the silica particles in the highest energy states (so the weakest bond strengths) dissolve, while the rest remains unaltered. In this way, silica dissolution from the gel/pristine glass interface can make sense. On the other hand, the lower the number of siloxane bonds that a silica particle has, the easier it will dissolve. Particles on the gel/solution interface evidently have a lower number of siloxane bonds than particles inside the glass/gel. So, it looks more evident that silica dissolves from the glass/solution interface than from inside the glass. An additional problem is that possibly the pore structure in the gel changes, making a diffusion coefficient in the gel time or position dependent.

Although the silica diffusion coefficient in the gel is a fit parameter, intended to lead to better agreement between experimentally measured dissolution data and model predictions, its fitted value is generally very inaccurate. Remember 4.2.2.1, in particular expression (53-54), showing that the silica diffusion coefficient only enters the predicted dissolution data by the length *L**, making that the value of the silica diffusion coefficient is highly correlated with all other parameters of the silica diffusion part of both models (the correlation with the saturation constant C* was illustrated more extensively in 4.2.2.1) and resulting in a high relative error of the silica diffusion coefficient. Besides, in some cases (weak diffusion) the value of the silica diffusion coefficient hardly affects the predicted behaviour.

Although silica diffusion is uncertain, it is possible to estimate by comparison with other media having similar porosities and pore sizes as the gel, an expected value for the silica diffusion coefficient in the gel. If fitting dissolution data leads to similar values, this would support the assumption of silica diffusion. The next two sections provide such estimates. It has already been mentioned that due to the hypothesis of a linear concentration gradient in the gel, made in both models, only the value of the effective diffusion coefficient matters (see expression (54) and the explanations around expression (59)). Since at least the magnitude of the porosity of the gel is more or less known (estimations based on the amount of boron and alkalis in the glass), it is possible to discuss the pore diffusion coefficient instead of the effective diffusion coefficient (remember expression (19)). Besides, we also discuss the value of the apparent silica diffusion coefficient, since (i) it has at least been measured, and (ii) it might become relevant if the assumption of a stationary linear profile (expressions (29), (42) and (50)) made by both models is not valid.

5.4.1 The pore diffusion coefficient

In porous media, the pore diffusion coefficient is nearly similar for most ionic aqueous species [32]. In boom clay, its value is about 2 10^{-10} m^2/s to 5 10^{-10} m^2/s for a porosity of about 0.35 to 0.4 at around 25°C. Measurements of the silica diffusion coefficient in boom clay lead to a slightly lower value: 6 10^{-11} to 1 10^{-10} m^2/s [33].

Pore diffusion coefficients in porous media do not tend to differ much from the self diffusion coefficient of water (around 2 10^{-9} m^2/s [32]). In partially saturated porous media, it is possible to measure the diffusion coefficient as a function of volumetric water content. Measurements show a gradual decrease of the diffusion coefficient as the water content decreases, followed by a steep drop-off at low water contents due to the loss of continuous pathways (see Figure 6). The diffusion coefficients for all materials fall into a narrow range and demonstrate that the diffusion coefficient is dependent primarily on water content, and secondary on the material type. According to Figure 6, an estimated gel porosity (= volumetric water content) of 0.2 for glasses should lead to a gel pore diffusion with an order of magnitude around 10^{-10} m^2/s.

A similar trend as in Figure 6 is seen in Figure 7 and Figure 8, showing the impact of the pore radius on the water diffusion coefficient in zeolites. For large pores (pore sizes larger than ≈ 7 Å), diffusion in the pores is nearly as fast as in molecular water (and largely independent of pore size). For smaller pores, the pore size has an enormous impact on the water diffusion coefficient. Measured gel pore sizes in glass (gel) are listed in Figure 9. Almost all values here are larger than 7 Å, so that the expected pore diffusion coefficient is again around 10^{-10} m^2/s.

According to Rebiscoul [26], the final gel can consist of two sub layers: an open porous layer at solution side and a dense layer at the glass side. In this case, diffusion through the dense layer is rate limiting, and diffusion through the porous part is not very relevant. The resulting overall diffusion coefficient will then be much smaller than the estimates from Figures 6 to 9. Based on element profiles, Aertsens [34] also mentions very low values (10^{-21} to 10^{-19} m^2/sec) for the diffusion coefficient in the gel.

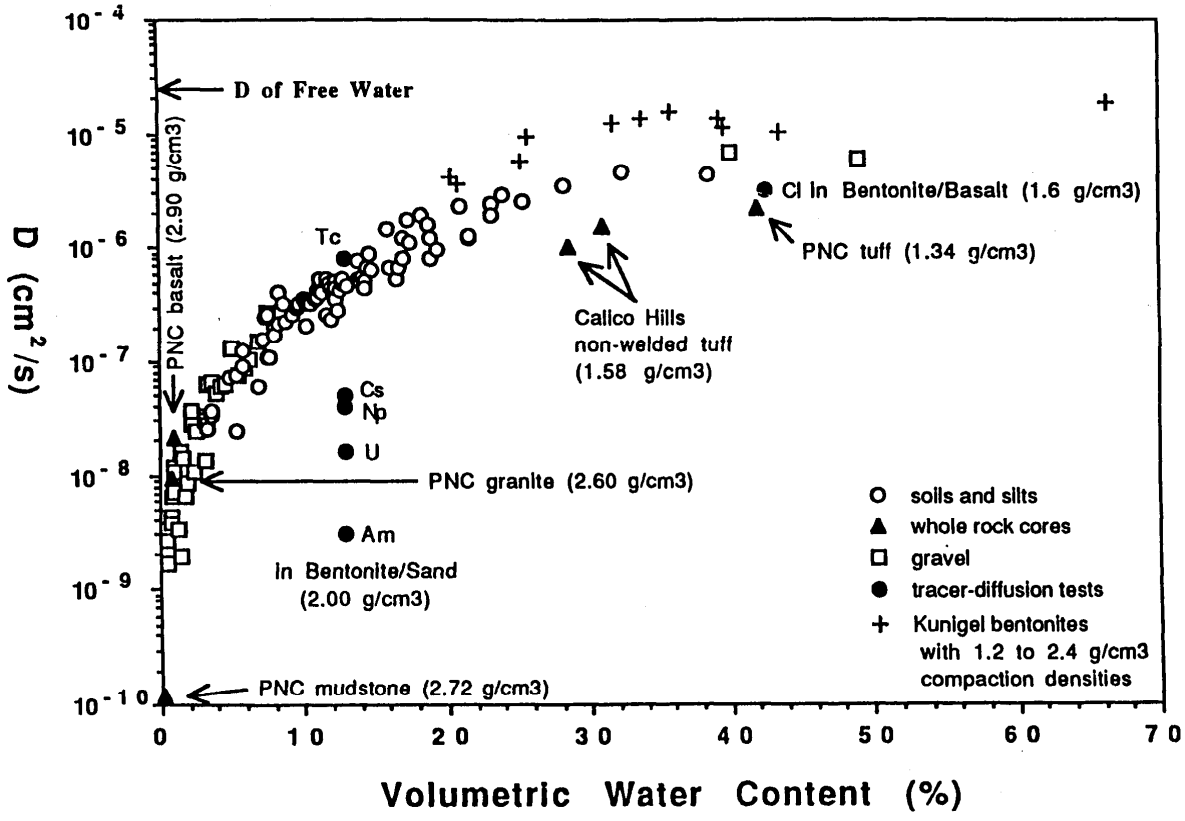

Figure 6 (from [32]): Compilation of measured effective diffusion coefficients as a function of volumetric water content for a variety of repository and geological materials

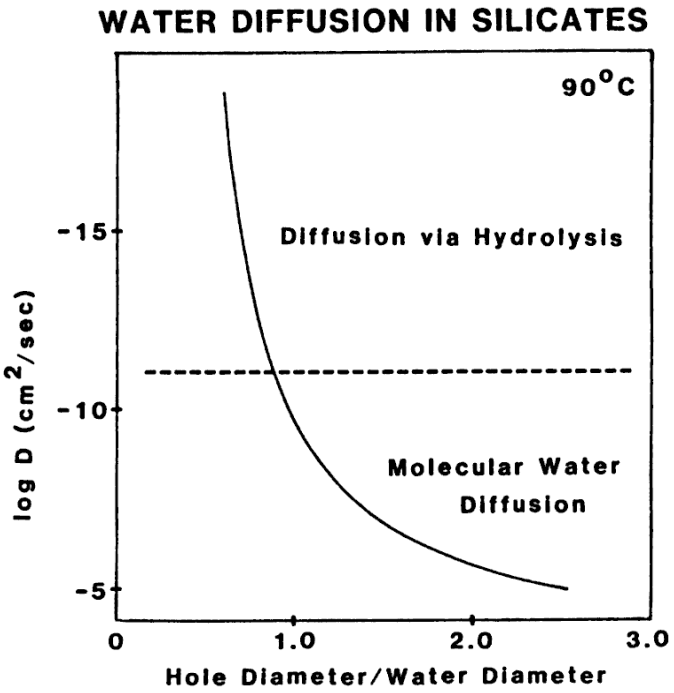

Figure 7 (from [35]): Water diffusion coefficient as a function of pore size. The size of water is 2.8 Å

Zeolite	Pore Radius Ångstroms	D (cm^2/s)	D° (cm^2/s)	E_a (kcal/mole)	TC°
Analcime	2.2-2.4	$2.0x10^{-13}$	$1.5x10^{-1}$	17.0	46
Heulandite	2.4-7.8	$2.1x10^{-8}$	$7.6x10^{-1}$	11.0	45
Chabazite	3.7-4.2	$1.3x10^{-7}$	$1.2x10^{-1}$	8.7	45
Gmelinite	3.4-6.9	$5.8x10^{-8}$	$2.0x10^{-2}$	8.1	45
Na-X	~7.4	$2.1x10^{-5}$	-------	6.9	40
Ca-X	~7.4	$2.4x10^{-5}$	-------	6.8	40
Water	2.8	$3.9x10^{-5}$	$5.6x10^{-2}$	4.6	45

Figure 8 (from [36]): Water diffusion coefficient in some zeolites versus pore size

Reference	**Pore size**	**Method**
Trotignon [37]	larger than 0.6 nm	infrared spectroscopy
Vernas [38]	1.5 to 2.5 nm	X-ray diffusion (??)
	6 nm	gas adsorption
Deruelle [39,40]	4 nm (pseudo-dynamic test)	Thermoporometry, X-ray diff
	2 nm (static conditions)	Thermoporometry, X-ray diff
Belyustin [41]	5 to 8 Å	
Bunker [42]	10 Å and more	Transmission electron micrographs
Rebiscoul [26]	5 nm and 8 nm	in situ X-ray reflectometry

Figure 9: Glass pore sizes mentioned in the literature

5.4.2 The apparent diffusion coefficient

Since apparent diffusion coefficient D_{app} is the ratio of the pore diffusion coefficient D_p and the retardation factor R (see expression (13)), the retardation coefficient needs to be estimated in order to know the apparent diffusion coefficient.

Therefore, note that substituting expression (9) in expression (8) with D_p = 0 leads to the linear rate law (4) with

$$\mu S = \frac{SA}{V} k_f \qquad \textit{and} \qquad \lambda = \frac{SA}{V} k_f \frac{1}{C_{sat}} = \frac{k_b}{V} \tag{65}$$

At first sight, the expressions (65) do not make much sense. The linear rate law is derived for silica dissolution of a solid in a finite volume V and the silica dissolution rate constant k_f is a surface reaction rate. In the kinetically coupled diffusion model, the reaction rate constant μ concerns a three dimensional bulk dissolution rate, and concepts like volume V or surface SA simply do not exist.

However, the 'equilibrium expressions' (14) and (3) are similar as well: they both provide equilibrium as the ratio of a forward rate constant and a backward rate constant. So, silica retardation is linked to silica solubility. This can be quantified by substituting the expressions (65) in expression (10), leading to

$$R = 1 + \frac{\lambda}{\mu} = \frac{S}{C_{sat}} \tag{66}$$

According to this expression, low silica solubility corresponds to high silica retardation. Since at high pH, the total silica concentration in solution rises due to silica dissociation, it makes sense to expect limited silica retardation at high pH.

The experimentally observed silica saturation concentration of approximately 10^{-3} mole/litre (at 90°C) can be converted to a dimensionless number by expressing it as the probability that a 'site' in solution is occupied by silica. This probability is $10^{-3}/(55+10^{-3}) \approx 1.8\ 10^{-5}$ with 55 mole/litre the water concentration. Assuming a dimensionless silica solubility of $2\ 10^{-5}$ and a bulk silica concentration S of the order of 10^{-1} (the amount of silica in bulk glass), expression (26) gives a retardation coefficient of the order of 10^4. For comparison, in boom clay a silica retardation coefficient between 100 and 300 is measured [34].

The apparent silica diffusion coefficient in the gel has been directly measured by Valle [43]. Already altered glass samples were placed in a solution doped with tracer silica. After some time, the sample is withdrawn from the solution and the apparent tracer silica diffusion coefficient is measured by SIMS profiles. The value of the measured apparent silica diffusion coefficient depends on how the gel of the altered glasses was formed: if formed in dynamic solutions with little silica, a value around $4\ 10^{-12}$ m^2/s is measured. In similar static conditions, this value was lower: between $5\ 10^{-14}$ and $4\ 10^{-13}$ m^2/s are measured for glasses altered in solutions containing most of the glass elements. For these three types of (already) altered glasses, a lower value of the apparent silica diffusion coefficient also means a lower value of the forward rate k_f of the 'second alteration': for the third type of gel (with an apparent silica diffusion coefficient lower than 10^{-18} m^2/sec), the forward rate of the already altered glass was 120 times lower than the corresponding forward rate during the first alteration (see also section 4.3.3). These measurements by Valle clearly illustrate the 'protective effect' (see section 4.3.3), and thus the variation with time of the values of the model parameters, but they do not prove the exactness of the silica diffusion/dissolution mechanism as stated in both *r(t)* and GM. Assuming a silica retardation coefficient of the order of 10^2 to 10^4 (see previous paragraph) values of $5\ 10^{-14}$ to $4\ 10^{-12}$ m^2/s (for the two first types of altered glass) are consistent with a silica pore diffusion coefficient of the order of 10^{-10} m^2/sec, as suggested for porous media. In that case, gels are not 'protective' and silica diffusion is hardly relevant in the overall dissolution behaviour of both models.

5.5 The water diffusion coefficient in the diffusion layer

The water diffusion coefficient in the diffusion layer can be measured from element profiles of the diffusion layer. Typical values of the diffusion coefficient in the diffusion layer are mentioned in [34]. Some of these values are obtained from element profiles, others from measuring dissolution rates at silica 'saturation'. Although, the values depend on the model used, they are typically between 10^{-19} m^2/sec and 10^{-22} m^2/sec.

5.6 The $K_{d,i}$ values for boron and lithium in the diffusion layer

It is already mentioned in Section 4.2.1 that contrary to what the name (notation) of these parameters suggests, these parameters are in no way sorption constants K_d as defined in expressions (15-16). For estimates of $K_{d,i}$ values we refer to 4.2.1. Remember from there also that due to correlations with the water diffusion coefficient in the diffusion layer it is not expected that $K_{d,i}$ values can be determined from dissolution data alone.

6. Summary: Description of the models used in GLAMOR

The models used in GLAMOR are the *r(t)* models [1] and GM2003 [2]. GM2003 is a more recent and not yet published version of GM2001, published in [2]. In the meantime, more recent versions than GM2003 have been developed, but are not discussed in the present report.

Both the *r(t)* model and the GM2003 are to a large extent similar. They both rely on silica diffusion. This is described in nearly the same way, which is briefly explained next. The major difference between both models is that GM also considers water diffusion through the diffusion layer. So, afterwards, it is shown how this is accounted for in GM.

6.1 Silica diffusion in the gel

During glass dissolution, it is assumed that the position of the interface between the glass and the solution, in which it dissolves, remains unchanged. Glass dissolution is described by the progression of an alteration front, where the glass is transformed into a gel. The thickness of the gel increases as a function of time. It is assumed that at the gel/pristine glass interface, the glass dissolves according to a linear rate law:

$$r(t) = k_f \left(1 - \frac{C}{C_{sat}} \right) + r_{final} \qquad (67)$$

with *r(t)* the dissolution rate, *C(t)* the silica concentration in the gel pore solution at the gel/pristine glass interface, k_f the maximal glass alteration rate, C_{sat} a 'silica saturation' constant, and r_{final} a final dissolution rate. All three parameters will be discussed in more detail later. From the gel/pristine glass interface, the silica diffuses towards solution with a diffusion coefficient $D_{Si,gel}$. The solution itself is assumed to be well stirred, so that the concentration of dissolved glass components is the same everywhere in solution. At the gel/pristine glass interface, not only silica but also fast dissolving glass components like boron and alkalis dissolve into solution. These components are assumed to diffuse so fast in the gel, that their concentration throughout the gel is constant and equal to their concentration in solution. Besides, at the gel/pristine glass interface all boron and alkalis present in the glass dissolve, but only part of the silica dissolves. The not-dissolving silica is retained to form the gel. Both models allow the use of next silica retention function:

$$f_{Si}(C) = 1 - \exp(-\alpha C) \qquad (68)$$

where α is a fit parameter (unit: $(g/litre)^{-1}$). Note that expression (68) assures that no silica is retained in the gel when the silica concentration in solution is zero. Since then there is no silica retained to form the gel, and since the model assumes a gel, it remains unclear where this gel consists of at the initial solution / glass interface. At high silica concentration in solution, almost all silica is retained in the gel. Apart from expression (68), the GM2003 model also allows the use of a constant silica retention factor f_{ret} ($f_{Si}(C) = f_{ret}$ for all C). Both models do not fully solve the diffusion equation describing the diffusion of silica through the gel. Instead, they both use the additional assumption of a stationary state in the gel: the concentration gradient of dissolved silica in the gel is constant.

Now that the silica diffusion mechanism used in both models is explained, we briefly discuss the resulting parameters:

- the maximal dissolution rate k_f: Since this rate can easily be measured, none of both models considers it as a fit parameter. Both models use the measured value. In experiments, this maximal dissolution rate k_f depends on the pH in solution. At some temperatures (50°C, 90°C and 150°C) the pH dependency of the maximal dissolution rate is known. At these temperatures, *r(t)* allows to take this dependency automatically into account since the program has a geochemical part, calculating pH. The *r(t)* computer code can be used in two ways: either at fixed pH, either at calculated pH (with at the just mentioned temperatures an automatic adjusting of the maximal dissolution rate to pH)

- the silica saturation concentration C_{sat}: this (fit) parameter is still discussed farther on. Theoretically, it should be easy to measure it, since according to the linear rate law, it is the concentration at which silica dissolution should stop. In reality, the situation is more complex due to pH variations in the solution and changes in the glass/gel structure during glass dissolution. The *r(t)* model even allows silica concentrations higher than C_{sat}

- the final dissolution rate r_{final}. The status of this parameter is not entirely clear. In the published texts of both models [1, 2], this parameter is not mentioned at all. Still, it is included in both models, and it was used during the GLAMOR project (in particular by the *r(t)* model). Although the theoretical origin of this parameter is not entirely clear, it is related to the fact that even at 'silica saturation' the transformation of pristine glass into gel can go on (since glass is a metastable instead of a stable state). Besides, a (constant) final rate is sometimes observed experimentally.

  Due to the obscurity of the final rate, it is not surprising that both models apply it in a different way. In GM, the final rate only relates to boron and alkali dissolution. In *r(t),* it also concerns silica dissolution, allowing to increase calculated silica concentrations above the 'silica saturation concentration' C_{sat} and rising questions about the meaning of this parameter

- the silica diffusion coefficient in the gel: Despite the fact that the model *r(t)* pretends to use an apparent silica diffusion coefficient (although it is in fact an effective diffusion coefficient) and GM a pore diffusion coefficient, both models describe silica diffusion in the gel in exactly the same way, and the values of the diffusion coefficients used by both models can exactly be compared (see appendix for more information). Although, the silica diffusion coefficient in the gel is surely the most problematic parameter used in both models: the reported values for it vary over many orders of magnitude, independent measurements of its value hardly exist and there are doubts about the relevance of silica diffusion for describing glass dissolution (other models like e.g. STORM [MC GRAIL-2005] describe glass dissolution without taking a silica diffusion coefficient in the gel into account). Besides, a theoretical analysis (see appendix) shows that the fitted value of the silica diffusion coefficient in the gel is strongly correlated with the values of the other model parameters (so that the resulting error on it is quite large) and that in some cases it can even be nearly impossible to estimate it

- the silica retention function: After the silica 'saturation concentration' and the silica diffusion coefficient in the gel, this is the third (official) fit parameter of both models. The used (empirical) expression is identical in both models, so that it is straightforward to compare the fit values provided by each model. According to the silica retention function, there is no silica retention when the silica concentration in solution is zero (which is the case at the start of most glass dissolution experiments). Since there is no siilca retained to form the gel, and since the model assumes a gel, it remains unclear where this gel consists of at the initial solution/glass interface.

The differences of the silica diffusion part of both models are:

- *r(t)* is coupled with a geochemical part, calculating e.g. pH and allowing for some cases automatic adoption of the maximal dissolution rate to pH.
- although both models use at first sight the same linear rate law, due to silica dissociation this is not so in the model of variable pH of the *r(t)* model (see section 4.3.2.1 for the details)
- the final dissolution rate in GM only refers to boron and the alkalis, while in *r(t)* it also concerns silica dissolution.

6.2 GM: water diffusion in the diffusion layer

The most essential difference between *r(t)* and GM is that apart from silica diffusion/dissolution, GM also considers diffusion in the diffusion layer. Element profile measurements clearly show a layer (called diffusion layer) between the gel and the pristine glass where diffusion profiles of water, boron and the alkalis exist. Water diffusion is described by the solution of the diffusion advection equation

$$\frac{\partial C_{H2O}}{\partial t} = D_{H2O} \frac{\partial^2 C_{H2O}}{\partial x^2} - r(t) \frac{\partial C_{H2O}}{\partial x} \qquad (69)$$

with C_{H20} the water concentration in the diffusion layer, D_{H2O} the water diffusion coefficient in the diffusion layer and *r(t)* the glass dissolution rate (which is known by solving the silica diffusion part first). This diffusion equation is completed by two constant concentration boundary conditions (one at the diffusion layer/gel interface and one at the diffusion layer/pristine glass interface). This equation is solved numerically, but a good analytical approximation seems possible as well.

Expression (44) is introduced to relate the leached concentration of boron/alkalis out of the diffusion layer to the amount of water diffused into the diffusion layer. In this expression, a retention coefficient $K_{d,i}$ is introduced for each element *i*, being boron or an alkali.

Fitting the dissolution data of boron and lithium, the GM2003 model has three additional parameters (compared to *r(t)*):

- the water diffusion coefficient D_{H2O}
- *a* $K_{d,B}$ values for boron and a $K_{d,Li}$ value for lithium.

Since the boron/lithium concentrations in solution also depend on the *r(t)* parameters, we do not expect that by fitting dissolution data alone, accurate values can be obtained for all GM parameters. Since fitting with more fit parameters always leads to better fits but also to a larger uncertainty of the values on the fit parameters, it is evident that the value of additional parameters D_{H2O}, $K_{d,B}$ and $K_{d,Li}$ will be correlated also to the values of the fit parameters of the silica diffusion part. The values of these parameters in turn will get less accurate by the addition of the parameters of the water diffusion part. Besides, also a strong correlation between the parameter D_{H2O} on one hand and $K_{d,B}$ and $K_{d,Li}$ on the other hand, has been shown. Summarizing, when fitting with GM, it is advised not to fit all parameters but to assign to some of them a constant value.

References

1 Ribet I., Gin S., Minet Y., Vernaz E., Chaix P., Do Quang R.,
Long-term behaviour of nuclear glass: the r(t) operational model,
Global (9-13 september 2001, Paris)

2 Grambow B., Müller R.,
First-order dissolution rate law and the role of surface layers in glass performance assessment,
J. Nucl. Mat., Vol. 298, p.112-124, 2001

3 Kuhn W., Bunnell L.,
Results of testing the Grambow rate law for use in HWVP glass durability correlations,
PNNL report PNNL-11070 UC-810 (Richland, Washington, USA), 1996

4 Advocat T., Couchan J.L., Crovisier J.L., Guy C., Daux V., Jégou C., Gin. S., Vernaz E.,
Borosilicate nuclear waste glass alteration kinetics: chemical inhibition and affinity control,
Mat. Res. Soc. Symp. Proc., Vol. 506, p. 63-70, 1997

5 Jégou C.,
Mise en évidence expérimentale des mécanismes limitant l'altération du verre R7T7 en milieu aqueux. Critique et proposition d'évolution du formalisme cinétique,
Ph. D. thesis (Université deMontpellier II), 1998

6 Abraitis P., Mc Grail B., Trivedi D.,
The effects of silicic acid, aluminate ion activity and hydrosilicate gel development on the dissolution rate of a simulated British Magnox waste glass,
Mat. Res. Soc. Symp. Proc., Vol. 556, p. 401-408, 1999

7 Abraitis P., Livens F., Monteith J., Small J., Trivedi D., Vaughan D., Wogelius R.,
The kinetics and mechanisms of simulated British Magnox waste glass dissolution as a function of pH, silicic acidity and time in low temperature aqueous systems,
Appl. Geochem. 15(9), p. 1399-1416, 2000

8 Mc Grail B., Icenhower J., Rodriguez E.,
Origins of discrepancies between kinetic rate law theory and experiments in the Na_2O-B_2O_3-SiO_2 system,
Mat. Res. Soc. Symp. Proc., Vol. 713, p. 537-546, 2002

9 Aagaard P., Helgeson H.,
Thermodynamic and kinetic constraints on reaction rates among minerals and aqueous solutions. I. Theoretical considerations
American J. of Science, Vol. 282, p. 237-285, 1982

10 Lasaga A.,
Rate laws of chemical reactions,
in Kinetics of geochemical processes, eds. A. Lasaga, R. Kirkpatrick, Review in mineralogy, v8, p. 1-110, 1981

11 Pelmenschikov A., Strandh H., Petterson L., Leszczynski J.,
Lattice resistance to hydrolysis of Si-O-Si bonds of silicate minerals: ab initio calculations of a single water attack onto the (001) and (111) □-cristobalite surfaces,
J. Phys. Chem. B, Vol. 104, p. 5779-5783, 2000

12 Aertsens M.,
Testing the Grambow glass dissolution model by comparing it with Monte Carlo simulation results,
Mat. Res. Soc. Symp. Proc., Vol. 556, p. 409-419, 1999

13 Abrajano T., Bates J., Bradley J.,
Analytical electron microscopy of leached nuclear waste glasses,
Ceramic transactions : nuclear waste management III, ed. Mellinger G. (Am. Ceram. Soc. Proc. 9, Westerville, OH), p. 211-229, 1990

14 Dran J., Petit J., Brousse C.,
Mechanism of aqueous dissolution of silicate glasses,
Nature, Vol. 319, p. 485-487, 1986

15 Knauss K., Bourcier W., McKeegan K., Merzbacher C., Nguyen N., Ryerson F., Smith D., Weed H., Newton L.,
Dissolution kinetics of a simple analogue nuclear waste glass as a function of pH, time and temperature,
Mat. Res. Soc. Symp. Proc., Vol. 176, p. 371-381, 1990

16 Advocat T.,
Hydrolysis of R7T7 nuclear waste glass in dilute media : mechanisms and rate as a function of pH,
Mat. Res. Soc. Symp. Proc., Vol. 212, p. 57-64, 1991

17 Xiao Y., Lasaga A.,
Ab initio quantum mechanical studies of the kinetics and mechanisms of silicate dissolution: H^+ (H_30^+) catalysis,
Geochim. Cosmochim. Acta, Vol. 58, p. 5379-5400, 1994

18 Xiao Y., Lasaga A.,
Ab initio quantum mechanical studies of the kinetics and mechanisms of quartz dissolution: OH^- catalysis,
Geochim. Cosmochim. Acta, Vol. 60, p. 2283-2295, 1996

19 Böhm T., Chudek J.,
Structural changes during glass corrosion,
Fundamentals of Glass Science and Technology (Glafo, Växjö,Sweden), p. 476-481, 1997

20 Bunker B., Tallant D., Headley T., Turner G., Kirkpatrick R.,
The structure of leached sodium borosilicate glass,
Phys. Chem. Glasses, Vol. 29, p. 106-119, 1988

21 Bach H., Grosskopf K., March P.,
In-depth analysis of elements and properties of hydrated subsurface layers on optical surfaces of SiO_2-BaO-B_2O_3 with SIMS, IBSCA, RBS and NRA, 1. Experimental procedures and results,
Glas tech. Ber., Vol. 60, N° 1, p. 21-30, 1987

22 Bach H., Grosskopf K., March P.,
In depth analysis of elements and properties of hydrated subsurface layers on optical surfaces of SiO_2-BaO-B_2O_3 with SIMS, IBSCA, RBS and NRA, 2. Discussion of results,
Glas tech. Ber., Vol. 60, N° 1, p. 33-46, 1987

23 Carroll S., Maxwell R., Bourcier W., Martin S., Hulsey S.,
Evaluation of silica-water surface chemistry using NMR spectroscopy,
Geochim. Cosmochim. Acta, Vol. 66, p. 913-926, 2002

24 Scholze H.,
Glass,
Springer Verlag, 1991

25 Rebiscoul D., Van der Lee A., Frugier P., Ayral A., Gin S.,
X-ray reflectometry characterization of SON68 glass alteration films,
J. Non-Cryst. Solids, Vol. 325, p. 113-123, 2003

26 Rebiscoul D., Van der Lee A., Rieutord F., Né F., Spalla O., El-Mansouri A., Frugier P., Ayral A., Gin S.,
Morphological evolution of alteration layers formed during nuclear glass alteration: new evidence of a gel as a diffusive barrier,
J. Nucl. Mat, Vol. 326, p. 9-18, 2004

27 Chick L., Pederson L.,
The relationship between reaction layer thickness and leach rate for nuclear waste glasses,
Mat. Res. Soc. Symp. Proc., Vol. 26, p. 635-642, 1984

28 Xing S., Buechele A., Pegg I.,
Effect of surface layers on the dissolution of nuclear waste glasses,
Mat. Res. Soc. Symp. Proc., Vol. 333,p. 541-548, 1994

29 Mac Grail B.P.: http://www.pnl.gov/agg/technologies/stormcode.stm

30 Werme L., Björner I., Bart G., Zwicky H., Grambow B., Lutze W., Ewing R., Magrabi C.,
Chemical corrosion of highly radioactive borosilicate nuclear waste glass under simulated repository conditions,
J. Mater. Res., Vol. 5, p. 1130-1146, 1990

31 Grambow B.,
Private communication

32 The Status of Near-field Modelling (OECD, rue André Pascal, Paris), 1992

33 Aertsens M., De Cannière P., Moors H.,
Modelling of silica diffusion experiments with ^{32}Si in boom clay,
J. Cont. Hydrology, Vol. 61, p. 117-129, 2003

34 Aertsens M., Lemmens K., Van Iseghem P.,
Fitting element profiles for predicting glass dissolution rates in synthetic interstitial clay water,
Mat. Res. Soc. Symp. Proc., Vol. 757, p. 167-174, 2003

35 Bunker B.,
Molecular mechanisms for corrosion of silica and silicate glasses,
J. Non-Cryst. Solids, Vol. 179, p. 300-308, 1994

36 Casey W., Bunker B.,
Leaching of mineral and glass surfaces during dissolution,
in 'Mineral-Water interface geochemistry', ed. Hochella M., White A., Mineral. Soc. Am. Rev. Mineral. 23, p. 397-426, 1990

37 Trotignon L., Petit J., Dran J.,
Nature of leached layers formed on borosilicate glasses during aqueous corrosion,
Ceramic transactions : nuclear waste management III, ed. Mellinger G., (Am. Ceram. Soc. Proc. 9, Westerville, OH), p. 229-240, 1991

38 Vernaz E., Dussossoy J.,
Current state of knowledge of nuclear waste glass corrosion mechanisms : the case of R7T7 glass,
Applied Geochem., Suppl. Issue no 1, p. 13-22, 1992

39 Deruelle O., Barboux P., Spalla O., Ricol S., Lambard J., Vernaz E.,
Morphology of altered layers on glass,
in 'Glass, scientifc research for High performance containment' (CEA/ Valrhô, summer session proc.), p. 393-402, 1998

40 Deruelle O., Spalla O., Barboux P., Lambard J.,
Growth and ripening of porous layers in water altered glasses,
J. Non Cryst. Solids, Vol. 261, p. 237-251, 2000

41 Belyustin A.,

Concentration distribution of ions in the subsurface layers of alkali silicate glasses treated with aqueous solutions,
Sov. J. Glass Phys. Chem., Vol.7 (3), p. 169-188, 1981

42 Bunker B.,
Waste glass leaching: chemistry and kinetics,
Mat. Res. Soc. Symp. Proc., Vol. 84, p. 493-507, 1987

43 Valle N.,
Tracage isotopique (29Si et 18O) des mécanismes de l'altération du verre de confinement des déchets nucléaires: SON68,
Ph. D. Thesis, Centre de Recherches pétrographiques et géochimiques, Nancy (France), 2000

44 G. Wicks, A. Lodding, M. Molecke, Aqueous alteration of nuclear waste glasses and metal package materials. MRS Bulletin Vol XVIII, No9, Sept 1993, 32-39

45 A. Lodding, Characterization of corroded ceramics by SIMS. Chapter 4 in *Corrosion of glass, ceramics and ceramic superconductors*. Ed D.E. Clark and B.K. Zoitos. Noyes Publ., 1991, 103-121

46 ASTM C 1220 – 92. Standard test method for static leaching of monolithic waste forms for disposal of radioactive waste (1992)

47 Standard practice for measurement of the glass dissolution rate using the single-pass-flow-through test method. Method submitted to ASTM for approval.

ANNEX II

Input data sheets for the selected experiments in WP2

	Parameters of the Experiment						
Ref	*Reference Number Experiment**			A1	A2	A3	A4
Ref	*Reference Number input data set**						
t0	Date (Start of Experiment)			03/12/1997	25/03/1998	25/03/1998	25/03/1998
glass sample	Glass Sample Reference						
	Type of Glass*			R7T7 type (SON68)	R7T7 type (SON68)	R7T7 type (SON68)	R7T7 type (SON68)
	Sample Shape (Powder/Monolith)*			Powder	Powder	Powder	Powder
	If Monolith : Surface State (polished/nonpolished; grade)*						
	If Powder : Sample Granulometric Range (+ 95% conf. interval)	lower	µm	8	63	63	63
		higher	µm	10	100	100	100
	Mass		g	51,66	4,651	4,651	4,651
	Specific Surface Area of powder *(+ 95% conf. interval)		cm²/g	5807	860 (5%)	860 (5%)	860 (5%)
	Method for determination of specific surface area*			BET	BET (Kr)	BET (Kr)	BET (Kr)
Reactor	Type*			PTFE	PTFE	PTFE	PTFE
	Volume		ml	180	120	120	120
	number of reactors*	1 reactor is san	(Y/N)	Y	Y	Y	Y
		1 reactor per te	(Y/N)	N	N	N	N
Stirring	(Y/N)*			Y	Y	Y	Y
Solution	Type*			high purity water	high purity water	high purity water + KOH	high purity water + KOH
Solids	Type*						
	Dry mass of solid / SA of glass* (+ 95% conf. interval)		g/cm²				
Type	Experimental Mode: static/dynamic*			static	static	static	static
	If Dynamic : Leaching Solution Flow Rate*		ml/day				
	If Static : Volume of leaching solution (+ 95% conf. interval)		ml	150,8	80	80	80
	If Static : SA/V ratio* (+ 95% conf. interval)		cm^-1	2000	50	50	50
pH	Imposed pH (Y/N)*			N	N	Y	Y
	If imposed pH : Value* (+ 95% tolerance)					7 (6,5-7,5)	8 (7,7-8,5)
	If imposed pH : Buffer						
Temperature	Temperature of the Experiment* (+ 95% conf. interval)		°C	90	90	90	90
Pressure	If different from ambient pressure: pressure of the Experiment (bars)* (+ 95% conf. interval)						
	Document/File for Reference*	internal		logbook			
		external		N	Y	Y	Y
	Analyses and Results						
sampling	if 1 reactor is sampled repeatedly: volume *		ml	1,2	1,2	1,2	1,2
	No Filtration (D), Filtration (F), Ultrafiltration (U)*			U	U	U	U
	If Filtration: Mesh Size *		µm				
	If ultrafiltration: MWCO*		dalton	10000	10000	10000	10000
	type of solution analyses*			ICP-AES	ICP-AES	ICP-AES	ICP-AES
	analysed elements/ions*			Si, B, Na, Li, Mo, Al, Ca	Si, B, Na, Al, Ca, Li, Mo	Si, B, Na, Al, Ca, Li, Mo	Si, B, Na, Al, Ca, Li, Mo
	Element Concentration vs Duration Data in mg/l : ouput sheet reference*			A1-out	A2-out	A3-out	A4-out
	pH vs Duration Data in mg/l : output sheet reference*			A1-out	A2-out	A3-out	A4-out
	Eh vs Duration Data in mg/l : output sheet reference			-	-	-	-
solid analysis	Glass mass loss vs Duration Data in mg/l : output sheet reference			A1-out	A2-out	A3-out	A4-out
	If surface analysis performed: type*			TEM	-	-	-
glass	**Glass composition (wt % oxides)***						
	SiO2			45,12	45,48	45,48	45,48
	B2O3			13,92	14,02	14,02	14,02
	Na2O			10,06	9,86	9,86	9,86

	Parameters of the Experiment						
Ref	*Reference Number Experiment**			A5	A6	A7	A8
Ref	*Reference Number input data set**						
t0	Date (Start of Experiment)			25/03/1998	25/03/1998	25/03/1998	25/03/1998
glass sample	Glass Sample Reference						
	Type of Glass*			R7T7 type (SON68)	R7T7 type (SON68)	R7T7 type (SON68)	R7T7 type (SON68)
	Sample Shape (Powder/Monolith)*			Powder	Powder	Powder	Powder
	If Monolith : Surface State (polished/nonpolished; grade)*						
	If Powder : Sample Granulometric Range (+ 95% conf. interval)	lower	µm	63	63	63	63
		higher	µm	100	100	100	100
	Mass		g	4,651	4,651	4,651	4,651
	Specific Surface Area of powder *(+ 95% conf. interval)		cm²/g	860 (5%)	860 (5%)	860 (5%)	860 (5%)
	Method for determination of specific surface area*			BET (Kr)	BET (Kr)	BET (Kr)	BET (Kr)
Reactor	Type*			PTFE	PTFE	PTFE	PTFE
	Volume		ml	120	120	120	120
	number of reactors*	1 reactor is san	(Y/N)	Y	Y	Y	Y
		1 reactor per te	(Y/N)	N	N	N	N
Stirring	(Y/N)*			Y	Y	Y	Y
Solution	Type*			high purity water + KOH	high purity water + KOH	high purity water + KOH	high purity water + KOH
Solids	Type*						
	Dry mass of solid / SA of glass* (+ 95% conf. interval)		g/cm²				
Type	Experimental Mode: static/dynamic*			static	static	static	static
	If Dynamic : Leaching Solution Flow Rate*		ml/day				
	If Static : Volume of leaching solution (+ 95% conf. interval)		ml	80	80	80	80
	If Static : SA/V ratio* (+ 95% conf. interval)		cm^-1	50	50	50	50
pH	Imposed pH (Y/N)*			Y	Y	Y	Y
	If imposed pH : Value* (+ 95% tolerance)			9,5 (9,2-9,7)	10 (9,7-10,2)	10,5 (10,3-10,8)	11 (10,8-11,1)
	If imposed pH : Buffer						
Temperature	Temperature of the Experiment* (+ 95% conf. interval)		°C	90	90	90	90
Pressure	If different from ambient pressure: pressure of the Experiment (bars)* (+ 95% conf. interval)						
	Document/File for Reference*	internal					
		external		Y	Y	Y	Y
	Analyses and Results						
sampling	if 1 reactor is sampled repeatedly: volume *		ml	1,2	1,2	1,2	1,2
	No Filtration (D), Filtration (F), Ultrafiltration (U)*			U	U	U	U
	If Filtration: Mesh Size *		µm				
	If ultrafiltration: MWCO*		dalton	10000	10000	10000	10000
	type of solution analyses*			ICP-AES	ICP-AES	ICP-AES	ICP-AES
	analysed elements/ions*			Si, B, Na, Al, Ca, Li, Mo	Si, B, Na, Al, Ca, Li, Mo	Si, B, Na, Al, Ca, Li, Mo	Si, B, Na, Al, Ca, Li, Mo
	Element Concentration vs Duration Data in mg/l : ouput sheet reference*			A5-out	A6-out	A7-out	A8-out
	pH vs Duration Data in mg/l : output sheet reference*			A5-out	A6-out	A7-out	A8-out
	Eh vs Duration Data in mg/l : output sheet reference			-	-	-	-
solid analysis	Glass mass loss vs Duration Data in mg/l : output sheet reference			A5-out	A6-out	A7-out	A8-out
	If surface analysis performed: type*			-	-	-	-
glass	**Glass composition (wt % oxides)***						
	SiO2			45,48	45,48	45,48	45,48
	B2O3			14,02	14,02	14,02	14,02
	Na2O			9,86	9,86	9,86	9,86

	Parameters of the Experiment						
Ref	*Reference Number Experiment**			A9	A10	A11	A12
Ref	*Reference Number input data set**						
t0	Date (Start of Experiment)			25/03/1998			
glass sample	Glass Sample Reference						
	Type of Glass*			R7T7 type (SON68)	R7T7 type (SON68)	R7T7 type (SON68)	R7T7 type (SON68)
	Sample Shape (Powder/Monolith)*			Powder	Powder	Powder	Powder
	If Monolith : Surface State (polished/nonpolished; grade)*						
	If Powder : Sample Granulometric Range (+ 95% conf. interval)	lower	µm	63	125	125	125
		higher	µm	100	250	250	250
	Mass		g	4,651	0,6818	0,6818	0,6818
	Specific Surface Area of powder *(+ 95% conf. interval)		cm²/g	860 (5%)	264	264	264
	Method for determination of specific surface area*			BET (Kr)	BET (Kr)	BET (Kr)	BET (Kr)
Reactor	Type*			PTFE	PTFE	PTFE	PTFE
	Volume		ml	120	120	120	120
	number of reactors*	1 reactor is san	(Y/N)	Y	Y	Y	Y
		1 reactor per te	(Y/N)	N	N	N	N
Stirring	(Y/N)*			Y	Y	Y	Y
Solution	Type*			high purity water + KOH	high purity water + KOH	KOH (pH 8) + 60 ppm Si	KOH (pH 8) + 120 ppm Si
Solids	Type*						
	Dry mass of solid / SA of glass* (+ 95% conf. interval)		g/cm²				
Type	Experimental Mode: static/dynamic*			static	dynamic	dynamic	dynamic
	If Dynamic : Leaching Solution Flow Rate*		ml/day		144	144	144
	If Static : Volume of leaching solution (+ 95% conf. interval)		ml	80			
	If Static : SA/V ratio* (+ 95% conf. interval)		cm^-1	50			
pH	Imposed pH (Y/N)*			Y	Y	Y	Y
	If imposed pH : Value* (+ 95% tolerance)			11,5 (10,8-11,5)	8 ((8-8,20)	8 ((8-8,20)	8 ((8-8,20)
	If imposed pH : Buffer						
Temperature	Temperature of the Experiment* (+ 95% conf. interval)		°C	90	90	90	90
Pressure	If different from ambient pressure: pressure of the Experiment (bars)* (+ 95% conf. interval)						
	Document/File for Reference*	internal					
		external		Y	Y	Y	Y
	Analyses and Results						
sampling	if 1 reactor is sampled repeatedly: volume *		ml	1,2	2	2	2
	No Filtration (D), Filtration (F), Ultrafiltration (U)*			U	U	U	U
	If Filtration: Mesh Size *		µm				
	If ultrafiltration: MWCO*		dalton	10000	10000	10000	10000
	type of solution analyses*			ICP-AES	ICP-AES	ICP-AES	ICP-AES
	analysed elements/ions*			Si, B, Na, Al, Ca, Li, Mo	Si, B, Na, Al, Ca, Li, Mo	Si, B, Na, Al, Ca, Li, Mo	Si, B, Na, Al, Ca, Li, Mo
	Element Concentration vs Duration Data in mg/l : ouput sheet reference*			A9-out	A10-out	A11-out	A12-out
	pH vs Duration Data in mg/l : output sheet reference*			A9-out	A10-out	A11-out	A12-out
	Eh vs Duration Data in mg/l : output sheet reference			-	-	-	-
solid analysis	Glass mass loss vs Duration Data in mg/l : output sheet reference			A9-out	A10-out	A11-out	A12-out
	If surface analysis performed: type*			-	-	-	-
glass	**Glass composition (wt % oxides)***						
	SiO2			45,48	45,48	45,48	45,48
	B2O3			14,02	14,02	14,02	14,02
	Na2O			9,86	9,86	9,86	9,86

	Parameters of the Experiment							
Ref	*Reference Number Experiment**			A9	A10	A11	A13	A14
Ref	*Reference Number input data set**							
t0	Date (Start of Experiment)			25/03/1998				
glass sample	Glass Sample Reference							
	Type of Glass*			R7T7 type (SON68)	R7T7 type (SON68)	R7T7 type (SON68)	R7T7 type (SON68)	R7T7 type (SON68)
	Sample Shape (Powder/Monolith)*			Powder	Powder	Powder	Powder	Powder
	If Monolith : Surface State (polished/nonpolished; grade)*							
	If Powder : Sample Granulometric Range (+ 95% conf. interval)	lower	µm	63	125	125	63	63
		higher	µm	100	250	250	100	100
	Mass		g	4,651	0,6818	0,6818	17,52	17,52
	Specific Surface Area of powder *(+ 95% conf. interval)		cm²/g	860 (5%)	264	264	855	855
	Method for determination of specific surface area*			BET (Kr)	BET (Kr)	BET (Kr)	BET (Kr)	BET (Kr)
Reactor	Type*			PTFE	PTFE	PTFE	PTFE	PTFE
	Volume		ml	120	120	120	1000	1000
	number of reactors*	1 reactor is san	(Y/N)	Y	Y	Y	Y	Y
		1 reactor per te	(Y/N)	N	N	N	N	N
Stirring	(Y/N)*			Y	Y	Y	Y	Y
Solution	Type*			high purity water + KOH	high purity water + KOH	KOH (pH 8) + 60 ppm Si	KOH (pH 9,0)	KOH (pH 9,0) + 100ppm P
Solids	Type*							
	Dry mass of solid / SA of glass* (+ 95% conf. interval)		g/cm²					
Type	Experimental Mode: static/dynamic*			static	dynamic	dynamic	static	static
	If Dynamic : Leaching Solution Flow Rate*		ml/day		144	144		
	If Static : Volume of leaching solution (+ 95% conf. interval)		ml	80			1000	1000
	If Static : SA/V ratio* (+ 95% conf. interval)		cm^-1	50			15	15
pH	Imposed pH (Y/N)*			Y	Y	Y	Y	Y
	If imposed pH : Value* (+ 95% tolerance)			11,5 (10,8-11,5)	8 ((8-8,20)	8 ((8-8,20)	9 (8,9-9,2)	9 (8,9-9,2)
	If imposed pH : Buffer							
Temperature	Temperature of the Experiment* (+ 95% conf. interval)		°C	90	90	90	90	90
Pressure	If different from ambient pressure: pressure of the Experiment (bars)* (+ 95% conf. interval)							
	Document/File for Reference*	internal						
		external		Y	Y	Y	Y	Y
	Analyses and Results							
sampling	if 1 reactor is sampled repeatedly: volume *		ml	1,2	2	2	3	3
	No Filtration (D), Filtration (F), Ultrafiltration (U)*			U	U	U	F, U	F, U
	If Filtration: Mesh Size *		µm				F : 0,45 µm	F : 0,45 µm
	If ultrafiltration: MWCO*		dalton	10000	10000	10000	U : 10000 D	U : 10000 D
	type of solution analyses*			ICP-AES	ICP-AES	ICP-AES	ICP-AES	ICP-AES
	analysed elements/ions*			Si, B, Na, Al, Ca, Li, Mo	Si, B, Na, Al, Ca, Li, Mo	Si, B, Na, Al, Ca, Li, Mo	Si, B, Na, Al, P	Si, B, Al, P
	Element Concentration vs Duration Data in mg/l : ouput sheet reference*			A9-out	A10-out	A11-out	A13-out	A114-out
	pH vs Duration Data in mg/l : output sheet reference*			A9-out	A10-out	A11-out	A13-out	A114-out
	Eh vs Duration Data in mg/l : output sheet reference			-	-	-	-	-
solid analysis	Glass mass loss vs Duration Data in mg/l : output sheet reference			A9-out	A10-out	A11-out	A13-out	A114-out
	If surface analysis performed: type*			-	-	-	STEM	STEM
glass	**Glass composition (wt % oxides)***							
	SiO2			45,48	45,48	45,48	45,48	45,48
	B2O3			14,02	14,02	14,02	14,02	14,02
	Na2O			9,86	9,86	9,86	9,86	9,86

	Parameters of the Experiment							
Ref	*Reference Number Experiment**			A15	A16	A17	A18	A19
Ref	*Reference Number input data set**							
t0	Date (Start of Experiment)			23/02/1998	24/08/1998	1991	1989	sept-83
glass sample	Glass Sample Reference							TAV-6
	Type of Glass*			R7T7 type (SON68)	R7T7 type (SON68)	R7T7 type (SON68)	R7T7 type (SON68)	R7T7 type (SON68)
	Sample Shape (Powder/Monolith)*			Powder	Powder	monolith	monolith	monolith
	If Monolith : Surface State (polished/nonpolished; grade)*					polished	polished	polished
	If Powder : Sample Granulometric Range (+ 95% conf. interval)	lower	µm	40	40			
		higher	µm	63	63			
	Mass		g	5,766	5,766		3	≈ 800
	Specific Surface Area of powder *(+ 95% conf. interval)		cm^2/g	1300	1300			
	Method for determination of specific surface area*			BET (Kr)	BET (Kr)			
Reactor	Type*			PTFE	PTFE	PTFE	Stainless steel	Stainless steel
	Volume		ml	180	180	800	50	1149
	number of reactors*	1 reactor is san	(Y/N)	Y	Y	Y		Y
		1 reactor per te	(Y/N)	N	N		Y	
Stirring	(Y/N)*			Y	Y	Y		N
Solution	Type*			high purity water	KOH (pH 9,15 at 90°C)	high purity water	high purity water	Volvic water equilibrated with granite and sand
Solids	Type*							Granite, sand, corrosion products
	Dry mass of solid / SA of glass* (+ 95% conf. interval)		g/cm^2					See comments above
Type	Experimental Mode: static/dynamic*			static	static	static	static	dynamic
	If Dynamic : Leaching Solution Flow Rate*		ml/day					0.3 ml/day for 44 months and 0.2 ml/day after
	If Static : Volume of leaching solution (+ 95% conf. interval)		ml	150	150			
	SA/V ratio* (+ 95% conf. interval)		cm^-1	50	50	0,5	0,5	glass surface area: 253 cm^2 , leachate volume : 320 ml
pH	Imposed pH (Y/N)*			N	Y	N	N	N
	If imposed pH : Value* (+ 95% tolerance)				9			
	If imposed pH : Buffer							
Temperature	Temperature of the Experiment* (+ 95% conf. interval)		°C	90	90	90	150	90
Pressure	If different from ambient pressure: pressure of the Experiment (bars)* (+ 95% conf. interval)							100
	Document/File for Reference*	internal						
		external		Y	Y	PhD thesis Delage, 1992	PhD thesis Caurel, 1990	
	Analyses and Results							
sampling	if 1 reactor is sampled repeatedly: volume *		ml	1,2	1,2	5	5	18 ml for 44 months and 12 ml after
	No Filtration (D), Filtration (F), Ultrafiltration (U)*			U	U	F	D	D
	If Filtration: Mesh Size *		µm			0,45		
	If ultrafiltration: MWCO*		dalton	U : 10000 D	U : 10000 D			
	type of solution analyses*			ICP-AES	ICP-AES			
	analysed elements/ions*			Si, B, Na, Li, Mo, Al, Ca	Si, B	Si, B, Na, Li, Mo, Al, Ca, Z	Si, B, Na, Li, Mo, Ca, Sr, Z	Si, B, Na, Li, Mo, Al, Ca
	Element Concentration vs Duration Data in mg/l : ouput sheet reference*			A15-out	A16-out	A17-out	A18-out	A19-out
	pH vs Duration Data in mg/l : output sheet reference*			A15-out	A16-out	A17-out	A18-out	A19-out
	Eh vs Duration Data in mg/l : output sheet reference			-	-	-	-	-
solid analysis	Glass mass loss vs Duration Data in mg/l : output sheet reference			A15-out	A16-out	A17-out	A18-out	A19-out
	If surface analysis performed: type*							
glass	**Glass composition (wt % oxides)***							
	SiO2			45,48	45,48	45,48	45,48	45,48
	B2O3			14,02	14,02	14,02	14,02	14,02
	Na2O			9,86	9,86	9,86	9,86	9,86

	Parameters of the Experiment					
Ref	*Reference Number Experiment**			A20	A21	A22
Ref	*Reference Number input data set**					
t0	Date (Start of Experiment)			march-90	21/09/1999	21/09/1999
glass sample	Glass Sample Reference			TAV-20		
	Type of Glass*			R7T7 type (SON68)	AVM (AVM6)	AVM (AVM10)
	Sample Shape (Powder/Monolith)*			fractured monolith	powder	powder
	If Monolith : Surface State (polished/nonpolished; grade)*			non polished		
	If Powder : Sample Granulometric Range (+ 95% conf. interval)	lower	µm		63	63
		higher	µm		125	125
	Mass		g	≈ 800	30	30
	Specific Surface Area of powder *(+ 95% conf. interval)		cm^2/g		550	550
	Method for determination of specific surface area*					
Reactor	Type*			Stainless steel	PTFE	PTFE
	Volume		ml	1149	500	500
	number of reactors*	1 reactor is san	(Y/N)	Y	Y	Y
		1 reactor per te	(Y/N)		N	N
Stirring	(Y/N)*			N	N	N
Solution	Type*			Clay water in equilibrium with Boom clay	high purity water	high purity water
Solids	Type*			Boom clay, sand, corrosion products		
	Dry mass of solid / SA of glass* (+ 95% conf. interval)		g/cm^2	See comments above		
Type	Experimental Mode: static/dynamic*			dynamic	static	static
	If Dynamic : Leaching Solution Flow Rate*		ml/day	0.4 ml/day		
	If Static : Volume of leaching solution (+ 95% conf. interval)		ml		300	300
	SA/V ratio* (+ 95% conf. interval)		cm^-1	glass surface area: 3100 cm^2 , leachate volume : 510 ml	55	55
pH	Imposed pH (Y/N)*			N	N	N
	If imposed pH : Value* (+ 95% tolerance)					
	If imposed pH : Buffer					
Temperature	Temperature of the Experiment* (+ 95% conf. interval)		°C	90	50	50
Pressure	If different from ambient pressure: pressure of the Experiment (bars)* (+ 95% conf. interval)			100		
	Document/File for Reference*	internal				
		external				
	Analyses and Results					
sampling	if 1 reactor is sampled repeatedly: volume *		ml	12	2	2
	No Filtration (D), Filtration (F), Ultrafiltration (U)*			F	U	U
	If Filtration: Mesh Size *		µm	0,45		
	If ultrafiltration: MWCO*		dalton		10000	10000
	type of solution analyses*				ICP-AES	ICP-AES
	analysed elements/ions*			Si, B, Na, Li, Mo, Al, Ca	Si,B,Na,Li,Al	Si,B,Na,Li,Al
	Element Concentration vs Duration Data in mg/l : ouput sheet reference*			A20-out	AVM6-out	AVM10-out
	pH vs Duration Data in mg/l : output sheet reference*			A20-out	AVM6-out	AVM10-out
	Eh vs Duration Data in mg/l : output sheet reference			-		
solid analysis	Glass mass loss vs Duration Data in mg/l : output sheet reference			A20-out	AVM6-out	AVM10-out
	If surface analysis performed: type*					
glass	**Glass composition (wt % oxides)***					
	SiO2			45,48	44,49	38,5
	B2O3			14,02	19,5	16,75
	Na2O			9,86	15,5	15

	Parameters of the Experiment						
Ref	*Reference Number Experiment**			B1	B2	B3	B4
Ref	*Reference Number input data set**						
t0	Date (Start of Experiment)			16/09/1997	29/11/1996	03/03/1997	06/07/1998
glass sample	Glass Sample Reference			CJ1	CJ3	CJ6	CJ9
	Type of Glass*			Simplified	Simplified	Simplified	Simplified
	Sample Shape (Powder/Monolith)*			Powder	Powder	Powder	Powder
	If Monolith : Surface State (polished/nonpolished; grade)*						
	If Powder : Sample Granulometric Range (+ 95% conf. interval)	lower	µm	40	40	40	40
		higher	µm	100	100	100	100
	Mass		g	28,88	30,769	32,87	30,01
	Specific Surface Area of powder *(+ 95% conf. interval)		cm²/g	831	780	730	800
	Method for determination of specific surface area*			BET	BET	BET	BET
Reactor	Type*			PTFE	PTFE	PTFE	PTFE
	Volume		ml	500	500	500	500
	number of reactors*	1 reactor is san	(Y/N)	Y	Y	Y	Y
		1 reactor per te	(Y/N)	N	N	N	N
Stirring	(Y/N)*			Y	Y	Y	Y
Solution	Type*			high purity water	high purity water	high purity water	high purity water
Solids	Type*						
	Dry mass of solid / SA of glass* (+ 95% conf. interval)		g/cm²				
Type	Experimental Mode: static/dynamic*			static	static	static	static
	If Dynamic : Leaching Solution Flow Rate*		ml/day				
	If Static : Volume of leaching solution (+ 95% conf. interval)		ml	300	300	300	300
	If Static : SA/V ratio* (+ 95% conf. interval)		cm^-1	80	80	80	80
pH	Imposed pH (Y/N)*			N	N	N	N
	If imposed pH : Value* (+ 95% tolerance)						
	If imposed pH : Buffer						
Temperature	Temperature of the Experiment* (+ 95% conf. interval)		°C	90	90	90	90
Pressure	If different from ambient pressure: pressure of the Experiment (bars)* (+ 95% conf. interval)						
	Document/File for Reference*	internal		logbook	logbook	logbook	logbook
		external		Y	Y	Y	Y
	Analyses and Results						
sampling	if 1 reactor is sampled repeatedly: volume *		ml	2	2	2	2
	No Filtration (D), Filtration (F), Ultrafiltration (U)*			U	U	U	U
	If Filtration: Mesh Size *		µm				
	If ultrafiltration: MWCO*		dalton	10000	10000	10000	10000
	type of solution analyses*			ICP-AES	ICP-AES	ICP-AES	ICP-AES
	analysed elements/ions*			Si, B, Na	Si, B, Na, Al, Ca	Si, B, Na, Al, Ca, Li	Si, B, Na, Ca
	Element Concentration vs Duration Data in mg/l : ouput sheet reference*			B1-out	B2-out	B3-out	B4-out
	pH vs Duration Data in mg/l : output sheet reference*			B1-out	B2-out	B3-out	B4-out
	Eh vs Duration Data in mg/l : output sheet reference			-	-	-	-
solid analysis	Glass mass loss vs Duration Data in mg/l : output sheet reference			B1-out	B2-out	B3-out	B4-out
	If surface analysis performed: type*			TEM	TEM	TEM	TEM
glass	**Glass composition (wt % oxides)***						
	SiO2			65,56	58,07	52,66	59,8
	B2O3			20,23	17,92	16,25	18,45
	Na2O			14,21	12,59	11,34	12,95

	Parameters of the Experiment					
Ref	*Reference Number Experiment**			SCKgl31/42	SCKgl46/57	SCKgl151/162
Ref	*Reference Number input data set**			SCKgl31/42-in	SCKgl46/57-in	SCKgl151/162-in
t0	Date (Start of Experiment)			1997-1998	1997-1998	1997-1998
glass sample	Glass Sample Reference			batch 1862, 1863, 1865, 1867	batch 1862, 1863, 1865, 1867	batch 1862, 1863, 1865, 1868
	Type of Glass*			R7T7	R7T7	R7T7
	Sample Shape (Powder/Monolith)*			monolith	Powder + monolith	monolith
	If Monolith : Surface State (polished/nonpolished; grade)*			P500 (Fepa norm)	P500 (Fepa norm)	P500 (Fepa norm)
	If Powder : Sample Granulometric Range (+ 95% conf. interval)	lower	µm		125	
		higher	µm		250	
	Specific Surface Area of powder *(+ 95% conf. interval)		cm^2/g		118,5 (?)	
	Method for determination of specific surface area*				calculation for spherical particles	
Reactor	Type*			Stainless steel with PTFE lining	Stainless steel with PTFE lining	Stainless steel with PTFE lining
	Volume		ml	22	22	22
	number of reactors*	1 reactor is san	(Y/N)	N	N	N
		1 reactor per te	(Y/N)	Y	Y	Y
Stirring	(Y/N)*			N	N	N
Solution	Type*			clay water	clay water	clay water + Boom Clay
Solids	Type*					Boom Clay
	Dry mass of solid / SA of glas* (+ 95% conf. interval)		g/cm^2			0,82 (5%)
Type	Experimental Mode: static/dynamic*			static	static	static
	If Dynamic : Leaching Solution Flow Rate*		ml/day			
	If Static : Volume of leaching solution (+ 95% conf. interval)		ml	14 to 15 (1%)	14 to 15 (1%)	14 to 15 (2,5%)
	If Static : SA/V ratio* (+ 95% conf. interval)		cm^-1	1 (5%)	25 (?)	1 (5%)
pH	Imposed pH (Y/N)*			N	N	N
	If imposed pH : Value* (+ 95% tolerance)					
	If imposed pH : Buffer					
Temperature	Temperature of the Experiment* (+ 95% conf. interval)		°C	90 (2)	90 (2)	90 (2)
Pressure	If different from ambient pressure: pressure of the Experiment (bars)* (+ 95% conf. interval)					
	Document/File for Reference*	internal		logbook	logbook	logbook
		external				
	Analyses and Results					
sampling	if 1 reactor is sampled repeatedly: volume *					
	No Filtration (D), Filtration (F), Ultrafiltration (U)*			F,U	F,U	U
	If Filtration: Mesh Size *		µm	0,45	0,45	
	If ultrafiltration: MWCO*		dalton	10 000	10 000	10 000
	type of solution analyses*			ICP-AES	ICP-AES	ICP-AES
	analysed elements/ions*			Si, B, Na, Li, Mo, Al, Ca, Fe, Mg	Si, B, Na, Li, Mo, Al, Ca, Fe, Mg	Si, B, Na, Li, Mo, Al, Ca, Fe, Mg
	Element Concentration vs Duration Data in mg/l : ouput sheet reference*			SCKgl31/42-out	SCKgl46/57-out	SCKgl151/162-out
	pH vs Duration Data in mg/l : output sheet reference*			SCKgl31/42-out	SCKgl46/57-out	SCKgl151/162-out
	Eh vs Duration Data in mg/l : output sheet reference				SCKgl46/57-out	SCKgl151/162-out
solid analysis	Glass mass loss vs Duration Data in mg/l : output sheet reference			SCKgl1/12-out	SCKgl46/57-out	SCKgl151/162-out
	If surface analysis performed: type*			SIMS		SIMS
glass	**Glass composition (wt % oxides)***					
	SiO2			45,48	45,48	45,48
	B2O3			14,02	14,02	14,02
	Na2O			9,86	9,86	9,86

	Parameters of the Experiment						
Ref	*Reference Number Experiment**			FZK1	FZK2	FZK3	FZK4
Ref	*Reference Number input data set**						
t0	Date (Start of Experiment)			19/08/1997	19/08/1997	19/08/1997	19/08/1997
glass sample	Glass Sample Reference						
	Type of Glass*			GP WAK 1	GP WAK 1	GP WAK 1	GP WAK 1
	Sample Shape (Powder/Monolith)*			Powder	Powder	Powder	Powder
	If Monolith : Surface State (polished/nonpolished; grade)*						
	If Powder : Sample Granulometric Range (+ 95% conf. interval)	lower	µm	100	100	100	100
		higher	µm	200	200	200	200
	Mass		g	2,52	2,52	2,52	2,52
	Specific Surface Area of powder *(+ 95% conf. interval)		cm^2/g	427	427	427	427
	Method for determination of specific surface area*			BET(Kr)	BET(Kr)	BET(Kr)	BET(Kr)
Reactor	Type*			Borosilicatglas	Borosilicatglas	Borosilicatglas	Borosilicatglas
	Volume		ml	150	150	150	150
	number of reactors*	1 reactor	(Y/N)	Y	Y	Y	Y
		1 reactor	(Y/N)	N	N	N	N
Stirring	(Y/N)*			Y	Y	Y	Y
Solution	Type*			DI water,air saturated	DI water,air saturated	DI water,air saturated	DI water,air saturated
Solids	Type*						
	Dry mass of solid / SA of glass* (+ 95% conf. interval)		g/cm^2				
Type	Experimental Mode: static/dynamic*			static	static	static	static
	If Dynamic : Leaching Solution Flow Rate*		ml/day				
	If Static : Volume of leaching solution (+ 95% conf. interval)		ml	100	100	100	100
	If Static : SA/V ratio* (+ 95% conf. interval)		cm^-1	10+/-1	10+/-1	10+/-1	10+/-1
pH	Imposed pH (Y/N)*			Y	Y	Y	Y
	If imposed pH : Value* (+ 95% tolerance)			2.6 +/-0.02	3.0 +/-0.15	3.5 +/-0.2	4 +/-0.5
	If imposed pH : Buffer (which?) or pH-Stat			pH-stat	pH-stat	pH-stat	pH-stat
Temperature	Temperature of the Experiment* (+ 95% conf. interval)		°C	50+/-0.1	50+/-0.1	50+/-0.1	50+/-0.1
Pressure	If different from ambient pressure: pressure of the Experiment (bars)* (+ 95% conf. interval)						
	Document/File for Reference*	internal		ExpZweigengl/pH2.5	ExpZweigengl/pH3	ExpZweigengl/pH3.5	ExpZweigengl/pH4
		external		Y	Y	Y	Y
	Analyses and Results						
sampling	if 1 reactor is sampled repeatedly: volume *		ml	1	1	1	1
	No Filtration (D), Filtration (F), Ultrafiltration (U)*			F/U	F/U	F/U	F/U
	If Filtration: Mesh Size *		µm	0,45	0,45	0,45	0,45
	If ultrafiltration: MWCO*		nm	1,8	1,8	1,8	1,8
	type of solution analyses*			ICP-AES	ICP-AES	ICP-AES	ICP-AES
	analysed elements/ions*			Si, B, Li, Mo, Al, Ca	Si, B, Li, Mo, Al, Ca	Si, B, Li, Mo, Al, Ca	Si, B, Li, Mo, Al, Ca
	Element Concentration vs Duration Data in mg/l : ouput sheet reference*			FZK1-out	FZK2-out	FZK3-out	FZK4-out
	pH vs Duration Data in : output sheet reference*			FZK1-out	FZK2-out	FZK3-out	FZK4-out
	Eh vs Duration Data in : output sheet reference			-	-	-	-
solid analysis	Glass mass loss vs Duration Data in mg/l : output sheet reference			FZK1-out	FZK2-out	FZK3-out	FZK4-out
	If surface analysis performed: type*						
glass	**Glass composition (wt % oxides)***			**WAK**	**WAK**	**WAK**	**WAK**
	SiO2			50,4	50,4	50,4	50,4
	B2O3			14,8	14,8	14,8	14,8
	Na2O			10,3	10,3	10,3	10,3

	Parameters of the Experiment						
Ref	*Reference Number Experiment**			FZK5	FZK6	FZK7	FZK8
Ref	*Reference Number input data set**						
t0	Date (Start of Experiment)			19/08/1997	08/04/1998	08/04/1998	07/04/1998
glass sample	Glass Sample Reference						
	Type of Glass*			GP WAK 1	GP WAK 1	GP WAK 1	GP WAK 1
	Sample Shape (Powder/Monolith)*			Powder	Powder	Powder	Powder
	If Monolith : Surface State (polished/nonpolished; grade)*						
	If Powder : Sample Granulometric Range (+ 95% conf. interval)	lower	µm	100	100	100	100
		higher	µm	200	200	200	200
	Mass		g	2,52	2,52	2,52	2,52
	Specific Surface Area of powder *(+ 95% conf. interval)		cm^2/g	427	427	427	427
	Method for determination of specific surface area*			BET(Kr)	BET(Kr)	BET(Kr)	BET(Kr)
Reactor	Type*			Borosilicatglas	Borosilicatglas	Borosilicatglas	Borosilicatglas
	Volume		ml	150	150	150	150
	number of reactors*	1 reactor	(Y/N)	Y	Y	Y	Y
		1 reactor	(Y/N)	N	N	N	N
Stirring	(Y/N)*			Y	Y	Y	Y
Solution	Type*			DI water,air saturated	DI water,air saturated	DI water,air saturated	DI water,air saturated
Solids	Type*						
	Dry mass of solid / SA of glass* (+ 95% conf. interval)		g/cm^2				
Type	Experimental Mode: static/dynamic*			static	static	static	static
	If Dynamic : Leaching Solution Flow Rate*		ml/day				
	If Static : Volume of leaching solution (+ 95% conf. interval)		ml	100	100	100	100
	If Static : SA/V ratio* (+ 95% conf. interval)		cm^-1	10+/-1	10+/-1	10+/-1	10+/-1
pH	Imposed pH (Y/N)*			Y	Y	Y	Y
	If imposed pH : Value* (+ 95% tolerance)			4.5 +/-1.5	5.1 +/-0.1	6.1 +/-0.1	7.1 +/-0.02
	If imposed pH : Buffer (which?) or pH-Stat			pH-stat	pH-stat	pH-stat	pH-stat
Temperature	Temperature of the Experiment* (+ 95% conf. interval)		°C	50+/-0.1	50+/-0.1	50+/-0.1	50+/-0.1
Pressure	If different from ambient pressure: pressure of the Experiment (bars)* (+ 95% conf. interval)						
	Document/File for Reference*	internal		ExpZweigengl/pH4.5	ExpZweigengl/G01_pH5	ExpZweigengl/G02_pH6	ExpZweigengl/G04_pH7
		external		Y	Y	Y	Y
	Analyses and Results						
sampling	if 1 reactor is sampled repeatedly: volume *		ml	1	1	1	1
	No Filtration (D), Filtration (F), Ultrafiltration (U)*			F/U	F/U	F/U	F/U
	If Filtration: Mesh Size *		µm	0,45	0,45	0,45	0,45
	If ultrafiltration: MWCO*		nm	1,8	1,8	1,8	1,8
	type of solution analyses*			ICP-AES	ICP-AES	ICP-AES	ICP-AES
	analysed elements/ions*			Si, B, Li, Mo, Al, Ca	Si, B, Li, Mo, Al, Ca	Si, B, Li, Mo, Al, Ca	Si, B, Li, Mo, Al, Ca
	Element Concentration vs Duration Data in mg/l : ouput sheet reference*			FZK5-out	FZK6-out	FZK7-out	FZK8-out
	pH vs Duration Data in : output sheet reference*			FZK5-out	FZK6-out	FZK7-out	FZK8-out
	Eh vs Duration Data in : output sheet reference			-	-	-	-
solid analysis	Glass mass loss vs Duration Data in mg/l : output sheet reference			FZK5-out	FZK6-out	FZK7-out	FZK8-out
	If surface analysis performed: type*						
glass	**Glass composition (wt % oxides)***			**WAK**	**WAK**	**WAK**	**WAK**
	SiO2			50,4	50,4	50,4	50,4
	B2O3			14,8	14,8	14,8	14,8
	Na2O			10,3	10,3	10,3	10,3

	Parameters of the Experiment					
Ref	*Reference Number Experiment**			FZK9	FZK10	FZK11
Ref	*Reference Number input data set**					
t0	Date (Start of Experiment)			07/04/1998	08/04/1998	06/04/1998
glass sample	Glass Sample Reference					
	Type of Glass*			GP WAK 1	GP WAK 1	GP WAK 1
	Sample Shape (Powder/Monolith)*			Powder	Powder	Powder
	If Monolith : Surface State (polished/nonpolished; grade)*					
	If Powder : Sample Granulometric Range (+ 95% conf. interval)	lower	µm	100	100	100
		higher	µm	200	200	200
	Mass		g	2,52	2,52	2,52
	Specific Surface Area of powder *(+ 95% conf. interval)		cm²/g	427	427	427
	Method for determination of specific surface area*			BET(Kr)	BET(Kr)	BET(Kr)
Reactor	Type*			Borosilicatglas	Borosilicatglas	Borosilicatglas
	Volume		ml	150	150	150
	number of reactors*	1 reactor	(Y/N)	Y	Y	Y
		1 reactor	(Y/N)	N	N	N
Stirring	(Y/N)*			Y	Y	Y
Solution	Type*			DI water,air saturated	DI water,air saturated	DI water,air saturated
Solids	Type*					
	Dry mass of solid / SA of glass* (+ 95% conf. interval)		g/cm²			
Type	Experimental Mode: static/dynamic*			static	static	static
	If Dynamic : Leaching Solution Flow Rate*		ml/day			
	If Static : Volume of leaching solution (+ 95% conf. interval)		ml	100	100	100
	If Static : SA/V ratio* (+ 95% conf. interval)		cm^-1	10+/-1	10+/-1	10+/-1
pH	Imposed pH (Y/N)*			Y	Y	Y
	If imposed pH : Value* (+ 95% tolerance)			8.1 +/-0.1	9.1 +/-0.1	10.1 +/-0.2
	If imposed pH : Buffer (which?) or pH-Stat			pH-stat	pH-stat	pH-stat
Temperature	Temperature of the Experiment* (+ 95% conf. interval)		°C	50+/-0.1	50+/-0.1	50+/-0.1
Pressure	If different from ambient pressure: pressure of the Experiment (bars)* (+ 95% conf. interval)					
	Document/File for Reference*	internal		ExpZweigengl/G06_pH8	ExpZweigengl/G07_pH9	ExpZweigengl/G08_pH1
		external		Y	Y	Y
	Analyses and Results					
sampling	if 1 reactor is sampled repeatedly: volume *		ml	1	1	1
	No Filtration (D), Filtration (F), Ultrafiltration (U)*			F/U	F/U	F/U
	If Filtration: Mesh Size *		µm	0,45	0,45	0,45
	If ultrafiltration: MWCO*		nm	1,8	1,8	1,8
	type of solution analyses*			ICP-AES	ICP-AES	ICP-AES
	analysed elements/ions*			Si, B, Li, Mo, Al, Ca	Si, B, Li, Mo, Al, Ca	Si, B, Li, Mo, Al, Ca
	Element Concentration vs Duration Data in mg/l : ouput sheet reference*			FZK8-out	FZK8-out	FZK8-out
	pH vs Duration Data in : output sheet reference*			FZK8-out	FZK8-out	FZK8-out
	Eh vs Duration Data in : output sheet reference			-	-	-
solid analysis	Glass mass loss vs Duration Data in mg/l : output sheet reference			FZK8-out	FZK8-out	FZK8-out
	If surface analysis performed: type*					
glass	**Glass composition (wt % oxides)***			**WAK**	**WAK**	**WAK**
	SiO2			50,4	50,4	50,4
	B2O3			14,8	14,8	14,8
	Na2O			10,3	10,3	10,3

	Parameters of the Experiment			E1	E2	E3
Ref	*Reference Number Experiment**					
Ref	*Reference Number input data set**					
t0	Date (Start of Experiment)			18/02/02	18/02/02	18/02/02
glass sample	Glass Sample Reference					
	Type of Glass*			R7T7 type SON 68	R7T7 type SON 68	R7T7 type SON 68
	Sample Shape (Powder/Monolith)*			powder	powder	monolith
	If Monolith : Surface State (polished/nonpolished; grade)*					polished
	If Powder : Sample Granulometric Range (+ 95% conf. interval)	lower	µm	0		
		higher	µm	20	5	
	Mass		g	0,3	0,3	
	Specific Surface Area of powder *(+ 95% conf. interval)		cm²/g	0,5056	1,39	
	Method for determination of specific surface area*			BET (Kr)		
Reactor	Type*			PTFE	PTFE	PTFE
	Volume		ml	35	35	35
	number of reactors*	1 reactor	(Y/N)	Y	Y	Y
		1 reactor	(Y/N)	N	N	N
Stirring	(Y/N)*			N	N	N
Solution	Type*			60 mg/L silica, 380 mg/L B, >1g/L Na	60 mg/L silica, 380 mg/L B, >1g/L Na	60 mg/L silica, 380 mg/L B, >1g/L Na
Solids	Type*					
	Dry mass of solid / SA of glass* (+ 95% conf. interval)		g/cm²			
Type	Experimental Mode: static/dynamic*			dynamic	dynamic	dynamic
	If Dynamic : Leaching Solution Flow Rate*		ml/day	14,4	14,4	14,4
	If Static : Volume of leaching solution (+ 95% conf. interval)		ml			
	If Static : SA/V ratio* (+ 95% conf. interval)		cm^-1			
pH	Imposed pH (Y/N)*			Y	Y	Y
	If imposed pH : Value* (+ 95% tolerance)			5	5	5
	If imposed pH : Buffer (which?) or pH-Stat			buffer CH3COOH/CH3COO-, Na+	buffer CH3COOH/CH3COO-, Na+	buffer CH3COOH/CH3COO-, Na+
Temperature	Temperature of the Experiment* (+ 95% conf. interval)		°C	50	50	50
Pressure	If different from ambient pressure: pressure of the Experiment (bars)* (+ 95% conf. interval)					
	Document/File for Reference*	internal				
		external				
	Analyses and Results					
sampling	if 1 reactor is sampled repeatedly: volume *		ml			
	No Filtration (D), Filtration (F), Ultrafiltration (U)*			D	D	D
	If Filtration: Mesh Size *		µm			
	If ultrafiltration: MWCO*		nm			
	type of solution analyses*			ICP-MS	ICP-MS	ICP-MS
	analysed elements/ions*			Li,Cs,Mo,Si	Li,Cs,Mo,Si	Li,Cs,Mo,Si
	Element Concentration vs Duration Data in mg/l : ouput sheet reference*			E1-out	E2-out	E3-out
	pH vs Duration Data in : output sheet reference*			E1-out	E2-out	E3-out
	Eh vs Duration Data in : output sheet reference					
solid analysis	Glass mass loss vs Duration Data in mg/l : output sheet reference					
	If surface analysis performed: type*			BEM, FTIR	FTIR	BEM, FTIR
glass	**Glass composition (wt % oxides)***					
	SiO2			45,48	45,48	45,48
	B2O3			14,02	14,02	14,02
	Na2O			9,86	9,86	9,86

Parameters of the Experiment			E5	E6	E7
*Reference Number Experiment**					
*Reference Number input data set**					
Date (Start of Experiment)			15/04/02	15/04/02	15/04/02
Glass Sample Reference					
Type of Glass*			R7T7 type SON 68	R7T7 type SON 68	R7T7 type SON 68
Sample Shape (Powder/Monolith)*			powder	monolith	powder
If Monolith : Surface State (polished/nonpolished; grade)*				polished	
If Powder : Sample Granulometric Range (+ 95% conf. interval)	lower	µm			
	higher	µm	5		20
Mass		g			0,5056
Specific Surface Area of powder *(+ 95% conf. interval)		cm²/g	1,39		BET (Kr)
Method for determination of specific surface area*					
Type*			PTFE	PTFE	PTFE
Volume		ml	35	35	35
number of reactors*	1 reactor	(Y/N)	Y	Y	Y
	1 reactor	(Y/N)	N	N	N
(Y/N)*			N	N	N
Type*			60 mg/L silica, 380 mg/L B, >1g/L Na	60 mg/L silica, 380 mg/L B, >1g/L Na	60 mg/L silica, 380 mg/L B, >1g/L Na
Type*					
Dry mass of solid / SA of glass* (+ 95% conf. interval)		g/cm²			
Experimental Mode: static/dynamic*			dynamic	dynamic	dynamic
If Dynamic : Leaching Solution Flow Rate*		ml/day	14,4	14,4	14,4
If Static : Volume of leaching solution (+ 95% conf. interval)		ml			
If Static : SA/V ratio* (+ 95% conf. interval)		cm^-1			
Imposed pH (Y/N)*			Y	Y	Y
If imposed pH : Value* (+ 95% tolerance)			7,2	7,2	9,8
If imposed pH : Buffer (which?) or pH-Stat			buffer citric acid /NaOH	buffer citric acid /NaOH	
Temperature of the Experiment* (+ 95% conf. interval)		°C	50	50	50
If different from ambient pressure: pressure of the Experiment (bars)* (+ 95% conf. interval)					
Document/File for Reference*	internal				
	external				
Analyses and Results					
if 1 reactor is sampled repeatedly: volume *		ml			
No Filtration (D), Filtration (F), Ultrafiltration (U)*			D	D	D
If Filtration: Mesh Size *		µm			
If ultrafiltration: MWCO*		nm			
type of solution analyses*			ICP-MS	ICP-MS	ICP-MS
analysed elements/ions*			Li,Cs,Mo,Si	Li,Cs,Mo,Si	Li,Cs,Mo,Si
Element Concentration vs Duration Data in mg/l : ouput sheet reference*			E5-out	E6-out	E7-out
pH vs Duration Data in : output sheet reference*			E5-out	E6-out	E7-out
Eh vs Duration Data in : output sheet reference					
Glass mass loss vs Duration Data in mg/l : output sheet reference					
If surface analysis performed: type*			FTIR	BEM, FTIR	FTIR
Glass composition (wt % oxides)*					
SiO2			45,48	45,48	45,48
B2O3			14,02	14,02	14,02
Na2O			9,86	9,86	9,86

ANNEX III

Composition of the glasses studied in GLAMOR

Glass composition (wt % oxides)*	SON68	AVM6	AVM10	CJ1	CJ3	CJ6	CJ9	MW	GPWAK1
SiO2	45,48	44,49	38,5	65,56	58,07	52,66	59,8	46,73	50,4
B2O3	14,02	19,5	16,75	20,23	17,92	16,25	18,45	16,53	14,8
Na2O	9,86	15,5	15	14,21	12,59	11,34	12,95	8,09	10,3
Al2O3	4,91	9	12,5		6,27	5,68		5,65	2,6
MgO		3,8	6					5,55	1,8
CaO	4,04	0,2	0,2		5,15	4,66	5,31	0,01	4,5
Li2O	1,98	0,4	0,4			2,28		3,81	2,9
Fe2O3	2,91	1,9	1,9					2,63	2,19
NiO	0,74	0,3	0,3					0,3	0,34
Cr2O3	0,51	0,45	0,45					0,46	0,58
ZnO	2,5								
F		1,8							
SO3		0,1	0,1					0,07	
P2O5	0,28		2					0,17	0,44
SrO	0,33	0,04	0,12					0,33	0,11
ZrO2	2,65	0,19	0,53			3,07	3,49	1,59	0,76
TiO2								0,01	1
MoO3	1,70	0,29	0,82					1,69	1,05
MnO2	0,72	0,06	0,17						0,4
Cs2O	1,42	0,14	0,39					1,1	0,69
BaO	0,60	0,07	0,19					0,53	0,54
Y2O3	0,20	0,02	0,07					0,17	0,15
La2O3	0,90	0,11	0,3					0,47	0,5
Ce2O3	0,93	0,11	0,33			4,55		0,93	0,41
Nd2O3	1,59	0,18	0,51					1,51	1,51
Pr2O3	0,44	0,05	0,15					0,63	0,34
Gd2O3		0,23	0,66					0,01	0,07
UO2	0,52								
ThO2	0,33								
Ag2O	0,03	0,04	0,11					0,01	0,02
CdO	0,03	0,5	0,5					0,01	0,02
SnO2	0,02							0,01	0,01
Sb2O3	0,01		0,01					0,01	
TeO2	0,23	0,03	0,08					0,1	0,15
RuO2		0,15	0,44					0,61	0,61
Rh									
Pd		0,1	0,27						
K2O									
CoO	0,12								
Cl			0,1						
Rh2O3									
PdO									0,31
Sm2O3								0,28	0,29
RbO2								0,08	0,06
Eu2O3								0,01	0,03
total	**100**	**99,75**	**99,85**	**100**	**100**	**100,49**	**100**	**100,09**	**99,88**

ANNEX IV

Overview of model simulations made by CEA and Subatech

A1 Experiment — SON68 glass, T=90°C, free pH, HPW, S/V=200 000 m^{-1}

Fits by CEA

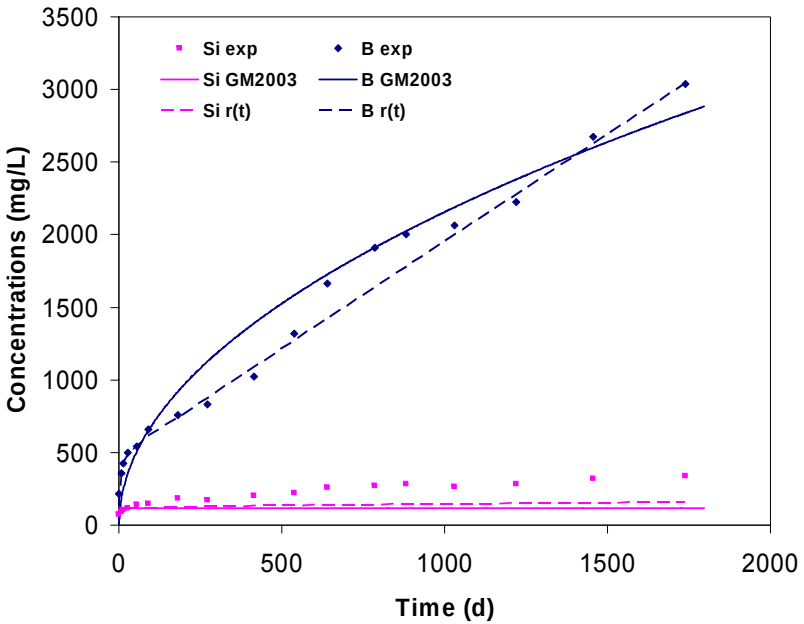

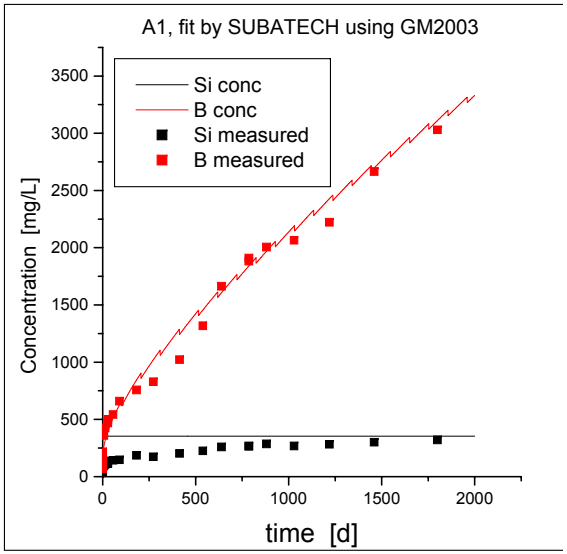

A1		r_o (g.m^{-2}.day^{-1})	C*/ K_{SiO2} (ppm)	Dg/D_{Si} (m².s^{-1})	α(ppm^{-1})	r_{fin}(g.m^{-2}.day^{-1})	D_{H20} (m².s^{-1})	Kd_B (kg.m^{-3})
CEA	R(t)	3.22	32	1.0 10^{-19}	0.038	1.5 10^{-4}	n.c.	n.c.
	GM2003	0.7	115	5.2 10^{-14}	0.005	1.0 10^{-11}	5.0 10^{-23}	70
Subatech	R(t)	?	?	?	?	?	n.c.	n.c.
	GM2003	0.7	85	5.2 10^{-14}	0.014	7.0 10^{-8}	2.5 10^{-23}	100

A2 Experiment — SON68 glass, T=90°C, free pH, HPW, S/V=5000 m^{-1}

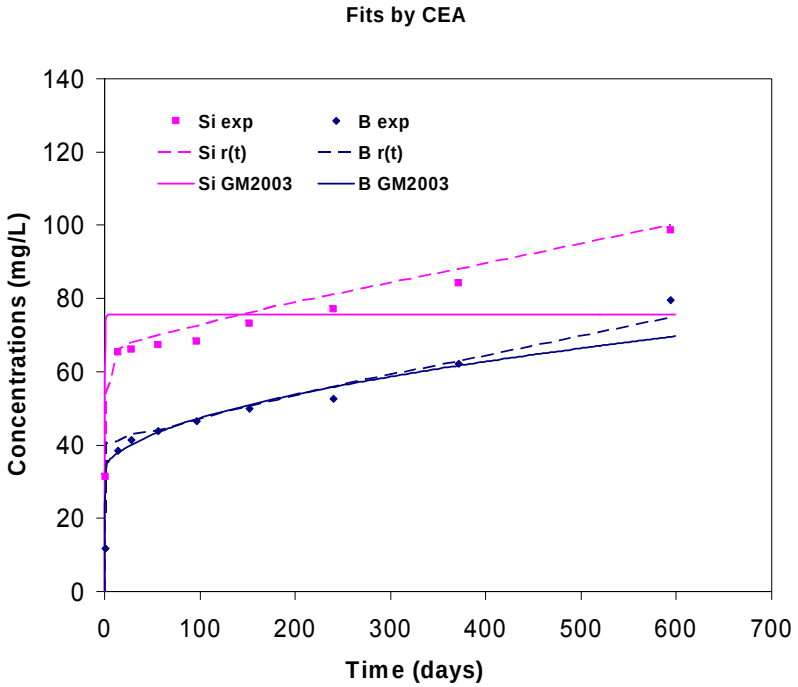

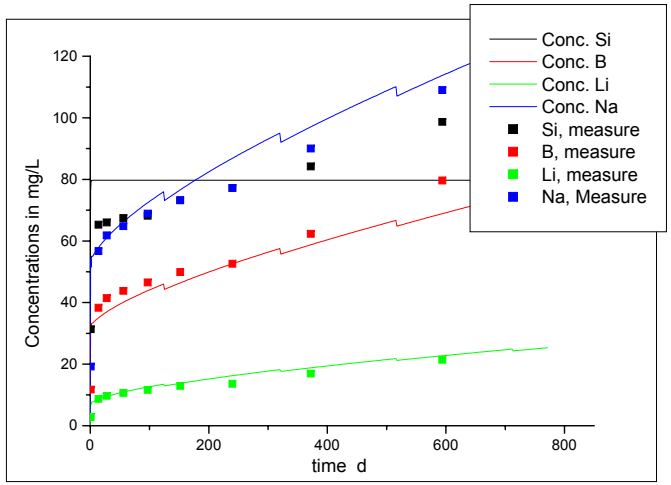

A2		r_o (g.m^{-2}.day^{-1})	C*/ K_{SiO2} (ppm)	Dg/D_{Si} (m².s^{-1})	α(ppm^{-1})	r_{fin}(g.m^{-2}.day^{-1})	D_{H20} (m².s^{-1})	Kd_B (kg.m^{-3})
CEA	R(t)	2.6	26	1.0 10^{-14}	0.02	2.5 10^{-4}	n.c.	n.c.
	GM2003	0.7	75	5.2 10^{-15}	0.02	1.0 10^{-11}	8.0 10^{-24}	5
Subatech	R(t)	?	?	?	?	?	n.c.	n.c.
	GM2003	0.7	95	5.2 10^{-14}	0.015	7.0 10^{-8}	4.0 10^{-23}	100

A3 Experiment — SON68 glass, T=90°C, pH=7, KOH, S/V=5000 m^{-1}

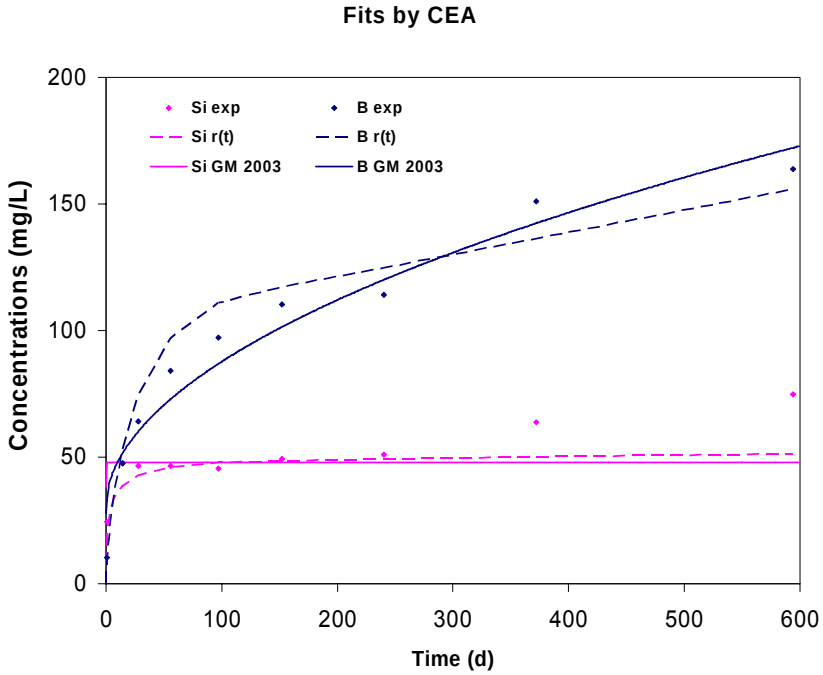

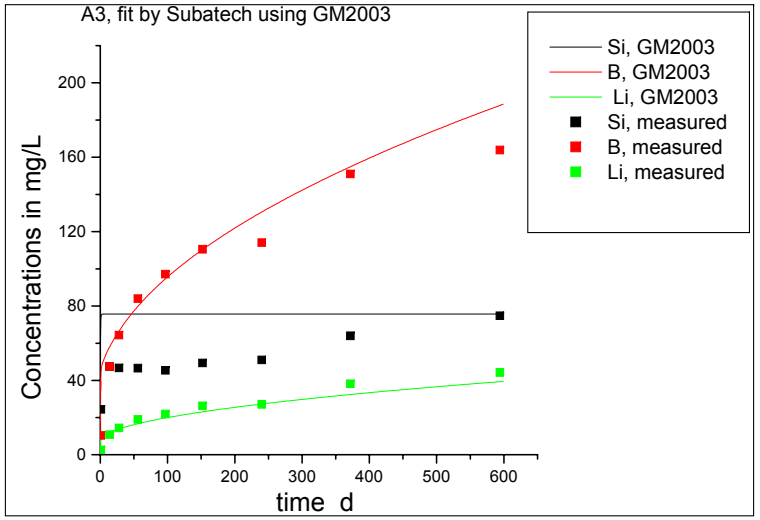

A3		r_o (g.m^{-2}.day^{-1})	C*/ K_{SiO2} (ppm)	Dg/D_{Si} (m².s^{-1})	α(ppm^{-1})	r_{fin}(g.m^{-2}.day^{-1})	D_{H20} (m².s^{-1})	Kd_B (kg.m^{-3})
CEA	R(t)	0.4	48	1.0 10^{-17}	0.078	3.0 10^{-4}	n.c.	n.c.
	GM2003	0.7	48	5.2 10^{-14}	0.02	1.0 10^{-11}	3.0 10^{-22}	30
Subatech	R(t)	?	?	?		?	n.c.	n.c.
	GM2003	0.7	75	5.2 10^{-14}	0.02	7.0 10^{-8}	1.0 10^{-21}	100

A4 Experiment — SON68 glass, T=90°C, pH=8, KOH, S/V=5000 m^{-1}

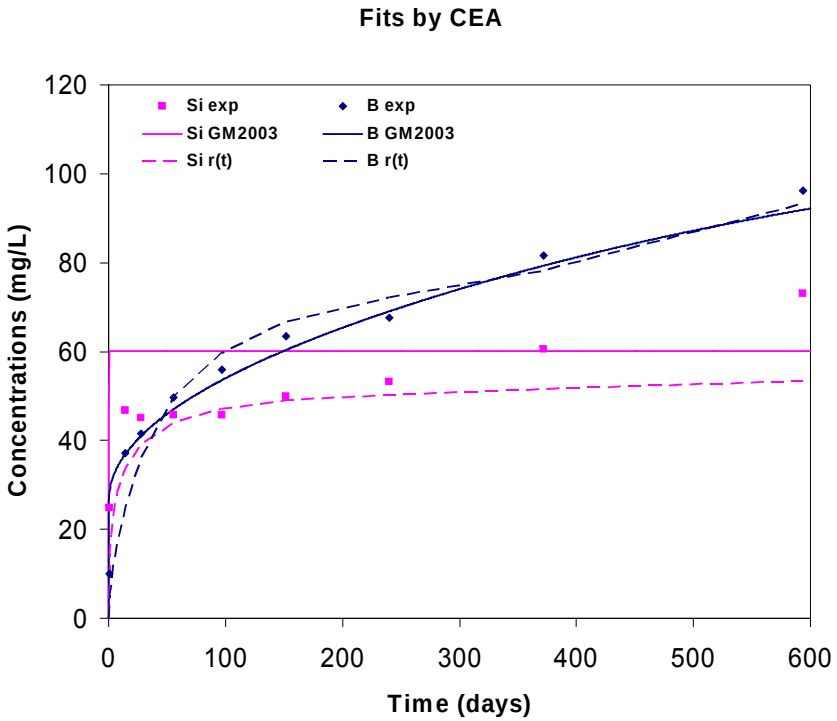

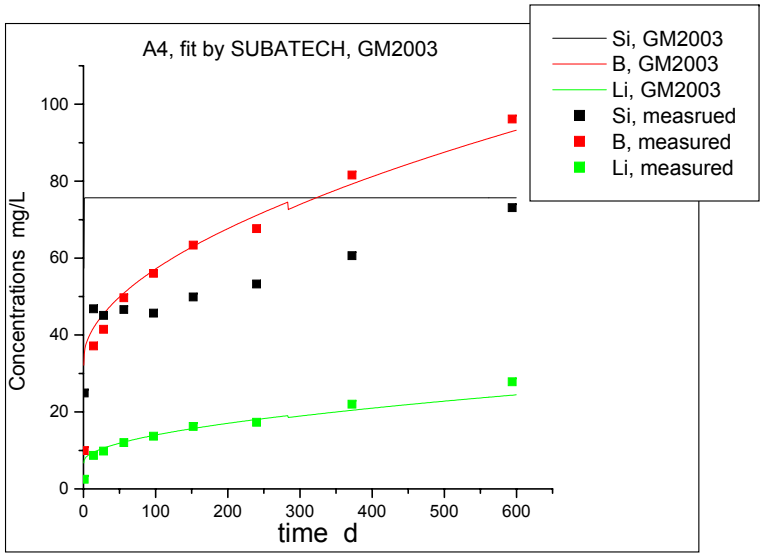

A4		r_o (g.m^{-2}.day^{-1})	C*/ K_{SiO2} (ppm)	Dg/D_{Si} (m².s^{-1})	α(ppm^{-1})	r_{fin}(g.m^{-2}.day^{-1})	D_{H20} (m².s^{-1})	Kd_B (kg.m^{-3})
CEA	R(t)	0.95	45	3.0 10^{-18}	0.061	2.0 10^{-4}	n.c.	n.c.
	GM2003	0.7	60	5.2 10^{-15}	0.025	1.0 10^{-11}	1.3 10^{-22}	70
Subatech	R(t)	?	?	?	?	?	n.c.	n.c.
	GM2003	0.7	75	5.2 10^{-14}	0.02	7.0 10^{-8}	1.5 10^{-22}	100

A5 Experiment — SON68 glass, T=90°C, pH=9.5, KOH, S/V=5000 m^{-1}

Fits by CEA

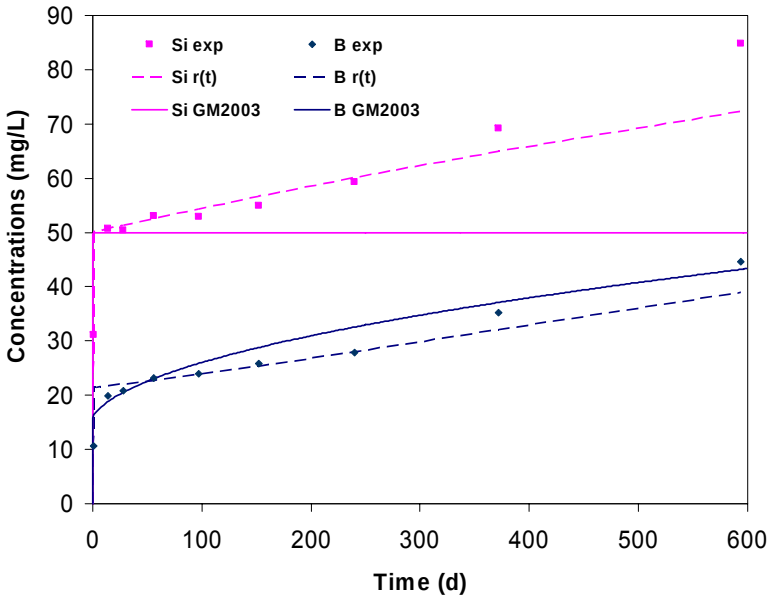

fit by Subatech

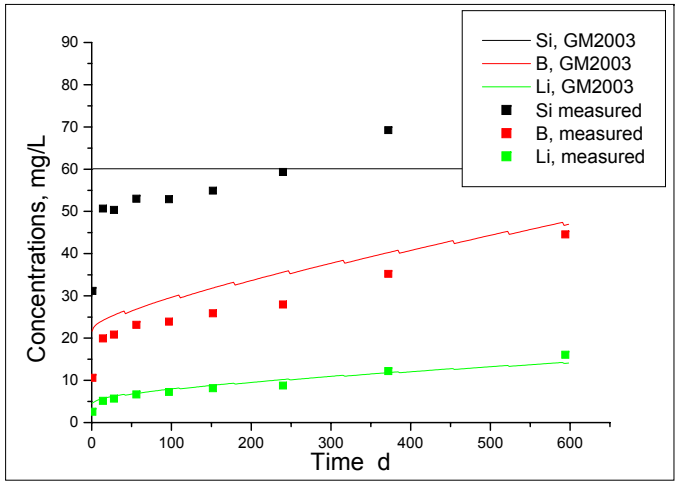

A5		r_o (g.m^{-2}.day^{-1})	C*/ K_{SiO2} (ppm)	Dg/D_{Si} (m².s^{-1})	α(ppm^{-1})	r_{fin}(g.m^{-2}.day^{-1})	D_{H20} (m².s^{-1})	Kd_B (kg.m^{-3})
CEA	R(t)	3.6	11	1.0 10^{-14}	0.017	1.0 10^{-4}	n.c.	n.c.
	GM2003	0.7	50	5.2 10^{-15}	0.016	1.0 10^{-11}	2.5 10^{-23}	70
Subatech	R(t)	?	?	?	?	?	n.c.	n.c.
	GM2003	0.7	60	5.2 10^{-14}	0.017	7.0 10^{-8}	1.0 10^{-23}	100

A6 Experiment — SON68 glass, T=90°C, pH=10, KOH, S/V=5000 m^{-1}

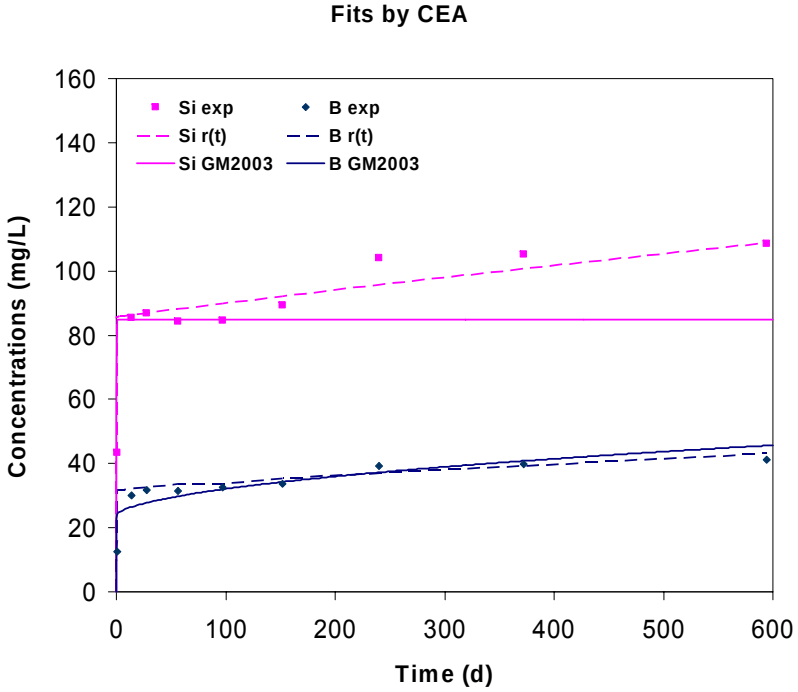

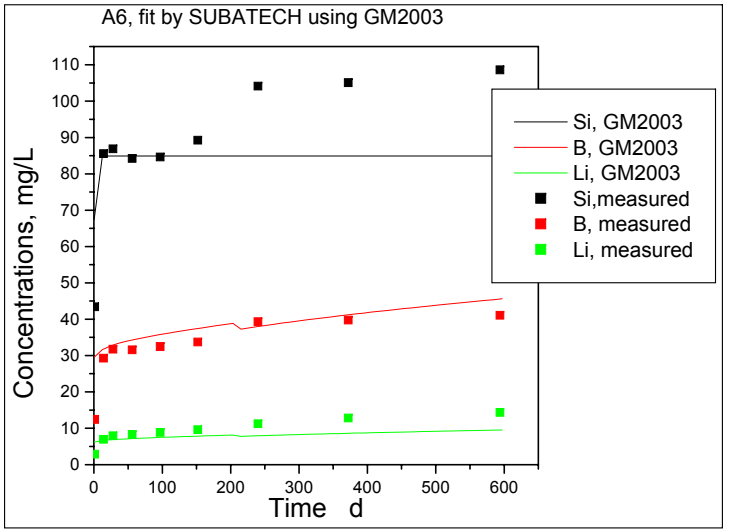

A6		r_o (g.m^{-2}.day^{-1})	C*/ K_{SiO2} (ppm)	Dg/D_{Si} (m².s^{-1})	α(ppm^{-1})	r_{fin}(g.m^{-2}.day^{-1})	D_{H20} (m².s^{-1})	Kd_B (kg.m^{-3})
CEA	R(t)	5.73	7	1.0 10^{-14}	0.008	8.0 10^{-5}	n.c.	n.c.
	GM2003	0.7	85	5.2 10^{-15}	0.008	1.0 10^{-11}	2.0 10^{-23}	90
Subatech	R(t)	?	?	?	?	?	n.c.	n.c.
	GM2003	0.7	75	5.2 10^{-14}	0.012	7.0 10^{-8}	1.0 10^{-23}	100

A7 Experiment — SON68 glass, T=90°C, pH=10.5, KOH, S/V=5000 m^{-1}

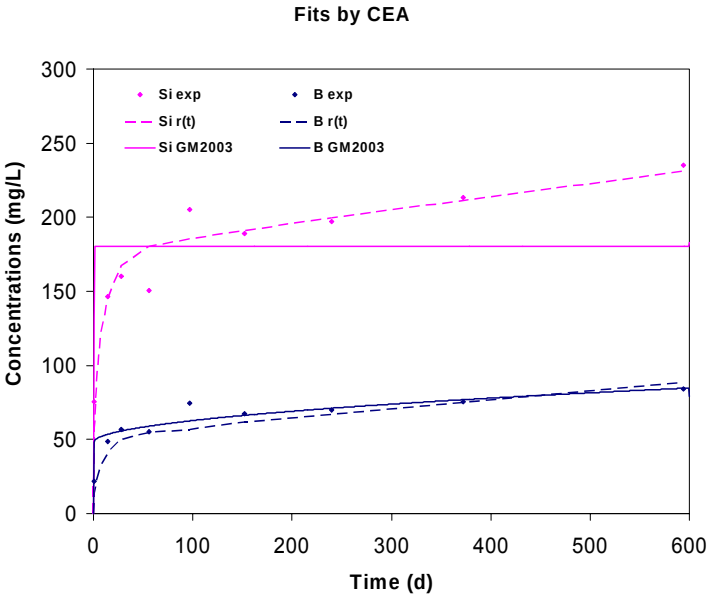

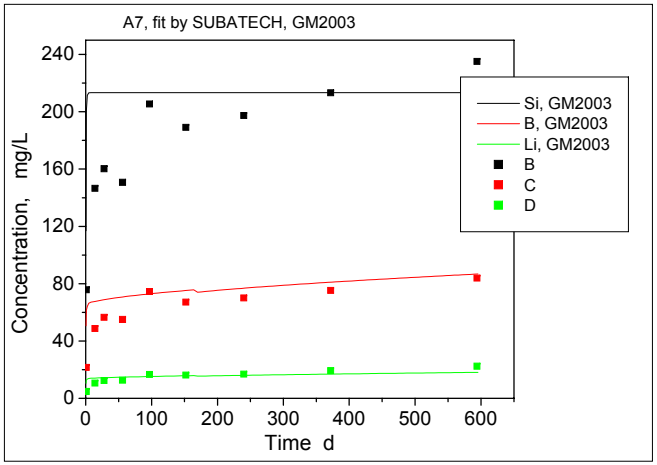

A7		r_o (g.m^{-2}.day^{-1})	C*/ K_{SiO2} (ppm)	Dg/D_{Si} (m².s^{-1})	α(ppm^{-1})	r_{fin}(g.m^{-2}.day^{-1})	D_{H20} (m².s^{-1})	Kd_B (kg.m^{-3})
CEA	R(t)	8.98	5	1.0 10^{-17}	0.004	2.0 10^{-4}	n.c.	n.c.
	GM2003	0.7	180	5.2 10^{-14}	0.003	1.0 10^{-11}	4.0 10^{-23}	70
Subatech	R(t)	?	?	?	?	?	n.c.	n.c.
	GM2003	0.7	213	5.2 10^{-14}	0.005	7.0 10^{-8}	2.0 10^{-23}	100

A8 Experiment — SON68 glass, T=90°C, pH=11, KOH, S/V=5000 m^{-1}

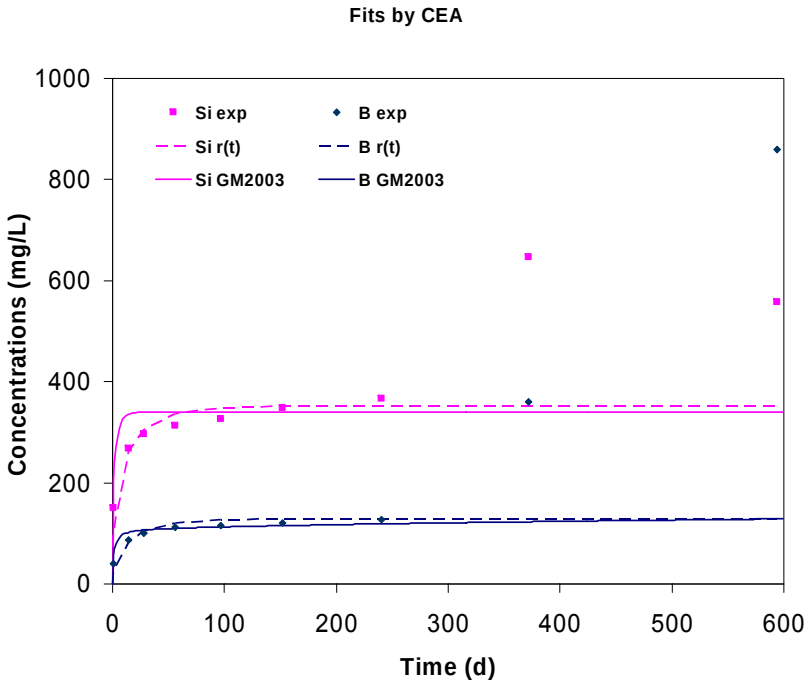

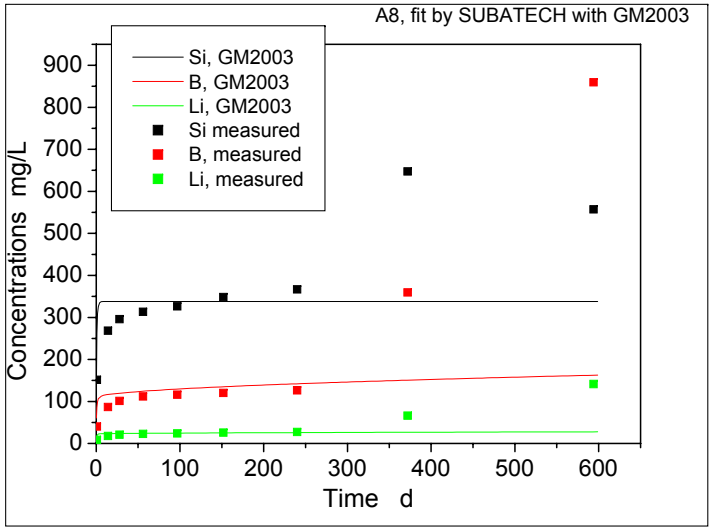

A8		r_o (g.m^{-2}.day^{-1})	C*/ K_{SiO2} (ppm)	Dg/D_{Si} (m².s^{-1})	α(ppm^{-1})	r_{fin}(g.m^{-2}.day^{-1})	D_{H20} (m².s^{-1})	Kd_B (kg.m^{-3})
CEA	R(t)	14	3.1	1.7 10^{-17}	0.003	1.0 10^{-8}	n.c.	n.c.
	GM2003	0.7	340	5.2 10^{-15}	0.002	1.0 10^{-11}	2.0 10^{-23}	70
Subatech	R(t)	?	?	?	?	?	n.c.	n.c.
	GM2003	0.7	338	5.2 10^{-14}	0.003	7.0 10^{-8}	2.0 10^{-23}	100

A9 Experiment — SON68 glass, T=90°C, pH=11.5, KOH, S/V=5000 m^{-1}

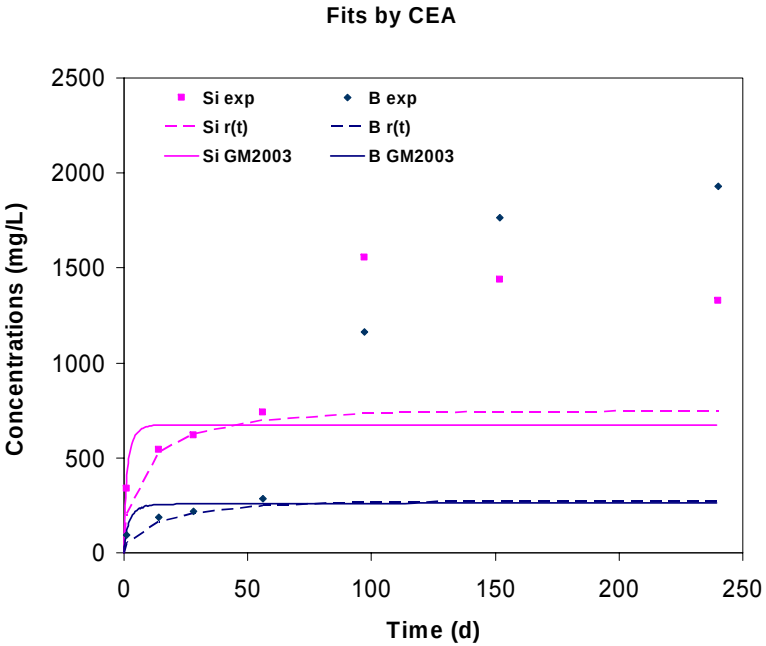

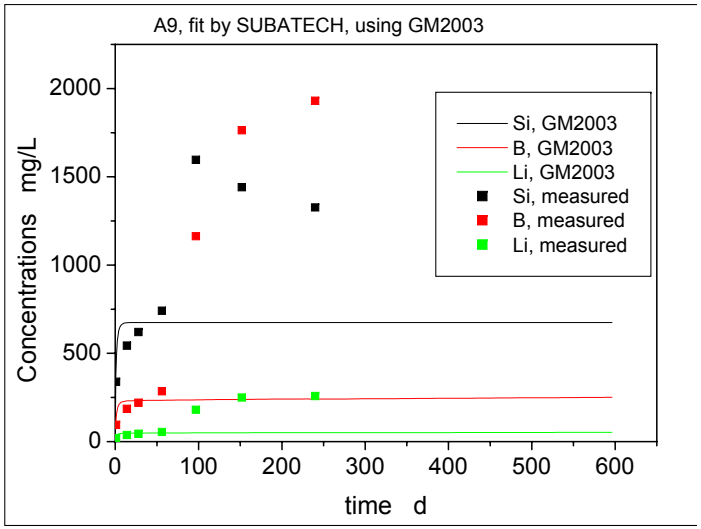

A9		r_o (g.m^{-2}.day^{-1})	C*/ K_{SiO2} (ppm)	Dg/D_{Si} (m².s^{-1})	α(ppm^{-1})	r_{fin}(g.m^{-2}.day^{-1})	D_{H20} (m².s^{-1})	Kd_B (kg.m^{-3})
CEA	R(t)	22	2	3.0 10^{-17}	0.0014	1.0 10^{-8}	n.c.	n.c.
	GM2003	0.7	674	5.2 10^{-14}	0.0016	1.0 10^{-11}	2.0 10^{-23}	70
Subatech	R(t)	?	?	?	?	?	n.c.	n.c.
	GM2003	0.7	674	5.2 10^{-14}	0.0015	7.0 10^{-8}	2.0 10^{-23}	100

CURTI Experiment — SON68 glass, T=90°C, pH=9.7, KOH, S/V=1200 m^{-1}

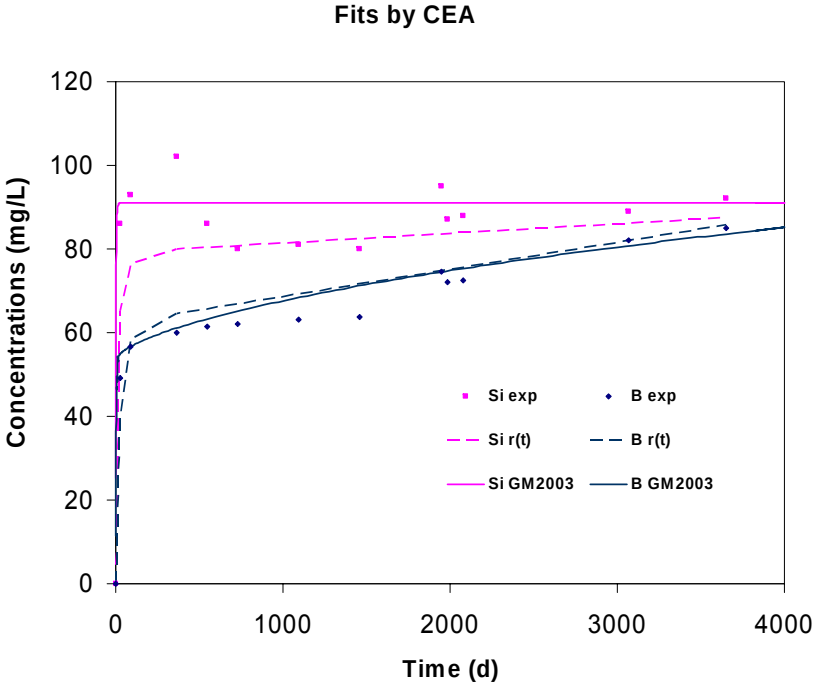

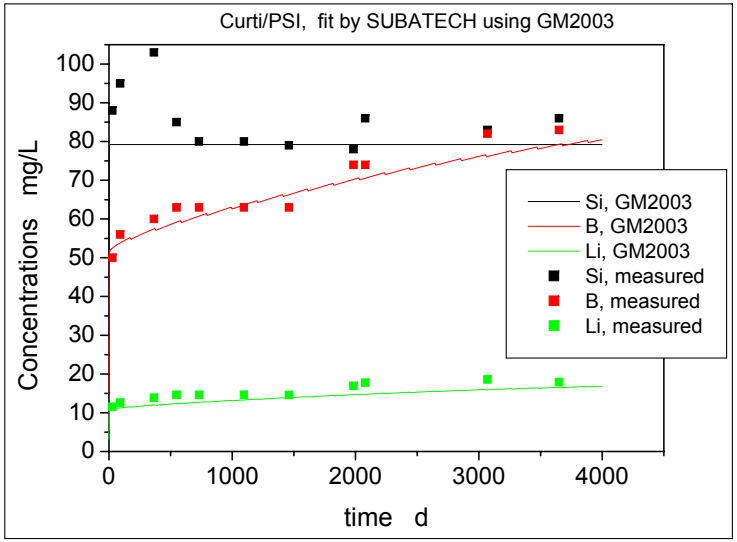

CURTI		r_o (g.m^{-2}.day^{-1})	C*/ K_{SiO2} (ppm)	Dg/D_{Si} (m².s^{-1})	α(ppm^{-1})	r_{fin}(g.m^{-2}.day^{-1})	D_{H20} (m².s^{-1})	Kd_B (kg.m^{-3})
CEA	R(t)	4.38	2	8.0 10^{-17}	0.028	1.0 10^{-4}	n.c.	n.c.
	GM2003	0.7	90	5.2 10^{-14}	0.02	1.0 10^{-11}	2.5 10^{-23}	10
Subatech	R(t)	?	?	?	?	?	n.c.	n.c.
	GM2003	0.7	84.9	5.2 10^{-14}	0.027	7.0 10^{-8}	2.5 10^{-23}	100

A10 Experiment SON68 glass, T=90°C, pH=8, KOH, S/V=150 m^{-1}, 144 mL/day

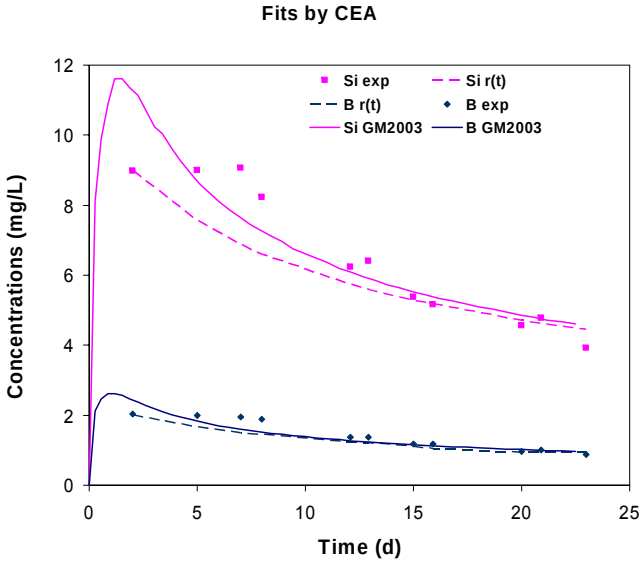

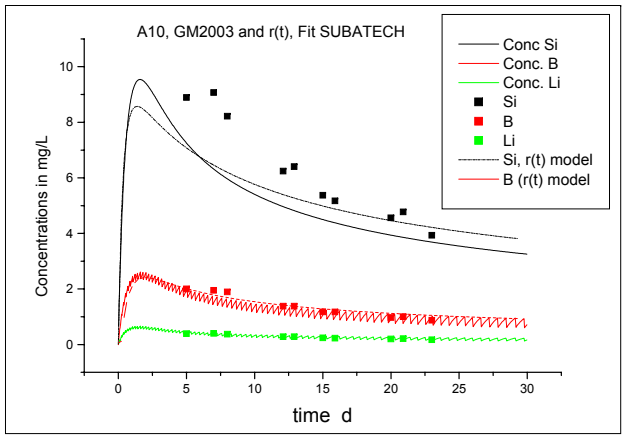

A10		$r_{o\ (}$g.m^{-2}.day^{-1})	C*/ K_{SiO2} (ppm)	Dg/D_{Si} (m².s^{-1})	α(ppm^{-1})	r_{fin}(g.m^{-2}.day^{-1})	D_{H20} (m².s^{-1})	Kd_B (kg.m$^{-3)}$
CEA	R(t)	0.95	18.6	7.0 10^{-14}	0.011	1.0 10^{-8}	n.c.	n.c.
	GM2003	0.7	95	7.0 10^{-14}	0.002	1.0 10^{-11}	1.0 10^{-23}	70
Subatech	R(t)	0.7	36	1.7·10^{-13}	0.024	7.0 10^{-8}	n.c.	n.c.
	GM2003	0.7	85	5.2 10^{-14}	0.014	7.0 10^{-8}	2.0 10^{-20}	100

A11 Experiment SON68 glass, T=90°C, pH=8, 60 ppm Si, S/V=150 m^{-1}, 144 mL/day

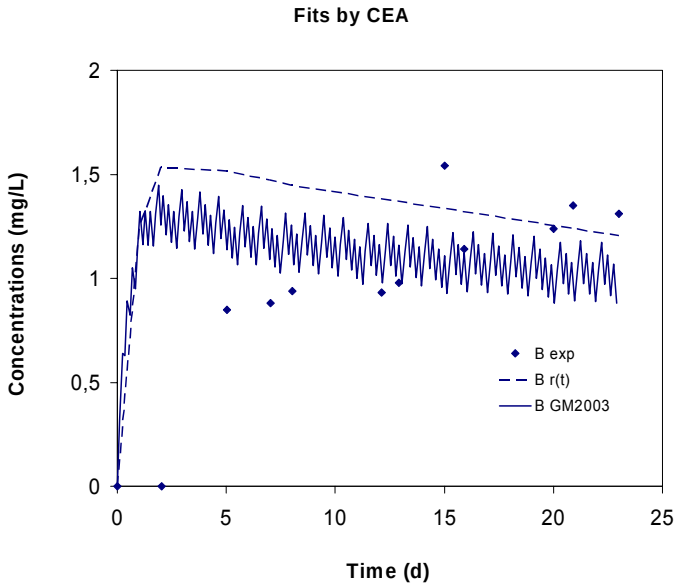

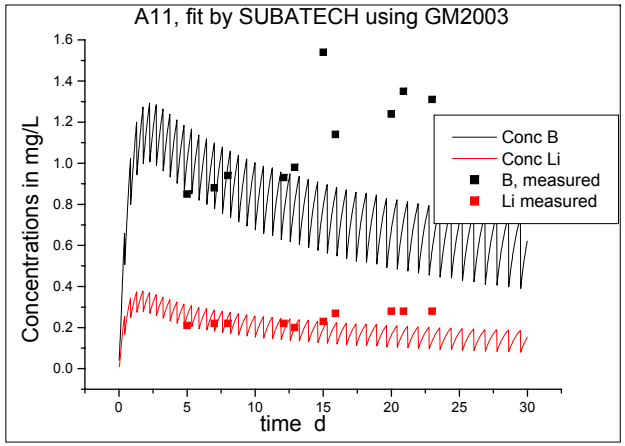

Remarque: the fit using GM2003 is bette by CEA, but with the goal of maintaining the parameter set of experiment A10, not optimisation was attempted

A11		r_o (g.m^{-2}.day^{-1})	C*/ K_{SiO2} (ppm)	Dg/D_{Si} (m².s^{-1})	α(ppm^{-1})	r_{fin}(g.m^{-2}.day^{-1})	D_{H20} (m².s^{-1})	Kd_B (kg.m^{-3})
CEA	R(t)	0.95	85	7.0 10^{-14}	0.009	1.0 10^{-8}	n.c.	n.c.
	GM2003	0.7	84.9	7.0 10^{-14}	0.04	1.0 10^{-11}	8.0 10^{-21}	30
Subatech	R(t)	?	?	?	?	?	n.c.	n.c.
	GM2003	0.7	85	5.2 10^{-14}	0.014	7.0 10^{-8}	2.0 10^{-20}	100

A12 Experiment SON68 glass, T=90°C, pH=8, 120 ppm Si, S/V=150 m^{-1}, 144 mL/day

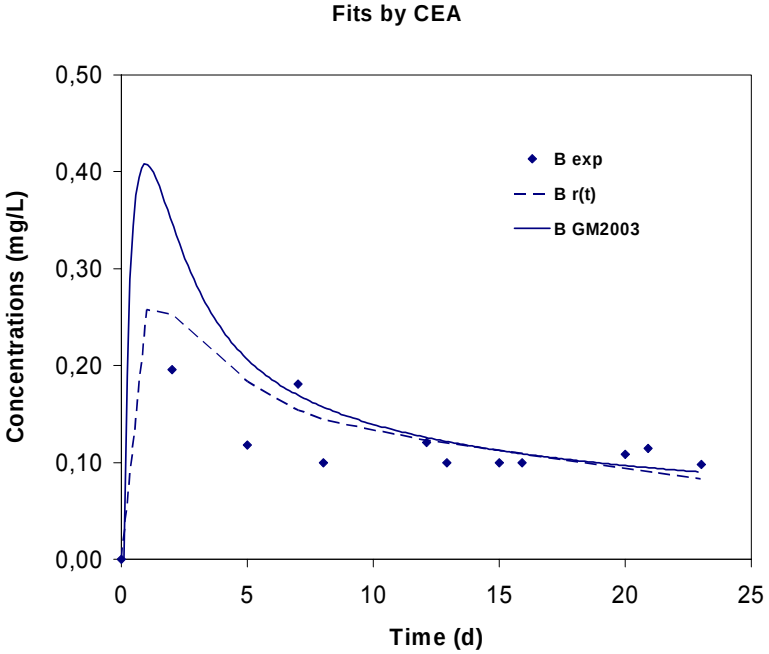

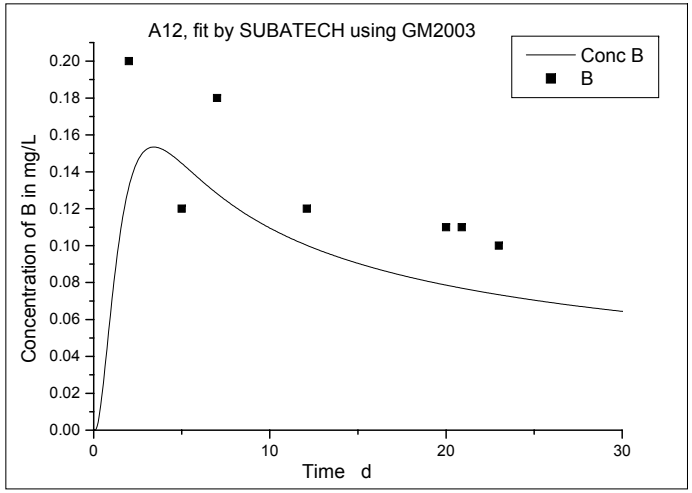

A12		r_o (g.m^{-2}.day^{-1})	C*/ K_{SiO2} (ppm)	Dg/D_{Si} (m².s^{-1})	α(ppm^{-1})	r_{fin}(g.m^{-2}.day^{-1})	D_{H20} (m².s^{-1})	Kd_B (kg.m^{-3})
CEA	R(t)	0.95	120	7.0 10^{-16}	0.001	1.0 10^{-8}	n.c.	n.c.
	GM2003	0.7	120	7.0 10^{-14}	0.03	1.0 10^{-11}	1.0 10^{-20}	30
Subatech	R(t)	?	?	?	?	?	n.c.	n.c.
	GM2003	0.7	85	5.2.0 10^{-14}	0.014	7.0 10^{-8}	2.0 10^{-20}	100

A13 Experiment — SON68 glass, T=90°C, pH=9, KOH, S/V=1500 m^{-1}

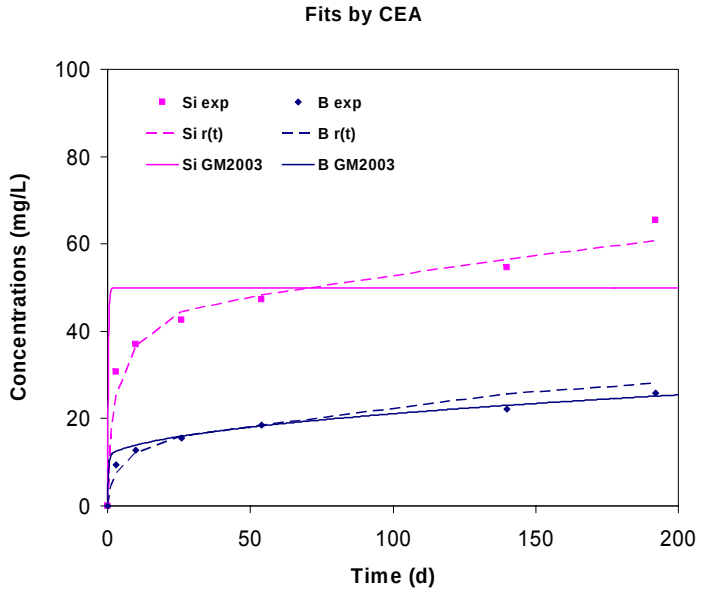

A13		r_o (g.m^{-2}.day^{-1})	C*/ K_{SiO2} (ppm)	Dg/D_{Si} (m².s^{-1})	α(ppm^{-1})	r_{fin}(g.m^{-2}.day^{-1})	D_{H20} (m².s^{-1})	Kd_B (kg.m^{-3})
CEA	R(t)	2.33	22	4.0 10^{-17}	0.023	1.0 10^{-3}	n.c.	n.c.
	GM2003	0.7	50	5.2 10^{-14}	0.002	1.0 10^{-11}	8.0 10^{-23}	20
Subatech	R(t)	?	?	?	?	?	n.c.	n.c.
	GM2003	?	?	?	?	?	?	?

A14 Experiment — SON68 glass, T=90°C, pH=9, 100 ppm P, S/V=1500 m^{-1}

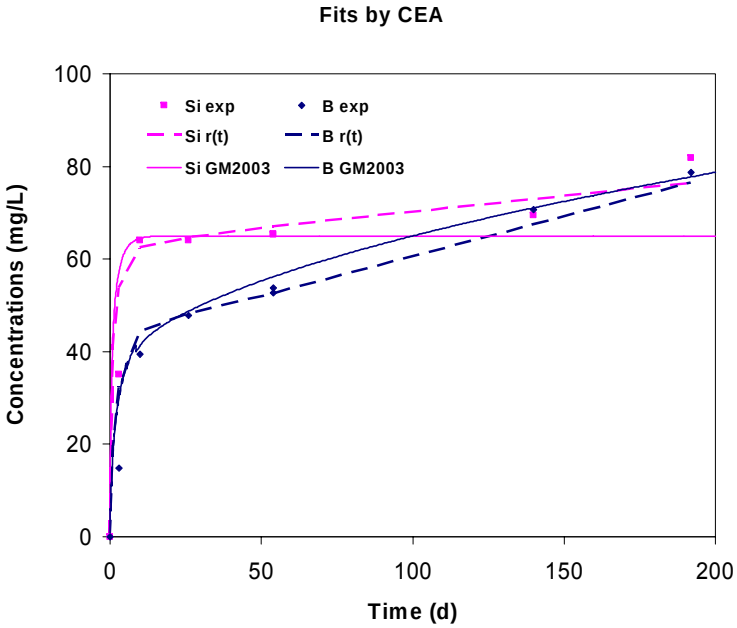

A14		r_o (g.m^{-2}.day^{-1})	C*/ K_{SiO2} (ppm)	Dg/D_{Si} (m².s^{-1})	α(ppm^{-1})	r_{fin}(g.m^{-2}.day^{-1})	D_{H20} (m².s^{-1})	Kd_B (kg.m^{-3})
CEA	R(t)	2.33	30	5.0 10^{-16}	0.033	2.3 10^{-3}	n.c.	n.c.
	GM2003	0.7	65	5.2 10^{-15}	0.025	1.0 10^{-11}	8.0 10^{-22}	20
Subatech	R(t)	?	?	?	?	?	n.c.	n.c.
	GM2003	?	?	?	?	?	?	?

A15 Experiment — SON68 glass, T=90°C, free pH, HPW, S/V=5000 m^{-1}

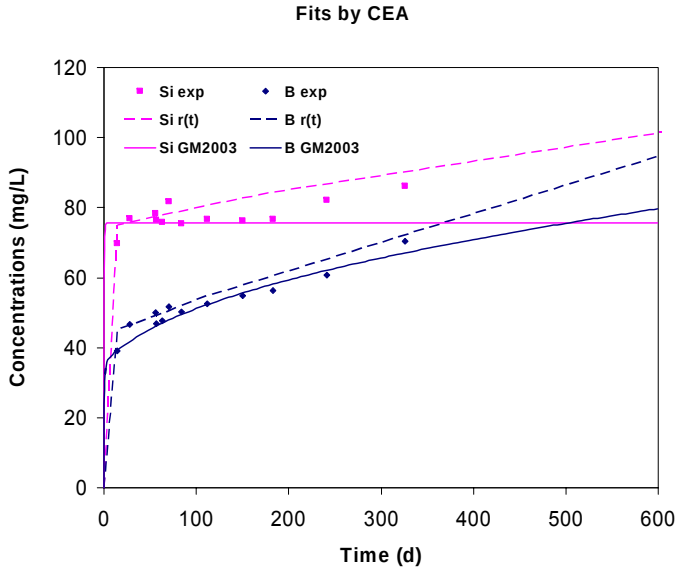

A15		r_o (g.m^{-2}.day^{-1})	C*/ K_{SiO2} (ppm)	Dg/D_{Si} (m².s^{-1})	α(ppm^{-1})	r_{fin}(g.m^{-2}.day^{-1})	D_{H20} (m².s^{-1})	Kd_B (kg.m^{-3})
CEA	R(t)	2.33	35	$5.0\ 10^{-16}$	0.02	$3.0\ 10^{-4}$	n.c.	n.c.
	GM2003	0.7	75	$5.2\ 10^{-15}$	0.02	$1.0\ 10^{-11}$	$1.2\ 10^{-23}$	4
Subatech	R(t)	?	?	?	?	?	n.c.	n.c.
	GM2003	?	?	?	?	?	?	?

A16 Experiment — SON68 glass, T=90°C, pH=9, KOH, S/V=5000 m^{-1}

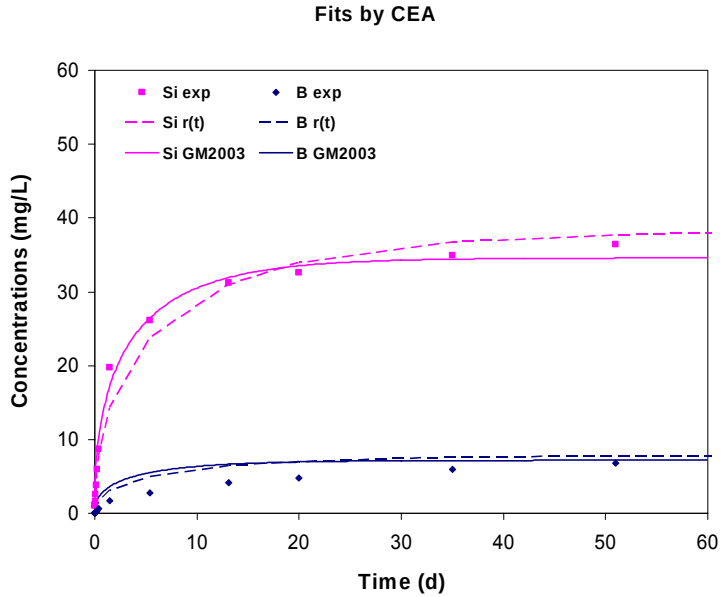

A16		r_o (g.m^{-2}.day^{-1})	C*/ K_{SiO2} (ppm)	Dg/D_{Si} (m².s^{-1})	α(ppm^{-1})	r_{fin}(g.m^{-2}.day^{-1})	D_{H20} (m².s^{-1})	Kd_B (kg.m^{-3})
CEA	R(t)	2.33	18	2.0 10^{-18}	0.0001	1.0 10^{-8}	n.c.	n.c.
	GM2003	0.7	75	1.7 10^{-17}	1.0 10^{-5}	1.0 10^{-11}	1.2 10^{-25}	100
Subatech	R(t)	?	?	?	?	?	n.c.	n.c.
	GM2003	?	?	?	?	?	?	?

A17 Experiment — SON68 glass, T=90°C, free pH, HPW, S/V=50 m^{-1}

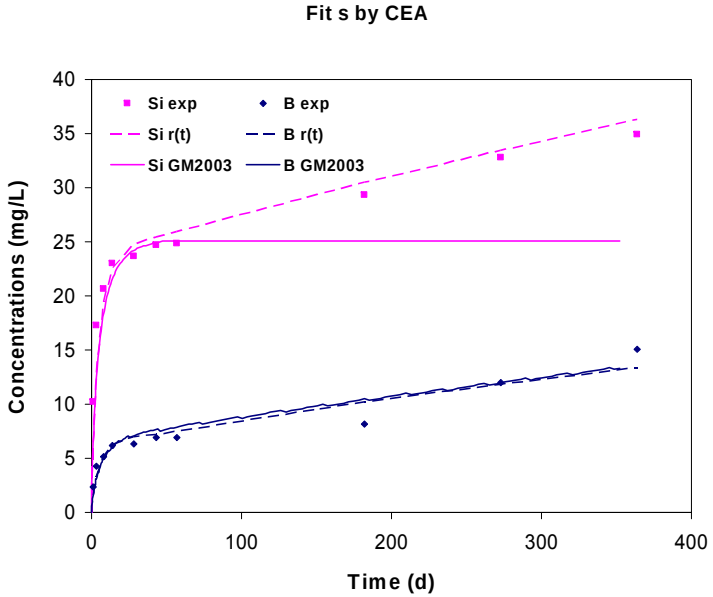

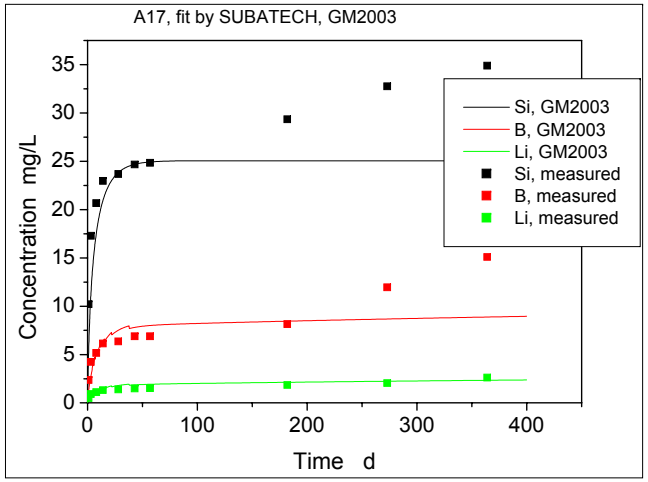

A17		r_o (g.m^{-2}.day^{-1})	C*/ K_{SiO2} (ppm)	Dg/D_{Si} (m².s^{-1})	α(ppm^{-1})	r_{fin}(g.m^{-2}.day^{-1})	D_{H20} (m².s^{-1})	Kd_B (kg.m^{-3})
CEA	R(t)	1.33	16	$5.0\ 10^{-14}$	0.023	$6.5\ 10^{-3}$	n.c.	n.c.
	GM2003	0.7	25	$2.6\ 10^{-13}$	0.022	$1.0\ 10^{-11}$	$5.0\ 10^{-21}$	100
Subatech	R(t)	?	?	?	?	?	n.c.	n.c.
	GM2003	0.7	25	$2.5\ 10^{-13}$	0.028	$7.0\ 10^{-8}$	$2.0\ 10^{-21}$	100

A18 Experiment — SON68 glass, T=150°C, free pH, HPW, S/V=50 m^{-1}

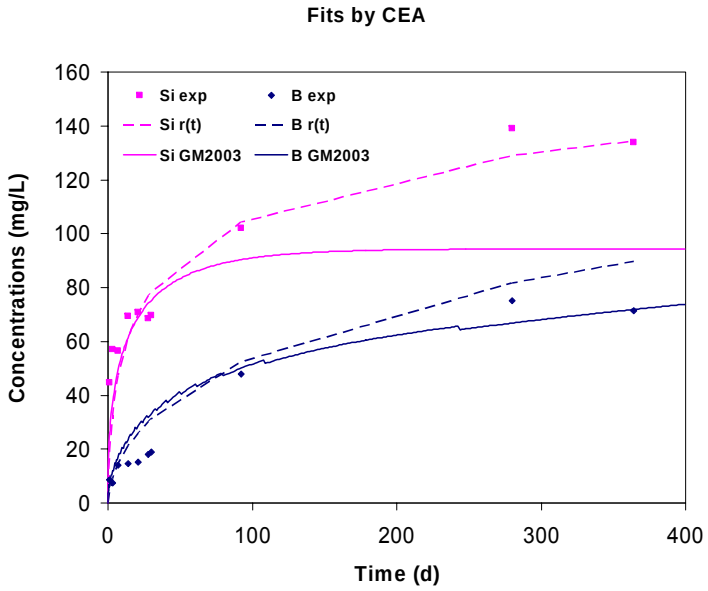

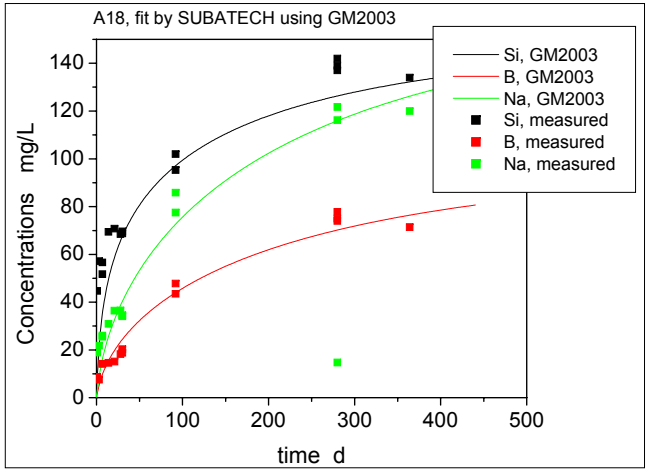

A18		r_o (g.m^{-2}.day^{-1})	C*/ K_{SiO2} (ppm)	Dg/D_{Si} (m².s^{-1})	α(ppm^{-1})	r_{fin}(g.m^{-2}.day^{-1})	D_{H20} (m².s^{-1})	Kd_B (kg.m^{-3})
CEA	R(t)	14.43	60	$5.0\ 10^{-14}$	0.015	$1.5\ 10^{-3}$	n.c.	n.c.
	GM2003	18	94	$1.4\ 10^{-13}$	0.011	$1.0\ 10^{-11}$	$1.0\ 10^{-19}$	100
Subatech	R(t)	?	?	?	?	?	n.c.	n.c.
	GM2003	18	133	$7.0\ 10^{-14}$	0.019	$7{\cdot}10^{-8}$	$2.0\ 10^{-26}$	100

A21 Experiment — AVM6 glass, T=50°C, free pH, HPW, S/V=5500 m^{-1}

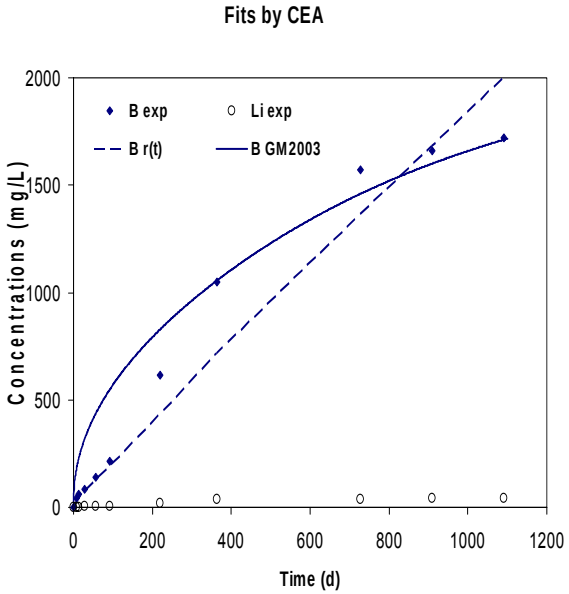

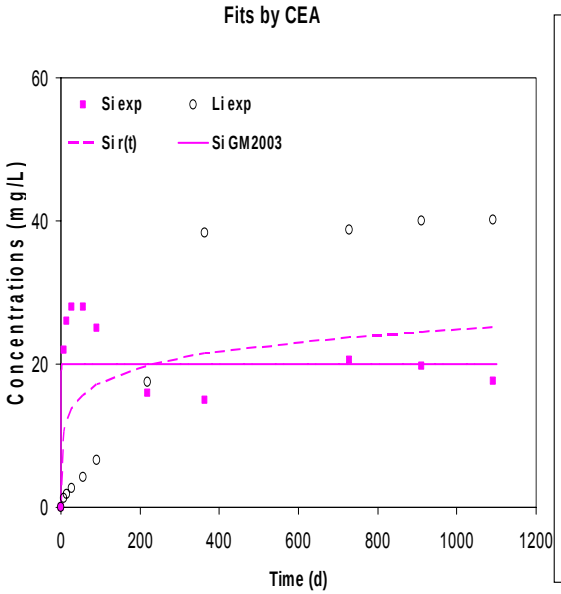

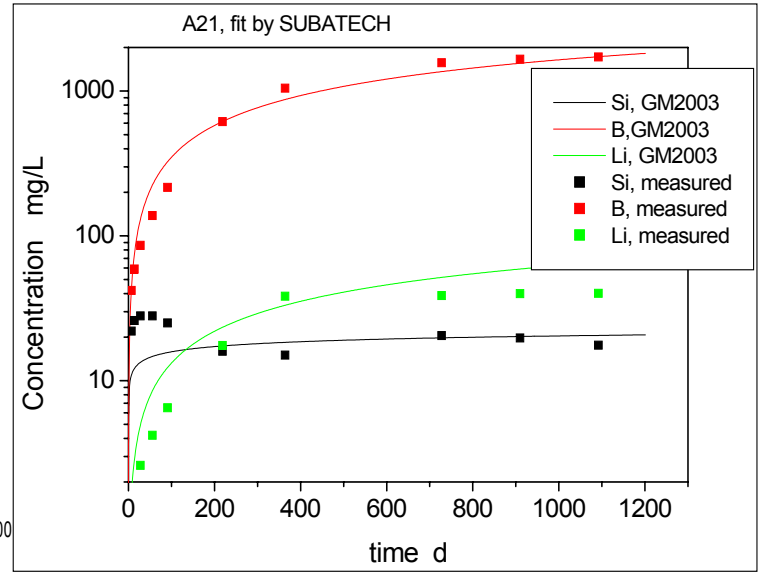

A21		r_o (g.m^{-2}.day^{-1})	C*/ K_{SiO2} (ppm)	Dg/D_{Si} (m².s^{-1})	α(ppm^{-1})	r_{fin}(g.m^{-2}.day^{-1})	D_{H20} (m².s^{-1})	Kd_B (kg.m^{-3})
CEA	R(t)	0.02	10	5.0 10^{-14}	0.003	5.0 10^{-3}	n.c.	n.c.
	GM2003	0.04	20	2.8 10^{-13}	0.15	1.0 10^{-11}	3.0 10^{-20}	100
Subatech	R(t)	?	?	?	?	?	n.c.	n.c.
	GM2003	0.04	20	2.8 10^{-13}	0.419	7.0 10^{-8}	3.0 10^{-24}	100

A22 Experiment — AVM10 glass, T=50°C, free pH, HPW, S/V=5500 m^{-1}

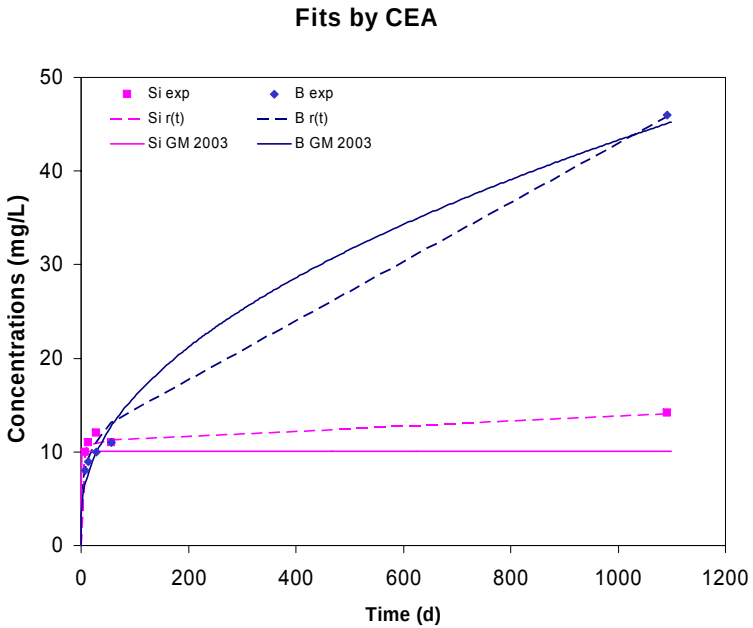

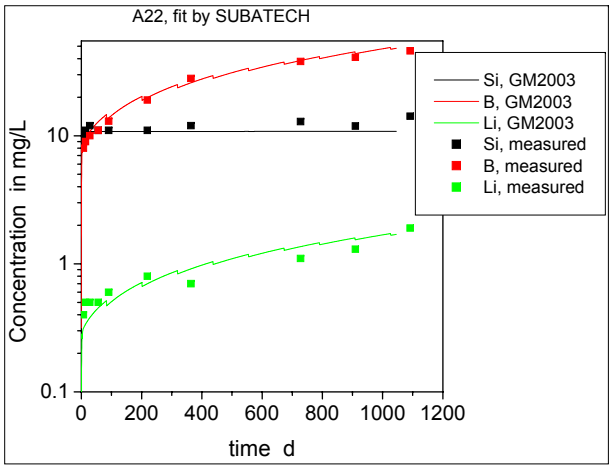

A22		r_o (g.m^{-2}.day^{-1})	C*/ K_{SiO2} (ppm)	Dg/D_{Si} (m².s^{-1})	α(ppm^{-1})	r_{fin}(g.m^{-2}.day^{-1})	D_{H20} (m².s^{-1})	Kd_B (kg.m^{-3})
CEA	R(t)	0.02	14	4.0 10^{-18}	0.25	3.0 10^{-4}	n.c.	n.c.
	GM2003	0.04	10	3.7 10^{-14}	0.089	1.0 10^{-11}	6.0 10^{-24}	20
Subatech	R(t)	?	?	?	?	?	n.c.	n.c.
	GM2003	0.04	10	2.8 10^{-13}	0.158	7.0 10^{-8}	6.5 10^{-24}	100

B1 Experiment — CJ1 glass, T=90°C, free pH, HPW, S/V=8000 m^{-1}

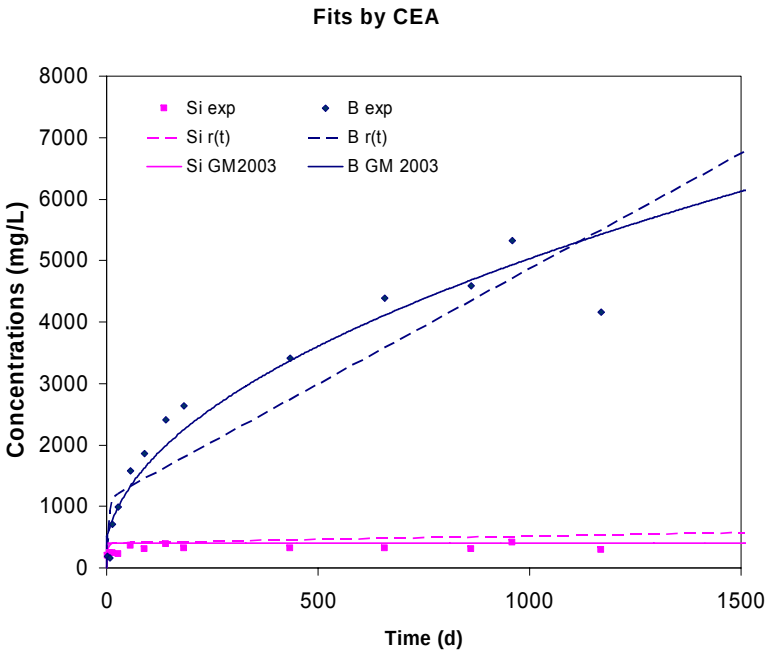

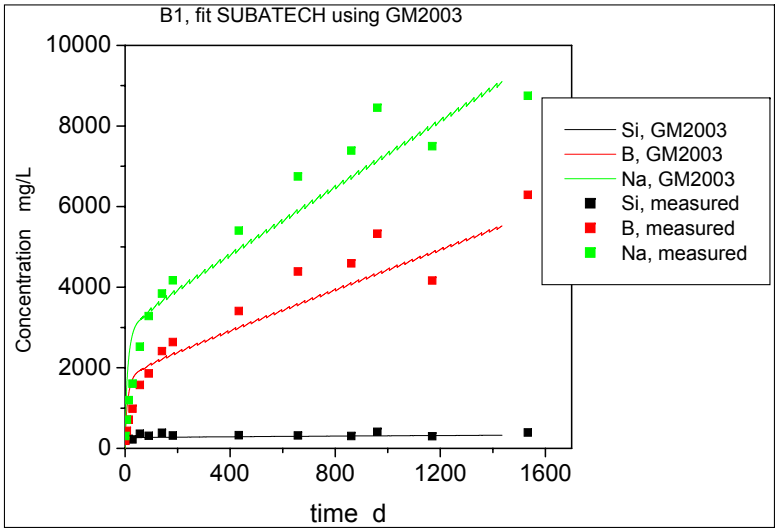

B1		r_o (g.m^{-2}.day^{-1})	C*/ K_{SiO2} (ppm)	Dg/D_{Si} (m².s^{-1})	α(ppm^{-1})	r_{fin}(g.m^{-2}.day^{-1})	D_{H20} (m².s^{-1})	Kd_B (kg.m^{-3})
CEA	R(t)	1.5	240	1.0 10^{-14}	0.01	7.0 10^{-3}	n.c.	n.c.
	GM2003	1.5	401	5.2 10^{-14}	0.004	1.0 10^{-11}	2.0 10^{-20}	10
Subatech	R(t)	?	?	?	?	?	n.c.	n.c.
	GM2003	1.5	157	5.2 10^{-14}	0.031	4.7 10^{-3}	2.0 10^{-24}	10

B4 Experiment — CJ9 glass, T=90°C, free pH, HPW, S/V=8000 m^{-1}

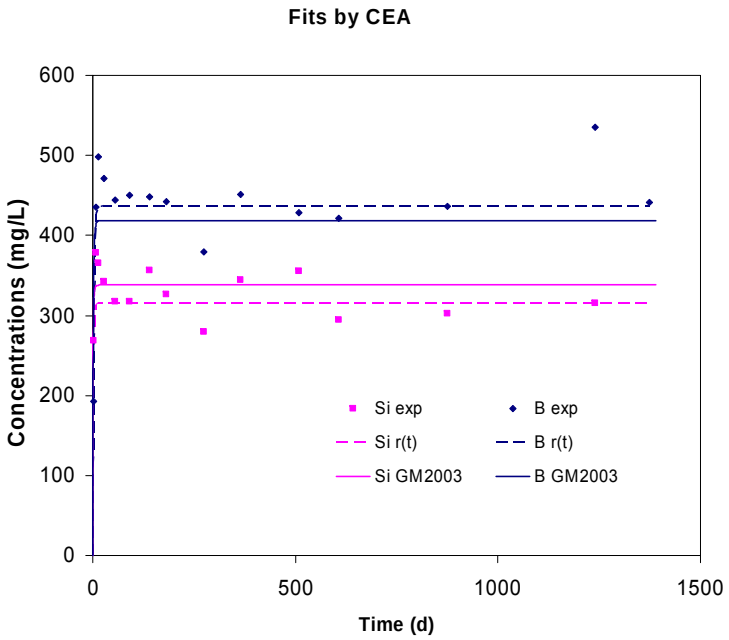

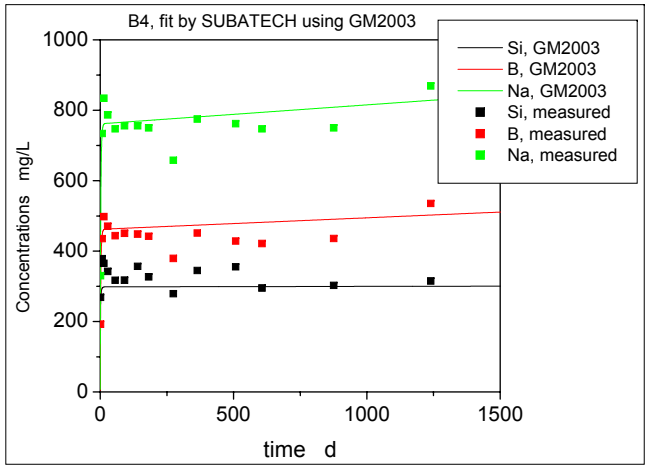

B4		r_o (g.m^{-2}.day^{-1})	C*/ K_{SiO2} (ppm)	Dg/D_{Si} (m².s^{-1})	α(ppm^{-1})	r_{fin}(g.m^{-2}.day^{-1})	D_{H20} (m².s^{-1})	Kd_B (kg.m^{-3})
CEA	R(t)	1.5	220	$1.0\ 10^{-14}$	0.01	$7.0\ 10^{-8}$	n.c.	n.c.
	GM2003	1.5	338	$5.2\ 10^{-14}$	0.008	$1.0\ 10^{-11}$	$2.0\ 10^{-26}$	10
Subatech	R(t)	?	?	?	?	?	n.c.	n.c.
	GM2003	1.5	221	$5.2\ 10^{-14}$	0.014	$7.0\ 10^{-5}$	$2.0\ 10^{-26}$	10

FZK2 Experiment — GPWAK1 glass, T=50°C, pH=3, S/V=1000 m^{-1}

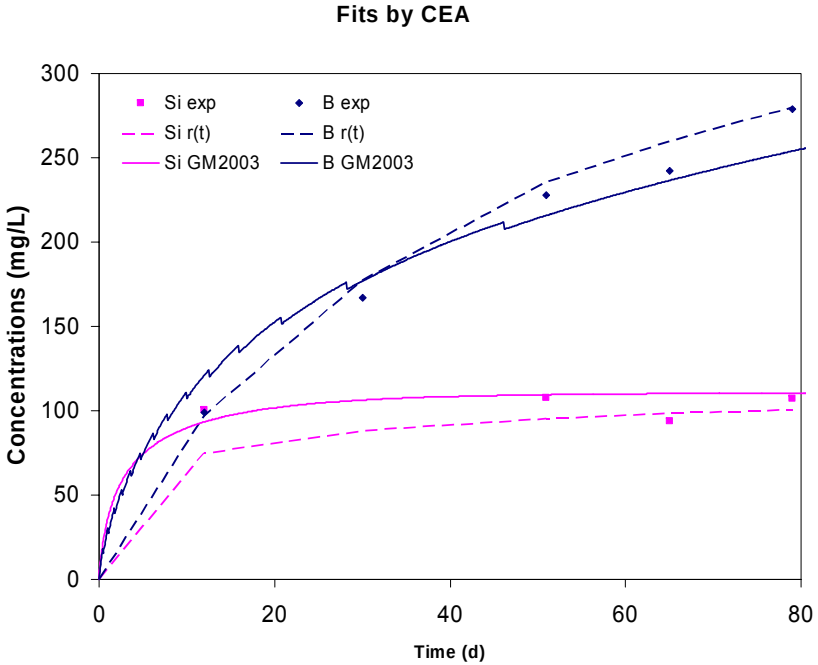

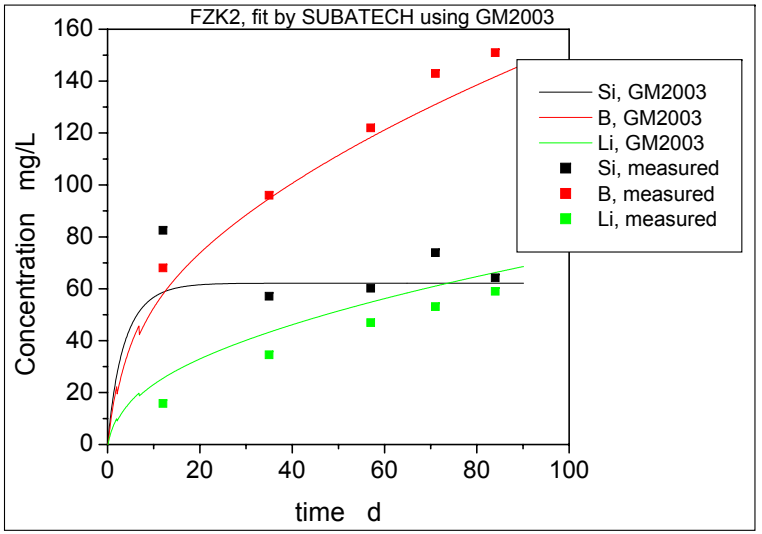

FZK2		$r_{o\,(}$g.m^{-2}.day^{-1})	C*/ K_{SiO2} (ppm)	Dg/D_{Si} (m².s^{-1})	α(ppm^{-1})	r_{fin}(g.m^{-2}.day^{-1})	D_{H20} (m².s^{-1})	Kd_B (kg.m^{-3})
CEA	R(t)	0.27	110	3.0 10^{-15}	0.04	1.0 10^{-8}	n.c.	n.c.
	GM2003	0.27	110	2.8 10^{-14}	0.019	1.0 10^{-11}	8.0 10^{-20}	30
Subatech	R(t)	?	?	?	?	?	n.c.	n.c.
	GM2003	0.09	62	2.8 10^{-14}	0.005	7.0 10^{-8}	1.3 10^{-19}	100

FZK6 Experiment — GPWAK1 glass, T=50°C, pH=5.1, S/V=1000 m^{-1}

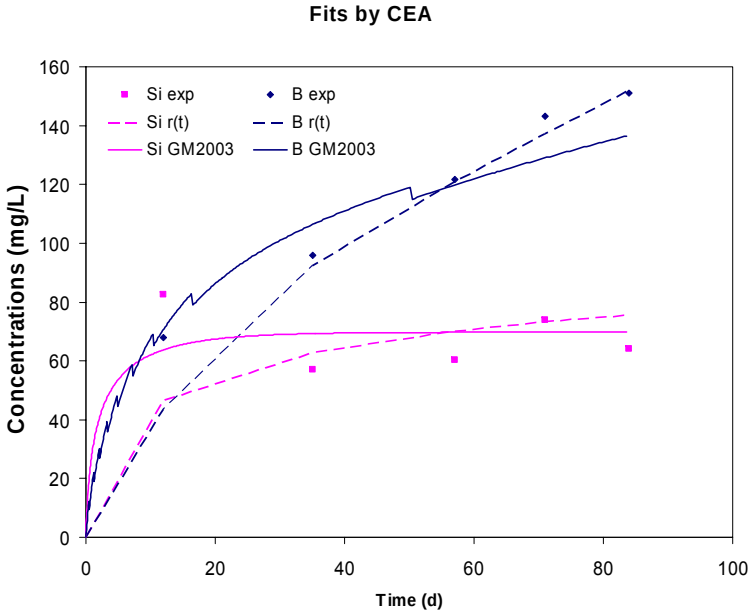

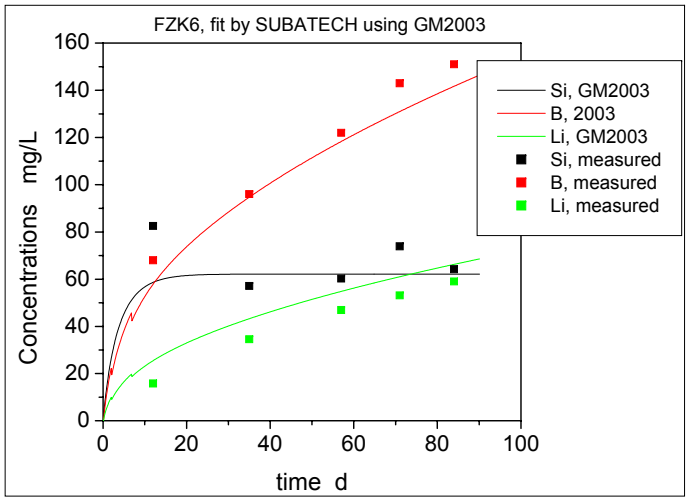

FZK6		r_o (g.m^{-2}.day^{-1})	C*/ K_{SiO2} (ppm)	Dg/D_{Si} (m².s^{-1})	α(ppm^{-1})	r_{fin}(g.m^{-2}.day^{-1})	D_{H20} (m².s^{-1})	Kd_B (kg.m^{-3})
CEA	R(t)	0.27	110	9.7 10^{-17}	0.04	1.0 10^{-8}	n.c.	n.c.
	GM2003	0.27	69	2.8 10^{-14}	0.03	1.0 10^{-11}	2.0 10^{-20}	30
Subatech	R(t)	?	?	?	?	?	n.c.	n.c.
	GM2003	0.09	62	2.8 10^{-14}	0.005	7.0 10^{-8}	1.3 10^{-19}	100

FZK8 Experiment — GPWAK1 glass, T=50°C, pH=7.1, S/V=1000 m^{-1}

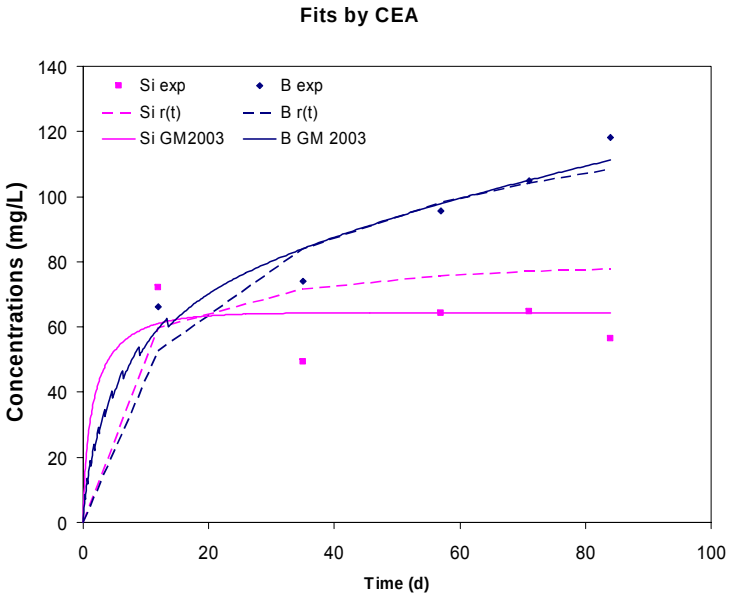

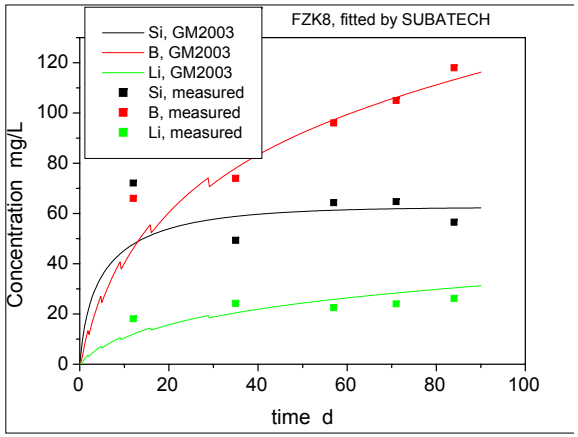

FZK8		r_o (g.m^{-2}.day^{-1})	C*/ K_{SiO2} (ppm)	Dg/D_{Si} (m².s^{-1})	α(ppm^{-1})	r_{fin}(g.m^{-2}.day^{-1})	D_{H20} (m².s^{-1})	Kd_B (kg.m^{-3})
CEA	R(t)	0.27	63.4	1.0 10^{-15}	0.055	1.0 10^{-8}	n.c.	n.c.
	GM2003	0.27	64	2.8 10^{-14}	0.028	1.0 10^{-11}	7.0 10^{-21}	10
Subatech	R(t)	?	?	?	?	?	n.c.	n.c.
	GM2003	0.09	61	2.8 10^{-14}	0.029	7.0 10^{-8}	5.0 10^{-20}	100

FZK10 Experiment — GPWAK1 glass, T=50°C, pH=9.1, S/V=1000 m^{-1}

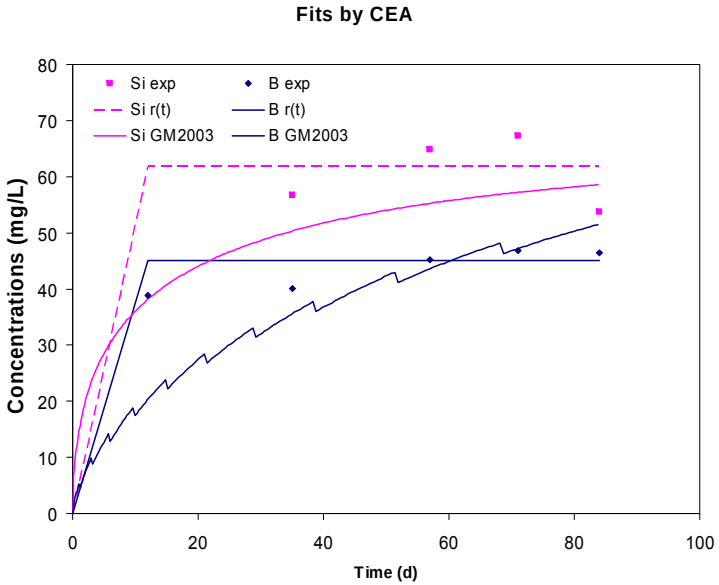

FZK10		$r_{o\ (}$g.m^{-2}.day^{-1})	C*/ K_{SiO2} (ppm)	Dg/D_{Si} (m².s^{-1})	α(ppm^{-1})	r_{fin}(g.m^{-2}.day^{-1})	D_{H20} (m².s^{-1})	Kd_B (kg.m$^{-3)}$
CEA	R(t)	0.27	40	1.0 10^{-14}	0.035	1.0 10^{-8}	n.c.	n.c.
	GM2003	0.27	64	2.8 10^{-16}	0.033	1.0 10^{-11}	2.0 10^{-21}	100
Subatech	R(t)	?	?	?	?	?	n.c.	n.c.
	GM2003	0.09	62	2.8 10^{-14}	0.035	7.0 10^{-8}	5.0 10^{-23}	100

E1 Experiment SON68 glass, T=50°C, pH=5.8, S/V=4000 m^{-1}, F=14.4 mL/day, 120 ppm Si

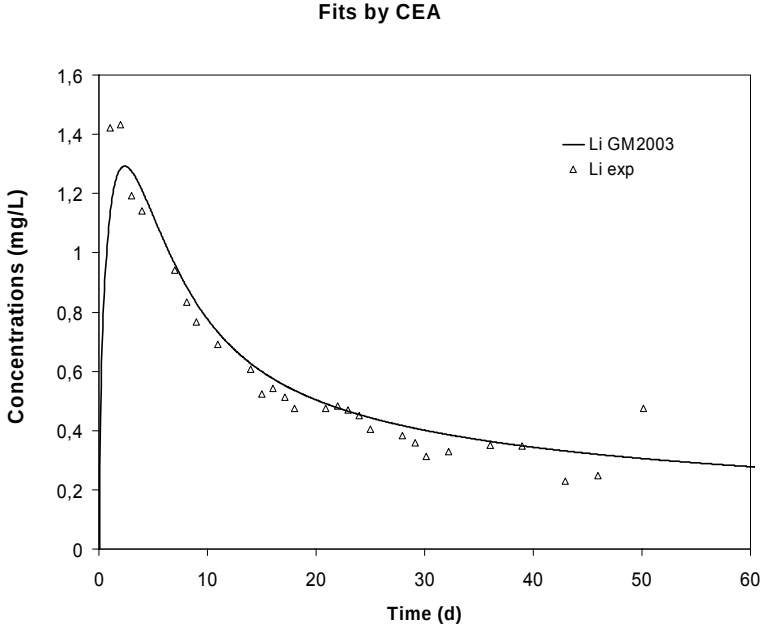

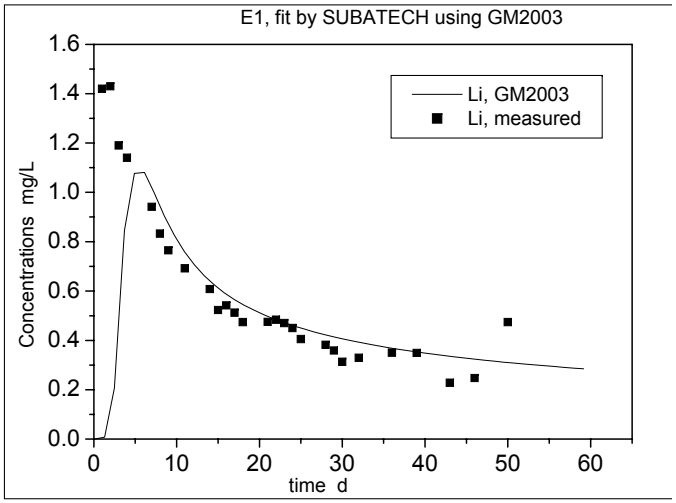

E1		r_o (g.m^{-2}.day^{-1})	C*/ K_{SiO2} (ppm)	Dg/D_{Si} (m².s^{-1})	α(ppm^{-1})	r_{fin}(g.m^{-2}.day^{-1})	D_{H20} (m².s^{-1})	Kd_{Li} (kg.m^{-3})
CEA	R(t)	Not performed						
	GM2003	0.04	64	2.8 10^{-16}	0.033	1.0 10^{-11}	2.0 10^{-21}	100
Subatech	R(t)	Fit not possible						
	GM2003	0.04	12	2.8 10^{-14}	0.05	7·10^{-8}	4.0 10^{-22}	10

E2 Experiment SON68 glass, T=50°C, pH=6, S/V=12000 m^{-1}, F=14.4 mL/day, 120 ppm Si

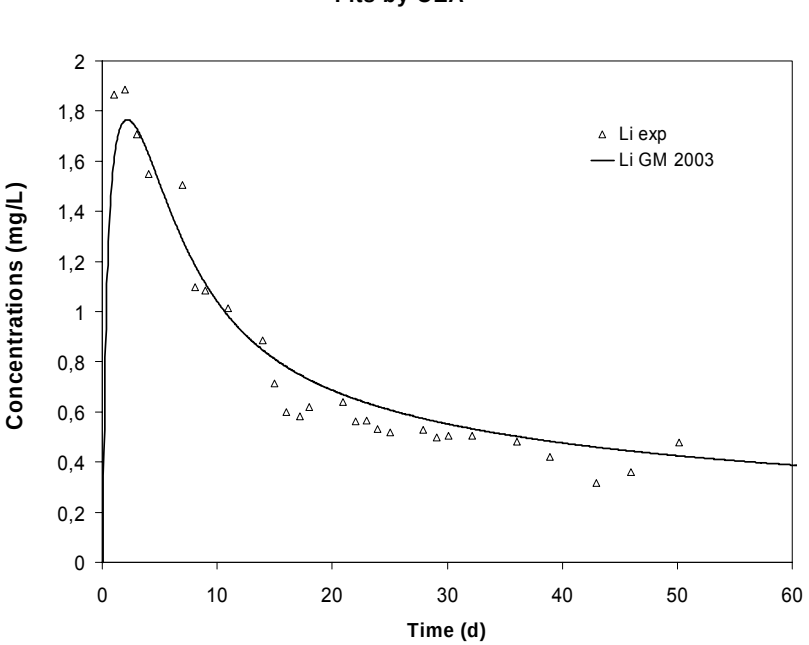

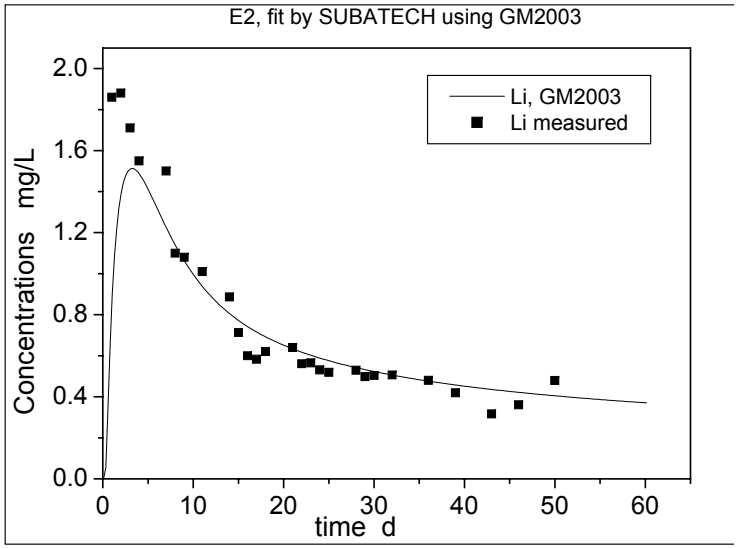

E2		r_o (g.m^{-2}.day^{-1})	C*/ K_{SiO2} (ppm)	Dg/D_{Si} (m².s^{-1})	α(ppm^{-1})	r_{fin}(g.m^{-2}.day^{-1})	D_{H20} (m².s^{-1})	Kd_{Li} (kg.m^{-3})
CEA	R(t)	Not performed						
	GM2003	0.04	29	2.8 10^{-14}	0.086	1.0 10^{-11}	1.0 10^{-22}	100
Subatech	R(t)	?	?	?	?	?	n.c.	n.c.
	GM2003	0.04	12	2.8 10^{-14}	0.05	7.0 10^{-8}	8.0 10^{-23}	10

E3 Experiment SON68 glass, T=50°C, pH=6.6, S/V=12000 m^{-1}, F=14.4 mL/day, 120 ppm Si

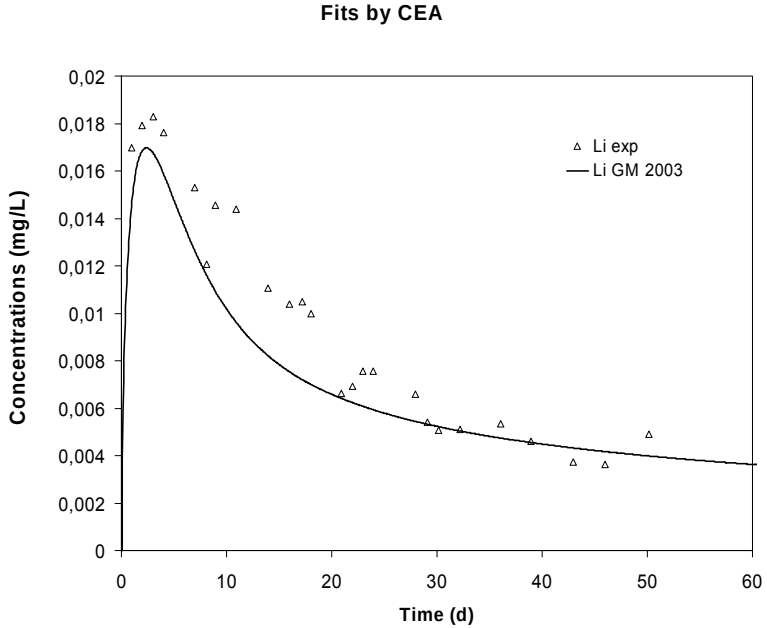

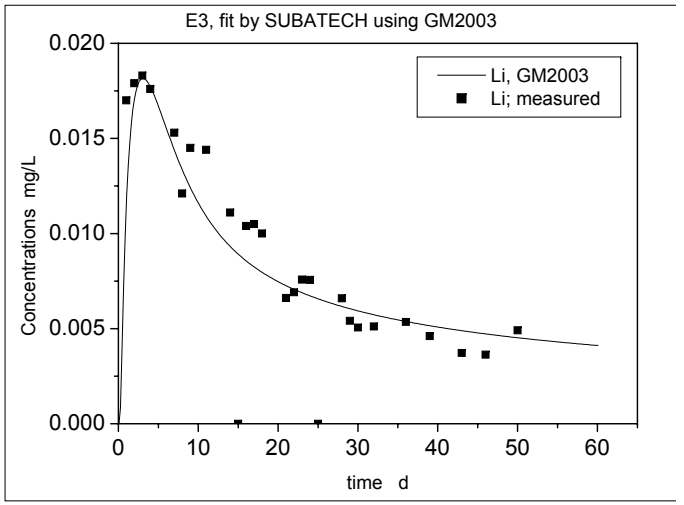

E3		r_o (g.m^{-2}.day^{-1})	C*/ K_{SiO2} (ppm)	Dg/D_{Si} (m^2.s^{-1})	α (ppm^{-1})	r_{fin} (g.m^{-2}.day^{-1})	D_{H20} (m^2.s^{-1})	Kd_{Li} (kg.m^{-3})
CEA	R(t)	Not performed						
	GM2003	0.04	29	$2.8\ 10^{-14}$	0.086	$1.0\ 10^{-11}$	$5.0\ 10^{-22}$	100
Subatech	R(t)	Fit not possible						
	GM2003	0.04	12	$2.8\ 10^{-14}$	0.05	$7.0\ 10^{-8}$	$2.5\ 10^{-21}$	10

E5 Experiment SON68 glass, T=50°C, pH=7.2, S/V=12000 m^{-1}, F=14.4 mL/day, 120 ppm Si

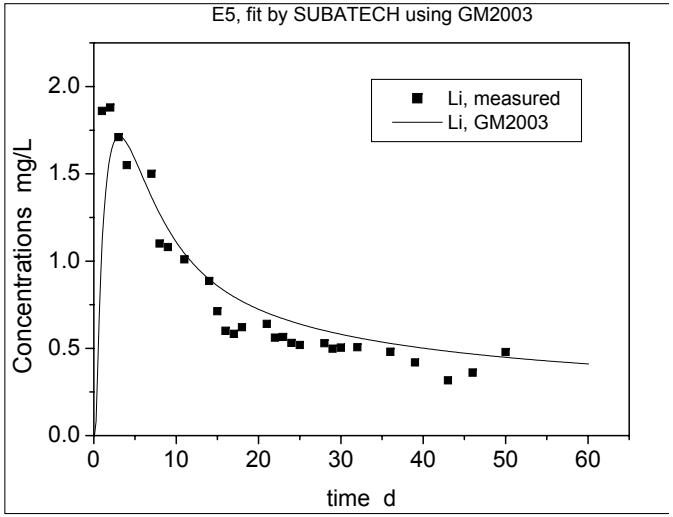

E5		r_o (g.m^{-2}.day^{-1})	C*/ K_{SiO2} (ppm)	Dg/D_{Si} (m².s^{-1})	α (ppm^{-1})	r_{fin} (g.m^{-2}.day^{-1})	D_{H20} (m².s^{-1})	Kd_{Li} (kg.m^{-3})
CEA	R(t)	Not performed						
	GM2003							
Subatech	R(t)	Fit not possible						
	GM2003	0.04	12	2.8 10^{-14}	0.05	7.0 10^{-8}	1.0 10^{-22}	10

E7 Experiment SON68 glass, T=50°C, pH=9.8, S/V=4300 m^{-1}, F=14.4 mL/day, 120 ppm Si

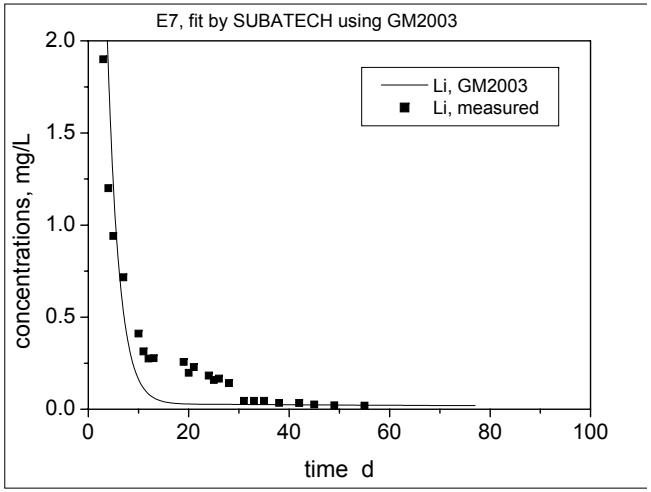

* fit required hypothesis of an initial release of 10 ppm Li. Another option to fit would be that the diffusion coefficient is not constant in time or space

E7		r_o ($g.m^{-2}.day^{-1}$)	C*/ K_{SiO2} (ppm)	Dg/D_{Si} ($m^2.s^{-1}$)	α (ppm^{-1})	r_{fin} ($g.m^{-2}.day^{-1}$)	D_{H20} ($m^2.s^{-1}$)	Kd_{Li} ($kg.m^{-3}$)
CEA	R(t)	Not performed						
	GM2003							
Subatech	R(t)	Fit not possible						
	GM2003	0.04	26	$2.8\ 10^{-14}$	0.09	$1.0\ 10^{-8}$	$3.0\ 10^{-24}$	10

E9 Experiment SON68 glass, T=90°C, pH=7.5, S/V=12000 m^{-1}, F=14.4 mL/day, 120 ppm Si

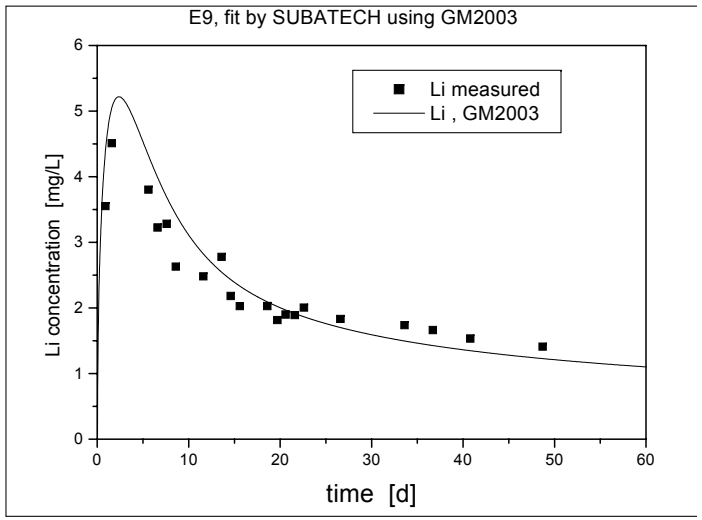

E9		r_o (g.m^{-2}.day^{-1})	C*/ K_{SiO2} (ppm)	Dg/D_{Si} (m².s^{-1})	α (ppm^{-1})	r_{fin} (g.m^{-2}.day^{-1})	D_{H20} (m².s^{-1})	Kd_{Li} (kg.m^{-3})
CEA	R(t)	Not performed						
	GM2003							
Subatech	R(t)	Fit not possible						
	GM2003	0.7	76	5.2 10^{-14}	0.05	7.0 10^{-8}	8.0 10^{-22}	10

E11 Experiment SON68 glass, T=90°C, pH=8.1, S/V=4300 m^{-1}, F=14.4 mL/day, 120 ppm Si

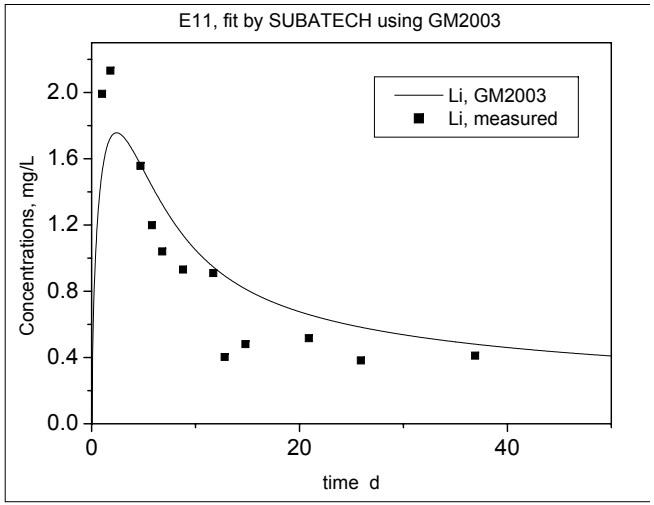

E11		$r_{o\,(}$ g.m^{-2}.day^{-1})	C*/ K_{SiO2} (ppm)	Dg/D_{Si} (m².s^{-1})	α (ppm^{-1})	r_{fin} (g.m^{-2}.day^{-1})	D_{H20} (m².s^{-1})	Kd_{Li} (kg.m$^{-3)}$
CEA	R(t)	Not performed						
	GM2003							
Subatech	R(t)	Fit not possible						
	GM2003	0.7	76	5.2 10^{-14}	0.03	7.0 10^{-8}	5.0 10^{-22}	10

E15 Experiment SON68 glass, T=90°C, pH=8.9, S/V=12000 m^{-1}, F=14.4 mL/day, 120 ppm Si

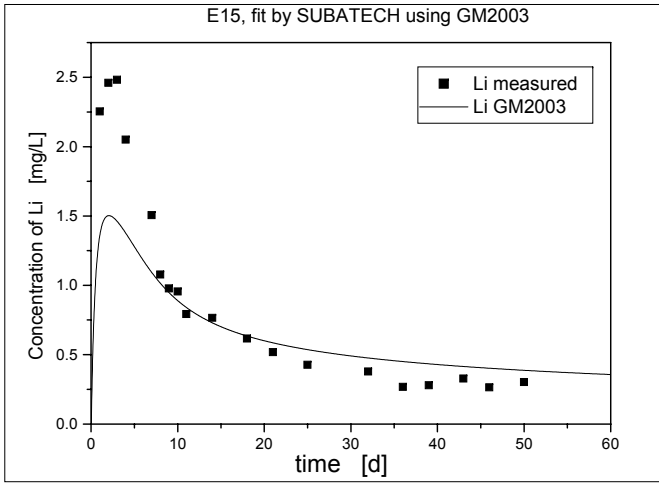

E15		r_o (g.m^{-2}.day^{-1})	C*/ K_{SiO2} (ppm)	Dg/D_{Si} (m².s^{-1})	α (ppm^{-1})	r_{fin} (g.m^{-2}.day^{-1})	D_{H20} (m².s^{-1})	Kd_{Li} (kg.m^{-3})
CEA	R(t)	Not performed						
	GM2003							
Subatech	R(t)	Fit not possible						
	GM2003	0.7	76	5.2 10^{-14}	0.03	7.0 10^{-8}	5.0 10^{-23}	10

E16 Experiment SON68 glass, T=90°C, pH=8.9, S/V=26 m^{-1}, F=14.4 mL/day, 120 ppm Si

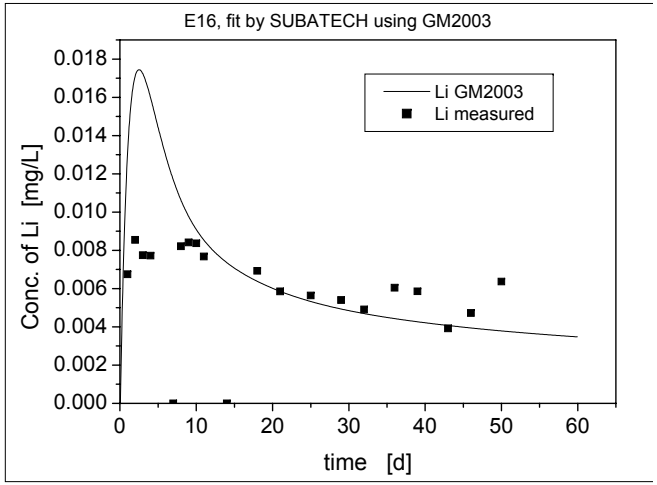

E16		r_o (g.m^{-2}.day^{-1})	C*/ K_{SiO2} (ppm)	Dg/D_{Si} (m².s^{-1})	α (ppm^{-1})	r_{fin} (g.m^{-2}.day^{-1})	D_{H20} (m².s^{-1})	Kd_{Li} (kg.m^{-3})
CEA	R(t)	Not performed						
	GM2003							
Subatech	R(t)	Fit not possible						
	GM2003	0.7	76	5.2 10^{-14}	0.03	7.0 10^{-8}	2.0 10^{-21}	10

SCK-GL31-42 Experiment R7T7 glass, T=90°C, pH=8.6, S/V=100 m^{-1}, static, clay water

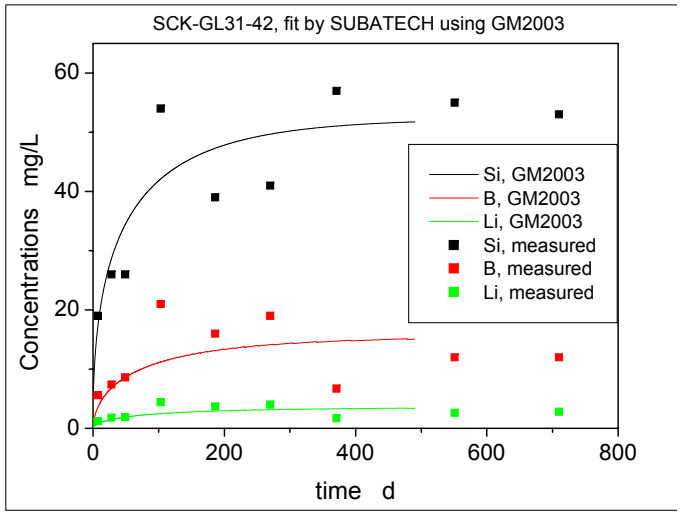

SCK-GL31-42		$r_{o\,(}$g.m^{-2}.day^{-1})	C*/ K_{SiO2} (ppm)	Dg/D_{Si} (m².s^{-1})	α (ppm^{-1})	r_{fin} (g.m^{-2}.day^{-1})	D_{H20} (m².s^{-1})	Kd_B (kg.m$^{-3)}$
CEA	R(t)	Not performed						
	GM2003							
Subatech	R(t)	Not performed						
	GM2003	0.7	46	5.2 10^{-15}	0.012	7.0 10^{-8}	1.2 10^{-22}	10